UNIVERSITY OF SOUTHAMPTON

FACULTY OF MEDICINE

Clinical Experimental Sciences

Interactions between *Pseudomonas aeruginosa* Bacteria and Corneal Fibroblasts in Human Microbial Keratitis

by

Ahmad Elsahn MBBCh FRCS(Glasg)

Thesis for the degree of Doctor of Philosophy

February 2016

UNIVERSITY OF SOUTHAMPTON

ABSTRACT

FACULTY OF MEDICINE

Clinical Experimental Sciences

Thesis for the degree of Doctor of Philosophy

INTERACTIONS BETWEEN PSEUDOMONAS AERUGINOSA BACTERIA AND CORNEAL FIBROBLASTS IN HUMAN MICROBIAL KERATITIS

Ahmad Fathy Elsahn

Microbial keratitis (MK) is a leading cause of blindness in the developing world. *Pseudomonas aeruginosa* (PA) is the most common pathogen isolated from contact lens related MK, and is usually associated with significant visual complications. The intact corneal epithelium forms a strong barrier to bacterial penetration into deeper tissue, and only when bacteria reach the stroma, through a breach in the epithelium, does a typical ulcer develop, with stromal suppuration and necrosis. Since corneal fibroblasts are one of the most prominent cellular components in the stroma, they probably have an important role in the pathogenesis of corneal ulceration.

The aim of this study was to establish an *in vitro* model of PA microbial keratitis in order to examine the microbiological, biochemical and ultrastructural changes associated with live infection of primary human corneal fibroblasts (hCF) with PA, and to assess the role of these cells in the initiation and progression of the pathogenesis of the disease.

Human corneal fibroblast monolayers were infected with bacteria, and bacterial association was assessed at 3, 6 and 9h, bacterial invasion was assessed at 9h and cytokine profiles were assessed at 9 and 24 h post challenge. Host cell death was assessed at 9h using a lactate dehydrogenase assay (LDH). Gentamicin was added at 3h to eliminate all extra cellular bacteria and limit pathogen induced effects, and bacterial replication and survival and its effect on host cell viability were assessed. Induction of cytokine and matrix metalloproteinase (MMP) production by hCF in response to PA infection was assessed by a sandwich immunoassay and a gelatine zymography.

To examine the interactions of PA with the cornea as an organ, donor corneal buttons remaining after DSEK were incubated in a medium inoculated with PA for 3-9h, then processed for scanning and transmission electron microscopy. Scanning and Transmission Electron Micrographs (SEM/TEM)

of bacterial association and invasion of corneal cells were acquired and showed that bacteria associated to superficial epithelial cells but only invaded and colonized the stroma in the presence of a mechanical breach to the epithelial basement membrane.

PAO1 bacteria caused monolayer disruption within 24h with all infective doses (10^1-10^8 CFU/mL). PAO1 associated to hCF in a dose- and time-dependant manner utilizing type IV pilus and flagella. Bacterial internalization was detected by the gentamicin assay, which also demonstrated the ability of PAO1 to survive and replicate within the fibroblasts, and was dependant on the SRC tyrosine kinase and the actin microfilament system, where internalisation was diminished when these systems were inhibited. Cytotoxicity was observed by 9h post challenge, and was reliant on bacterial type III secretion system and flagella, where mutant bacterial strains induced less cytotoxicity. The more virulent PA14 bacteria induced more cytotoxicity than PAO1. The presence of intracellular bacteria did not affect cell viability in the presence of gentamicin.

In response to PAO1 infection, hCF produced the pro-inflammatory IL-1β and GM-CSF, although GM-CSF seems to be released later than IL-1β as shown by protecting the cells with gentamicin 3h post challenge. Infection with PA14 caused an earlier and more potent cytokine production than PAO1, reflecting the pattern of cytotoxicity. Bacterial components did not have a significant effect on cytokine production by corneal fibroblasts. Cytokine production was partly reliant on bacterial type III secretion system and flagella, and wild type PA14 strains induced an earlier and more potent IL-1β production by infected corneal fibroblasts.

Gelatine zymography showed that hCF produce specific MMPs in response to live PA challenge for 24h, and these MMPs were not released in response to treatment with individual bacterial components and virulence factors. Bacteria alone produced alkaline protease, a bacterial MMP. Sandwich immunoassays showed that MMP-1, MMP-2, MMP-3 and MMP-9 were produced by infected fibroblasts to a level similar to uninfected cells. Gentamicin protected cells produced more MMPs than unprotected cells.

TABLE of CONTENTS

ABSTRACT ... i

LIST OF FIGURES ... viii

LIST OF TABLES ... x

PRESENTED WORK, PUBLICATIONS AND AWARDS ... xii

DECLARATION OF AUTHORSHIP ... xiv

ACKNOWLEDGEMENTS ... xv

DEFINITIONS AND ABBREVIATIONS ... xvi

Chapter 1 : INTRODUCTION ... 1

1.1 The global impact of corneal blindness ... 2

1.2 The Host: Structure and function of the normal cornea ... 5

1.2.1 Macroscopic anatomy of cornea ... 5

1.2.2 Microscopic anatomy of the cornea ... 7

1.2.3 Maintenance of normal corneal integrity ... 17

1.3 The Pathogen: Biology of *Pseudomonas aeruginosa* ... 18

1.3.1 Background ... 18

1.3.2 Culture Morphology and Cell structure ... 19

1.3.3 Pathogenesis and Virulence ... 25

1.3.4 Clinical Significance ... 34

1.4 The Barrier: Innate corneal defences against infection ... 36

1.4.1 Background ... 36

1.4.2 The ocular immune privilege ... 36

1.4.3 Corneal barriers against infection ... 39

1.5 The Challenge: Pathogenesis of microbial keratitis ... 43

1.5.1 Background ... 43

1.5.2 Pathogen recognition and innate immunity in the corneal epithelium ... 43

1.5.3 Recruitment of immune cells into the cornea ... 45

1.5.4 Proteases involved in the pathogenesis of corneal ulceration ... 46

1.6 Hypothesis and Objectives ... 50

1.6.1 Hypothesis ... 50

1.6.2 Objectives ... 50

Chapter 2 : MATERIALS and METHODS 51

2.1 General preparation of bacteria and host tissue 52

2.1.1 Bacteria 52

2.1.2 Cell culture model 53

2.1.3 Whole tissue model 54

2.2 Challenge of human corneal tissue with bacteria 55

2.2.1 Preparation of bacteria 55

2.2.2 Infection of corneal donor buttons 55

2.2.3 Infection of corneal fibroblasts 56

2.3 Measurement of total bacterial association 57

2.3.1 Viable counting assays 57

2.3.2 Scanning Electron Microscopy (SEM) 57

2.3.3 Assessment of the role of TFP and flagella in bacterial association to fibroblasts 58

2.3.4 Laser scanning confocal microscopy 58

2.4 Measurement of bacterial invasion 59

2.4.1 Gentamicin protection assays 59

2.4.2 Transmission Electron Microscopy (TEM) 59

2.4.3 Assessment of the effect of ciprofloxacin on intracellular bacteria 60

2.4.4 Measurement of bacterial survival and replication inside invaded fibroblasts 60

2.4.5 Assessment of the role of the SRC kinase system in bacterial internalization 61

2.5 Assessment of bacteria-induced cytotoxicity 64

2.5.1 Assessment of fibroblast cytotoxicity associated with live infection 64

2.5.2 Assessment of the effect of intracellular bacteria on fibroblast viability 64

2.5.3 Assessment of the effect of bacterial virulence on cytotoxicity 65

2.5.4 Assessment of the role of bacterial virulence factors on cytotoxicity 65

2.6 Assessment of host cell response to bacterial infection 66

2.6.1 Assessment of corneal fibroblast cytokine release associated with live infection 66

2.6.2 Assessment of corneal fibroblast MMP release associated with live infection 68

2.7 Statistical analysis and graphs 70

Chapter 3 : RESULTS 71

3.1 Bacterial association to corneal fibroblasts 72

3.1.1 Total association 72

3.1.2 Electron microscopy 73

3.1.3 The role of pili and flagella in PA association to corneal fibroblasts 75

3.2 Bacterial invasion of corneal fibroblasts 78

3.2.1 Gentamicin protection assays 78

3.2.2 Electron microscopy 80

3.2.3 Effect of ciprofloxacin on internalized bacteria 80

3.2.4 Bacterial survival and replication inside invaded fibroblasts 83

3.2.5 The role of the SRC kinase system in bacterial internalization 85

3.3 Bacterial cytotoxic effect on corneal fibroblasts 87

3.3.1 Lactate dehydrogenase (LDH) Assays 87

3.3.2 Effect of intracellular bacteria on fibroblast viability 87

3.3.3 Effect of bacterial virulence on cytotoxicity 90

3.3.4 The role of flagella and type III secretion system in cytotoxicity 92

Chapter 4 : RESULTS 94

4.1 Cytokine production by corneal fibroblasts 95

4.1.1 Cytokine production in response to live PAO1 infection 95

4.1.2 Cytokine production by infected corneal fibroblasts protected with gentamicin 95

4.1.3 Early cytokine production by infected corneal fibroblasts 95

4.1.4 The role of individual bacterial cellular components on cytokine production 100

4.1.5 Effect of bacterial virulence on cytokine production 102

4.1.6 The role of flagellin and type III secretion system in cytokine production 102

4.2 Matrix Metalloprotease (MMP) Production by Corneal Fibroblasts 105

4.2.1 Gelatine Zymography 105

4.2.2 Sandwich immunoassay 107

Chapter 5 : RESULTS 115

5.1 Model Design 116

5.2 Bacterial association to the corneal epithelium 117

5.2.1 Scanning electron microscopy 117

5.3 Bacterial penetration into corneal stroma 119

5.3.1 Light Microscopy 119

5.3.2 Transmission electron microscopy (TEM) 119

Chapter 6 : DISCUSSION 122

6.1 Host-pathogen interactions in microbial keratitis 123

6.1.1 *P. aeruginosa* bacteria associate to corneal fibroblasts 123

6.1.2 *P. aeruginosa* bacteria invade corneal fibroblasts 124

6.1.3 *P. aeruginosa* bacteria kill corneal fibroblasts 126

6.1.4 Corneal fibroblasts produce cytokines in response to *P. aeruginosa* infection 128

6.1.5 Corneal fibroblasts produce MMPs in response to *P. aeruginosa* infection 131

6.2 A model of microbial keratitis 133

6.2.1 Sequence of events in early microbial keratitis 134

6.3 Limitations and future work 136

6.3.1 Assessment of bacterial association and invasion in different strains**Error! Bookmark not defined.**

6.3.2 Removing infective medium to maintain steady infective dose 136

6.3.3 Assessment of cytokines and MMP release at more time points 137

6.3.4 Assessment of cytokine and MMP release in the presence of ciprofloxacin**Error! Bookmark not defined**

6.3.5 Testing the global cytokines and MMP release in the whole tissue model 137

6.3.6 Assessment of naïve corneal fibroblast response to a conditioned medium 137

6.3.7 Assessment of leukocyte response to cytokines released by infected fibroblasts 138

6.3.8 Introduction of leukocytes to the whole tissue model 138

Chapter 7 : APPENDICES 140

7.1 Reagents for Bacterial Culture 141

7.1.1 Luria-Bertani agar with 60µg/mL gentamicin 141

7.2 Reagents for Cell Culture and Infection 142

7.2.1 Corneal fibroblast culture medium (CFCM) 142

7.2.2 Corneal fibroblast infection medium (CFIM) 142

7.3 Reagents for cell culture 143

7.3.1 Decomplemented foetal bovine serum (dFBS) 143

7.3.2 Cytochalasin D (CD) solution 143

7.3.3 Saponin lysis solution 143

7.4 Reagents used in polymerase chain reaction (PCR) 144

7.4.1 Agarose gel 144

7.5 Reagents used in sandwich immunoassays 144

7.5.1 Reagents used in the Pro-Inflammatory 9-Plex assay 144

7.5.2 Reagents used in the V-PLEX Human IL-1β assay 145

7.5.3 Reagents used in the Human MMP Ultra-Sensitive assays 146

7.6 Reagents used in Zymography 147

7.6.1 Zymogram sample buffer (2X): 147

7.6.2 Zymogram running buffer (5X): 147

7.6.3 Zymogram staining buffer: 147

7.6.4 Zymogram de-staining buffer: 148

7.7 Reagents used in SDS-PAGE and Western blots 149

7.7.1 Separating (resolving) gel 149

7.7.2 Stacking gel 149

7.7.3 Sample buffer 149

7.7.4 Running buffer 150

7.7.5 Transfer (blotting) buffer 150

7.7.6 Blocking buffer 150

7.7.7 Pierce™ BCA Protein Assay 150

7.7.8 Serial dilutions of albumin standard 151

7.8 Miscellaneous reagents 151

7.8.1 PBS-Tween 151

LIST OF REFERENCES 152

LIST OF FIGURES

Figure 1.1 Microscopic anatomy of the cornea 9
Figure 1.2 Types of intercellular junctional complexes in the corneal epithelium 12
Figure 1.3 Transmission electron microscopy of the corneal stroma 15
Figure 1.4 Structure of the flagellum 21
Figure 1.5 Structure of the type-4 pilus 23
Figure 1.6 Structural characteristics and virulence factors of *P.aeruginosa* 24
Figure 2.1 Corneal fibroblast pre-treatment and infection using SRC kinase inhibitors 61
Figure 3.1 Total bacterial association of PAO1 bacteria to human corneal fibroblasts. 72
Figure 3.2 Scanning electron micrograph of bacterial association to human corneal fibroblasts. 74
Figure 3.3 Rate of growth of wild type and mutant PAO1 strains 75
Figure 3.4 Association of wild type and mutant PAO1 bacteria to corneal fibroblasts 76
Figure 3.5 Laser scanning confocal microscopy of PAO1 bacteria adhering to corneal fibroblasts 77
Figure 3.6 Gentamicin protection assay of bacterial invasion of human corneal fibroblasts. 79
Figure 3.7 Transmission electron micrograph of PAO1 bacteria invading corneal fibroblasts 81
Figure 3.8 Gentamicin-ciprofloxacin invasion assay 82
Figure 3.9 Bacterial survival and replication inside corneal fibroblasts. 84
Figure 3.10 Bacterial association to corneal fibroblasts pre-treated with inhibitors 85
Figure 3.11 Role of SRC tyrosine kinase and the actin microfilament system in bacterial internalisation 86
Figure 3.12 LDH release from infected fibroblasts as a percentage of maximum release by complete lysis of cells. 88
Figure 3.13 Effect of intracellular bacteria on LDH release 89
Figure 3.14 Effect of bacterial virulence on LDH release 90
Figure 3.15 Bacterial association to corneal fibroblasts infected with PAO1 and PA14 91
Figure 3.16 The role of bacterial flagella and type III secretion system in bacterial cytotoxic effects. 92
Figure 3.17 Bacterial Association to fibroblasts infected with wild type and mutant PA14 93
Figure 4.1 Cytokine production with live uninterrupted infection of corneal fibroblasts. 96
Figure 4.2. Cytokine production with gentamicin protection of corneal fibroblasts. 97
Figure 4.3. IL-1ß production by infected corneal fibroblasts at 9 and 24h post challenge as compared to uninfected controls 99

Figure 4.4 Interleukin-1ß production by corneal fibroblasts in response to challenge with live bacteria and various exotoxins and bacterial cellular components 100
Figure 4.5 Effect of bacterial virulence on cytokine production..... 103
Figure 4.6 The role of bacterial flagella and type III secretion system in cytokine production..... 104
Figure 4.7 Gelatine zymogram showing MMP release by corneal fibroblasts. 106
Figure 4.8 MMP production by corneal fibroblasts in response to challenge with live bacteria and individual bacterial components 108
Figure 4.9 MMP production by fibroblasts protected by gentamicin and unprotected cells 109
Figure 4.10 MMP production by corneal fibroblasts infected with PAO1 and PA14 at 9h 111
Figure 4.11 MMP production by corneal fibroblasts infected with PAO1 and PA14 at 24h 112
Figure 4.12 MMP production by corneal fibroblasts infected with wild type and mutant PA14 strains at 9h 113
Figure 4.13 MMP production by corneal fibroblasts infected with wild type and mutant PA14 strains at 24h 114
Figure 5.1 Human corneal DSEK button model 116
Figure 5.2 Scanning electron micrograph of bacterial association to the intact corneal epithelium. 118
Figure 5.3 Light micrograph of human corneal button..... 120
Figure 5.4 Scanning electron micrograph of bacterial association to scarified corneal epithelium... 120
Figure 5.5 Transmission electron micrograph of bacterial penetration into the corneal stroma. 121
Figure 6.1 Flow diagram of the sequence of events in early microbial keratitis 135
Figure 7.1 Serial dilution for calibrator solutions 145

LIST OF TABLES

Table 1.1 Causative organisms of microbial keratitis. 4
Table 1.2 Characteristics of corneal epithelial cells 12
Table 1.3 Diseases caused by Pseudomonas aeruginosa 35
Table 1.4 Factors contributing to ocular immune privilege 37
Table 1.5 Classes and types of matrix metalloproteinases (MMPs) 49
Table 2.1 Bacterial inocula and corresponding multiplicity of infection (MOI) 56
Table 3.1 Difference in bacterial association between wild type and mutant PAO1 strain 76
Table 3.2 Comparison between invasion rates in fibroblasts pre-treated with cytochalasin D and untreated cells. 79
Table 3.3 Difference between the number of recovered bacteria in gentamicin-treated and ciprofloxacin-treated fibroblasts 82
Table 3.4 Difference between intracellular bacterial counts at different time points. 84
Table 3.5 Difference in bacterial association in the presence and absence of inhibitors 85
Table 3.6 Comparison between bacterial internalisation in corneal fibroblasts pre-treated with SRC tyrosine kinase and actin microfilament system inhibitors and untreated cells 86
Table 3.7 Comparison between LDH release percentage in infected and unifected fibroblasts with and without gentamicin protection 89
Table 3.8 Difference between cytotoxicity induced by PA14 and PAO1 strains 90
Table 3.9 Difference in association between PA14 and PAO1 strains 91
Table 3.10 Difference between cytotoxicity induced by wild type and mutant PA14 strains 92
Table 3.11 Difference in association between wild type and mutant PA14 strains 93
Table 4.1 Comparison between cytokine levels released by uninfected cells and corneal fibroblasts protected with gentamicin after 24h of bacterial challenge. 98
Table 4.2 Comparison between IL-1ß release by corneal fibroblasts protected with gentamicin and uninfected cells after 9 and 24h of bacterial challenge. 99
Table 4.3 Difference between IL-1ß production by lysed uninfected corneal fibroblasts, and cells challenged with live bacteria and various exotoxins and bacterial cellular components 101
Table 4.4 Difference in IL-1β production between fibroblasts challenged with PA14 and with PAO1 across 3 different cell lines 103
Table 4.5 Difference in cytokine production between corneal fibroblasts infected with wild type PA14 and with mutant PA14 strains PA14*Δpopb* and PA14*ΔflgK* 104
Table 4.6 MMP production by infected gentamicin protected and unprotected corneal fibroblasts 109

Table 4.7 MMP production by infected and uninfected gentamicin protected fibroblasts 109
Table 4.8 Difference in MMP production between fibroblasts infected with PAO1 and PA14 at 9h 111
Table 4.9 Difference in MMP production between fibroblasts infected with PAO1 and PA14 at 24h 112
Table 4.10 Difference in MMP production between corneal fibroblasts infected for 9h with wild type and mutant PA14 strains 113
Table 4.11 Difference in MMP production between corneal fibroblasts infected for 24h with wild type and mutant PA14 strains 114
Table 7.1 Luria-Bertani agar with gentamicin 141
Table 7.2 Corneal fibroblast culture medium (CFCM) 142
Table 7.3 Corneal fibroblast infection medium 142
Table 7.4 Saponin lysis solution 143
Table 7.5 Zymogram sample buffer 147
Table 7.6 Zymogram running buffer 147
Table 7.7 Zymogram staining buffer 147
Table 7.8 Zymogram de-staining buffer 148
Table 7.9 Separating gel for SDS-PAGE 149
Table 7.10 Stacking gel for SDS-PAGE 149
Table 7.11 Sample buffer for SDS-PAGE 149
Table 7.12 Running buffer for SDS-PAGE 150
Table 7.13 Pierce™ BCA Protein Assay Kit 150
Table 7.14 Serial dilutions of albumin standard in BCA assay 151

PRESENTED WORK, PUBLICATIONS AND AWARDS

Posters and Presentations

May 2014	Primary Human Corneal Fibroblasts Release Specific MMPs in response to live *Pseudomonas aeruginosa* infection in-vitro. Poster. Association for Research in Vision and Ophthalmology (ARVO) Annual meeting. Orlando, FL, USA
April 2014	Bacterial Infection of the Cornea. Oral Presentation. Wessex Regional Study Day, Southampton Eye Unit. Southampton, UK
July 2013	*Pseudomonas aeruginosa* Microbial Keratitis: Understanding the Pathogenesis. Rapid Fire Presentation. Oxford Ophthalmological Congress. Oxford, UK
July 2013	Microbiological and Electron Microscopic Assessment of *Pseudomonas aeruginosa* Infection of Primary Human Corneal Fibroblasts and Epithelial Cells. Poster. Oxford Ophthalmological Congress. Oxford, UK
May 2013	Early Events of *Pseudomonas aeruginosa* Microbial Keratitis: An Electron Microscopic Study. Oral Presentation. 21st VISTA Scientific Corneal Conference. Seattle, WA, USA
May 2013	Microbiological and Electron Microscopic Assessment of *Pseudomonas aeruginosa* Association and Invasion of Human Corneal Cells *in-vitro.* Poster. Association for Research in Vision and Ophthalmology (ARVO) Annual meeting. Seattle, WA, USA
November 2012	*Pseudomonas* Infection of the Cornea: Research Update. Oral Presentation. Weekly Corneal Teaching, Southampton Eye Unit. Southampton, UK
May 2012	Cytopathic and Immunologic Effects of *Pseudomonas aeruginosa* Infection of Human Corneal Fibroblasts. Oral Presentation. 20th VISTA Scientific Corneal Conference. Fort Lauderdale, FL, USA
May 2012	Interactions of *Pseudomonas aeruginosa* with Human Corneal Fibroblasts *in-vitro*. Poster. Association for Research in Vision and Ophthalmology (ARVO) Annual meeting. Fort Lauderdale, FL, USA
March 2012	Early Events in *Pseudomonas aeruginosa* Infection of Human Corneal Cells. Wessex Regional Study Day, Salisbury District General Hospital. Salisbury, UK

Publications

- Taube MA, del Mar Cendra M, **Elsahn A**, Christodoulides M, Hossain P. Pattern recognition receptors in microbial keratitis. Eye (Lond). 2015 Nov;29(11):1399-415. Review.

Awards

- National Institute for Health Research Biomedical Research Centre for Ophthalmology grant

Upcoming Activities

- A poster presentation entitled 'The role of type 4 pilus, flagella and type III secretion system in the interactions between Pseudomonas aeruginosa bacteria and corneal fibroblasts in human microbial keratitis' has been accepted for presentation as a poster in the upcoming Association for Research in Vision and Ophthalmology (ARVO) Annual meeting on 1-5 May 2016 in Seattle, WA, USA
- An author's manuscript entitled 'Interactions between Pseudomonas aeruginosa bacteria and corneal fibroblasts in human microbial keratitis' is being prepared for submission to the Investigative Ophthalmology & Visual Science (IOVS) journal

DECLARATION OF AUTHORSHIP

I, Ahmad Elsahn, declare that the thesis entitled “Interactions between *Pseudomonas aeruginosa* bacteria and corneal fibroblasts in human microbial keratitis” and the work presented in it are my own and has been generated by me as the result of my own original research.

I confirm that:

1. This work was done wholly or mainly while in candidature for a research degree at this University;
2. Where any part of this thesis has previously been submitted for a degree or any other qualification at this University or any other institution, this has been clearly stated;
3. Where I have consulted the published work of others, this is always clearly attributed;
4. Where I have quoted from the work of others, the source is always given. With the exception of such quotations, this thesis is entirely my own work;
5. I have acknowledged all main sources of help;
6. Where the thesis is based on work done by myself jointly with others, I have made clear exactly what was done by others and what I have contributed myself;
7. None of this work has been published before submission

Signed: .....

Date: .....

ACKNOWLEDGEMENTS

I would like to express my deep gratitude to Prof Myron Christodoulides, my academic supervisor, for his invaluable support throughout the course of my studies. His leadership and professionalism set an example that will always influence and inspire me.

I would also like to express my gratitude to Mr Parwez Hossain, my clinical supervisor, for his support and mentorship. He supported and believed in me from the very start, and his encouragement and positive influence were invaluable to me.

I am eternally grateful to my wife, Yasmine, and my children, Hosna and Adam, who always encouraged and supported me through the good and challenging times of my journey. Yasmine was always there with me, always patient and understanding, and would always help me up and push me forward when I fall.

I would like to acknowledge Professor George O'Toole (University of Dartmouth, USA) and Professor Tim Tolker-Nielssen (University of Copenhagen, Denmark) for providing the strains for this study.

I am truly grateful to my colleagues in the molecular microbiology department (Rachel, Cynthia, Jay, Colette, Cate, Mar, Emma, Hania, Anish) for their continuous support and encouragement, and for the incredible times we shared together. Thank you all for being another family to me.

An important part of this work would not have been possible without the invaluable help, guidance and support from the staff of the Biomedical Imaging Unit, particularly Anton, David and Patricia, whom I've learned so much from.

I would like to deeply thank the British Council for the Prevention of Blindness, the Royal College of Surgeons of Edinburgh, the National Eye Research Centre and the Gift of Sight foundation for providing the funding to carry out this work.

I would like to deeply thank the theatre staff in Southampton Eye Unit, particularly Yvonne, for their help and support during the collection of samples necessary for this study.

I am ever so grateful to my colleagues and consultants in Southampton Eye Unit and the eye research group in the Faculty of Medicine, particularly Professor Andrew Lottery, for including me in their activities and seminars and for always treating me as part of the team.

I am grateful to the Faculty of Medicine for offering the opportunity for such an excellent research degree and for the valuable support and guidance throughout the years of study in the University.

DEFINITIONS AND ABBREVIATIONS

BCA	bicinchoninic acid
CD	Cytochalasin D
CF	Corneal fibroblasts
CFCM	Corneal fibroblast culture medium
CFIM	Corneal fibroblast infection medium
CFU	Colony forming unit
dFCS	Decomplemented foetal calf serum
DSEK	Descemet's stripping endothelial keratoplasty
GFP	Green fluorescent protein
GM-CSF	Granulocyte monocyte colony stimulating factor
hCFs	Human corneal fibroblasts
IL-1β	Interleukin 1-beta
LDH	Lactate dehydrogenase
MK	Microbial keratitis
MMP	Matrix metalloproteinase
MOI	Multiplicity of infection
PA	*Pseudomonas aeruginosa*
PBS	Phosphate buffered saline
PCR	Polymerase chain reaction
SDS-PAGE	Sodium dodecyl sulphate-polyacrylamide gel electrophoresis
SEM	Scanning electron microscopy
TEM	Transmission electron microscopy
TFP	Type IV pilus
TNF-α	Tumour necrosis factor-alpha
TTSS	Type III secretion system
WT	Wild type bacteria

Chapter 1 : **INTRODUCTION**

1.1 The global impact of corneal blindness

The World Health Organization (WHO) Prevention of Blindness and Deafness Programme reports in its most recent systematic search and review to obtain a global estimate of visual impairment that the estimated number of people visually impaired in the world is 285 million, 39 million of which are blind.[1] Corneal opacities accounted for 7-15% of the world's blind population, making it the 3rd most common cause of blindness.[2, 3] In some regions, such as Saudi Arabia and India, the prevalence of corneal blindness can be as high as 25%,[4-7] and in Malawi[8] and Bangladesh,[9] corneal scarring was accountable for 39–55% of unilateral blindness. Unlike other major causes of blindness, like cataract, glaucoma and macular degeneration, corneal blindness frequently affects all age groups, including people of working age, making it a major public health problem, with significant long term socio-economic implications.[10]

Corneal opacification is the third most common cause of childhood blindness worldwide, after non-corneal causes such as congenital cataract and glaucoma,[10] and is often due to a single episode of infection, such as ophthalmia neonatorum resulting from Neisseria gonorrhoea and Chlamydia trachomatis infections.[2] Surveys of child blindness in Africa have shown that approximately 70% of all visual disability in this group is caused by corneal opacification.[11] Patients suffering corneal blindness endure long term loss of vision, reduced quality of life and decreased productivity. In addition, there are significant costs to patients and carers, such as lost income and distress from pain and discomfort.[12] Blind children have a lifetime of increased morbidity ahead of them, and even increased mortality, with up to 60% of blind children dying within 1 year of becoming blind.[10]

The aetiology of corneal blindness is diverse and varies according to ocular diseases endemic to each geographic location. Important diseases classically associated with corneal blindness include trachoma, onchocerciasis, leprosy, ophthalmia neonatorum, and xerophthalmia.[13] Trachoma remains the world's leading infectious cause of blindness and ocular morbidity. It is estimated by WHO that, at present, there are about 4.9 million people already blind from trachomatous corneal scarring and an additional 10 million suffering from trichiasis which puts them at risk of corneal blindness.[14] Onchocerciasis is another major cause of blindness in the world, although the incidence of onchocerciasis-related blindness has been declining since the introduction of the onchocerciasis control programme.[15] Leprosy causes corneal scarring from interstitial keratitis, exposure keratitis due to lagophthalmos and loss of corneal sensation. Despite remarkable progress in the management of leprosy in the past few decades, corneal complications are still a significant cause of corneal blindness, affecting 10-12 million people, with approximately 250,000 blind from the disease,

mostly in Africa and the southern India.[16] Xerophthalmia and Ophthalmia neonatorum are important causes of blindness in children.[17]

Although these diseases remain a big public health problem, the introduction of control programs by the WHO has been successful in decreasing their incidence. This, in addition to worldwide decline in the number of cases of trachoma, has drawn attention to other causes of corneal blindness. These include trauma, microbial keratitis and the use of traditional eye medicines, which are often contaminated and can provide a route for the spread of pathogens.[17]

There is an estimated 1.5-2 million people that develop corneal ulceration every year in developing countries.[17] In a recent study by Wang *et al,*[18] infectious keratitis accounted for as much as 40% of childhood and 20% of adult corneal blindness in their study population in China, whereas Rapoza *et al*[19] and Bowman *et al*[20] reported corneal infections, including trachoma, were the leading cause of unilateral and bilateral corneal blindness in central Tanzania and Gambia, respectively. In the Nepal blindness survey, corneal trauma and ulceration were the second most common cause of unilateral visual loss after cataract, accounting for 7.9% of all blind eyes.[21] All this clearly shows that corneal infection is a significant public health problem, yet it is alarmingly under-diagnosed and under-treated, that some consider it a 'silent epidemic' in the developing world.[22]

Infectious keratitis can be caused by bacteria, viruses, fungi, protozoa, and parasites (Table 1.1).[23-37] On a global level, common risk factors for the disease include ocular trauma, contact lens wear, recent ocular surgery, pre-existing ocular surface disease, dry eyes, lid deformity, corneal sensational impairment, chronic use of topical steroids, and systemic immunosuppression.[38-41] These risk factors and causative organisms, however, vary tremendously with geographical location; for instance, non-surgical trauma to the eye accounted for 48.6–65.4% of all corneal ulcers in Nepal and India,[42, 43] but only accounted for 27% of all cases at a large county trauma referral centre in the United States.[44]

Contact lens wear accounts for up to 50.3% of cases of microbial keratitis[45] in the western world, and the estimated annual incidence of microbial keratitis per 10,000 contact lens wearers is up to 25.4 (95 % CI, 14.6-29.5) for extended wear of silicone hydrogel lenses.[46] *Pseudomonas aeruginosa* is the most commonly isolated causative organism for contact lens associated microbial keratitis,[47-50] accounting for up to 68.8% of isolates.[47] *Pseudomonas aeruginosa* microbial keratitis is not only one of the most significant types of the disease, but also one of the most devastating, causing significant morbidity and disability.

Table 1.1 Causative organisms of microbial keratitis.

BACTERIAL	Gram positive	Gram negative
	Staphylococcus spp (aureus, epidermidis)	*Pseudomonas aeruginosa*
	Streptococcus pneumoniae	*Moraxella spp*
	Streptococcus pyogenes	*Klebsiella pneumoniae*
	Streptococcus viridans	*Enterobacter aerogenes*
	Corynbacterium diphtheroides	*Serratia spp (marcescens, liquefaciens)*
	Nocardia spp	*Acinetobacter spp*
	Propionibacteria acnes	*Enterococcus spp*
	Bacillus spp	*Burkholderia cepacia*
	Mycobacterium spp	*Escherichia coli*
	Micrococcus spp	*Stenotrophomonas maltophilia*
	Actinomyces spp	*Neisseria gonorrhoeae*
		Haemophilus spp
		Kingella kingae
		Pseudomonas spp (non-aeruginosa)
		Citrobacter spp
		Aeromonas spp
CHLAMYDIAL	*C trachomatis, psittaci*	
FUNGAL	*Fusarium spp*	
	Aspergillus spp (flavus, fumigatus, niger, terreus and nidulans)	
	Alternaria spp	
	Cuvularia spp	
	Lasiodiplodia theobromae	
	Paecilomyces spp	
	Penicillium spp	
	Scedosporium apiospermum	
	Cephaliophora irregularis	
	Cladosporium cladosporoides	
	Cylindrocarpon spp	
	Exserohilum rostratum	
	Bipolaris spp	
	Candida spp	
	Pythium insidiosum	
VIRAL	Herpes simplex virus type 1	
	Varicella zoster virus	
	Human adenovirus (serotypes 8, 19, and 37)	
	Enterovirus type 70	
	Coxsackievirus type 24	
	Echovirus type 13	
	Poliovirus type 3	
	Cytomegalovirus	
PARASITIC	*Acanthamoeba spp (castellani, polyphaga and culbertsoni)*	
	Microsporidia spp	
	Hartmannella spp	
	Vahlkampfia spp	
	Dictyostelium polycephalum	
	Phthriasis palpebrarum	
	Oestrus ovis	
NEMATODAL	*Loa loa*	
	Onchocerca volvulus	

1.2 The Host: Structure and function of the normal cornea

1.2.1 Macroscopic anatomy of cornea

The cornea is a transparent avascular tissue that is exposed to the external environment. The anterior corneal surface is covered by the tear film, and the posterior surface is in direct contact with the aqueous humor.[51] The adult human cornea measures 11 to 12 mm horizontally and 9 to 11 mm vertically. It is approximately 0.5 mm thick at the centre, and its thickness increases gradually toward the periphery, where it is about 0.7 mm thick.[52] The shape of the anterior corneal surface is convex, although the curvature along the corneal surface is not constant, and aspheric, where it is steeper and almost spherical at the centre, with a radius of curvature between 7.5 and 8.0 mm, and flatter towards the periphery. The refractive power of the cornea is 40 to 44 dioptres, which constitutes about two-thirds of the total refractive power of the eye.[51]

The cornea is one of the few avascular tissues in the body. It is also one of the most heavily innervated tissues in the body, and the density of nerve endings in the cornea is about 300 to 400 times greater than that in the skin.[53] Most of the sensory nerves in the cornea are derived from the long ciliary nerves of the ophthalmic branch of the trigeminal nerve, entering the cornea mostly as a continuation the nerves in the suprachoroidal space. Approximately 43 nerve bundles enter the cornea, predominantly in the mid and deep stroma, evenly distributed through the limbal circumference. Corneal nerves penetrate Bowman's layer perpendicularly and vertically (i.e. from inferior to superior) in the mid-peripheral cornea, to form a sub basal nerve plexus.[54] The cornea contains peptidergic, sympathetic, and parasympathetic nerve fibres, with various neurotransmitters, including substance P, calcitonin gene-related peptide, neuropeptide Y, vasoactive intestinal peptide, galanin, methionine-encephalin, catecholamines, and acetylcholine.[55-62]

Corneal epithelial and endothelial cells are metabolically active and require adenosine triphosphate (ATP) as an energy source, which is obtained by glycolysis under aerobic conditions. A supply of glucose and oxygen is thus essential to maintain the normal metabolic functions of the cornea.[63-66] Glucose is obtained by diffusion from the aqueous humor, whereas oxygen is obtained primarily by diffusion from the tear fluid, which absorbs oxygen from air, and to a lesser extent by diffusion from the aqueous humor and limbal circulation. Disruption of oxygen supply to the cornea, such as that associated with contact lens wear, can lead to corneal hypoxia and consequent stromal oedema.[67] Closure of the eyelids during sleep also reduces the amount of oxygen that reaches the cornea, which can change corneal metabolism from aerobic to anaerobic, with consequent accumulation of lactate.[68, 69]

The corneal surface is covered by the tear fluid, which protects the cornea from dehydration and helps to maintain the epithelial surface smooth. It contains almost all of the biochemical components of blood, including albumin and globulins, but few of the cellular components. The thickness and volume of the tear film are about 7 μm and 6.5 ± 0.3 μl, respectively. The tear film consists of three layers: a superficial lipid layer (~0.1 μm), an aqueous layer (~7 μm), and a mucin layer (0.02 to 0.05 μm).[70] The constituents of the superficial lipid layer of the tear film are secreted by Meibomian glands and other secretory glands of the eyelid, the aqueous layer is secreted by the main and accessory lacrimal glands, and the mucin layer is produced by goblet cells in the conjunctival epithelium and corneal epithelial cells. More than 98% of the total volume of the tear film is water, but it also contains many biologically important molecules, including electrolytes, glucose, immunoglobulins, lactoferrin, lysozyme, albumin, and oxygen, in addition to several biologically active substances such as histamine, prostaglandins, growth factors, and cytokines. Thus, the tear film serves not only as a lubricant and source of nutrients for the corneal epithelium but also as a source of regulatory factors required for epithelial maintenance and repair[71-75] and modulation of corneal epithelial migration, proliferation, and differentiation.[76, 77] In pathological conditions such as allergic keratoconjunctivitis, corneal trauma, or corneal infection, tear fluid provides a path for various inflammatory cells, growth factors, and inflammatory cytokines derived from the palpebral or bulbar conjunctiva to reach the cornea. The tear fluid of individuals with corneal ulceration also contains matrix metalloproteinases (MMPs) that degrade extracellular matrix proteins such as collagen and basement membrane components.[78-81]

1.2.2 Microscopic anatomy of the cornea

The structure of the cornea is relatively simple, consisting of five layers: the epithelium, Bowman's layer, the stroma, Descemet's membrane, and the endothelium (Figure 1.1 A). The epithelium, stroma and endothelium are cellular layers, whereas Bowman's layer and Descemet's membrane are acellular and act as interfaces. Epithelial cells are embryologically derived from the surface ectoderm, whereas stromal keratocytes (corneal fibroblasts) and endothelial cells are of neural crest (neuroectodermal) origin. Components of the cornea interact with each other to maintain its integrity and function.[51]

The optical properties of the cornea are determined by its transparency, surface smoothness, contour, and refractive index. Corneal transparency is mostly attributable to the arrangement of collagen fibres in the stroma.[51] Both the mean diameter of each collagen fibre and the mean distance between collagen fibres are relatively homogeneous and are less than half of the wavelength of visible light (400 to 700 nm). This anatomic arrangement is thought to be responsible for the fact that scattering of an incident ray of light by each collagen fibre is cancelled by interference from rays scattered by neighbouring collagen fibres,[82] allowing light to pass through the cornea with minimal scatter. If the diameter of, or the distance between, collagen fibres become disorganized (as occurs in fibrosis or oedema), incident rays are scattered randomly and the corneal transparency is significantly affected.

1.2.2.1 The epithelium

The corneal epithelium is composed of non-keratinized stratified squamous epithelial cells, spanning a thickness, which is constant over the entire corneal surface, of approximately 50 µm, about 10% of the total thickness of the cornea. There are 5-6 layers of three different types of epithelial cells (Figure 1.1 B), and although the corneal epithelium is normally non-keratinized, it may develop keratinization under certain pathological conditions, such as vitamin A deficiency.[83]

The surface of the corneal epithelium consists of 2-3 layers of terminally differentiated superficial cells. These cells are flat and polygonal with a diameter of 40-60 µm and a thickness of 2-6 µm. Their surface is covered with microvilli, which form microplicae[84] that increase the surface area of each cell and thereby promote the absorption of oxygen and nutrients from tear fluid.

Superficial cells are well differentiated, and so they do not proliferate, exhibit a low metabolic activity and contain fewer organelles and less RNA than do the other types of corneal epithelial cells. Numerous glycoprotein and glycolipid molecules are embedded in the cell membrane of epithelial cells and are collectively known as the glycocalyx. These molecules interact with the mucinous layer

of the tear film and help to maintain its structure.[84, 85] Two different types of superficial cells are present in the corneal epithelium: large, dark cells and small, light cells. The former are mature, have a dense coat of microvilli, and are about to undergo desquamation into the tear film; the latter have fewer microvilli and are thought to be younger.

Although superficial cell desquamation occurs in normal physiologic conditions, apoptosis and increased desquamation can occur under conditions of stress, such as ultraviolet radiation, hypoxia, infection or mechanical injury.[86-89] Apoptosis contributes to stromal keratocyte cell turnover under normal conditions, but it is not clear whether it is also involved in normal epithelial cell turnover.

Beneath the superficial cells of the corneal epithelium lie 2-3 layers of wing cells, so called because of their characteristic wing-like shape. Wing cells are in an intermediate state of differentiation between basal and superficial cells and are rich in intracellular keratin tonofilaments, but have sparse cytoplasmic organelles.[90, 91] The cell membranes of adjacent wing cells interdigitate and have numerous desmosomes and gap junctions between them (see Figure 1.2).

Basal epithelial form a single layer resting on the basement membrane. Neighbouring cells are joined laterally by desmosomes, gap junctions, and adherens junctions (zonula adherens). They are the only epithelial cells capable of mitosis, giving rise to wing cells, which in turn differentiate in to superficial flat cells. The latter desquamate into the tear film approximately 7-14 days after differentiation.[92] Due to their mitotic activity, basal cells demonstrate numerous intracellular organelle, free ribosomes, rough endoplasmic reticulum, mitochondria, centrioles, microfilaments, microtubules, and glycogen granules, in contrast to wing cells or superficial cells, which have less organelles.[51] The posterior surfaces of the basal cells lie flat over the basement membrane, and are adherent to it with hemidesmosomes and anchoring fibrils. The later consist of type VII collagen and penetrate the basement membrane into the stroma, where they, in addition to stromal type I collagen, form anchoring plaques. This arrangement is critical in maintaining the stability of the entire epithelium by ensuring the adhesion of the epithelial cells to the basement membrane and underlying stroma, and its disruption leads to recurrent epithelial erosions.[93]

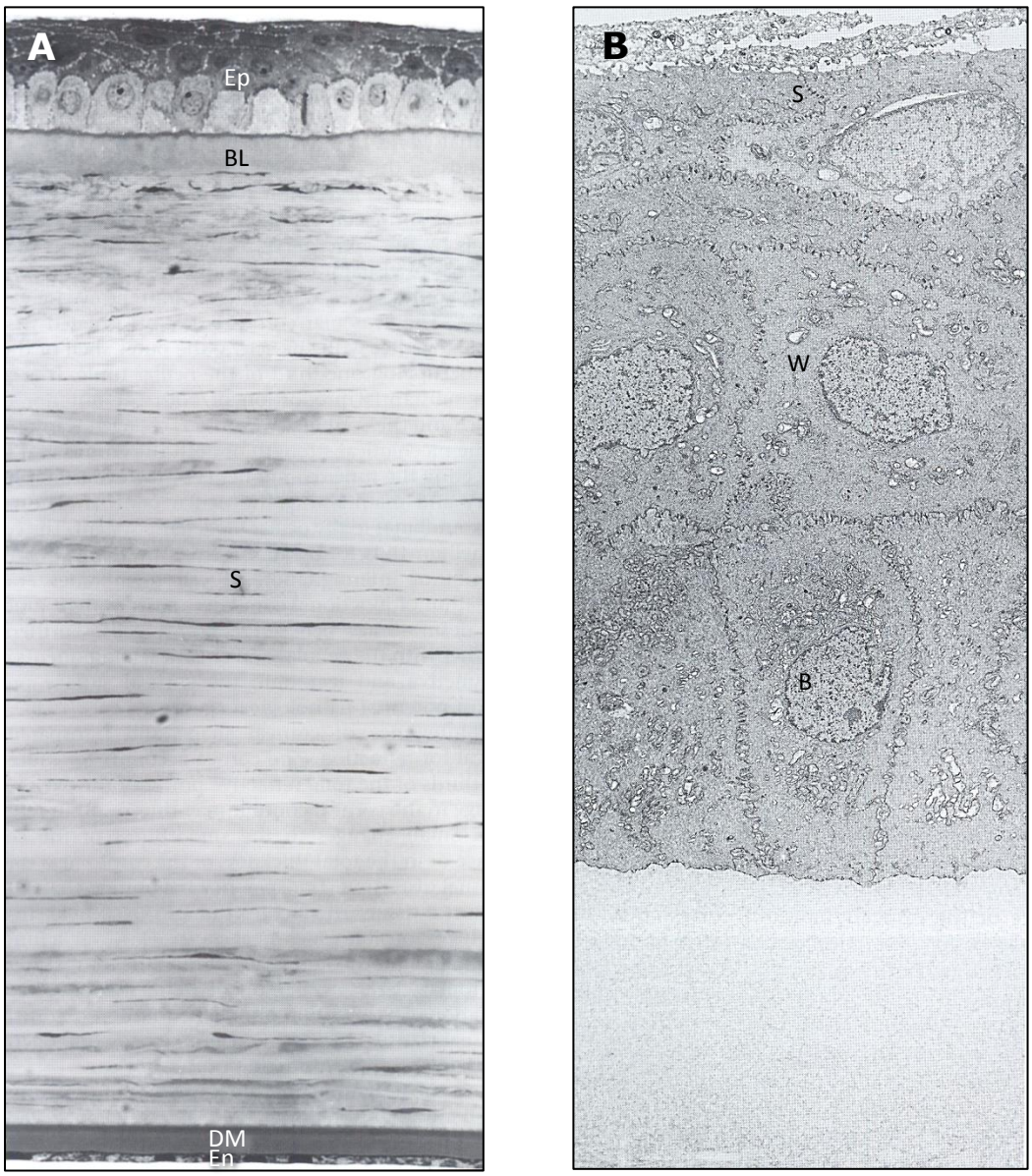

Figure 1.1 Microscopic anatomy of the cornea

A, Histology of the cornea showing the epithelium (Ep), Bowman's layer (BL), the stroma (S), Descemet's membrane (DM), and the endothelium (En). **B**, Scanning electron microscopy of the corneal epithelium, comprising a basal cell layer (B), 2-3 layers of wing cells (W), and 2-3 layers of superficial cells (S). (Reproduced with permission from Krachmer et al, Cornea. Mosby. 2005)

The basal epithelial cells synthesize and secrete type IV collagen and laminin, which are major components that form the basement membrane, along with fibronectin, heparan sulphate, type VII collagen, proteoglycans and fibrin.[94] When examined by transmission electron microscopy, the basement membrane is 40-60 nm thick and is composed of a pale layer (the lamina lucida) immediately posterior to the cell membrane of the epithelial basal cells and an electron-dense layer (the lamina densa) adjacent to the stroma.

The presence of the basement membrane between the basal epithelium and the underlying stroma fixes the polarity of epithelial cells, which is important in the virulence of microbes and the pathogenesis of microbial keratitis.[95-97] It provides a matrix on which cells can migrate and is important for maintenance of the stratified and well-organized structure of the corneal epithelium. It also appears to play a prominent role in epithelial wound healing, particularly fibronectin. Fibronectin is thought to provide a temporary matrix over which cells can migrate during the transition period between epithelial debridement and the formation of a new basement membrane, which can take more than a week, and although type IV collagen and laminin are essential for maintenance of the steady state of the corneal epithelium, fibronectin appears to play a more important role under conditions of acute injury to it.[98]

After damage to the corneal epithelium, actively migrating epithelial cells no longer manifest gap junctions or desmosomes in the wounded region lacking a basement membrane. Reestablishment of the continuity of the corneal epithelium is accompanied by the synthesis and deposition of basement membrane proteins and by the reassembly of the various types of junctional apparatus, suggesting that the presence of the basement membrane may be required for reformation of cell-cell junctions in the corneal epithelium.[99]

The epithelium functions as barrier to various external biological and chemical insults. This is achieved by a variety of junctional complexes between epithelial cells and the interdigitation of adjacent cell membranes, which, together, form an effective barrier against the influx of fluid and chemical molecules into the underlying stroma, thereby preventing corneal oedema and blurred vision. Superficial cells are bound together by tight junctions, which form the main component of the superficial epithelial barrier, whereas basal cells and wing cells have gap junctions that allow the passage of nutrients and different molecules between cells. Adherens junctions and desmosomes are present in all layers of the epithelium and help to maintain the structural integrity of the epithelium.[51]

The epithelium also acts as a barrier to microbial penetration into deeper layers of the cornea, mainly through the enzymes and cytokines of the tear film, the desquamation of surface epithelial cells, the tight junctions between adjacent epithelial cells, and the epithelial basement membrane, with its pores that are too small to allow bacterial penetration into the stroma.[100] Rapid renewal and the formation of intercellular junctions between corneal epithelial cells help to protect the cornea from microbial challenge. Both cell-cell and cell-matrix interactions are important for maintenance of the normal stratified structure and physiological functions of the corneal epithelium.[51] The characteristics of the different types of intercellular junctional complexes present between the corneal epithelium are summarized in Table 1.2 and in Figure 1.2.

Cellular components of the epithelium also play an important role in corneal immunology. Dendritic Langerhans cells, bone marrow derived specialized macrophages involved in antigen processing, are abundant at the periphery of the corneal epithelium but are not present in the central region of the normal cornea.[101-103] These cells express human lymphocyte antigen (HLA) class II molecules and are thought to function in the afferent arm of the ocular immune response by presenting antigens to T cells.[104] In addition, their numbers are increased in conditions characterized by ocular inflammation and are reduced by treatment with corticosteroids.[105] Injury to the central cornea results in the rapid migration of peripheral Langerhans cells to the damaged area.[106]

The tear film covered epithelium largely contributes to maintaining the smooth optical surface necessary for the sharp focusing of light onto the retina. Loss of the smooth contour of the epithelium, like in epithelial defects or irregularities or in dry eyes, leads to scattering of light, degradation of image quality and consequent blurring of vision.

Table 1.2 Characteristics of corneal epithelial cells

	Shape	Layers	Size	Junctional Complexes	Cytoplasmic Organelles
Superficial Cells	Flat	2-4	Diameter: 40-60 Thickness: 2-6 µm	Desmosomes Tight Junctions (zonula occludens)	Sparse
Wing Cells	Wing-like	2-3	Variable	Desmosomes Gap junctions	Sparse
Basal Cells	Columnar	1	Diameter: 8-10 µm Thickness: 18-20 µm	Desmosomes Gap junctions Hemidesmosomes (zonula adherens)	Prominent mitochondria and Golgi apparatus

(Reproduced with permission from Krachmer et al, Cornea. Mosby. 2005)

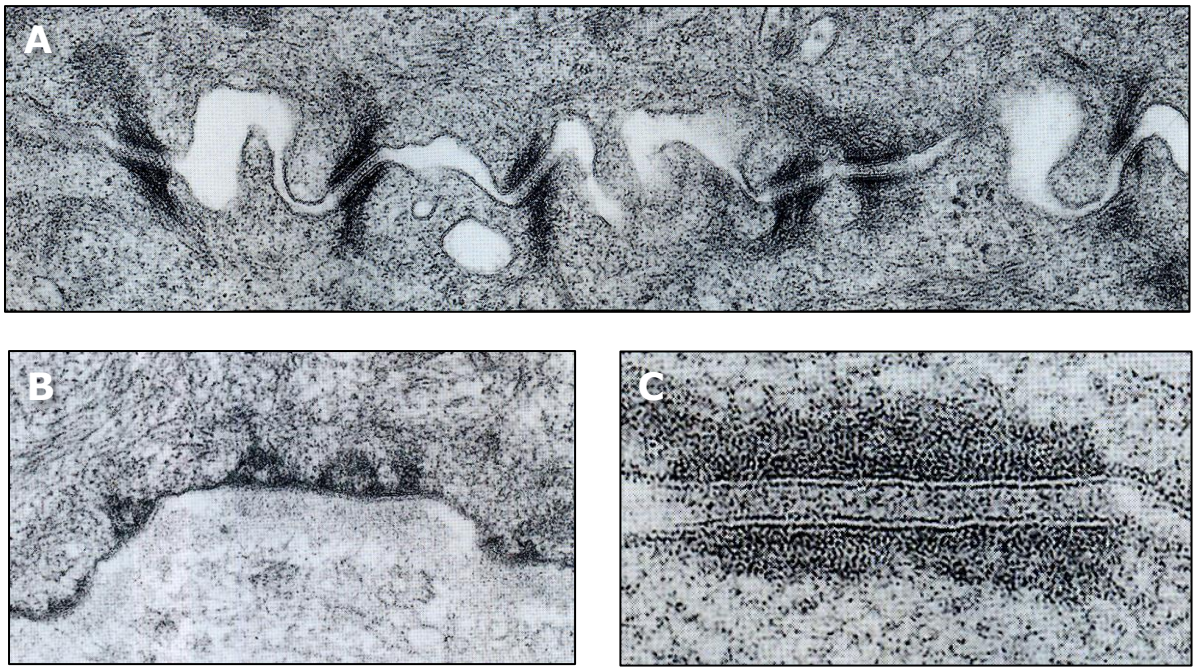

Figure 1.2 Types of intercellular junctional complexes in the corneal epithelium

A, Interdigitations and junctional complexes at lateral surfaces of epithelial cells. **B**, Hemidesmosomes at the basal surface of basal epithelial cells. **C**, Gap junctions between basal epithelial cells. (Reproduced with permission from Krachmer et al, Cornea. Mosby. 2005)

1.2.2.2 Bowman's layer

Lying directly posterior to the epithelial basement membrane is Bowman's layer, an acellular layer of relatively randomly arranged collagen fibres and proteoglycans that is 12 μm thick. The collagen fibres of this layer are primarily collagen types I and III and measure 20-30 nm in diameter, smaller than stromal collagen fibres.[107-109] It is considered to be the anterior portion of the corneal stroma, and its collagen fibres appear continuous with stromal collagen fibres and are synthesized by stromal fibroblasts.

The physiological role of Bowman's layer is unclear. Many of the functions originally attributed to it are now known to be mediated by the epithelial basement membrane. Bowman's layer does not regenerate after injury or Excimer laser surgery, and yet a normal epithelium is formed and maintained even in the absence of Bowman's layer. Furthermore, many mammals do not have a Bowman's layer but still exhibit a well-organized epithelial structure.[110]

1.2.2.3 The stroma

The corneal stroma constitutes more than 90% of the thickness of the cornea (Figure 1.1), and many of the properties of the cornea, such as transparency, shape stability and tensile strength are attributable to the anatomic and biochemical properties of the stroma. One of the most important functions of the stroma is maintenance of corneal transparency. This is achieved by the regular arrangement, uniform diameter and continuous slow production and degradation of its collagen fibres. In addition, the epithelial and endothelial cells play an important role in maintaining the biological activities of keratocytes and the arrangement of collagen fibres through their regulation of the water content of the stroma.[111]

The corneal stroma consists of extracellular matrix, stromal cells and nerve fibres. The cellular components only comprise 2-3% of the total volume of the stroma, with the remaining portion mostly comprised of extracellular matrix containing collagen and glycosaminoglycans. Collagen constitutes more than 70% of the dry weight of the cornea and is mostly type I, in addition to smaller amounts of types III, V and VI.[112-116]

Keratocytes are the predominant cellular components of the corneal stroma and are thought to turn over every 2-3 years. The spindle-shaped keratocytes are scattered between the lamellae of the stroma and extend long processes that are connected to neighbouring cells at their tips by gap junctions (Figure 1.3).[117] The detection of fluorescent dye transfer between neighbouring keratocytes suggests that the gap junctions in these cells are functional and serve to transmit intercellular signals.[118] Damage to the corneal stroma results in a loss of the network connections of

keratocytes near the site of injury; this leads to activation of keratocytes, which play an essential role in corneal stromal wound healing as well as in the pathogenesis of corneal ulceration.[119]

Keratocytes possess an extensive intracellular cytoskeleton, including prominent actin filaments, which allows them to contract, and may be responsible for the maintenance of corneal shape and the packed structure of collagen in the stroma. The shape and function of keratocytes are regulated by the extracellular environment. Keratocytes cultured in a collagen gel become less active mitotically, appear similar to keratocytes in situ and provide a model system for studying keratocyte biology.[120, 121] Keratocytes in the normal cornea are inactive but are rapidly activated to fibroblast and myofibroblasts phenotypes by various types of insult to the stroma. Activated fibroblasts at the site of a persistent epithelial defect may contribute to stromal dissolution by increasing their synthesis and secretion of collagen-degrading enzymes, like matrix metalloproteinases (MMPs), and by exhibiting phagocytic activity for foreign material.[119]

The collagen fibres in the stroma are highly uniform in diameter (22.5 to 35 nm), and the distances between collagen fibres are also highly uniform (41.4 ± 0.5 nm).[122, 123] This regular arrangement is of paramount importance in determining corneal transparency, and any disturbance in the uniformity of the inter-fibre distance, like what occurs during stromal oedema or scarring, can result in a loss of corneal transparency. In the corneal stroma, the collagen fibres form about 300 lamellae, each lamella courses parallel to the surface of the cornea from one limbus to the other, and then run along the limbal circumference. The turnover of collagen molecules in the cornea is slow, requiring 2-3 years.[124]

Various glycosaminoglycans are present between collagen fibres in the corneal stroma and they have the ability to absorb and retain large amounts of water. All of these glycosaminoglycans bind to core proteins to form proteoglycans, with the exception of hyaluronan (formerly known as hyaluronic acid). Keratan sulphate is the main glycosaminoglycan in the cornea, constituting about 65% of the total glycosaminoglycan content. Other glycosaminoglycans include chondroitin sulphate and dermatan sulphate.[125] The major glycosaminoglycan in the embryonic eye is hyaluronan, which is present during morphogenesis of the corneal stroma but its amount is reduced after the stroma has formed. The reduction of hyaluronan as the structure of the cornea is established during embryonic development is accompanied by an increase in the amounts of keratan sulphate, chondroitin sulphate, and dermatan sulphate, giving rise to the glycosaminoglycan composition of the adult stroma.[126]

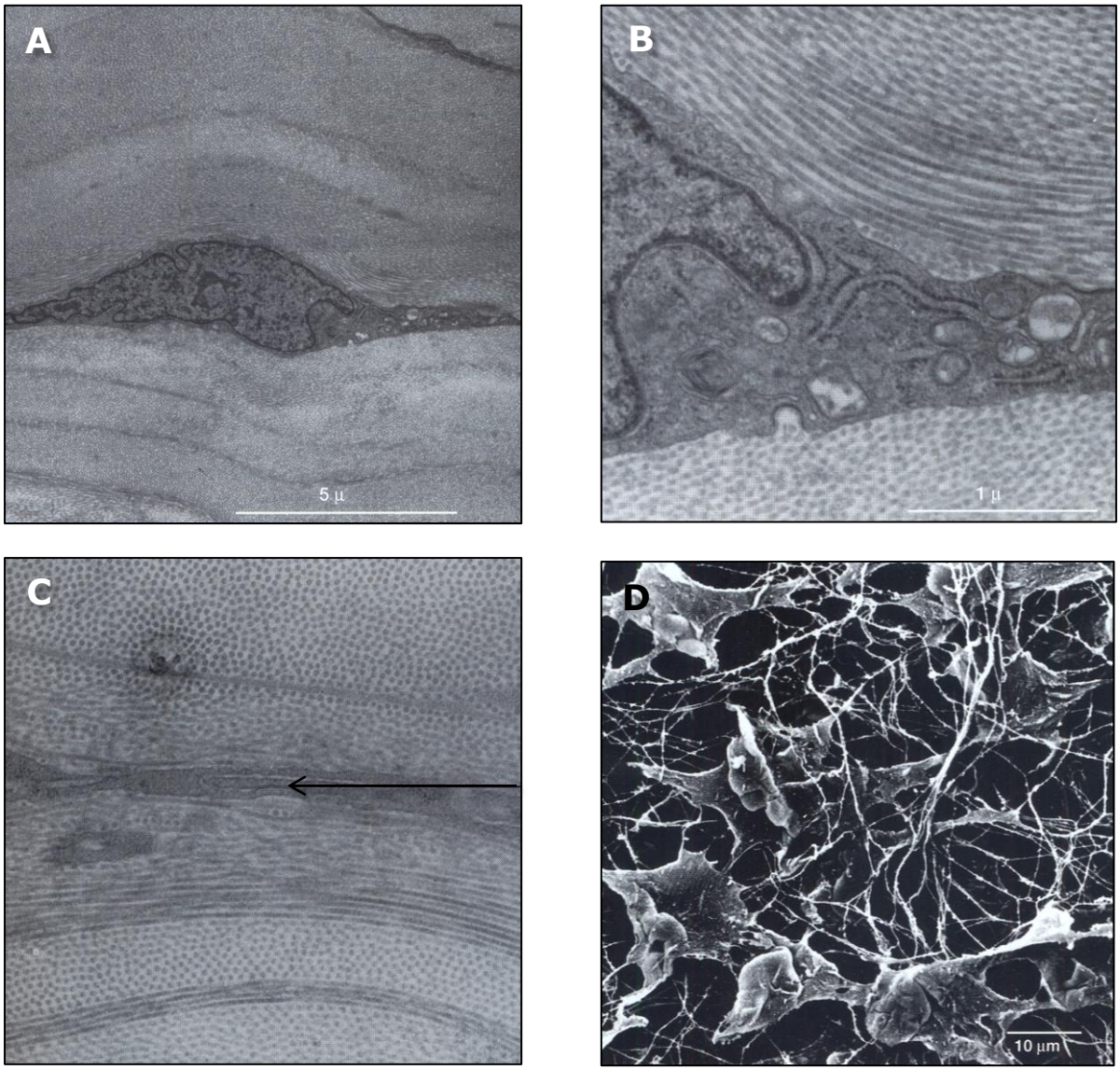

Figure 1.3 Transmission electron microscopy of the corneal stroma

A, Keratocyte lying between collagen fibres. **B**, Higher magnification view of A showing the orientation of collagen fibres in relation to the keratocyte. **C**, Gap junction between two adjacent keratocytes (arrow). **D**, Three-dimensional view of keratocytes in a rat cornea after digestion by collagen. (Reproduced with permission from Krachmer et al, Cornea. Mosby. 2005)

1.2.2.4 Descemet's membrane

Descemet's membrane comprises the basement membrane of the corneal endothelial cells, and measures about 8-10 µm thick. It is mostly composed of type IV collagen and lammin[127] but also contains fibronectin.[128, 129] Although its collagen fibres are not continuous with those of the stroma, unlike Bowman's layer, Descemet's membrane adheres tightly to the posterior surface of the corneal stroma and reflects any change in the shape of the stroma, and if the corneal stroma swells, the folding of Descemet's membrane can be observed clinically.

Descemet's membrane is tough and resistant to enzymatic degradation by MMPs, however, it can be torn easily on exposure to shearing stress. In cases of corneal ulceration, Descemet's membrane remains intact but protrudes outwards as a descemetocele as a result of the intraocular pressure and dissolution of the overlying stroma.[51]

1.2.2.5 The endothelium

The endothelial cells form a single layer posterior to Descemet's membrane in a characteristic well-arranged mosaic pattern. These cells have a uniform polygonal (mostly hexagonal) shape and a uniform size, with 5 µm in thickness and 20 µm in diameter.[130] An increase in the variability of cell area is termed polymegathism, whereas deviation from hexagonality of shape is referred to as pleomorphism. Both polymegathism and pleomorphism are important markers of endothelial damage, where normal endothelial cells fill the gaps left behind by lost cells. Although corneal endothelial cells proliferate in cell culture conditions, they do not proliferate *in vivo* in humans, suggesting that despite their ability to undergo mitosis, there may be factors in aqueous humor or other components in their surrounding environment may inhibit their proliferation.[131, 132] Endothelial cell density in the normal, healthy cornea decreases with age.[133]

Endothelial cells contain a large nucleus and abundant cytoplasmic organelles, including mitochondria, endoplasmic reticulum, free ribosomes, and Golgi apparatus, indicating that the cells are metabolically active and have secretory functions.[130] The anterior surface of endothelial cells is flat and directly adjacent to Descemet's membrane, whereas the posterior, free surface of the cells forms microvilli and marginal folds that protrude into the anterior chamber, thereby maximizing the surface area exposed to aqueous humor.[134] The endothelial cells interdigitate[135] and contain various junctional complexes, including zonula occludens, macula occludens, and macula adherens. They do not possess desmosomes, but do have gap junctions which allow the transfer of small molecules and electrolytes between the endothelial cells; this arrangement provides a leaky barrier to aqueous humour.[136] Loss or damage to corneal endothelial cells results in corneal oedema.

1.2.3 Maintenance of normal corneal integrity

The normal anatomical and biochemical structure of the extracellular matrix (ECM) of the corneal stroma is a prerequisite for a normally functioning cornea. Keratocytes maintain the stromal ECM by continually synthesising new collagen and glycosaminoglycans and degrading older, damaged components using ECM degrading enzymes, like MMPs, in a highly regulated process that is essential for the maintenance of corneal homeostasis.[137] On the other hand, although keratocytes grow relatively quickly in cell cultures, they seem to have a lower mitotic activity *in vivo,* indicating that their growth may be regulated by the surrounding collagen and ECM components.[121]

Collagen degradation by corneal keratocytes is regulated by various growth factors and cytokines. Under certain conditions of insult, such as injury, infections, and immunologic reactions, resident stromal keratocytes lose their quiescence and attain an activated phenotype, enter into the cell cycle and their cell size and organelle content increase. They begin to exhibit a fusiform shape, multiple nucleoli and a lack of cytoplasmic granules, and subsequently migrate to the site of injury.[137] A number of growth factors and cytokines contribute to the activation of keratocytes, including, for example, IL-1α, which is expressed by the corneal epithelium and released into the stroma upon injury, and has been identified as an important mediator for the expression of the collagenase gene in activated fibroblasts.[119]

1.3 The Pathogen: Biology of *Pseudomonas aeruginosa*

1.3.1 Background

Pseudomonas aeruginosa is a gram-negative, asporogenic, monoflagellated, rod-shaped bacterium that measures about 1-5 µm long and 0.5-1.0 µm wide. It belongs to phylum Proteobacteria, class Gamma proteobacteria, order Pseudomonadales, family pseudomonadaceae, genus pseudomonas, and species *Pseudomonas aueroginosa*. The word *Pseudomonas* means "false unit", from the Greek *pseudo* (Greek: false) and *monas* (Greek: a single unit). The stem word *mon* was used early in the history of microbiology to refer to germs, e.g., Kingdom Monera. The species name *aeruginosa* is a Latin word meaning "copper rust", which describes the blue-green bacterial pigment seen in laboratory cultures of the species.[138]

P. aeruginosa was first described as a distinct bacterial species at the end of the nineteenth century, after the development of sterile culture media by Pasteur. In 1882, a pharmacist named Carle Gessard published the first scientific study on P. aeruginosa, entitled “On the blue and green coloration of bandages”. This study showed *P. aeruginosa’s* characteristic water-soluble pigmentation which, on exposure to ultraviolet light, fluoresced blue-green light.[139] This was later attributed to the siderophores pyoverdin and pyocyanin (from "pyocyaneus" referring to "blue pus" characteristic of suppurative infections caused by *P. aeruginosa*), which also reflected the organism’s old names; *Bacillus pyocyaneus*, *Bakterium aeruginosa*, *Pseudomonas polycolor*, and *Pseudomonas pyocyaneus*.

P. aeruginosa is a very ubiquitous organism,[140] and it catabolizes a wide range of organic molecules, including organic compounds like benzoate,[141] among many other organic compounds for growth. On the other hand, organic growth factors are not essential for its growth, and it is even occasionally observed growing in distilled water,[142] which clearly indicates its minimal nutritional requirements. In the laboratory, the simplest medium for growth of *Pseudomonas aeruginosa* consists of acetate as a source of carbon and ammonium sulphate as a source of nitrogen. Its optimum temperature for growth is 37^{o}C, but it is able to grow at temperatures as high as 42^{o}C. [143] Its tolerance to a wide variety of physical conditions, including temperature, contributes to its ecological success as an opportunistic pathogen. It has a natural predilection to exist in soil and water, which is demonstrated in its predilection to grow in moist environments.[144]

Although the organism primarily utilizes aerobic respiration for energy production, it is also a facultative anaerobe, and, in the absence of oxygen, can utilize nitrate and other terminal electron acceptors for respiration.[145] Even in the absence of those, it is still able to ferment arginine

by substrate-level phosphorylation.[146] As a result, *P. aeruginosa* has been found in a wide range of different environments such as soil, water, humans, animals, plants, sewage, and hospitals. It is also capable of growth in diesel and jet fuel, where it is known as a hydrocarbon-using microorganism, causing microbial corrosion.[147, 148]

The typical *Pseudomonas* bacterium in nature might be found in a biofilm, attached to some surface or substrate, or in a planktonic form, as a single cell actively motile by means of polar flagella. It is commonly found in soil and water, and is a very important soil bacterium that is capable of breaking down polycyclic aromatic hydrocarbons and making rhamnolipids, quinolones, hydrogen cyanide, phenazines, and lectins.[149] It is a commensal of the human gut, and is the predominant inhabitant of oligotropic aquatic ecosystems, containing high-dissolved oxygen content but low plant nutrients throughout, making it the most abundant organism on earth.[140]

There are several strains of *Pseudomonas aeruginosa*; these include strain PAO1, strain PA7, strain PA14, and strain 2192. Most of these were isolated based on their distinctive grapelike odour of aminoacetophenone, pyocyanin production, and the colonies' structure on agar media.[150]

1.3.2 Culture Morphology and Cell structure

P. aeruginosa isolates may produce several colony types (Figure 1.6 A and B). Natural isolates from soil or water typically produce a small, rough colony. Clinical samples, in general, demonstrate two smooth colony types. One type has a fried-egg appearance, which is large, smooth, with flat edges and an elevated appearance. Another type, frequently obtained from respiratory and urinary tract secretions, has a mucoid appearance, possibly due to the production of alginate slime. The smooth and mucoid colonies are presumed to play a role in colonization and virulence.[151]

1.3.2.1. Cell surface and outer membrane:

P. aeruginosa is a Gram-negative microbe, with an outer membrane and a cell wall. Its outer membrane contains Protein F (OprF), which functions both as a structural protein, maintaining the bacterial cell shape, and as a porin, allowing certain molecules and ions to come into the cells. Protein F provides *P. aeruginosa* outer membrane with an exclusion limit of 500 Da, thus lowering the permeability of the outer membrane, which serves the organism well since this would decrease the intake of harmful substances into the cell and give *P. aeruginosa* a high resistance to antibiotics.[152]

Lipopolysaccharides belong to a group of polysaccharides that are present on the bacterial cell surface and serve as a barrier between the cell wall and the surrounding environment. They form structural components of biofilms, play an important role in maintaining outer membrane structural integrity and are important mediators for host-pathogen interactions and bacterial virulence. In *P. aeruginosa* infection during late stage cystic fibrosis, the exopolysaccharide alginate is responsible for the mucoid phenotype of the isolated offending strains.[153, 154]

1.3.2.1 Flagellum and Pili:

P. aeruginosa utilize pili and polar flagella for motility and for association to target cells. The flagellum is a sheathless long appendage extending from one pole of the bacterium that consists of various combinations of at least 10 heat labile antigens. These antigens, together with the heat stable somatic O-antigen, form the basis of serological classification of the organism.[155] In addition to using it for motility, *P. aeruginosa* uses its single polar flagellum to also display chemotaxis to sugars and other useful molecules in the surrounding environment. According to the size and the antigenicity of the flagellin subunit, *P. aeruginosa* strains are classified to have either A-type or B-type flagella. The flagellum is very important during the early stages of infection, as it can attach to and invade host tissues.[156]

The bacterial flagellum can be subdivided into three components (Figure 1.4). The first is the basal body, which anchors the flagellum to the cell membrane, provides the power for rotation, and secretes the other two components. The second component is the hook, which serves as a flexible universal joint changing the angle of flagellar rotation. The third is the helical filament, which is composed primarily of the protein flagellin. The junction between the hook and the basal body has the core rotor structure, or the switch complex, which consists of an axial rod, the FliF ring, and the C ring, which is composed of the conserved multi-domain proteins FliG, FliM, and FliN.[157] FliG lies close to the membrane and is involved in torque generation. FliM lies in the middle of the rotor and interacts with phosphorylated CheY (a signalling protein). FliN is located at the cytoplasmic end of the rotor and is essential for flagellar assembly and switching.[158] Bacterial locomotion is achieved by rotating the flagella, and forward propulsion is achieved by counter clockwise (CCW) rotation, whereas a change in direction is achieved by switching to clockwise CW) rotation. It appears that the binding of CheY-P to FliM (and possibly FliN) promotes a conformational change within the rotor to change its rotation sense from CCW to CW.[158]

Bacteria use flagella for locomotion and, equally, for association to inert surfaces or target cells. This would make one wonder; how do bacteria know when to 'swim-or-stick'? How does an individual bacterium recognize the proximity to a target surface and switch from swimming freely in its environment to sticking to a surface? How to switch from a motile to a sessile lifestyle? This can be explained by surface sensing, a sensory transduction mechanism that determines the phase of the switch and often involves the bacterial flagellum.[159] As such, flagella are not only important in propulsion and locomotion of bacteria, but also have a critical mechano-sensory role in the initial stages of bacterial association to target surfaces.[157] The swim-or-stick switch involves the inhibition of flagellar synthesis and rotation coupled with increased synthesis of the polymers and structures that are required for long-term attachment to a surface, such as pili.

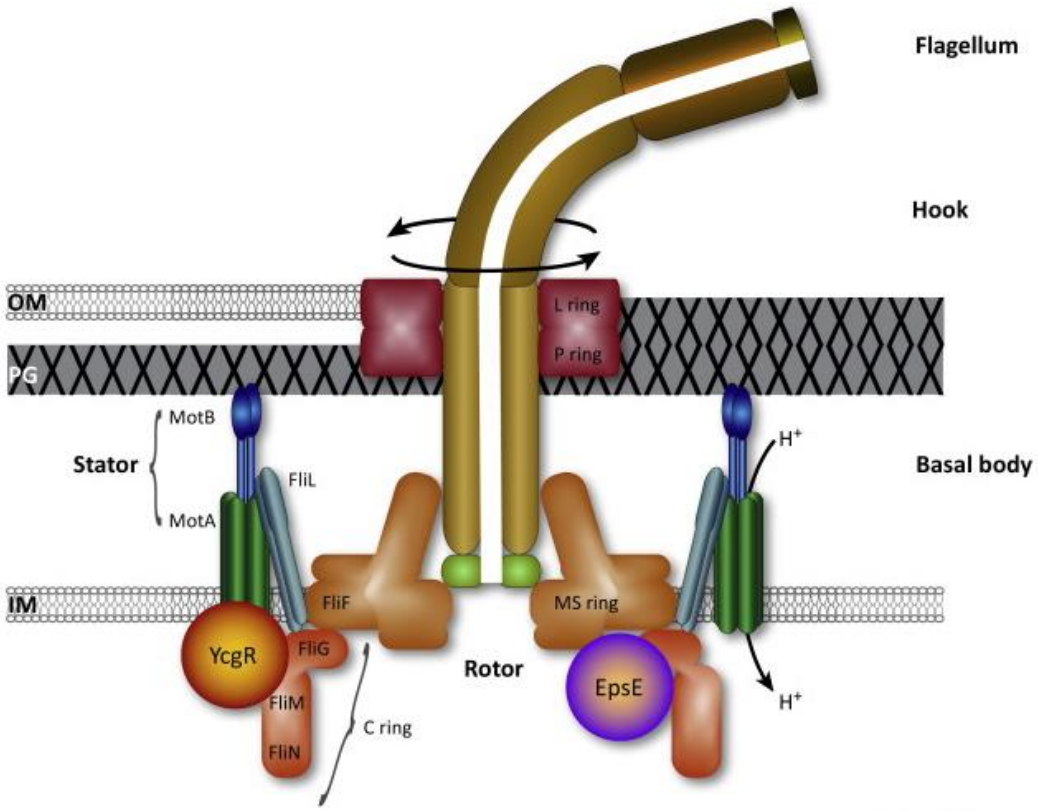

Figure 1.4 Structure of the flagellum

Shematic representation of the main components of the flagellum. The motor is composed of the stator (MotA and MotB proteins) and the rotor (C ring, composed of FliG, FliM, and FliN). Ion (H+ or Na+) flow through the MotAB channel provides the power to rotate the flagellum. The left side of the diagram represents a schematic of the Gram-negative structure with the YcgR brake. *IM, inner membrane; OM, outer membrane; PG, peptidoglycan*. *Modified with permission from Belas et al., 2014.*

Pili, or fimbriae, are another type of polar filaments that extend from the surface of the bacterium (Figure 1.6 D). Most clinical isolates of *P.aeruginosa* are palliated, and it has been suggested that it is the tips of the pili, which can be either N-methyl-phenyl-alanine (NMePhe) or type IV pili (TFP), that enhance the organism's association to host cells.[160] Pili are made up of homopolymers from the protein pilin, which is encoded by the pilA gene. In *Neisseria gonorrhoea*, which also has type IV pili, it has been shown that pili are markers of virulence and that they may have antiphagocytotic properties.[161] *P. aeruginosa* also uses its pili to achieve a special type of motility, termed twitching motility, in which the pilus is extended, attached to the target surface, then retracted, pulling the organism in the desired direction of travel.[162]

The structure of *P. aeruginosa* TFP has been proposed by Watts *et al*. and Folkhard *et al.* (Figure 1.5). Pilin, or PilA, protein subunits form a hollow cylindrical structure by means of a helical array arrangement. The outer diameter of this structure is about 5 nm and that of the central channel is about 1.2 nm.[163, 164] The *P. aeruginosa* TFP displays pilin subunits with tip-base differentiation and a structural domain of pilin which is only accessible at the tip of the pilus, and only this part is responsible for the adhesion function.[161] Functionally, the assembly of pilin subunit promotes the extension of TFP, and disassembly promotes retraction.[165] This process of assembly/disassembly is driven by the AAA-ATPases PilF (extension) and PilT1/PilT2 (retraction) (Figure 1.5). The outer membrane channel of the TFP machinery is formed by PilQ, whereas PilM, PilN, and PilO, are involved in pilus assembly and may couple the cytoplasmic and periplasmic sides of the pilus.[166]

Overall, *P. aeruginosa* flagellum and pili have similar functionality (for attachment) and structure (both are filamentous structures on the surface of the cell), and their motility is controlled by RpoN, especially during initial attachment to the human host and under low nutrient conditions.[167, 168] The main difference between them is that TFP bind to host N-glycans at the apical surfaces of polarized epithelial cells, whereas flagella bind to the heparan sulphate chains of heparan sulphate proteoglycans at the basolateral surfaces of the polarized epithelium.[96]

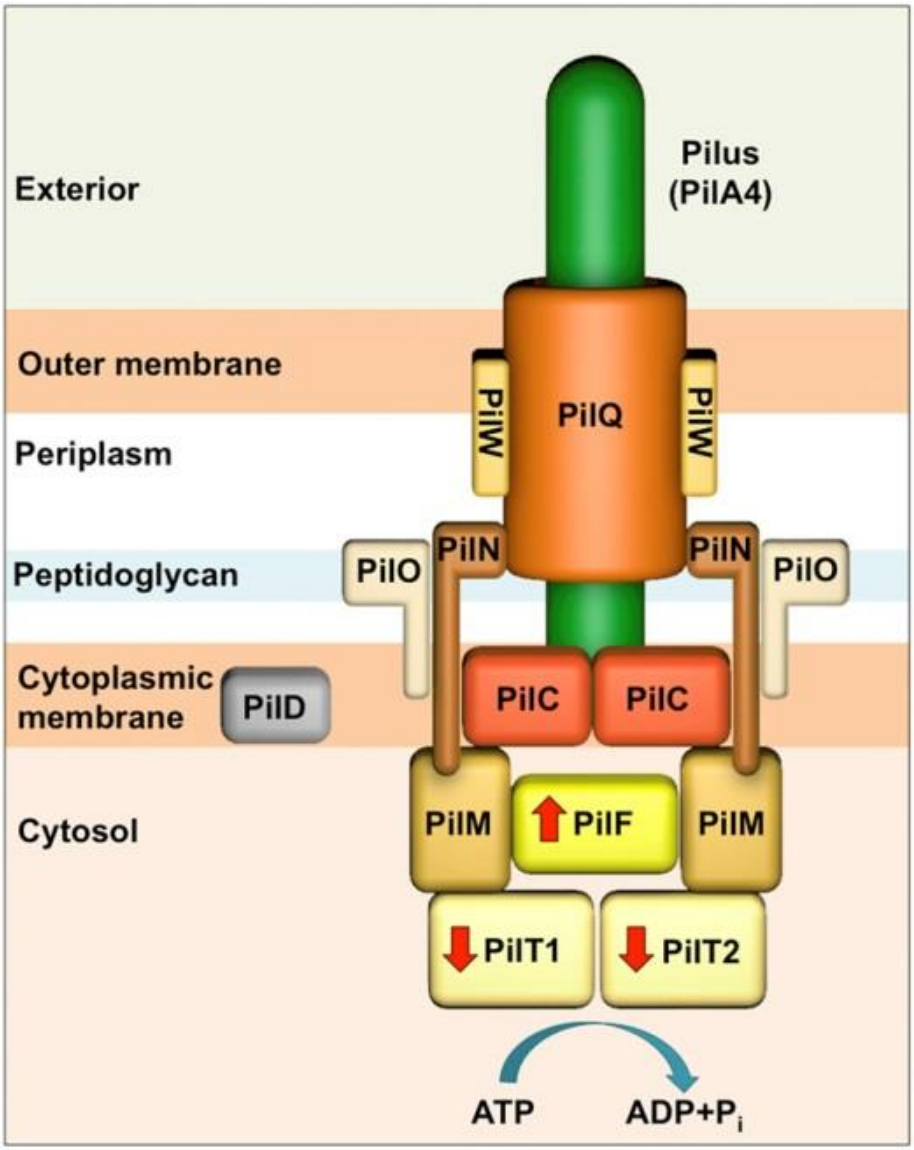

Figure 1.5 Structure of the type-4 pilus

Schematic representation of the TFP structure in *Thermus thermophiles,* which is representative of the pilus. The type IV pilus machinery is formed from at least 10 different proteins. The PilQ (orange) forms a channel in the outer membrane for secretion of PilA4 (green). PilW (light orange) is involved in DNA transport, PilQ assembly, and pilus extension. PilC (red) is located in the inner membrane and is essential for pilus formation. PilM (light brown), PilN (dark brown), and PilO (beige) possibly connect the periplasmic and cytoplasmic sides of the pilus. The cytoplasmic ATPases PilF (bright yellow) and PilT1/PilT2 (pale yellow) drive pilus extension and retraction (red arrows). *Modified with permission from Gold et al., 2015*

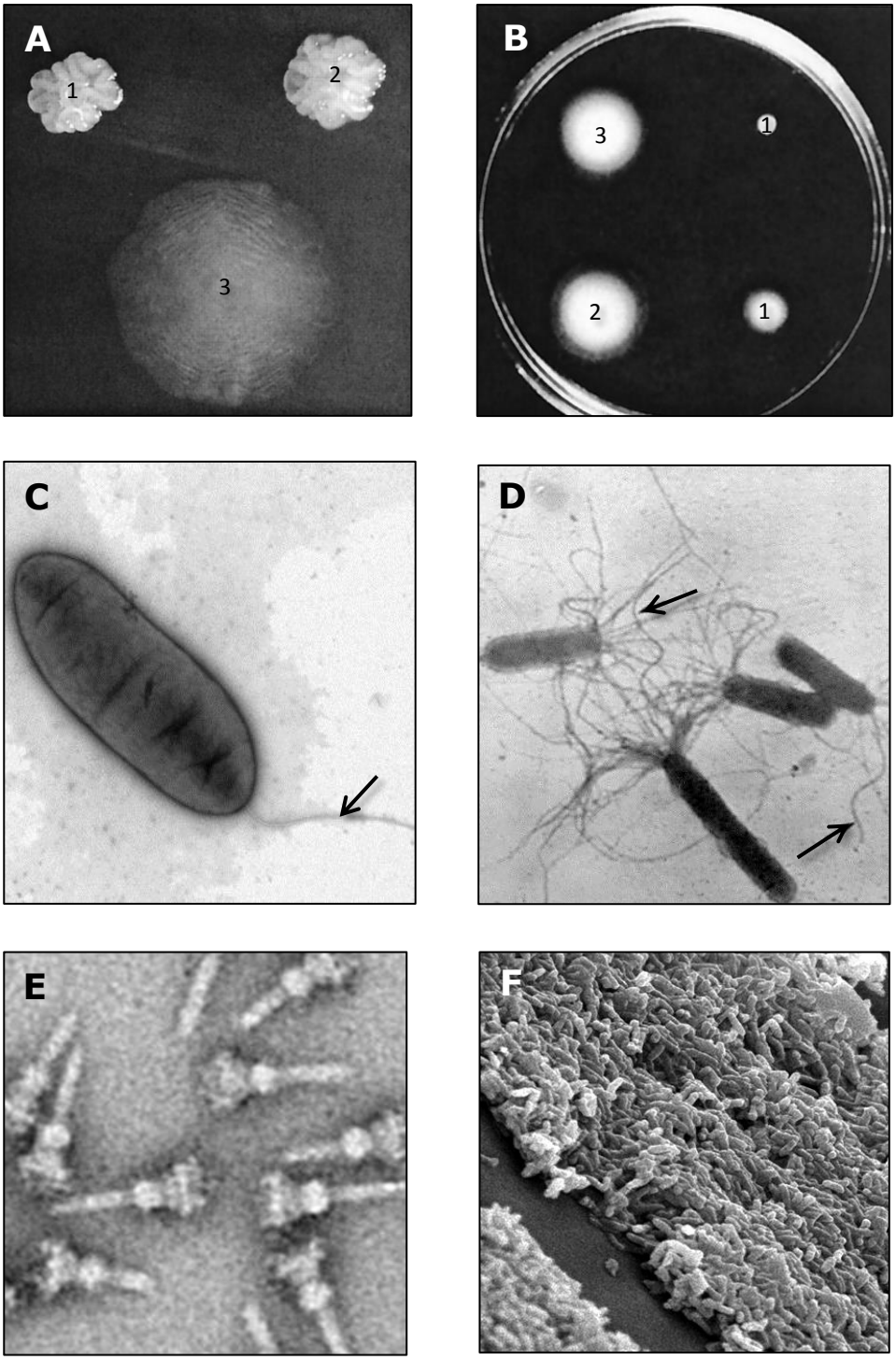

Figure 1.6 Structural characteristics and virulence factors of *P.aeruginosa*

A and **B**, Colony morphology of *P.aeruginosa* strain wspF (1), wspR (2) and PAO1 (3). **C**, pili and flagella (arrow). **D**, flagella (arrows). **E**, Needle complex of the type III secretion system (from *S. typhimurium*). **F**, *P.aeruginosa*biofilm. (Reproduced with permission from: D'Argenio DA, *et al*. J Bacteriol, 2002. 184(23): p. 6481-9.[**A,B**]; Carrion O, *et al*. Int J Syst Evol Microbiol, 2011. 61(Pt 10): p. 2401-5.[**C**]; Nunn D. Trends Cell Biol, 1999. 9(10): p. 402-8.[**D**]; Schraidt O, *et al*. PLoS Pathog. 2010 Apr 1;6(4):e1000824.[**E**]; Fu W, et al. Antimicrob Agents Chemother. 2010 Jan;54(1):397-404. [**F**])

1.3.2.2 Genomic structure:

P. aeruginosa has a unique genomic structure. It possesses a single and supercoiled circular chromosome in the cytoplasm in addition to numerous chromosome-mobilizing plasmids that are instrumental in its pathogenicity. Among these plasmids, the TEM, OXA, and PSE plasmids encode beta lactamase production, which is a key factor in its antibiotic resistance. The genome is relatively large containing 5.3-7.0 Mega base pairs, and the first complete genome sequencing was performed for strain PAO1,[169] derived from an Australian wound isolate from the 1950s. The PAO1 strain has been, and still is, the most common reference for genetic and functional studies on *P. aeruginosa*. The PAO1 genome consists of a circular chromosome containing 6,264,403 base pairs that encode for 5,570 predicted open reading frames and protein sequences, making it the largest bacterial genome to ever be sequenced, with almost the same genetic complexity as simple eukaryotes.[169]

The second *P. aeruginosa* genome sequence was published for strain PA14,[170] a clinical isolate displaying higher virulence than PAO1. In cystic fibrosis (CF) patients, strain LESB58 was found to be highly transmissible and can potentially also cause severe infections in non-CF human hosts.[170, 171] Strain PA7 is a clinical isolate from Argentina with an unusual antimicrobial multi-resistance pattern. It shares only 93.5% nucleotide identity in the core genome with the other sequenced strains, making it a taxonomic outlier within the species. Some of the numerous differences between PA7 and PAO1, including the complete absence of exoS, exoU, exoT and exoY of the type 3 secretion system, are probably the result of a frame shift mutation in the mvfR quorum sensing regulatory gene.[172]

1.3.3 Pathogenesis and Virulence

The pathogenesis of *Pseudomonas* infections is probably multifactorial, as suggested by the number and the diversity of virulence factors possessed by the bacterium, which is to be expected in the wide range of diseases caused by *Pseudomonas aeruginosa*. The virulence of *P. aeruginosa* can be attributed to several factors; Adhesins, in the form of fimbriae, flagella, glycocalyx and alginate may help in association of the bacterium to the epithelium. Invasins**,** such as elastase, alkaline protease, phospholipase, lecithinase, leukocidin and siderophores all help in deeper invasion and dissemination. Toxins, like Exotoxin A and Exoenzyme S cause tissue destruction and cell death, thus enhancing dissemination. The capsule, lipopolysaccharides and biofilm slime layer all help in evading phagocytosis and host immune responses.

1.3.3.1 Association and locomotion:

P. aeruginosa is an opportunistic pathogen that rarely affects healthy individuals or breach intact host defences. It usually requires a substantial breach in first-line defences and epithelial barriers in order to initiate infection. Such a breach can result from a bypass of normal cutaneous or mucosal barriers (e.g., trauma, surgery, serious burns, or indwelling devices), disruption of the protective balance of normal mucosal flora by broad-spectrum antibiotics, or alteration of the immunologic defence mechanisms.[173]

The first step in *P. aeruginosa* infections is colonization of the altered epithelium. Association is primarily mediated by TFP (Figure 1.6 C and Figure 1.5), but several other non-pilus adhesins that may also be responsible for the binding to mucin have been described; their role in the infection process, however, remains unclear. Flagella (Figure 1.6 C and D and Figure 1.4), which are primarily responsible for motility, also act as adhesins to epithelial cells.[156, 160]

1.3.3.2 Invasion and dissemination:

The ability of *P. aeruginosa* to invade tissues depends on its resistance to phagocytosis and host immune defences, and the extracellular enzymes and toxins it produces that break down physical barriers and contribute to bacterial invasion. The bacterial capsule and slime layer effectively protect the bacteria from opsonisation by antibodies, complement deposition, and phagocytosis.[174] Proteases, haemolysins, cytotoxins and siderophores produced by *P. aeruginosa* can cause extensive tissue damage, bloodstream invasion, and dissemination.

Several proteases that are released by *P. aeruginosa*, including alkaline protease, LasA elastase, LasB elastase, protease IV and *P. aeruginosa* small protease (PASP), play a major role during acute *P. aeruginosa* infection.[175-183] Alkaline protease is a 50.4-kDa zinc-dependent metalloprotease of *P. aeruginosa* that utilizes type I secretion for its release.[184, 185]] LasA elastase is a 20-kDa zinc metalloendopeptidase that is synthesized as a pre-proenzyme with a 22-kDa amino-terminal propeptide, but little is known about its maturation and secretion.[186, 187] It degrades elastin to render it sensitive to degradation by other proteases such as LasB elastase, alkaline protease, and neutrophil elastase. LasA protease action on proteins, including elastin, is limited and directed mainly to Gly3 and Gly2-Ala sequences that are uncommon in most proteins.[188]

LasB elastase is a type II secreted, zinc-dependent metalloprotease that is initially released as a 52-kDa precursor protein which undergoes auto catalytic cleavage to produce the 33-kDa mature protease and an 18-kDa propeptide.[177, 188, 189] Premature activation of the enzyme is prevented by the propeptide region, which remains non-covalently associated to the elastase until interrupted by

host-specific factors.[190, 191] LasB elastase acts on a number of proteins including elastin, fibrin and collagen. It also lyses fibronectin to expose receptors for bacterial attachment on the surface epithelium. Studies in animal models show that *P. aeruginosa* mutants defective in LasB elastase production are less virulent than their parent strains, which supports the role of LasB elastase as a virulence factor.[192] LasB elastase can inactivate substances such as human immunoglobulin G and A, airway lysozyme and complement components, suggesting that LasB elastase probably interferes with host defence mechanisms.[193] In microbial keratitis, elastase and alkaline protease act together to destroy the ground substance of the cornea and other supporting structures composed of fibrin and elastin, and to inactivate gamma Interferon and tumour necrosis factor.[194]

Cytotoxins, such as the pore-forming protein Leukocidin, are important virulence factor. Although originally named leukocidin because of its effect on neutrophils, it appears to be cytotoxic to most eukaryotic cells, including epithelial cells. This protein probably causes cytotoxicity by increasing cell membrane permeability, ultimately leading to cell death.[195]

Haemolysins, like Phospholipase C, rhamnolipid and lecithinase, appear to act synergistically to break down lipids and lecithin, thereby contributing to tissue invasion through their cytotoxic effect[196]. Rhamnolipid, a rhamnose-containing glycolipid biosurfactant, inhibits the mucociliary transport and ciliary function of human respiratory epithelium, and is believed to solubilize the phospholipids of lung surfactant, making them more accessible to cleavage by phospholipase C, by its detergent like structure.[196]

Siderophores are iron chelating agents that maintain adequate intracellular levels of iron by scavenging and importing it from the extracellular environment.[197-199] During infections, *P. aeruginosa* produces yellow-green, water-soluble compounds known as pyoverdins, which are considered to be essential virulence factors, since they strongly compete with host cells to obtain the iron essential for their metabolism.[200] Pyocyanin is a blue secondary metabolite produced by *P. aeruginosa* that impairs the normal function of human nasal cilia, disrupts the epithelium and exerts a proinflammatory effect on phagocytes.[201] Pyochelin, a derivative of pyocyanin, sequesters iron from the environment to support the growth of the pathogen.[202]

1.3.3.3 Type III secretion system:

P. aeruginosa uses complex, needle-like structures on its surface that function in a highly regulated manner to transport effector proteins into host cells (Figure 1.6 E). These complex processes are collectively known as the type III secretion system (TTSS), and they constitute an important component of the organism's virulence. Thirty-six genes that are clustered together in the *P. aeruginosa* chromosome are involved in the biogenesis and regulation of the type III secretion system and encode for its complex structure. It is composed of five parts; first, proteins constituting the needle complex that transports substrates from the bacterial cytosol to the extracellular environment; second, proteins that translocate secreted proteins into host cells; third, proteins that regulate the secretion process; fourth, chaperone proteins that facilitate secretion of their cognate partners; and finally, the so called effector proteins that are injected into the host cells.[203]

The needle complex is 60–120 nm long and 6–10 nm wide, and is responsible for the transport of proteins through the bacterial cytoplasmic membrane, the peptidoglycan layer and the outer membrane.[204-206] The needle-like filament, which comprises subunits of the protein PscF, is thought to be a passageway through which secreted factors move and may also serve as a sensor for host cell contact.[207, 208]

Translocation proteins are specialized proteins that, upon contact with target host cells, accumulate on the tip of the TTSS needle and induce the formation of pores on host cell membranes. This creates a continuation between the bacterial and the host cell cytoplasms, allowing the transfer of bacterial effector proteins into the host cell.[209] There are three types of translocator proteins, two TTSS loci-encoded membrane hydrophobic translocators and one hydrophilic partner. The hydrophilic translocator PcrV does not directly associate to host cell membranes; rather it provides a platform to enhance the membrane pore formation by the hydrophobic translocators. The major hydrophobic translocator PopB and the minor hydrophobic translocator PopD have been shown to lyse cholesterol rich host cell membranes when associated with their common chaperones PcrH.[210]

The process of effector protein delivery across the host cell membrane is so efficient that less than 0.1% of secreted effector proteins escape to the extracellular environment.[211] Host cell death can be caused either directly, through pore-mediated increases in membrane permeability;[212-215] or indirectly, through the activation of broad cellular defence responses.[216] *P. aeruginosa* type III secretion and translocation apparatus also triggers the inflammasome-mediated activation of caspase 1 through Nod-like receptor ice protease activating factor (IPAF; also known as NLRD4),[217-220] which results in the production of the interleukins IL-1β and IL-18 and in pyroptosis.[212, 218, 219]

Some effector proteins bind to chaperones before they are secreted, which facilitate their bacterial cytosol storage and the appropriate delivery to the secretion apparatus.[221] SpcS (previously known as orf1) serves as a chaperone for both exoS and exoT and is required for their maximal secretion,[222, 223] while SpcU is a chaperone for exoU.[224]

Four effector proteins of the *P. aeruginosa* TTSS have been identified: ExoS, ExoT, ExoU and ExoY. In isolates from acute infections, the exoS gene is found in 58–72% of isolates, the exoU gene in 28-42%, the exoY gene in 89% and the exoT gene in 92–100%. Nearly all strains have either the exoS or the exoU gene but not both. The secreted effector proteins define the behaviour of a particular strain during infection, so exoS-secreting strains cause delayed cell death with features of apoptosis, whereas exoU secretion induces rapid host cell lysis.[225, 226]

ExoS is a bifunctional toxin that has both GTPase activating protein (GAP) activity and ADP ribosyl transferase (ADPRT) activity. The GAP domain targets the small GTPases Rho, Rac and cell division cycle 42 (CDC42), which maintain the organization of the host cell actin cytoskeleton. These regulatory GTPases normally switch between an active, GTP-bound form and an inactive, GDP-bound form, but the ExoS GAP domain largely maintains these enzymes in the GDP-bound, inactive form, leading to the disruption of the host cell actin cytoskeleton.[227, 228] This leads to host cell rounding and decreased internalization of *P. aeruginosa*, suggesting that the GAP domain of ExoS may have a role in preventing phagocytosis.[229-231]

P. aeruginosa has a clever mechanism in place to prevent ExoS from turning against it. It requires the binding of a eukaryotic host cofactor to bind to the ADPRT domain for the activation of ADPRT activity but not for GAP activity.[232, 233] This requirement ensures that ExoS is not activated until after it is injected into the host cell and bound to the host cell cofactor. Following its injection and activation, the ADPRT activity of ExoS causes an irreversible actin cytoskeleton disruption and inhibition of DNA synthesis, vesicular trafficking and endocytosis and cell death. This possibly contributes to a reduction in cell–cell adherence, which can facilitate *P. aeruginosa* penetration through epithelial barriers into deeper layers.[234-237]

In *P. aeruginosa* infections, there is rapid killing of host immune cells. This could either be the result of the direct cytotoxic effect of ExoS on these cells, or it may be a host cells response to the presence of ExoS to try and eliminate intoxicated cells.[203] The cell death that is induced has features of both apoptosis and necrosis.[235, 238]

ExoT shares 76% amino acid identity with ExoS and is also a bifunctional toxin with N-terminal GAP activity and carboxy-terminal ADPRT activity. Similar to ExoS, ExoT GAP activity towards Rac, Rho

and CDC42 causes disruption of the actin cytoskeleton that manifests as cell rounding, cell detachment and inhibition of cell migration and phagocytosis.[230, 231, 239, 240] ExoT ADPRT domain also requires binding to a host cell cofactor for activation.[241] However, unlike ExoS, ExoT ADP ribosylates CRKI at Arg20, which interferes with CRK signalling, causing the disruption of signalling to RAC1 and the blockage of cell division at the cytokinesis stage.[242, 243]

The GAP and ADPRT activities of ExoT work together to alter the host actin cytoskeleton and to inhibit cell migration, adhesion and proliferation. This blocks phagocytosis, disrupts epithelial barriers, and thus facilitates bacterial dissemination.[230, 243] ExoT has also been linked to delays in wound healing,[244, 245] and causes apoptosis-like cell death through its ADPRT activity, possibly due to the inhibition of CRK signalling.[246] The contribution of ExoT to disease in mammalian models is modest when compared to that of ExoU and ExoS.[230, 243]

ExoU is a potent phospholipase that is capable of causing rapid cell death in eukaryotic cells. It has a chaperone, SpcU, and requires a eukaryotic host cofactor for activation.[247, 248] ExoU possesses a patatin-like domain that confers phospholipase A2 (PLA2) activity, which hydrolyses the ester bond of the acyl group of phospholipids, resulting in the release of free fatty acids and lysophospholipids. This results in host cell death, characterized by rapid loss of plasma membrane integrity, within one to two hours, which is consistent with necrosis.[249, 250] ExoU killing is directed against phagocytes and epithelial cells, thereby promoting bacterial persistence and dissemination.[243, 251]

ExoY is a secreted adenylyl cyclase that has two extracellular adenylyl cyclase (CyaA) domains which act together to bind ATP. It requires a host cell cofactor for full enzymatic activity[252]. Injection of ExoY into mammalian cells results in an elevation of intracellular cAMP concentration,[253, 254] which leads to the disruption of the actin cytoskeleton[253, 255], inhibition of bacterial uptake by host cells[256] and increased endothelial permeability.[252, 257-260] Such activities would be predicted to lead to more severe disease but this has not been uniformly observed,[214, 261] and the significance of ExoY in infection remains unclear.[203]

1.3.3.4 Quorum sensing:

Bacteria are able to sense their environment, process information, and react appropriately; but they can also sense their own cell density, communicate with each other, and behave as a population instead of individual cells. This phenomenon is called quorum sensing or cell-to-cell signalling and is a common phenomenon described in many bacteria. Both Gram-positive and Gram-negative species utilize various signal molecules to mediate cell-to-cell communication.[253, 254, 262]

Quorum sensing (QS) is a global regulatory system that controls the expression of numerous genes and phenotypes, and is governed by the secretion and detection of signal molecules. When these signals reach a threshold concentration, they bind to specific receptor proteins, which then initiate transcription of the QS-controlled genes. This enables the majority of the bacterial population to simultaneously express a specific phenotype.[255]

Quorum sensing controls the expression of somewhere between 3 and 10% of the genome of *P. aeruginosa*;[256, 263] many of these genes either directly mediate the pathogenicity of *P.aeruginosa*, or play significant roles in the persistence of the organism during infection, mainly by contributing to the formation of biofilms that are able to withstand the actions of the immune system. The primary QS system in *P.aeruginosa* is the Las system, which encodes the proteins LasI and LasR.[264] The LasI protein catalyses the production of the AHL molecule, whereas LasR controls virulence factor production, including LasB elastase, LasA elastase (staphylolysin), alkaline protease, exotoxin A and LasI itself.[265-268] Another important QS system in *P.aeruginosa* is the Pseudomonas quinolone signal (PQS), which plays an important role in controlling the production of pyocyanin and rhamnolipid virulence factors.[269] It is therefore clear that QS controls a significant proportion of the virulence factors used by *P.aeruginosa* to mediate infection.

In order for *P. aeruginosa* to overcome host defences, the bacteria need to secrete extracellular virulence factors at high levels, and this is only attainable when the bacterial population reaches a certain density. Quorum sensing allows *P. aeruginosa* to coordinate the expression of virulence factors across the entire bacterial population through the regulated expression of their virulence genes. It can stimulate a host immune response[270] or disrupt the epithelial barrier function.[271] In microbial keratitis, because the host immune response usually results in severe corneal damage, including perforation of the globe and blindness,[272, 273] and because an intact barrier function is essential to defend against *P. aeruginosa* infection,[274, 275] QS could represent a virulence factor in their own right.[255]

1.3.3.5 Biofilm formation

The exceptional ability to survive and thrive in a hostile environment by colonizing surfaces is widespread among bacteria and is due to the sessile mode of growth and the formation of biofilms (Figure 1.6 F). The biofilm mode of growth is an ancient strategy that is extremely resistant to many hostile chemicals in the environment, including disinfectants and antibiotics like aminoglycosides, beta lactams and fluoroquinolones. Biofilms also provide bacteria the ability to avoid or overcome the host innate and active immune defence mechanisms.[276]

Biofilms are hydrophilic, and water is the predominant constituent of the biofilm. They consist of bacterial microcolonies, constituting 10–20% of the volume of the biofilm, surrounded by exopolysaccharide alginate produced by the bacteria, penetrated by minute anastomosing water channels that form a primitive circulatory system.[277] One-micrometer latex particles can migrate through these channels by convection, whereas soluble materials are transported by molecular diffusion through the water-filled matrix of the biofilm. An oxygen gradient is present from top to bottom in biofilms so that the bacteria at the base of the biofilm are surrounded by an anaerobic milieu inside the biofilm matrix, whereas the water-filled channels contain dissolved oxygen.[276]

The thicknesses of biofilms are variable and uneven (13–60 μm), and the growth rate of bacteria in biofilms is reduced compared with that of planktonic bacteria.[278] Coordinated activity of single cells inside the biofilm can be detected, and is caused by quorum sensing between cells of a similar nature, as can be seen between eukaryotic cells.[279] Bacterial biofilms are therefore dynamic masses of bacteria, and the proportion between the sessile biofilm and the detached planktonic bacteria depends on unspecific and immunologically specific defence mechanisms in addition to the presence of antibiotics.[276]

1.3.3.6 Antibiotic Resistance

Pseudomonas aeruginosa is notorious for its resistance to antibiotics and disinfectants,[280] and the antibiotic resistance of *P.aeruginosa* strains isolated from cystic fibrosis (CF) patients is significantly higher than strains isolated from non-CF patients.[281] The organism is naturally resistant to many antibiotics due to several factors. Firstly, it is intrinsically resistant to antimicrobial agents due to a combination of restricted permeability of its outer membrane and the efficient removal of antibiotic molecules that do penetrate by the action of efflux pumps. Secondly, it has the genetic capacity to express a wide array of resistance mechanisms, including mutation in chromosomal genes that regulate resistance. Finally, It can acquire additional resistance genes from other organisms (such as bacilli, actinomycetes and moulds) via plasmids (both R-factors and RTFs), horizontal gene transfer (mainly transduction and conjugation), transposons, and bacteriophages.[281]

Pseudomonas aeruginosa tends to colonize surfaces in the anionic polysaccharide alginate biofilm form, and this makes the bacteria resistant to therapeutic concentrations of antibiotics. The high bacterial cell density and the physical exclusion of the antibiotic inside the biofilm matrix are also factors that aid in the resistance of biofilms to antibiotics. A general stress response within the biofilm leads to physiological changes in the bacterial cells, where protective mechanisms and induced key metabolic processes are shut down.[282] The overall resistance is dependent on the interaction between the entire population of cells within the biofilm. This population is heterogeneous, containing fast- and slow-growing cells, with different modes of antibiotic resistance. Some of these bacteria are resistant through expression of inactivating enzymes and efflux pumps, others through non-expression of these systems.[283]

1.3.4 Clinical Significance

Most pseudomonads are known to be pathogens of plants rather than animals, but three *Pseudomonas* species are regularly pathogenic to humans: *Pseudomonas mallei*, *Pseudomonas pseudomallei* and *Pseudomonas aeruginosa*. *Pseudomonas mallei*, also known as *Burkholderia mallei,* causes a disease in horses known as glanders. *Pseudomonas pseudomallei,* also known as *Burkholderia pseudomallei,* is the agent of melioidosis, a highly fatal tropical disease of humans and other mammals, and is also an opportunistic pathogen contracted through the contamination of wounds with mud or soil.[284]

Pseudomonas aeruginosa is an opportunistic human pathogen, and it rarely infects healthy individuals. It often colonizes immunocompromised patients, like those with cystic fibrosis, cancer, or AIDS. It complicates 90% of cystic fibrosis cases and affects up to two thirds of critically-ill hospitalized patients, usually causing more devastating disease. It is also one of the leading Gram negative nosocomial infections, leading to a 40-60% mortality rate. Within the hospital, *P. aeruginosa* has numerous reservoirs, including disinfectants, respiratory equipment, food, sinks, taps, toilets, showers and mops. Furthermore, it is constantly reintroduced into the hospital environment on fruits, plants, vegetables, as well by visitors and patients transferred from other facilities. Spread occurs from patient to patient on the hands of hospital personnel, by direct patient contact with contaminated reservoirs, and by the ingestion of contaminated foods and water. The organism, however, also colonizes the oropharynx of up to 6% and is recovered from the faeces of 3-24% of healthy individuals.[140, 285]

Table 1.3 Diseases caused by Pseudomonas aeruginosa

Disease	Role of *P.aeruginosa*
Bacteraemia and septicaemia	*Pseudomonas aeruginosa* causes bacteraemia primarily in immunocompromised patients. Predisposing conditions include hematologic malignancies, immunodeficiency relating to AIDS, neutropenia, diabetes mellitus, and severe burns. Most *Pseudomonas* bacteraemia is acquired in hospitals and nursing homes. *Pseudomonas* accounts for about 25% of all hospital acquired Gram-negative bacteraemias.[286] *P.aeruginosa* septicaemia is rare, but it can be associated with high morbidity and mortality, as a result of the marked toxaemia, antibiotic resistance and severity of underlying disease.[287]
Bone and joint infections	*Pseudomonas* infections of bones and joints result from direct inoculation of the bacteria or the haematogenous spread of the bacteria from other primary sites of infection. Blood-borne infections are most often seen in IV drug users and in conjunction with urinary tract or pelvic infections. *P. aeruginosa* has a particular predilection for fibro-cartilaginous joints of the axial skeleton. It is the most common pathogen isolated in osteochondritis after puncture wounds of the foot, and causes chronic contiguous osteomyelitis, usually through direct inoculation of the bone.[288, 289]
Central nervous system infections	*Pseudomonas aeruginosa* causes meningitis and brain abscesses. The organism can invade the CNS from a contiguous structure such as the inner ear or a paranasal sinus. It can be directly inoculated during head trauma, surgery or invasive diagnostic procedures, or it can spread from a distant site of infection such as the urinary tract.[290]
Ear infections including otitis externa	*Pseudomonas aeruginosa* is the predominant bacterial pathogen in otitis externa, including swimmer's ear. The bacterium is infrequently found in the normal ear, but often colonizes the external auditory canal in association with injury, maceration, inflammation, or simply wet and humid conditions.[291]
Endocarditis	*Pseudomonas aeruginosa* infects heart valves of IV drug users and prosthetic heart valves. The organism establishes itself on the endocardium by direct invasion from the blood stream.[292, 293]
Eye infections	*Pseudomonas aeruginosa* can cause devastating infections in the eye. It is one of the most common causes of bacterial keratitis and it is the most common cause of contact lens associated microbial keratitis. It is one of the causative agents of infective endophthalmitis and has also been isolated as one of the etiologic agents of neonatal ophthalmia.[285]
Gastrointestinal infections	*Pseudomonas aeruginosa* can affect any part of the gastrointestinal tract from the oropharynx to the rectum, primarily in immunocompromised individuals. The organism has been implicated in perirectal infections, paediatric diarrhoea, typical gastroenteritis, and necrotizing enterocolitis. The gastrointestinal tract is also an important portal of entry in *P. aeruginosa* septicaemia and bacteraemia.[294]
Respiratory infections	Respiratory infections caused by *Pseudomonas aeruginosa* largely occur in individuals with a compromised lower respiratory tract or a compromised immunity. Primary pneumonia occurs in patients with chronic lung disease and congestive heart failure, whereas bacteraemic pneumonia commonly occurs in neutropenic cancer patients undergoing chemotherapy. Lower respiratory tract colonization of cystic fibrosis patients by mucoid strains of *P. aeruginosa* is common and almost impossible to eradicate.[295-298]
Skin and soft tissue infections	*Pseudomonas aeruginosa* can cause a variety of skin infections, both localized and diffuse. Common predisposing factors include burns, trauma, dermatitis, high moisture conditions such as those found in the toe webs of athletes, hikers and combat troops, in the perineal region and under diapers of infants, and on the skin of whirlpool and hot tub users. Individuals with AIDS can be easily infected. *P. aeruginosa* has also been implicated in folliculitis and in some resistant forms of acne vulgaris.[299-302]
Urinary tract infections	*Pseudomonas aeruginosa* is the third leading cause of hospital-acquired UTIs, accounting for about 12% of all infections of this type[303]. Urinary tract infections caused by *P. aeruginosa* are usually hospital-acquired and can occur via ascending or descending routes, usually secondary to urinary tract catheterization, instrumentation or surgery.[304]

1.4 The Barrier: Innate corneal defences against infection

1.4.1 Background

The normal inflammatory processes that occur in response to injury or infection to re-establish the integrity of the affected tissue can also cause significant injury to host tissue. This is because they depend on degradation of the affected tissue, proliferation of fibroblasts and new blood vessels to replace damaged structures, and tissue remodelling to restore the strength of the affected site. In most body surface tissues, this damage and scarring are acceptable outcomes, as they do not interfere with the primary function of the tissue. In the cornea, however, repair can result in significant loss of function, refractive distortion and opacity, leading to significant reduction in visual function, despite the full restoration of structural integrity. As a result, the cornea has evolved several complex adaptations to limit and regulate inflammation. At the same time, it has also developed formidable defences to prevent infection, and, in the event of an infection, additional adaptations that initiate robust immune and inflammatory responses to preserve ocular integrity.

1.4.2 The ocular immune privilege

Several sites in the body normally require tight regulation of inflammatory and immune responses to prevent potentially damaging consequences of these responses to delicate anatomic structures. These sites include the eye, the brain and the pregnant uterus and are collectively termed immune-privileged sites.[305, 306] The ocular immune privilege entails unique anatomic, physiologic, and immunoregulatory properties of immune and parenchymal cells, functioning as an integrated unit to develop a mechanism that supresses the intense local immunogenic inflammation that would have otherwise developed in its absence.[306] The ocular immune privilege is provided by several physiological and regulatory phenomena, including the anterior chamber associated immune deviation (ACAID) and soluble and cell membrane-bound immuno-suppressive factors in the anterior segment (Table 1.4). Ocular resident cells, such Müller cells in the retina, directly inhibit immune cells by secreting soluble factors and by contact-dependent mechanisms. The iris and ciliary body pigment epithelial cells, and the retinal pigment epithelium (RPE) inhibit T cells and even induce them to become T regulatory cells.[307] In addition, the conjunctiva -associated lymphoid tissue (CALT) is important in the induction of tolerance to ubiquitous non-pathogenic antigens.[308] The cornea and the retina are devoid of lymphatics in the native state, although lymphangiogenesis is induced in the inflamed cornea,[309] and this also contributes to the dampened immune responses in the quiescent eye.

Table 1.4 Factors contributing to ocular immune privilege

Factor	Location	Immune privilege effect
Blood ocular barrier	Tight junctions of epithelial cells, iris, ciliary body, vascular endothelial cells	Exclusion of macromolecules and inflammatory cells
TGF-β2 VIP Muller cells Pigmented epithelial cells	Aqueous humor Aqueous humor Retina Retina and uveal tract	Inhibition of T-cell proliferation
TGF-β2 VIP α-MSH Pigment epithelium	Aqueous humor Aqueous humor Aqueous humor Retina and uveal tract	Inhibition of IFN-γ release by Th1 cells
TGF-β2 CGRP α-MSH	Aqueous humor Aqueous humor Aqueous humor	Inhibition of pro-inflammatory factor release by macrophages
TGF-β2 MIF Qa-2	Aqueous humor Aqueous humor Cell membranes	Inhibition of NK-cell activity
ACAID TGF-β2 CGRP α-MSH VIP	Anterior chamber, vitreous Aqueous humor Aqueous humor Aqueous humor Aqueous humor	Inhibition of DTH
FasL	Cornea, retina, iris, ciliary body	Deletion of infiltrating inflammatory cells
Membrane-bound complement regulatory proteins CD55 Crry Soluble complement-regulatory proteins CD55 CD59 CD46 <1.3 kDa inhibitor of C1q	 Cornea Corneal epithelium, stroma Ciliary body Aqueous humor Aqueous humor Aqueous humor Aqueous humor	Inhibition of complement cascade

(Reproduced with permission from: Niederkorn JY. Crit Rev Immunol. 2002;22(1):13-46.)

ACAID, anterior chamber associated immune deviation; CGRP, calcitonin gene-related peptide; Crry, cell surface regulator of complement; DTH, delayed type hypersensitivity; FasL, Fas ligand; MSH, melanocyte stimulating hormone; TGF-β, transforming growth factor β; VIP, vasoactive intestinal peptide.

1.4.2.1 The Anterior Chamber Associated Immune Deviation

The Anterior Chamber Associated Immune Deviation (ACAID) is an unusual systemic immune response, whereby following the introduction of a foreign antigen into the anterior chamber of the eye, a signal is produced that communicates with the immune system through the spleen.[306] This leads to a series of events with several important features: inhibition of systemic delayed-type hypersensitivity, inhibition of complement-fixing antibody responses, maintenance of a normal cytotoxic T-cell and humoral immune response, and transfer of ACAID to immunologically naive recipients through antigen-specific splenic suppressor CD4+ and CD8+ T-cells.[306]

There are three phases of ACAID.[306] The first is the ocular phase, which involves the generation of an antigen-specific signal that is generated in the eye and delivered to the systemic immune system. This signal is produced by the F4/80+ antigen-presenting cells (APC) in the anterior chamber, which are exposed to a variety of immunosuppressive agents (Table 1.4). This leads to a reduced capacity to Th1 inducing IL-12, an enhanced production of the Th2 cytokine IL-10, a reduced expression of CD40 co-stimulatory molecule and the autocrine production of transforming growth factor-beta (TGF-ß).[306] In the second thymic phase, F4/80+ APC migrate to the thymus where they generate NK1+, CD8+, CD4- efferent cells, which suppress the delayed-type hypersensitivity. Finally, in the third splenic phase, which spans at least 7 days in the spleen, the F4/80+ APC migrate to the spleen where they generate CD8+ regulatory suppressor cells.

Two cell populations are responsible for ACAID. The first are CD4+ cells that produce increased amounts of IL-10 and decreased amounts of IFN-γ. These Th1 type cells are called afferent suppressor cells and are required to generate a second population of CD8+ cells, called the efferent suppressor cells, which in turn inhibit the expression of delayed-type hypersensitivity responses. T-cells bearing the γδ T-cell receptor and B cells are also required for ACAID.[310]

In addition to ACAID, many other immunoregulatory phenomena contribute to the ocular immune privilege (Table 6.6). The blood-ocular barrier, located at the tight junctions between the cells of the ciliary epithelium, physically provides a barrier to cellular infiltration. In addition, soluble factors inhibit a variety of immunological processes, including T-cell proliferation, IFN-γ production by Th1 cells, proinflammatory factors secreted by macrophages, natural killer (NK) cell activity and delayed hypersensitivity responses.[311] There are also both bound and soluble complement regulatory proteins that inhibit the complement cascade[312].

1.4.3 Corneal barriers against infection

Despite the continuous exposure of the cornea to ubiquitous microorganisms that naturally inhabit its surroundings, invasive infection rarely happens. Even when intact mouse or rat corneas were inoculated by extremely large inocula of both invasive and cytotoxic strains of *P. aeruginosa,* the ocular surface was rapidly cleared from offending bacteria without pathology.[313] In contrast, corneal epithelial cells cultured in vivo, interestingly, are easily invaded and killed by most clinical and laboratory isolates of *P. aeruginosa.*[314, 315] This suggests that the healthy eye possesses certain defence mechanisms against infection that are absent from laboratory cell culture conditions. Since these mechanisms are always present, even when the cornea is healthy, they are likely different from the host immune responses that are activated when an infection dose occur.[173]

Firstly, the conjunctiva lies immediately adjacent to the cornea, and it is provided with a system that detects antigens and induces an immune response by the direct action of the lymphatic cells or the secretion of soluble antibodies termed the conjunctiva -associated lymphoid tissue (CALT).[308] This system of lymphoid tissue was mainly observed in the palpebral conjunctiva, occurring in the form of a diffuse lymphoid layer of lymphocytes and plasma cells in the lamina propria and organized follicular lymphoid accumulations composed of B lymphocytes apically covered by lymphoepithelium. Thus, this system contains all components necessary for a complete immune response, which can serve an important function in the early protection against corneal infections.

An important in vivo factor missing in culture conditions is tear fluid. Although many *P. aeruginosa* strains grow readily in undiluted tear fluid despite its antimicrobial components, such as lactoferrin and lysozyme,[316, 317] tear fluid can protect both cultured corneal epithelial cells *in vitro* and injured and healing mouse corneas *in vivo* from infection by invasive and cytotoxic strains of *P. aeruginosa.*[318, 319] The tear fluid physically contributes to the cleansing of the ocular surface through the mechanical action of blinking, but it is also thought to directly act on corneal epithelial cells to make them more resistant to invasion and cytotoxicity by *P. aeruginosa.*[313] In one study, human corneal epithelial cells pre-treated with human tears were more resistant to invasion and cell death caused by *P. aeruginosa*,[320] and demonstrated an upregulation of nuclear factor kB (NF-kB) and activating protein 1 (AP-1), along with the up- and downregulation of genes encoding for cytokines, transcription factors and junctional proteins.[320]

In another study, tear fluid increased the barrier function of corneal epithelial cells *in vitro,*[319] which can help the multi-layered corneal epithelium protect itself against microbial traversal. This protective function of tear fluid may replace the well-established roles believed to be played by commensal microbes in modulating ocular homeostasis and innate immune defence.[173] Although tear fluid does not directly affect bacterial viability, it contains several factors that can bind microbes and suppress bacterial virulence factors, like mucins, secretory immunoglobulin A, and surfactant protein D, and this can ultimately alter the interactions between *P. aeruginosa* and corneal epithelial cells.[321-323]

In many host systems where there is interaction between bacteria and epithelial cells, bacteria tend to avoid the apical surfaces of epithelial cells. This has been observed in the gastrointestinal system, for instance, where gut bacteria, despite their enormous numbers, keep a zone that is about 50 µm wide free of microbes above the epithelial cell surface, and this is thought to be due to mucins and other antimicrobial factors present on the cell surface.[324, 325] A similar phenomenon has also been shown by live cell imaging of the corneal epithelium, where *P. aeruginosa* bacteria avoided the apical surfaces of corneal epithelial cells, and maintained a safe distance from the surface although always remaining within range of them.[315] This may be due to the presence of an environment similar to that of the gut, where mucins and other novel antimicrobial compounds are expressed from the surface.[326, 327] The apical surfaces of corneal epithelium cells are covered by a dense glycocalyx that is formed of MUC1, MUC4, and MUC16 mucins, and these are thought to be important in preventing association of bacteria, such as *P. aeruginosa* and *S. aureus*, to corneal epithelial cells.[328, 329] Lysates of human corneal epithelial cells contain keratin-derived antimicrobial peptides (KDAMPs), which rapidly kill several clinical isolates of *P. aeruginosa*, *S. pyogenes* and *S. aureus*. In mutant mice deficient in cytokeratin 6A, from which KDAMPs are derived, the antimicrobial activity of the corneal epithelial cell lysates was reduced, and the corneal epithelium was significantly more susceptible to bacterial association *in vivo.*[326]

Another factor that is different *in vivo* from culture conditions is the three dimensional arrangement of epithelial cells in the epithelium as a tissue, with all the junctional complexes and interactions between cells in different layers. The intact corneal epithelium is a formidable barrier to infection, and most animal models designed to study corneal infections bypass the epithelium by design, either by scarifying the epithelium, or by bypassing it all together and directly injecting the pathogens into the stroma. The pathology that occurs during microbial keratitis requires bacterial entry into the stroma, which then leads to the activation of inflammatory and immune responses and their subsequent damaging sequelae.[330, 331]

The resistance of the intact corneal epithelium to bacterial traversal can be attributed to a multitude of factors. As a first line of defence, superficial epithelial cells desquamate to reduce the microbial load of the offending inoculum. When *P. aeruginosa* is inoculated onto a healthy rat cornea, most internalized bacteria are found in cells that are readily shed from the eye with rinsing.[314] This supports the theory that internalization followed by desquamation is a mechanism for clearing bacteria that manage to adhere to the surface. Tight junctions between superficial cells are another major contributing factor, but other factors are also likely to be important. In a study where tissue paper blotting of the corneal surface was used to disrupt superficial tight junctions,[332] *P. aeruginosa* could adhere to superficial cells, but could not penetrate beyond the epithelial surface, despite the loss of barrier function to fluorescein. Thus, the loss of tight junctions promoted bacterial association to superficial cells, but prevented adherent bacteria from penetrating, suggesting that the corneal epithelial defences to these two initial steps of infection are separable, and involve multiple different factors.

In corneas treated with the calcium chelator ethylene glycol tetra-acetic acid (EGTA), bacteria were able to penetrate the epithelium, even after tissue paper blotting. This could be attributable to disruption of other types of cell-to-cell junctions in the absence of calcium, since their integrity is generally calcium-dependent,[332] or to other defence mechanisms of the corneal epithelial surface, such as surfactant protein D, whose activity is also calcium dependant.[333] This is supported by the observation that *P. aeruginosa* could partially traverse the tissue paper–blotted corneal epithelium of SP-D knockout mice *in vivo.*[332]

Other factors may be involved in epithelial defence against *P. aeruginosa* traversal. For instance, the corneas of mice deficient in myeloid differentiation primary response protein 88 (MyD88) are susceptible to *P. aeruginosa* penetration without the need for tissue paper blotting or EGTA treatment.[334] MyD88 is an essential component of toll-like receptor (TLR) signalling and IL-1R signalling, and its activity leads to activation of cytokines and chemokines, secretion of antimicrobial peptides, and recruitment of phagocytic cells.[335-338] It is important in the regulation of expression of antimicrobial peptides, like human beta defensin 2 (hBD-2) and cathelicidin LL-37, both of which are expressed by corneal epithelial cells stimulated by TLR or IL-1R agonists, and this may also demonstrate its involvement in corneal epithelial defence against bacterial association and traversal.[338, 339] In fact, hBD-2 has already been shown to be important in protecting the corneal epithelium against *P. aeruginosa* colonization.[340]

If *P. aeruginosa* bacteria do manage to traverse the multi-layered corneal epithelium and all of its defences, the epithelial basement membrane (basal lamina), composed mostly of extracellular matrix proteins, like laminin and type IV collagen, prevents them from actually entering the corneal stroma. This is because the basal lamina acts as a physical filter, as its pores are smaller than the size of most bacteria.[341] This may explain why even when the corneal epithelium is made susceptible to bacterial association and traversal, using either EGTA or MyD88 knockout mice, this does not always lead to microbial keratitis.[332, 334] Basal lamina extracellular matrix proteins can also form a chemical barrier to bacterial passage.[100] In addition, they improve the barrier function of the epithelial cells growing on top of them, possibly through the effects on junctional integrity or mucin and antimicrobial peptide expression of the cells.[173]

1.5 The Challenge: Pathogenesis of microbial keratitis

1.5.1 Background

When the bacteria do reach the corneal stroma, they are able to start colonizing the tissue, and a corneal ulcer develops. An ulcer is defined as a local epithelial defect with excavation of tissue and infiltration by immune cells. Break down of the corneal epithelium is a prerequisite for development of stromal melting and tissue loss, and a healthy corneal epithelium prevents stromal degradation and is essential for stromal healing, as demonstrated by several studies.[342] Most corneal ulcers are associated with a marked inflammatory response which typically involves dense infiltration of neutrophils and other leukocytes, and physical blockade or depletion of neutrophils and other leukocytes in animal models prevents ulceration[343, 344].

The typical stromal necrosis and tissue loss seen in microbial keratitis are caused by enzymatic degradation of extracellular matrix by pathogen and host released proteases. These involve the interplay of several host and pathogen factors that initiate and develop the progress of the pathogenesis. Although the infection is not initiated until the epithelial defences are overcome or bypassed, the cornea has additional innate defences and immune mechanisms that help to fight the infection. These mechanisms alert the immune system and recruit immune cells to the area, which in turn combat the offending microbes by phagocytosis and secretion of lytic enzymes, and by secreting cytokines and chemokines to recruit more immune cells to help with clearing out the pathogens.

1.5.2 Pathogen recognition and innate immunity in the corneal epithelium

One of the initial steps in the inflammatory process in relation to microbes is activation of the Toll-like receptor (TLR) family of pathogen recognition molecules. The TLR family is a class of single membrane-spanning non-catalytic receptors that recognize structurally conserved molecules derived from microbes, namely pathogen associated molecular patterns (PAMPs), once they have breached physical barriers, such as the corneal epithelium, and activate immune cell responses. Thirteen TLRs have been identified in humans and mice, which respond to lipids, proteins or nucleic acids.

TLR4, the most complex member of this receptor family, recognizes lipopolysaccharide (LPS), but it must be associated with the co-stimulatory molecules LPS binding protein (LBP), CD14, and MD-2 to recognise it.[345, 346] MD-2 is a bifunctional, 25-kD protein that is essential for TLR4 signalling by coupling endotoxin recognition to TLR4 activation. LBP and CD14 combine to extract single endotoxin molecules from endotoxin aggregates or from bacterial outer membrane and form monomeric endotoxin:CD14 complexes.[347] LPS is then transferred from CD14 to MD-2, which,

together with the other accessory molecules, facilitate recognition of the endotoxin at very low concentrations.[348, 349]

In *P. aeruginosa,* LPS and flagellin are recognised by TLR4 and TLR5 receptors, respectively,[350] initiating a pathway that involves recruiting the adaptor molecule MyD88, which mediates signalling by all TLRs except TLR3, and also mediates signalling by interleukin (IL)-1R and IL-18R. MyD88 recruits IL-1 receptor-associated kinase 1 (IRAK1) and IRAK4, and leads to activation of transforming growth factor (TGF)-β-associated kinase 1 (TAK1), the mitogen-activated protein (MAP) kinases p38MAPK and JNK8.[335] These MAP kinases mediate the phosphorylation of transcription factors NFκB and AP-1, and the transcription of proinflammatory and chemotactic cytokines.[351-354] TLR3 and TLR4 lead to activation of the TRIF-dependent pathway, and this leads to the production of type I interferons associated with viral infection. Thus, TLR4 activates cells through two independent signalling pathways, leading to a diverse and amplified response.[335]

Activation of the TLR4 and TLR3 receptors leads to recruitment of the adaptor molecule TIR domain-containing adaptor inducing IFN-β (TRIF),[355] which signals to the NF-kB and JNK pathways through RIP1 and TRAF6. TRIF also activates TRAF3, which leads to phosphorylation of IRF3 through TBK1 and IKK, and stimulates the production of type I interferons.[354, 356] The presence of TLR4 in *P. aeruginosa* corneal infection has also been associated with the release of antimicrobial factors such as inducible nitric oxide synthase (iNOS) and hBD-2.[357]

In cell cultures, human corneal epithelial cells respond to TLR2, TLR3, and TLR5 ligands by producing antimicrobial peptides, such as β-defensins and cathelicidin,[327, 338, 358] but, interestingly, are unresponsive to LPS.[359, 360] This is because, although TLR4 is constitutively expressed on the surface of human corneal epithelial cells, it is the MD-2 that is not expressed, and thus LPS responsiveness is only demonstrated in the presence of either exogenous MD-2 or by transfection with an MD-2 expressing plasmid.[360-362] This is supported by the finding that incubation with IFN-γ , which activates the Jak2/STAT1 pathway and the binding of p-STAT1 to IFN Gamma Activating Sites (GAS) on the MD-2 promoter, results in MD-2 gene and surface expression, and LPS responsiveness.[363] As IFN-γ is produced by infiltrating natural killer cells during *P. aeruginosa* corneal infection,[363, 364] it is likely that MD-2 expression and LPS responsiveness by corneal epithelial cells, that further contributes to the inflammatory response during active bacterial infection by producing pro-inflammatory and chemotactic cytokines, is secondary to that of myeloid immune cells.[365]

1.5.3 Recruitment of immune cells into the cornea

Recruitment of adaptor molecules MyD88 toTLR4 and TLR5, and recruitment of TIRAP and TRIF to TLR4, all lead to NF-κB translocation to the nucleus, and expression of pro-inflammatory and chemotactic cytokines. These include CXCL1/KC, which recruits neutrophils from limbal capillaries to the corneal stroma, and IL-1α and IL-1β, which then activate the IL-1R1 /MyD88 pathway in macrophages and resident corneal epithelial cells and keratocytes.[350]

Interleukin-1β (IL-1β) is a proinflammatory cytokine produced by activated macrophages and monocytes. It is involved in the generation of systemic and local responses to infection, injury, and immunological challenges and is the primary cause of chronic and acute inflammation. It is also a key player in the febrile response.[366] IL-1β is produced as an inactive cytoplasmic precursor (proIL-1β, p35) that must be cleaved to generate the mature active form (p17). The IL-1β-converting enzyme, better known as caspase-1[367-369] is required for this cleavage. Caspase-1 is a member of a family of inflammatory caspases, including human caspase-4 and -5, and mouse caspase-11 and -12, that contains an N-terminal caspase recruitment domain (CARD).[370]

Production of the mature IL-1β is a two-step process. Initially, the transcription of the 31kDa pro-form is induced, followed by post-translational cleavage of the preform to the 17kDa mature form.[371, 372] The assembly of a multiprotein complex containing one or more Nod-like receptors (NLRs), called inflammasomes, activates Caspase-1. Normally expressed in macrophages, the NLRC4 inflammasome, also termed IPAF, is activated by flagellin or type III secretion proteins, leading to caspase-1 recruitment and IL-1β cleavage.[365] The 31kD pro-IL-1β can be cleaved at different sites to produce the 18kD mature form of IL-1β by either caspase-1 or elastase, resulting in different sized cleavage products.[373, 374] It is thought that, during the early stages of infection, IL-1β processing by neutrophils plays an important role, while inflammasome activity by macrophage, and possibly neutrophil, contribute at a later stage.[365]

The recruitment of neutrophils from limbal blood vessels to the site of infection in the corneal stroma, and the subsequent bacterial killing, is likely due to the effect of both IL-1α and IL-1β acting together. When recruited, neutrophils generate reactive oxygen species (ROS) utilizing NADPH oxidase.[375] This production of ROS and MMPs, including collagenases, disrupts the extracellular matrix and prevents microbial dissemination.[376] In the cornea, this disruption of the collagen matrix results in loss of corneal clarity and impaired vision.

The normal corneal stroma was always believed to be devoid of myeloid immune cells, but it is now known that this is not entirely accurate. It is generally acknowledged that a number of corneal stimuli, including, infection, trauma, and cauterization, result in the presence of MHC class II+ dendritic cells (DC) in the central cornea, and this was, until recently, presumed to be entirely a result of de novo infiltration of these cells into the cornea.[377, 378] Recent studies, however, demonstrate that the central stroma contains exclusively MHC class II^{-} $CD80^{-}$ $CD86^{-}$ dendritic cells. Furthermore, corneas stained for CD14, an "immature" cell-surface marker reported to be associated with lack of differentiation of DC, demonstrate a large number of CD14+ cells in the stroma. This indicates that although myeloid cells are present in the normal stroma, they are undifferentiated monocytic precursor cells distinct from DC and macrophage populations present elsewhere. Thus, in contrast to other organs, where terminally differentiated populations of resident DC and/or macrophages outnumber colonizing precursors, large numbers of DC within the cornea remain in an undifferentiated state, and these cells only mature to a DC or a macrophage phenotype in response to inciting corneal stimuli.[379] Since corneal fibroblasts are the principal cell type present in the stroma, they may well have a role in immune activation when exposed to pathogens, perhaps as a first line of defence against progressive corneal ulceration. This has been described in other systems, and fibroblasts are regarded by some as resident sentinel cells capable of synthesizing chemokines, that initiate wound healing and clearance of invading microorganisms, and condition the cellular and cytokine environment in areas of inflammation by an array of factors they express.[380] In addition, fibroblasts can be activated to control extracellular matrix synthesis and produce cytokines and chemokines,[381, 382] which is analogous to cells of the immune system, such as macrophages and B and T lymphocytes.

1.5.4 Proteases involved in the pathogenesis of corneal ulceration

The progressive tissue destruction and necrosis seen in infective corneal ulceration is caused by several enzymes liberated by offending bacteria, as well as enzymes released by local host epithelial and stromal cells and infiltrating immune cells.[383-389] This process is thought to be sequential, initiated by bacterial exoenzymes, like alkaline protease and elastase, but maintained and exacerbated by proteases released by resident corneal cells[390] and stimulated inflammatory cells.[272, 391, 392] Three types of proteases appear to be important in the pathogenesis of stromal necrosis: The plasmin system, the matrix metalloproteases (MMPs), and the cysteine proteinases and cathepsins released during phagocytosis.

Plasmin is a serine protease that is mainly used by body tissues to dissolve fibrin clots, although it can hydrolyse other substrates, like fibronectin. It normally exists as the proenzyme plasminogen in

blood, tears, cornea, and aqueous humor,[94, 393, 394] and is converted into active plasmin by tissue plasminogen activator (t-PA) and urokinase plasminogen activator (u-PA).[395, 396] Plasminogen activators are present in many tissues, including the cornea,[94, 394] and on bacterial surfaces, where they facilitate bacterial penetration and migration by activating plasmin and dissolving fibrin clots. In the cornea, plasmin plays an important role in normal wound healing, where it dissolves the fibrin clot that fills the gap at the injury site, and allows epithelial cells to migrate and heal the defect. [94, 394]. Plasminogen is constitutively expressed in the cornea, and becomes activated by t-PA in the event of injury. If the epithelial healing is not achieved, however, the continuous expression of t-PA leads to persistent activation of plasmin, which can exacerbate stromal degradation,[94] either by its direct proteolytic action, or indirectly through activation of collagenase and other matrix metalloproteinases.[397] Corneal injury also leads to elevated plasmin levels in tears, which may promote stromal necrosis even further.[398]

Matrix metalloproteinases (MMP) are proteases that depend on zinc as an essential coenzyme and are important in degradation of the extracellular matrix. There are at least 17 different MMPs (Table 1.5) and they can be categorized into five groups: gelatineases (MMP-2 and 9), collagenases (MMP-1, 8, 13 and 18), stromelysins (MMP-3, 10 and 11) membrane-type MMPs, and others.[399, 400] Matrix metalloproteinases act on a variety of extracellular matrix molecules including interstitial collagens and proteoglycans. MMPs are synthesized and secreted as inactive pro enzymes and are activated by cleavage of their N-terminus, through a series of complex cascades, in the extracellular space.[401, 402] The activation MMP procollagenase is triggered by several factors. Initially, the conversion of plasminogen to plasmin after the secretion of t-PA partially activates procollagenase. This is then potentiated by the activity of other MMPs produced by activated fibroblasts. Collagenase activation is also triggered by pathogen factors, like LPS, and host factors, like inflammatory cytokines, like IL-1, and growth factors, like epidermal growth factor (EGF), platelet aggregating factor (PAF), and platelet-derived growth factor (PDGF).[403, 404]

Because of their strong proteolytic activity, MMPs production, activation and degradation are tightly regulated. They are typically only released when tissue remodelling is required, and once that is achieved, non-specific and specific protease inhibitors control their activity. One example of nonspecific protease inhibitors is α-2 macroglobulin, typically found in blood and interstitial fluids. Of the specific MMP inhibitors, termed tissue inhibitors of metalloproteinases (TIMPs), at least four have been described.[405] These proteins are typically produced and secreted by resident tissue cells, although some of them are found in plasma and in interstitial fluids.

The cornea is capable of producing at least four MMPs; gelatinase A, gelatinase B, collagenase-1 and stromelysin-1, although only gelatinase A has been isolated in the quiescent human and rodent cornea.[406-408] Gelatinase A can degrade fibronectin, denatured collagens, and basement membrane.[409] It is primarily present in the stroma, and because there is minimal stromal remodelling in normal cornea, it normally exists in its proenzyme form, associated with its inhibitor TIMP-2.[410] In the event of injury, stromelysin, collagenase and gelatinase B are produced in the cornea.[78, 407, 411] Stromelysin, which can degrade proteoglycans, can be detected in the cornea within 24 hours.[412] Gelatinase B is maximally elevated early following injury, and it seems to be important for remodelling of damaged basement membrane, and its down-regulation is required for normal re-epithelialization. Collagenase levels increase 1 to 4 weeks after injury and persist for at least 7 to 9 months. This difference in timing of the expression of specific MMPs suggests that they have specific roles during the wound healing process.[413]

Matrix metalloproteinases are thought to have significant roles in most corneal pathologies, including infectious keratitis. *P. aeruginosa*, for instance, produce MMPs that are inhibited by the MMP inhibitor galardin,[414] and in *P. aeruginosa* keratitis, systemic administration of antibodies against MMP inhibitors significantly exacerbated the ulcers in mice.[415] Thus, MMPs produced by *P. aeruginosa*, and neutralization of host inhibitors of MMPs, increase the virulence of *P. aeruginosa*. The development of new specific inhibitors of MMPs may prove to be beneficial in the treatment of infectious and non-infectious corneal ulcers and persistent epithelial defects.

A final group of proteases are those released during phagocytosis. These proteinases, namely cysteine proteinases and cathepsins, act primarily within lysosomes, and some of them, along with their inhibitors, have been identified within corneal cells, like cathepsin V, which is highly expressed in corneal epithelium.[416-420] On the other hand, numerous acid hydrolases are produced by phagocytic neutrophils and monocytes. During their maturation within the bone, neutrophils produce a group of serine proteases, including leukocyte elastase and cathepsin G that are active against many extracellular components, and store them in cytoplasmic granules until released at target tissues.[421] Monocytes, on the other hand, are capable of producing specific proteases tailored to the conditions of the site of inflammation. Both neutrophils and monocytes produce MMPs, and monocytes produce collagenase-1, stromelysin, gelatinease A, gelatinease B, and matrilysin, in addition to the unique MMP metalloelastase. In monocytes, these enzymes are not stored, but are newly synthesized at the site of inflammation as dictated by the surrounding inflammatory milieu.[51] The role of lysosomal proteinases in ulcer formation in infectious keratitis is not fully understood. Although the presence of active cathepsin B, D, and L has been demonstrated

in normal mouse corneal epithelium, and although their activities increase significantly during murine *P. aeruginosa* microbial keratitis,[422] the specific contribution of these proteases in corneal stromal loss has yet to be elucidated.

Table 1.5 Classes and types of matrix metalloproteinases (MMPs)

MMP	Substrate
Collagenases	Native type I, II, III collagens
MMP-1	
MMP-8	
MMP-13	
MMP-18	
Gelatineases	Native type IV, V, VII collagens and
MMP-2 (Gelatinase A)	gelatines
MMP-9 (Gelatinase B)	
Stomelysins	Proteoglycans, fibronectin
MMP-3	
MMP-10	
MMP-11	Serine protease inhibitors
Matrilysins	Gelatines, fibronectin
MMP-7	Gelatines, fibronectin
MMP-12	Elastin
MMP-19	
MMP-20	
Membrane-type MMPs	
MMP-14	Activation of progelatinase A
MMP-15	
MMP-16	
MMP-17	

(Reproduced with permission from Krachmer et al, Cornea. Mosby. 2005)

1.6 Hypothesis and Objectives

1.6.1 Hypothesis

In microbial keratitis, corneal fibroblasts interact with *P.aeruginosa* bacteria and are involved in the early pathogen recognition and immune signalling that lead to recruitment of immune cells and the start of the immune cascades necessary for clearance of the offending pathogens.

1.6.2 Objectives

- To determine whether or not *P. aeruginosa* interact with human corneal fibroblasts.
- To examine the dynamics of host-pathogen interactions in microbial keratitis with respect to bacterial association and internalization to corneal fibroblasts.
- To determine the cytotoxic effects of *P. aeruginosa* on corneal fibroblasts.
- To assess the host cell response to infection with respect to matrix metalloproteinase and pro-inflammatory cytokine release by corneal fibroblast at different time points.
- To determine the role of the different bacterial virulence factors during host-pathogen interactions in human microbial keratitis.

We were aware of the different challenges of trying to design and implement this model, and we had to utilise and optimise cross-disciplinary experience of immunology, microbiology and clinical ophthalmology in order to examine such a complex pathology.

Chapter 2 : **MATERIALS and METHODS**

2.1 General preparation of bacteria and host tissue

2.1.1 Bacteria

Pseudomonas aeruginosa wild type invasive strain PAO1 Holloway1C Stanier131 was obtained from NCIMB (Aberdeen, UK). Mutant *P. aeruginosa* strain PA14*ΔpopB* deficient in the PopB gene necessary for type III secretion system (TTSS), mutant strain PA14*ΔflgK* deficient in the FlgK gene necessary for normal flagellin and the parent wild type *P. aeruginosa* strain PA14 (PA14*WT*) were provided by Professor George O'Toole, University of Dartmouth, USA. Mutant green fluorescent protein (GFP) expressing *P. aeruginosa* PAO1 strain FliM tn7-GFP deficient in FliM gene necessary for normal flagella, mutant strain PilA tn7-GFP deficient in the PilA gene necessary for normal type IV pilus, mutant strain FliM PilA tn7-GFP deficient in both FliM and PilA gene and their parent strain PA tn7-GFP were acquired from Professor Tim Tolker-Nielssen, University of Copenhagen, Denmark

Strain	**Source**
PAO1 Holloway1C Stanier131	NCIMB, Aberdeen, UK
PA14*WT*	Professor George O'Toole, University of Dartmouth, USA
PA14*ΔflgK*	
PA14*ΔpopB*	
PA tn7-GFP	Professor Tim Tolker-Nielssen, University of Copenhagen, Denmark
FliM tn7-GFP	
PilA tn7-GFP	
FliM PilA tn7-GFP	

A master stock was made by adding a loopful of bacteria to sterile PBS to make a suspension, and this was stored in a liquid nitrogen tank. On the night before each experiment, PAO1 (Holloway1C Stanier131) and PA14 (WT, Δpopb and ΔflgK*)* were inoculated on nutrient agar (Oxoid, Basingstoke, UK) plates and grown over night, whereas PAO1 tnf-GFP (WT, FliM, PilA and FliM PilA) were grown on Luria-Bertani agar containing 60 µg/mL gentamicin (Appendix 7.1.1). Subsequent stocks were made and stored in a -80 C freezer using the Microbank system (Pro-Lab Diagnostics, Merseyside, UK). Inocula were prepared by suspending bacteria in corneal fibroblast infection medium (CFIM; Appendix 7.2.2).

2.1.2 Cell culture model

2.1.2.1 Isolation and culture of primary human keratocyte-derived corneal fibroblasts

Donor corneo-scleral rims remaining after corneal transplant procedures were obtained after the appropriate consent was taken from the donor. Five millilitres of corneal fibroblast culture medium (CFCM; Appendix 7.2.1) were placed into 30 ml universal container and 250 µl of 1 mg/ml collagenase solution in PBS was added to them. Under sterile conditions, the epithelium was scraped off the donor sample using a No. 15 scalpel blade and the donor rim was divided into 4 equal sections. For each section, the transparent corneal tissue was cut out, placed into universal container containing CFCM and collagenase and incubated with gentle shaking for 3h at 37^{o}C, after which the suspension was centrifuged at 1000 rpm (72 G) for 1 min. Under sterile conditions, the supernatant was carefully removed and discarded and the pellet was suspended in 7 ml of corneal culture medium and centrifuged at 2000 rpm (286 G) for 2 min. After repeating this process two more times, the pellet was suspended in 7 ml corneal culture medium, and the cell suspension was placed into 25 ml tissue culture flask. The flask was then incubated for 24 h at 37^{o}C, 5% (v/v) CO_2, checking cells for adherence and removing dead cells and replacing the culture medium under sterile conditions. The cells were incubated until the cells were >90% confluent, replacing culture medium every 3 days.

2.1.2.2 Expansion of corneal fibroblasts:

Once the cells were confluent, the medium was removed from the flask and 10 ml of sterile PBS was added to the flask, gently rocking, until the cells were thoroughly rinsed, after which the PBS was removed and replaced with 5 ml of Trypsin/EDTA solution (Sigma-Aldrich, Dorset, UK). The flask was incubated at 37^{o}C for 5 minutes, and then observed under a dissecting microscope until the complete dissociation of cells. Next, 7 ml of corneal culture medium were added to make a cell suspension, and the solution was centrifuged at 1000 rpm (72 G) for 4 minutes. The supernatant was discarded and the pellet was suspended in 9 ml of fresh medium. In a new flask, 3 ml of cell suspension were added to 7 ml of fresh culture medium and the flask was incubated for 24 h, after which adherence was checked under a dissecting microscope. Cells passaged between 3 and 6 times (P3-P6) were used in order to limit differentiation, as we noticed in our pilot experiments that cells at P7 or higher may be morphologically different. All cell culture preparation was done in a Class II safety cabinet.

2.1.2.3 Polymerase chain reaction (PCR) for detection of *Mycoplasma*

Corneal fibroblast cell cultures were tested for *Mycoplasma* contamination. Samples were prepared by taking 1 ml of culture medium from a confluent cell culture and centrifuging at 500g for 5 min. The supernatant was transferred to a fresh 1.5 ml Eppendorf tube and centrifuged at 15000g for 15 min, then the supernatant was decanted and the pellet suspended in 100 µl of fresh culture medium. For PCR setup, the PCR *Mycoplasma* test kit I/C (PromoCell, Heidelberg, Germany) was used. In each experiment, the kit negative and positive controls were included. For the sample mix, 2 µl of suspended pellet samples, 22 µl of rehydration buffer and 1 µl of DNA polymerase were added to dehydrated PCR tubes. A PCR programme was established according to the manufacturer's recommended settings (first cycle: 94^{o}C for 2 min; then 38 cycles: 94^{o}C for 30 s, 55^{o}C for 30 s, 72^{o}C for 40 s, then final cooling to 4-8^{o}C) and the reaction was run on a T3 thermal cycler (Biometra, Goettingen, Germany). After PCR, 10 µl of each control was run on a 2% (w/v) agarose gel (Appendix7.4.1) using a 5 mm combo, with electrophoresis at 100V for 40 min. The internal control band (479 base pairs) and the positive reaction band (265-278 base pairs) were visualised using a 2UV Transilluminator (BioDoc-It Systems, Upland, USA).

2.1.3 Whole tissue model

Donor corneal buttons left over from Descemet's stripping endothelial keratoplasty (DSEK) were collected after appropriate ethical approvals were obtained. Donor information from the eye bank was checked to ensure that they agreed for their donated corneas to be utilized for research purposes as well as transplant procedures. The buttons were transferred from eye theatres to our laboratories in the storage medium provided by the eye bank and stored at 4^{o}C until used in the infection experiments, within 72h of collection. The average age of donors was 78.8 years (range 65-88) with causes of death excluding those that would potentially affect our infection experiments (e.g. septicaemia).

2.2 Challenge of human corneal tissue with bacteria

2.2.1 Preparation of bacteria

An ampoule containing *P.aueruginosa* bacteria was transferred from the Microbank system to a Class II safety cabinet. Without allowing contents to thaw, a sterile plastic loop was used to capture one of the bacteria-laden pellets and transfer it to an agar plate, where the pellet was gently moved across the surface of the agar to spread the inoculum, after which the plate was incubated overnight in an incubator at 37^{o}C, 5% (v/v) CO_2. On the following day, a bacterial suspension was prepared by suspending bacteria, picked from the agar plate using a sterile loop, in 1-2 ml of sterile PBS. In order to prepare suspensions with known concentrations of bacteria, the optical density (OD) of an initial bacterial suspension was measured in 1% (w/v) SDS/0.1% (w/v) NaOH solution at a wavelength λ260 nm using a Hitachi U-1100 spectrophotometer (Hitachi, Tokyo, Japan) in UV transparent cuvettes (Starstedt, Nümbrecht, Germany). The optical density of the suspension was used to calculate the number of bacteria in the suspension and 10 fold serial dilutions were made by adding 100 µl of bacterial suspension to 900 µl sterile PBS, until the desired infecting doses were reached. Viable counting was performed by spreading 25 µl of the final bacterial suspension on the surface of the agar (adjusting for the total volume in the final calculation of bacterial counts), and was used to confirm the number of bacteria in the suspensions.

2.2.2 Infection of corneal donor buttons

In most cases, we used two donor buttons for our experiments. On the day of the experiment, the buttons were washed 4 times in warm sterile PBS, and one button was scarified by a 27 gauge needle to produce 4-5 linear epithelial scores that were deep enough to bypass the epithelium and score the underlying stroma. The buttons were then both bisected to yield 4 halves, and these were placed in a 24-well cell culture plate.

Bacterial suspensions were prepared to an infective dose of 10^7 CFU/mL (as above), and 1 mL was added to each tissue-containing well. The plates were incubated in an atmosphere of 5% (v/v) CO_2 at 37^{o}C for 3 or 9h. At these time points, the buttons were washed 4 times in warm sterile PBS and transferred to a container containing a fixative solution [3% (v/v) glutaraldehyde and 4% (v/v) formaldehyde in 0.1 M PIPES (1,4-Piperazinediethanesulfonic acid) buffer pH 7.2], fixed for a minimum of 1 hour, then processed for scanning or transmission electron microscopy, according to experiment. (See section2.3.2 for the methodology of electron microscopy).

2.2.3 Infection of corneal fibroblasts

Corneal fibroblasts were cultured to confluence in 24-well cell culture plates (Greiner Bio-One, Solingen, Germany). Cell quantification was carried out using the improved Neubauer cell counting chamber and trypan blue stain. The average cell count in a 24-well plate was 9.7 x 10^5/well (n=4 measurements). Before bacterial challenge, the CFCM in the wells was removed and the cell monolayers were gently rinsed 4 times in warm sterile phosphate buffered saline (PBS; Sigma-Aldrich, Dorset, UK) to remove any residual antibiotics.

Confluent corneal fibroblast monolayers were challenged in triplicate wells with bacterial suspension prepared by adding the bacteria to CFIM in 1ml volumes/well. Bacterial association was assessed at 3, 6, 9 and 24 hours. The concentration range of bacteria initially used was from low (10^1 and 10^2 CFU/mL) to intermediate (10^4 and 10^6 CFU/mL) to high (10^8 CFU/mL) and the corresponding multiplicity of infection (MOI) is shown in Table 2.1. Preliminary infection experiments demonstrated that high bacterial concentrations (>10^6 CFU/mL) led to an almost total destruction of the monolayers. Consequently, only bacterial concentrations of 10^1, 10^2, 10^3 and 10^4 were used.

Table 2.1 Bacterial inocula and corresponding multiplicity of infection (MOI)

Bacterial inoculum (CFU/mL)	**Multiplicity of infection** (bacteria/cell)
10^1	0.0001
10^2	0.001
10^3	0.01
10^4	0.1
10^5	1
10^6	10
10^7	100
10^8	1000

2.3 Measurement of total bacterial association

2.3.1 Viable counting assays

Corneal fibroblast monolayers were incubated for up to 24h and at each time point examined, the plate was transferred to the cabinet, the infection medium was removed and the cells were gently rinsed 4 times with warm sterile PBS to remove all non-associated bacteria. For the 9h and 24h time points, the infection medium was transferred to 1.5 ml Eppendorf tubes, centrifuged at 2200xg for 6 min, and the supernatants stored at -20°C for cytokine analysis (section 2.6.1). At each time point, fibroblasts were lysed by adding 250 µl of a saponin lysis solution (Appendix 7.3.3) to each well and incubating the plate for 15-20 minutes. Complete cell lysis was confirmed by observation under a light microscope, and a sterile plastic tip was used to mechanically aid in lysing the cells if necessary. Bacteria were quantified by viable counting, diluting the lysates in sterile PBS, and appropriate dilutions were inoculated onto nutrient agar plates (25 µl /plate) in triplicate and incubated overnight in an atmosphere of 5% (v/v) CO_2 at 37°C. Colony counts were quantified using a ProtoCOL model 60000 automated colony counter (Synoptics Ltd, Cambridge, UK).

2.3.2 Scanning Electron Microscopy (SEM)

Human corneal fibroblasts were grown to confluence on manufacturer collagen pre-coated transwells (ThinCerts™, transparent pore size 0.4 urn; Greiner Bio-one, Stonehouse, UK), challenged with a bacterial infective dose of 10^4 and 10^7 CFU/mL (MOI 0.1 and 100, respectively) and incubated in an atmosphere of 5% (v/v) CO_2 at 37°C for 3, 6 and 9h. Uninfected cells were included as negative controls. At each time point, the cells were washed 4 times with warm sterile PBS and then processed for SEM. Transwells were fixed for a minimum of 1h using a fixative solution [3% (v/v) glutaraldehyde and 4% (v/v) formaldehyde in 0.1 M PIPES (1,4-Piperazinediethanesulfonic acid) buffer pH 7.2] and were rinsed twice in buffer solution (0.1 M PIPES buffer) for 10min each. Then, a gradual concentration of ethanol [from 30%, 50%, 70%, 95% and up to 100% (v/v)] was used to dehydrate the samples (10min for each step and 20min for the final step). Cutting of the transwell membranes was done during the ethanol dehydration steps. Next, the cut membranes were critical-point dried and mounted onto metal stubs for the final sputter coating step. Coated specimens were viewed using the Quanta 200 scanning electron microscope (FEI, Hillsboro, USA) and several images were obtained for each specimen at magnifications of x3200 and up to x24000.

2.3.3 Assessment of the role of TFP and flagella in bacterial association to fibroblasts

In order to investigate the role of bacterial flagella (flg) and type IV pilus (TFP) in bacterial association to corneal fibroblasts, confluent fibroblast monolayers were challenged in triplicate with 10^7 CFU/mL (MOI 100) CFIM and incubated in an atmosphere of 5% (v/v) CO_2 at 37^{o}C for 3h. One triplicate was challenged with wild type PAO1 bacteria (PA tn7-GFP), another with mutant PAO1 strain FliM tn7-GFP deficient in flg, a third with mutant PAO1 strain PilA tn7-GFP deficient in TFP and a forth with mutant PAO1 strain FliM PilA tn7-GFP deficient in both flg and TFP (see section 2.1.1 for more details about bacterial strains). Viable counting assays were performed as described in section 2.3.1

2.3.4 Laser scanning confocal microscopy

The bacterial strains used in this set of experiments were green fluorescent protein (GFP) expressing PAO1 strains (section 2.1.1), which allowed for direct visualization of bacterial association to corneal fibroblasts. Confluent fibroblast monolayers were challenged in triplicate with 10^7 CFU/mL (MOI 100) CFIM and incubated in an atmosphere of 5% (v/v) CO_2 at 37^{o}C for 3h. At the given time point (3h), the cell monolayers were washed gently 4 times with warm PBS, and then fixed with paraformaldehyde 4% (w/v) in PBS for 30 min. The cells were washed with 50 mM ammonium bicarbonate, and then washed with warm PBS. Evans Blue 0.0025% (v/v) in PBS was then added to the cells and left for 20 min at 37^{o}C. The cell monolayers were washed thoroughly to remove all residual fixative, and were examined immediately after staining using the Leica TCS SP5 on the DM6000 inverted microscope stand. The field of view was 246 μm^3, using a HCX PlanoApo CS 63x 1.3 NA glycerol emersion objective lens=63x. The excitation laser had a wavelength of 488 and 561 nm, and the detection laser had wavelength ranges of 500-555 nm and 587-750 nm.

2.4 Measurement of bacterial invasion

2.4.1 Gentamicin protection assays

Confluent corneal fibroblast monolayers were challenged in triplicate with bacterial suspensions of 10^2 (MOI 0.001) and 10^4 CFU/mL (MOI 0.1) and incubated in an atmosphere of 5% (v/v) CO_2 at 37^{o}C for 9h. A higher bacterial infective dose (10^7 CFU/mL; MOI 100) was also used to challenge cell monolayers for a shorter time period (3h). In order to inhibit intracellular actin microfilament activity, monolayers were first pre-incubated with CFIM containing 2 µg/ml cytochalasin D (Appendix 7.3.2) for 30 min before adding the bacterial suspensions. At given time points, the cell monolayers were washed gently 4 times with warm PBS and then 1ml of CFIM containing 200 µg/ml of gentamicin (Sigma-Aldrich, Dorset, UK) was added to the wells and incubated at 37^{o}C for 90min. This was sufficient to destroy all extracellular bacteria (confirmed by sampling the medium and viable counting after incubating on nutrient agar, ensuring >99% bacterial killing) and allowed for quantification of internalized bacteria. Monolayers were then washed 4 times with warm PBS and lysed using saponin, and bacteria were quantified by viable counting on nutrient agar plates, as described above.

2.4.2 Transmission Electron Microscopy (TEM)

Human corneal fibroblasts were grown to confluence on collagen pre-coated transwells (ThinCerts™, transparent pore size 0.4 urn; Greiner Bio-one, Stonehouse, UK), challenged with a bacterial infective dose of 10^7 CFU/mL (MOI 100) and incubated in an atmosphere of 5% (v/v) CO_2 at 37^{o}C for 9h. Uninfected cells were used as negative controls. At the time point, the monolayers were washed 4 times with warm sterile PBS and then processed for TEM. Transwells were fixed for a minimum of 1h using a fixative solution [3% (v/v) glutaraldehyde and 4% (v/v) formaldehyde in 0.1 M PIPES (1,4-Piperazinediethanesulfonic acid) buffer pH 7.2], rinsed twice in buffer solution (0.1 M PIPES buffer) for 10min each and then fixed using post fixative [1% (w/v) osmium tetroxide in 0.1 M PIPES buffer, pH 7.2] for 1hr. Samples were briefly rinsed twice in PBS, and then a 2% (w/v) uranyl acetate solution was used for staining for 30min. A series of gradual concentrations of ethanol [from 30%, 50%, 70%, 95% and up to 100% (v/v)] was used to dehydrate the samples (10min for each step and 20min for the final step). Samples were incubated overnight, on a rotor (2rpm), in spur resin at a 50:50 ratio with acetonitrile. After that, the samples were placed in fresh spur resin and polymerised in an electric oven at 60°C for 20-24h. In preparation for microscopy, sample blocks were cut into ultrathin sections (about 90 nm thick) using glass knives on a Leica Reichert Ultracut E microtome (Leica, Wetzlar, Germany). A number of sections was stained with toluidine blue and checked under

light microscopy for the presence and positioning of cells, and then, when satisfactory, several sections per sample were fixed onto copper grids. Grids were stained using lead nitrate for 5min in the presence of NaOH capsules to absorb excess CO_2. Then, grids were briefly rinsed in distilled water and air dried. Sample viewing was done using the H7000 transmission electron microscope (Hitachi, Japan) at 75Kv and under different magnifications ranging from x3000 to x20000.

2.4.3 Assessment of the effect of ciprofloxacin on intracellular bacteria

Confluent fibroblast monolayers were challenged with PAO1 bacteria at a dose of 10^7 CFU/mL (MOI 100) for 3h, and then gently washed 4 times in warm sterile PBS. CFIM (1ml) containing 200 µg/ml of gentamicin was added to designated wells and ciprofloxacin (Sigma-Aldrich, Dorset, UK) at doses of 10, 50 and 200 µg/mL were added to separate wells and incubated at 37^{o}C for 90min. Monolayers were then washed 4 times with warm PBS and lysed using saponin, and bacteria were quantified by viable counting on nutrient agar plates, as described above.

2.4.4 Measurement of bacterial survival and replication inside invaded fibroblasts

Confluent corneal fibroblast monolayers were challenged in triplicate with bacterial suspensions of 10^7 CFU/mL (MOI 100) and incubated in an atmosphere of 5% (v/v) CO_2 at 37^{o}C for 24h. Infected CFIM was removed from the wells at 3h post challenge and the cell monolayers were washed gently 4 times with warm sterile PBS, after which 1ml of CFIM containing 200 µg/ml of gentamicin was added to the wells and the plates were returned to the incubator. At 24h, fibroblast monolayers were washed 4 times with warm PBS and lysed using saponin, and bacteria were quantified by viable counting on nutrient agar plates, as described above. Sterility was confirmed by sampling the extracellular medium and viable counting after incubating on nutrient agar overnight. Bacterial invasion was assessed at 90 min, 3h, 6h and 21h after adding the gentamicin using the method described above.

2.4.5 Assessment of the role of the SRC kinase system in bacterial internalization

To investigate the role of SRC tyrosine kinase in bacterial internalization, two sets of experiments were performed: a gentamicin protection assay to determine the direct effect of tyrosine kinase inhibitors on the number of internalized bacteria into corneal fibroblasts, and SDS-PAGE and western blot to detect the expression and upregulation of the enzymes during live infection.

2.4.5.1 Gentamicin protection assays

Corneal fibroblasts (CF) were cultured to confluence in 24-well cell culture plates, and triplicate monolayers were then pre-treated for 30 min with the tyrosine kinase inhibitors Genistein (GST – 10 µg/mL) and PP2 (3 µg/mL) and with the actin microfilament inhibitor cytochalasin D (CD – 10 µg/mL), one triplicate per inhibitor. One triplicate was not pre-treated with any inhibitors and was used as control. Infective medium was prepared by adding inhibitors to CFIM in the same concentration used for pre-treating the fibroblasts so that each pre-treated triplicate was infected by CFIM with the same inhibitor originally used (for example, monolayers pre-treated with 10 µg/mL CD were infected with CFIM containing 10 µg/mL CD).

Fibroblasts monolayers were challenged in triplicate with 10^7 CFU/mL (MOI 100) CFIM and incubated in an atmosphere of 5% (v/v) CO_2 at 37°C for 3h. To determine the effect of the inhibitors on the rate of bacterial growth, CFIM containing inhibitors was added to wells containing no fibroblasts, and the triplicates were incubated with the infected fibroblasts and treated in a similar manner.

At time point (3h), bacterial internalization was assessed as described in section 2.4.1. For the triplicate wells containing CFIM with inhibitors and no fibroblasts, bacteria were quantified by viable counting on nutrient agar plates immediately after the 3h incubation (Figure 2.1).

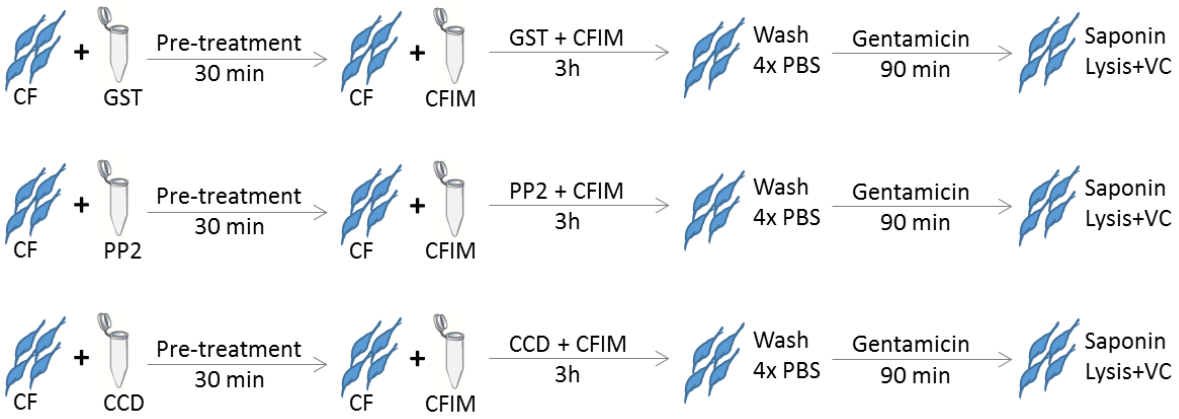

Figure 2.1 Corneal fibroblast pre-treatment and infection using SRC kinase inhibitors

2.4.5.2 Sodium dodecyl sulphate-polyacrylamide gel electrophoresis (SDS-PAGE)

In order to assess the presence and upregulation of SRC tyrosine kinase, SDS-PAGE with a 12% (w/v) acrylamide gel was performed in a second-dimension mini format electrophoresis system (Mini-PROTEAN; Bio-Rad, Hercules, CA, USA). Confluent corneal fibroblasts were challenged with 10^7 CFU/mL (MOI 100) CFIM and incubated in an atmosphere of 5% (v/v) CO_2 at 37^oC for 3h. At time point (3h), cell monolayers were washed 4 times with warm PBS, and then 100 µL of CytoBuster™ Protein Extraction Reagent (Fisher, Loughborough, UK) was added for 5 min, and the wells were mechanically scrapped by a plastic tip to ensure complete lysis of cells. The supernatants were stored in a -20 ^oC freezer.

A. Preparation of the gels

A separating gel (Appendix 7.7.1) was prepared between the 2 glass panes of the system after placing on a rubber spacer and fixing by clips to avoid leakage. After the separating gel was set, a stacking gel (Appendix 7.7.2) was introduced using a plastic liquid transfer pipette, a comb was placed on top to form the wells and the stacking gel was left to set for 1h at room temperature.

B. Determination of protein concentration

In order to determine and standardize the protein concentration in culture supernatant samples, a Pierce™ BCA Protein Assay Kit (Life Technologies, Paisley, UK) was used (Appendix 7.7.7). In this assay, the presence of proteins reduces Cu^{2+} to Cu^{1+} in an alkaline solution, and one molecule of the resultant Cu^{1+} chelates two molecules of bicinchoninic acid (BCA), resulting in an intense purple-coloured reaction product. Because of the highly sensitive and selective nature of the reaction, protein quantity can be determined by colorimetric detection.

Reagent A and Reagent B were mixed in a ratio of 50:1 to form BCA reagent, of which, a 200 µl aliquot was added to 25 µl of albumin standard (Appendix 07.7.8) or undiluted culture supernatant samples in a Nunc™ 96-well flat-bottomed polystyrene microtitre plate (Thermo-Scientific, Rockford, IL, USA). The plate was then incubated at 37^oC for 30 min, and the absorbance at 570 nm was read in an iMarkTM microplate reader (Bio-Rad, Hercules, CA, USA). The absorbance value of the albumin standards was plotted as a standard curve and the protein concentration of the samples was calculated by comparing the absorbance value with the standard curve.

C. Preparation and loading of the samples

After determining the protein concentration in each sample, all samples were diluted with distilled water so that they had similar protein concentrations. Twenty-five microliters of sample buffer (Appendix 7.7.3) were added to 100 µl of the adjusted samples, and the samples were boiled for 8 minutes. After carefully removing the comb and unpolymerized gel, the gels were placed into the electrophoresis system, and the tank was filled with running buffer (Appendix 7.7.4). SeeBlue® Plus2 Pre-stained Protein Standard (Life Technologies, Paisley, UK) (7 µl) and 20 µl of the boiled samples were added to the wells, and the gels were left to run at 170 V for 90 min or until all the bands have reached the bottom of the gels.

2.4.5.3 Western blotting

After the electrophoresis was finished, the SDS-PAGE gels containing the separated protein samples were immersed in transfer buffer (Appendix 07.7.5) and left on a gentle shaker for 15 min. For each gel, 6 layers of thick filter paper (3M, Bracknell, UK) and a piece of Amersham Hybond P 0.45 PVDF blotting membrane (GE Healthcare, Hatfield, UK) were cut to the same size as the gels and submerged in methanol for 5 min. A blotting sandwich was made by initially laying 3 layers of the filter paper on the bottom, followed by the blotting membrane, followed by the gel, and finally, the remaining 3 layers of filter paper. The sandwich was placed in a Trans-Blot SD semi-dry transfer cell (Bio-Rad, Hercules, CA, USA) at 10 V for 45 min. The membranes were then immersed in a blocking buffer (Appendix 7.7.6) and left on a gentle shaker for 1h, after which the buffer was replaced by 10 mL blocking buffer containing 18 µl anti-SRC antibody (Abcam, Cambridge, UK) and left, tightly covered, on a gentle shaker at room temperature overnight. After incubation, the membranes were washed 3x in PBS-Tween (Appendix 7.8.1), immersed in 10 mL PBS-Tween containing 4 µl goat anti-rabbit IgG HRP antibody, and left on a gentle shaker for 1h. The membranes were then washed 3x in PBS-Tween and read using a VersaDoc™MP 4000 imager (Bio-Rad, Hercules, CA, USA). A developing buffer was prepared using a Novex® ECL Chemiluminescent Substrate Reagent kit (Life Technologies, Paisley, UK) and a few drops of it were instilled on top of the membranes prior to reading.

2.5 Assessment of bacteria-induced cytotoxicity

2.5.1 Assessment of fibroblast cytotoxicity associated with live infection

Human corneal fibroblasts were grown to confluence in 96-well tissue culture plates (Greiner Bio-one, Stonehouse, UK). Cell quantification was carried out and the average count was $2.1x10^4$ cells/well (n=4 measurements). Confluent monolayers were maintained in CFCM. Bacterial inocula were prepared in CFIM at similar MOIs to those of previous infection experiments (see Table 2.1). The monolayers were gently rinsed with warm sterile PBS and then 200 µl/well of infective CFIM was added to triplicate wells. Uninfected control wells were also included for measurements of spontaneous LDH release and maximum LDH release by lysed uninfected cells as well as blank wells, containing only CFIM, for background measurements. Plates were incubated in an atmosphere of 5% (v/v) CO_2 at 37^oC for 9h. LDH measurements were carried out using the CytoTox 96® Non-Radioactive Cytotoxicity assay kit (Promega, Madison, WI, USA). The proprietary lysis solution (20 µl/well) was added to maximum LDH release wells 45min prior to the final time point to completely lyse the fibroblasts. Supernatants from each well were transferred to individual 1.5ml Eppendorf tubes and centrifuged at 2200g for 6 min to pellet the bacteria and dead cells. Next, 50 µl of supernatant from each tube was transferred to a 96-well measuring plate (Camlab, Cambridge, UK) to which 50 µl of the proprietary substrate mixture was added, followed by incubation in the dark at room temperature for 30min. A stop solution *(*50 µl/well*)* was added to all wells and the absorbance was read at 492nm using an iMark Absorbance Reader (Bio-Rad, USA). Cytotoxicity levels were calculated by dividing the average LDH release value of test sample by the average maximum LDH release value from lysed, uninfected cells using the following formula:

LDH release of test (%) = (LDH release of test/maximum LDH release) x 100

2.5.2 Assessment of the effect of intracellular bacteria on fibroblast viability

To investigate the effect of intracellular bacteria on fibroblast viability, corneal fibroblasts were grown to confluence in a 24-well plate, and monolayers were challenged in triplicate with bacterial suspensions of 10^7 CFU/mL (MOI 100) and incubated in an atmosphere of 5% (v/v) CO_2 at 37^oC for 9 and 24h. At 3h post challenge, infected and uninfected monolayers (n=3) were washed 4 times in warm PBS, and 1 mL of CFIM containing 200 µg/ml of gentamicin was added to each well and left for the remainder of the 9 or 24h period. LDH measurements were carried out at 9 and 24h as described above but with the addition of 100 µl/well of the proprietary lysis solution to maximum LDH release wells, 45min prior to the final time point (to compensate for the larger number of cells and the larger volume of the wells).

2.5.3 Assessment of the effect of bacterial virulence on cytotoxicity

In order to assess the impact of bacterial virulence on corneal fibroblast cytotoxicity, corneal fibroblasts were challenged with two different strains of *P. aeruginosa*: the 'invasive' strain PAO1 and the 'cytotoxic' strain PA14. Confluent fibroblast monolayers were challenged in triplicate with 10^7 CFU/mL (MOI 100) CFIM of each strain and incubated in an atmosphere of 5% (v/v) CO_2 at 37^{o}C for 9h. LDH measurement was carried out at 9h as described in section 2.5.

2.5.4 Assessment of the role of bacterial virulence factors on cytotoxicity

In order to investigate the role of bacterial flagella (flg) and type III secretion system (TTSS) in bacterial cytotoxic effects on corneal fibroblasts, an LDH cytotoxicity assay was carried out. Corneal fibroblasts were cultured to confluence in 24-well cell culture plates, and then challenged in triplicate with 10^7 CFU/mL (MOI 100) CFIM and incubated in an atmosphere of 5% (v/v) CO_2 at 37^{o}C for 9h. Triplicate wells were challenged with wild type PA14 bacteria (PA14*WT*), mutant PA14 bacteria deficient in TTSS (PA14*ΔPopb*) and mutant PA14 bacteria deficient in flagella (PA14*ΔFlgK*) (see section 2.1.1 for bacterial strains). LDH measurement was carried out at 9h as described in section 2.5.1.

2.6 Assessment of host cell response to bacterial infection

2.6.1 Assessment of corneal fibroblast cytokine release associated with live infection

2.6.1.1 Detection of cytokine release by a sandwich immunoassay technique

Confluent corneal fibroblast monolayers were challenged in triplicate with a bacterial infective dose of 10^1, 10^2, 10^3 and 10^4 CFU/mL (MOI 0.0001. 0.001, 0.01, 0.1, respectively). A subset of fibroblast monolayers was infected with a higher infective dose of bacteria (10^7 CFU/mL; MOI 100) and treated with gentamicin 3h post-challenge to destroy all extracellular bacteria (as described above). This allowed for the study of the effect of internalized bacteria on cytokine production with the preservation of fibroblasts until the end of the 9 or 24h time period. The plates were incubated in an atmosphere of 5% (v/v) CO_2 at 37^{o}C. Supernatants were collected at 9 and 24h post-challenge and centrifuged at 2200g for 6 min, and the samples were stored at -20°C. Cytokine analyses were carried out using the Human Pro-Inflammatory 9-Plex Tissue Culture Kit (MSD, Rockville, MD, USA) which employs a sandwich immunoassay format where capture antibodies are coated in a patterned array on the bottom of the wells of the plate. Initially, 150 µL of the 1% (w/v) Proprietary Blocker B solution were dispensed into each well, and the plate was incubated with vigorous shaking (300-1000 rpm) for 1 hour at room temperature. Thereafter, calibrator solutions were prepared (Appendix 7.5.1) and 25 µL were added per duplicate wells to the first 16 wells. In the remaining wells, 25 µL/well of each undiluted sample was added. The plate was sealed with an adhesive plate seal and incubated with vigorous shaking (300-1000 rpm) for a further 2h at room temperature, after which all wells were washed 3X with PBS + 0.05% (v/v) Tween-20. Thereafter, 25 µL of detection antibody solution (Appendix 7.5.1.2) were added to all wells, and the plate was sealed again with an adhesive plate seal and incubated for 1 to 2 hours with vigorous shaking (300-1000 rpm) at room temperature. The plate was then washed 3x in PBS, after which 150 µL of 2X Read Buffer T (Appendix7.5.1.3) were added, and the plate was immediately analysed using the SECTOR® Imager (MSD, Rockville, MD, USA).

2.6.1.2 Assessment of the effect of bacterial virulence on cytokine production

Corneal fibroblasts were challenged with *P.aeruginosa* PA14 strain and with PAO1 strain. Confluent fibroblast monolayers were challenged in triplicate with 10^7 CFU/mL (MOI 100) CFIM of each strain and incubated in an atmosphere of 5% (v/v) CO_2 at 37^{o}C for 24h. Supernatants were collected at 9 and 24h post challenge and spun at 2200xg for 6 min, and the samples were stored at -20°C. Cytokine analysis was carried out using the V-PLEX Human IL-1β Kit (MSD, Rockville, MD, USA) which employs a sandwich immunoassay format where capture antibodies are coated on independent and well-defined spots on the bottom of the wells of the plate. Initially, calibrator solutions were prepared (Appendix 7.5.2.1) and 50 µL/well were added in duplicate to the first 16 wells. In the remaining wells, 25 µL/well of the proprietary Diluent 2 and 25 µL/well of each undiluted sample were added. The plate was sealed with an adhesive plate seal and incubated with vigorous shaking (300-1000 rpm) for a further 2h at room temperature, after which all wells were washed 3X with PBS-Tween (Appendix 7.8.1). Thereafter, 25 µL of detection antibody solution (Appendix 7.5.1.27.5.2.2) were added to all wells, and the plate was sealed again with an adhesive plate seal and incubated for 1 to 2 hours with vigorous shaking (300-1000 rpm) at room temperature. The plate was then washed 3x in PBS-Tween, after which 150 µL of Read Buffer T (Appendix 7.5.1.3) were added, and the plate was immediately analysed using the SECTOR® Imager (MSD, Rockville, MD, USA).

2.6.1.3 Assessment of the role of bacterial virulence factors on cytokine production

Corneal fibroblasts were cultured to confluence in 24-well cell culture plates, and then challenged in triplicate with 10^7 CFU/mL (MOI 100) CFIM and incubated in an atmosphere of 5% (v/v) CO2 at 37oC for 9h. Similar to section 2.5.3, fibroblast triplicates were challenged with PA14WT, PA14ΔPopb and PA14ΔFlgK, and the cytokine analysis was carried out using the V-PLEX Human IL-1β Kit (MSD, Rockville, MD, USA) as described in section 0.

2.6.1.4 Assessment of the role of bacterial components on cytokine production

Confluent fibroblast monolayers were challenged in triplicates with live bacteria, heat killed bacteria, freeze-thaw killed bacteria and LPS, and controls included uninfected cells and lysed uninfected cells (see section 2.6.2.1). Culture supernatants were collected at 9 and 24h, and cytokine analysis was carried out using the V-PLEX Human IL-1β Kit (MSD, Rockville, MD, USA) as described in section 2.6.1.1.

2.6.2 Assessment of corneal fibroblast MMP release associated with live infection

2.6.2.1 Challenge of corneal fibroblast

Confluent corneal fibroblast monolayers were challenged in triplicate with live bacteria, heat killed (HK) bacteria and freeze-thaw (FT) killed bacteria, all with an infective dose equivalent to 10^7 CFU/mL. In addition, triplicate cell monolayers were challenged with 100 ng/mL of pure *Pseudomonas aeruginosa* lipopolysaccharide (LPS), and another set of monolayers was challenged with 10^7 CFU/mL (MOI 100) of live bacteria and then treated with 200 µg/mL gentamicin 3h post challenge. Negative controls included unchallenged cell monolayers and cells challenged only with 200 µg/mL gentamicin added 3h after start of experiment. Positive controls included live bacteria at a dose of 10^7 CFU/mL, suspended in medium with no fibroblasts; and fibroblast monolayers lysed with 100 µL of proprietary lysis solution (Promega, Madison, WI, USA) 45 minutes prior to the desired time point. Serum free CFIM was used in all wells.

Heat killed bacteria were prepared by heating a stock solution of 10^8 CFU/mL bacteria for 1h at 60°C using a water bath. The stock solution was then stored at 2-8°C, and a diluent of 10^7 CFU/mL (MOI 100) was used on the day of each experiment. Freeze-thaw killed bacteria were prepared by freezing a stock solution of 10^8 CFU/mL bacteria in a -80°C freezer overnight, then thawing the bacteria to 37°C in a water bath and repeating the freeze-thaw cycle until all bacteria were killed. Sterility of both heat-killed and freeze-thawed samples was verified by incubating a sample of each stock solution on nutrient agar plates overnight; this was repeated for freeze-thawing cycles until no bacterial growth was observed on the agar plates (8 cycles in total).

The plates were incubated in an atmosphere of 5% (v/v) CO_2 at 37^{o}C. Supernatants were collected at 9 and 24h post challenge and centrifuged at 2200g for 6 min, and the samples were stored at -20°C. Analyses were done within 2-4 weeks of collecting the supernatants using a sandwich immunoassay technique and a standard gelatine zymography.

2.6.2.2 Gelatin zymography

Culture supernatants were thawed on ice to room temperature, and 15 µL of each sample was added to 15µL of zymogram sample buffer (Appendix 7.6.1). Precast 10% (w/v) polyacrylamide gelatine 10-well gels (Bio-Rad, Hercules, CA, USA) were placed into a second-dimension mini format electrophoresis system (Mini-PROTEAN; Bio-Rad, Hercules, CA, USA), and the electrophoresis tank was filled with a zymogram running buffer (Appendix 7.6.2). On each gel, the first two wells were used for the protein ladder (Thermo-Scientific, Rockford, IL, USA) and for the MMP positive control (Sigma-Aldrich, Dorset, UK). No samples were added to the third well, and 10 µL of each sample was added to each of the remaining wells. The gels were left to run at 90 V for 2h or until all the bands have reached the bottom of the gels. The gels were then washed four times with a zymogram renaturation buffer (Bio-Rad, Hercules, CA, USA), gently shaking for 15 min. The gels were transferred to separate containers and washed once with a zymogram development buffer (Bio-Rad, Hercules, CA, USA), gently shaking for 30 min, and then incubated at 37°C for 40 h in development buffer containing 1% (w/v) sodium azide. After incubation, the gels were washed three times in distilled water, soaked in a zymogram staining buffer (Appendix 7.6.3) for 1h, and washed several times in a zymogram destaining buffer (Appendix 7.6.4), with gently shaking, until satisfactory destaining was achieved.

2.6.2.3 Detection of MMP release by a sandwich immunoassay technique

In order to detect the release of MMP-1, MMP-2, MMP-3 and MMP-9, the Human MMP-2 Ultra-Sensitive kit and the Human MMP 3-Plex Ultra-Sensitive kit (MSD, Rockville, MD, USA) were used. The method for both assays is identical, using the specific detection antibody for each kit.
Initially, 25 µL/well of the proprietary Diluent 2 were added to each well, and the plate was sealed with an adhesive plate seal and incubated with vigorous shaking (300-1000 rpm) for 30 min at room temperature. Calibrator solutions were prepared (Appendix 7.5.3.1) and 25 µL/well were added in duplicate to the first 16 wells, and, 25 µL/well of each undiluted sample were added to the remaining wells. The plate was sealed with an adhesive plate seal and incubated with vigorous shaking (300-1000 rpm) for 2h at room temperature, after which all wells were washed 3x with PBS-Tween (Appendix 7.8.1). Thereafter, 25 µL of detection antibody solution (Appendix 7.5.3.2) were added to all wells, and the plate was sealed again with an adhesive plate seal and incubated for 1 to 2 hours with vigorous shaking (300-1000 rpm) at room temperature. The plate was then washed 3x in PBS-Tween, after which 150 µL of Read Buffer T (Appendix 7.5.1.3) were added, and the plate was immediately analysed using the SECTOR® Imager (MSD, Rockville, MD, USA).

2.6.2.4 Assessment of the effect of bacterial virulence on MMP production by fibroblasts

In order to assess the impact of bacterial virulence on MMP release by corneal fibroblast in response to bacterial infection, corneal fibroblasts were challenged with the PA14 and the PAO1 strains. Confluent fibroblast monolayers were challenged in triplicate with 10^7 CFU/mL (MOI 100) CFIM of each strain and incubated in an atmosphere of 5% (v/v) CO_2 at 37^{o}C for 24h. Supernatants were collected at 24h post challenge and spun at 2200xg for 6 min, and the samples were stored at -20°C. Detection of MMP-1, MMP-2, MMP-3 and MMP-9 release was carried out using the the Human MMP-2 Ultra-Sensitive kit and the Human MMP 3-Plex Ultra-Sensitive kit (MSD, Rockville, MD, USA) as described in section 2.6.2.30.

2.6.2.5 Assessment of the role of bacterial virulence factors on MMP production by fibroblasts

To investigate the role of bacterial flagella (flg) and type III secretion system (TTSS) in influencing MMP production by corneal fibroblasts, a sandwich immunoassay technique was carried out. Similar to section 2.5.3, fibroblast triplicates were challenged with PA14ΔPopb and PA14ΔFlgK, and the detection of MMP-1, MMP-2, MMP-3 and MMP-9 release was carried out using the the Human MMP-2 Ultra-Sensitive kit and the Human MMP 3-Plex Ultra-Sensitive kit (MSD, Rockville, MD, USA) as described in section 02.6.2.3.

2.7 Statistical analysis and graphs

Statistical analysis was done using SPSS version 22.0 (IBM, Armonk, NY, USA). Graphs were made using GraphPad Prism 6 (GraphPad, La Jolla, CA, USA).

Chapter 3 **: RESULTS**

INTERACTIONS OF PSEUDOMONAS AERUGINOSA WITH CORNEAL FIBROBLASTS

3.1 Bacterial association to corneal fibroblasts

3.1.1 Total association

Primary human corneal fibroblasts (hCFs) confluent in tissue culture plates were challenged with various concentrations of PAO1 bacteria and bacterial association was measured and plotted against time and initial infective dose. Measurement of total association was done at different time points (3-24h), depending on the viability of the cells as demonstrated by visual inspection of fibroblast monolayers at each time point.

Results were obtained from 8 independent experiments with primary cell lines obtained from three different donor samples. PAO1 bacteria demonstrated a dose-dependent association with cell monolayers over time. Infection with 10^6 and 10^8 cfu/monolayer (MOI 10 and 1000, respectively) of bacteria led to a rapid saturation of the mono layers (**Figure 3.1** A) and monolayer destruction by 9-24h. On the other hand, all monolayers were visually intact at 9h after infection with lower doses of bacteria [10^1, 10^2, 10^3 and 10^4 cfu/monolayer (MOI 0.0001, 0.001, 0.01 and 0.1, respectively). For these lower MOI, the dose- and time-dependent association of PAO1 bacteria with CF was linear (**Figure 3.1** B). Monolayer destruction was observed at 24h with all infecting doses.

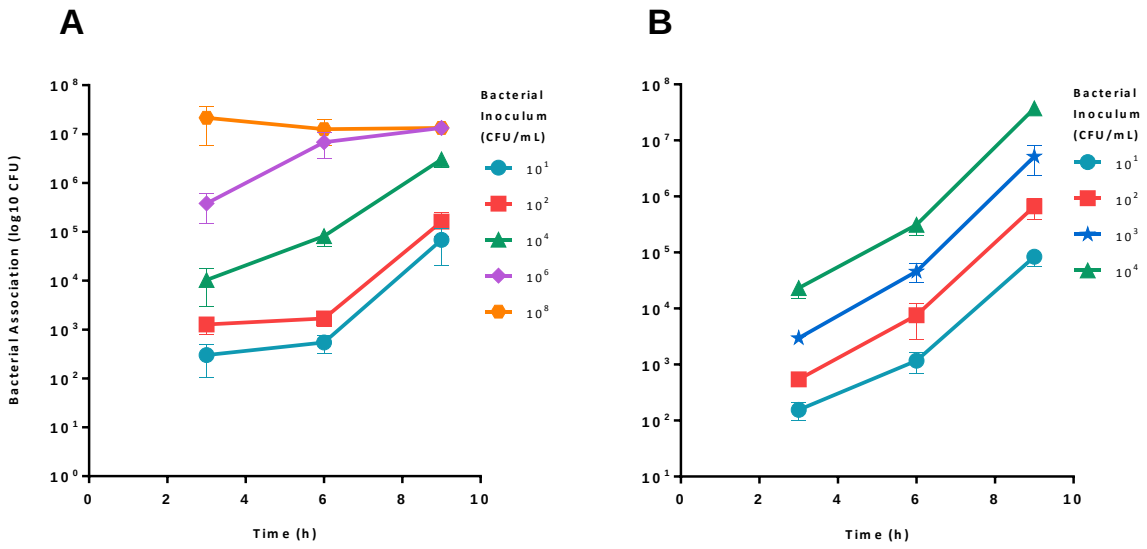

Figure 3.1 Total bacterial association of PAO1 bacteria to human corneal fibroblasts.

Corneal fibroblasts were challenged with 10^7 CFU/mL PAO1 for 3, 6, 9 and 24h. The association of PAO1 bacteria to corneal fibroblasts was dose- and time-dependant. The data symbols represent the mean number of associated bacteria and the error bars the standard error of the mean of 4 independent experiments. Where no error bars are visible, they fall within the symbol.

3.1.2 Electron microscopy

Viable counting assays demonstrated that PAO1 bacteria associated to human corneal fibroblasts *in-vitro*. To visually confirm the association of the bacteria to the surface of the fibroblasts, scanning electron microscopy (SEM) was used. Figure 3.2A shows uninfected fibroblasts with the characteristic fusiform shape and smooth surface with cellular projections, whereas Figure 3.2B shows the association of PAO1 bacteria to the surface of corneal fibroblasts at 3h post challenge with an infective dose of 10^4 CFU/mL (MOI 0.1). With a higher dose of infection (10^7 CFU/mL; MOI 100), a greater number of bacteria was observed associated to the surface of the fibroblasts (Figure 3.2C), with evidence of some bacteria penetrating beyond the cell membrane (Figure 3.2D). This supports the viable count findings from the association experiments, where PAO1 bacteria demonstrated a time-dependant association to human corneal fibroblasts, and suggests that bacteria may also invade the fibroblasts. At later time points, there was an almost complete destruction of fibroblast monolayers, and only cell debris and clusters of bacteria were observed scattered over the surface of the Transwell membrane (images not shown), suggesting that the classically invasive PAO1 bacteria can also be cytotoxic to corneal fibroblasts at high doses of infection.

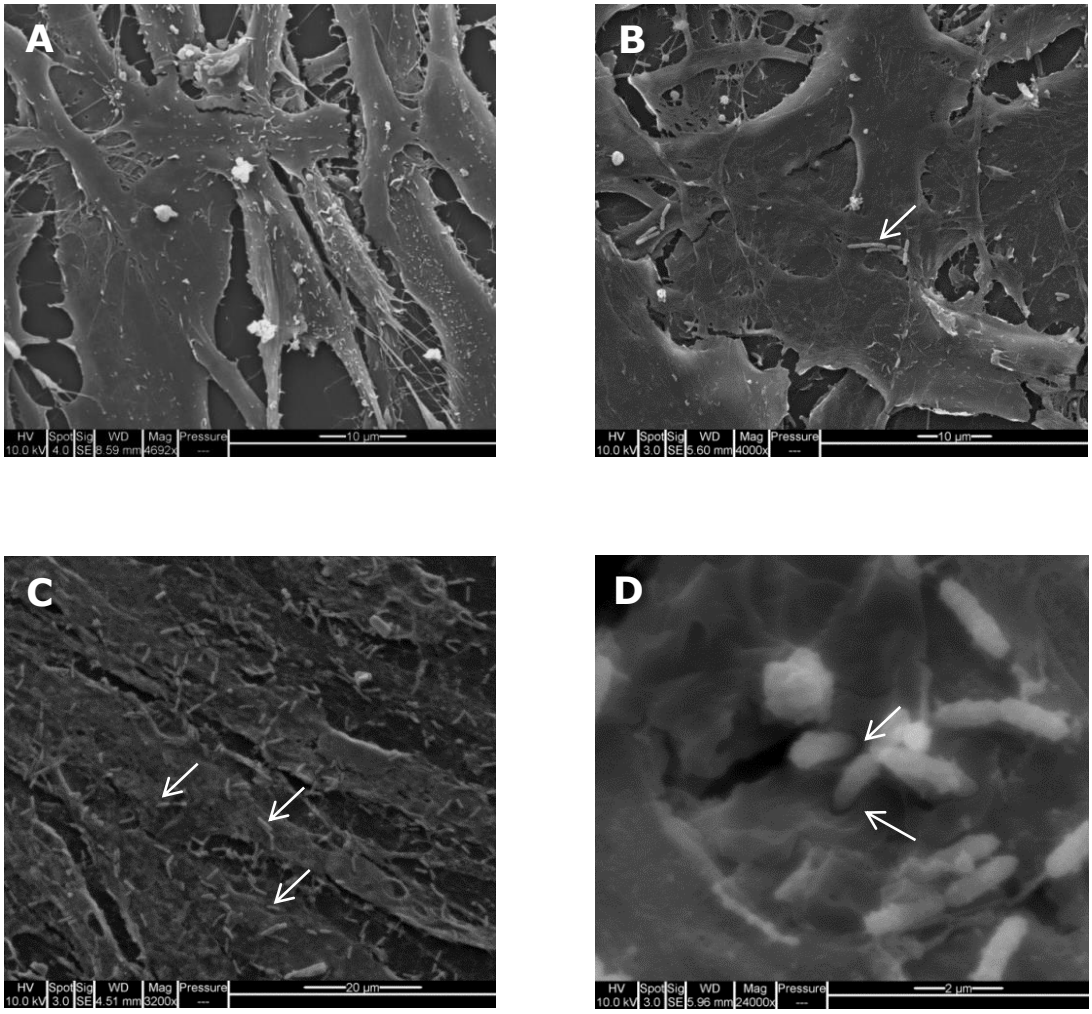

Figure 3.2 Scanning electron micrograph of bacterial association to human corneal fibroblasts.

Corneal fibroblasts were challenged with various doses of PAO1 and assessed at 3h. Associated bacteria can be seen associated to fibroblasts (B) as compared to uninfected fibroblasts with no bacteria (A). The arrows point to associated bacteria (B and C) and to bacteria seemingly penetrating the surface of the fibroblasts (D). [Original magnification= x4000 (A,B and C) and 24000x (D)].

3.1.3 The role of pili and flagella in PA association to corneal fibroblasts

Pseudomonas aeruginosa utilize type 4 pilus (TFP)[161] and flagella[156] to associate to target host cells. We sought to investigate the role of these adhesins in our microbial keratitis model by comparing the rate of bacterial association to corneal fibroblasts between wild type PAO1 bacteria and mutant strains deficient in TFP and/or flagella. Initially, we sought to ensure that all strains had the same rate of growth so that any difference in association would not be attributable to a difference in growth rates. We found that all strains had similar rates of growth (Figure 3.3).

Regarding the rate of bacterial association to corneal fibroblasts, we found that mutant strains had a significantly lower rate of association to corneal fibroblasts than wild type strains, suggesting that TFP and flagella play an important role in bacterial association to these cells. This was visually confirmed by scanning laser fluorescence microscopy (Figure 3.5) of interactions between GFP-expressing bacteria and hCFs, which showed an evident reduction in the number of associated mutant bacteria to corneal fibroblasts compared to wild type strains. There was no statistically significant difference in the rate of bacterial association between double mutant strain mutant strain FliM PilA tn7-GFP and either mutant strain FliM tn7-GFP or mutant strain PilA tn7-GFP (Table 3.1).

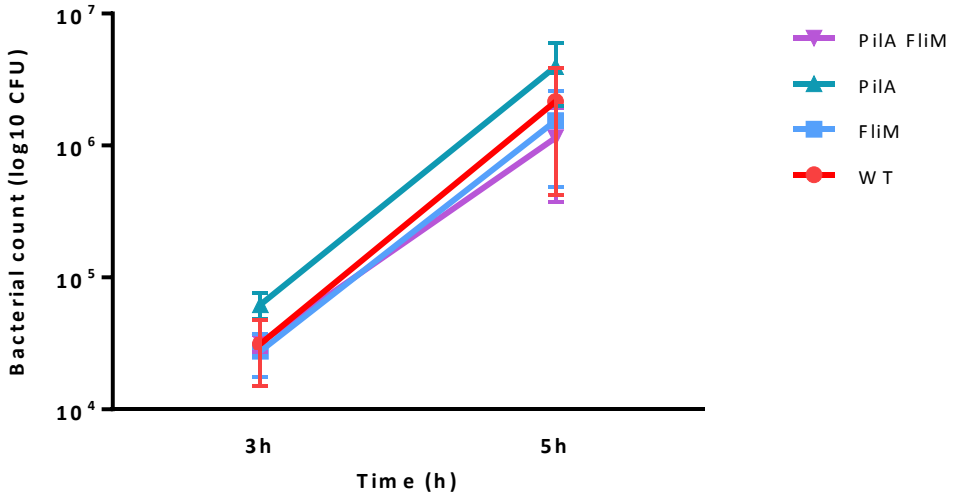

Figure 3.3 Rate of growth of wild type and mutant PAO1 strains

Wild type and mutant bacteria were left to grow in culture medium for 5h, and samples for viable counts were collected at 3 and 5h. The rate of growth of the wild type PAO1 (WT) strain, mutant strain FliM tn7-GFP deficient in FliM gene necessary for normal flagellin function, mutant strain PilA tn7-GFP deficient in the PilA gene necessary for normal type 4 pilus and mutant strain FliM PilA tn7-GFP deficient in both FliM and PilA gene was similar. The symbols represent the mean number of bacteria and the error represent the standard error of the mean of 3 independent experiments. Where no error bars are visible, they fall within the point.

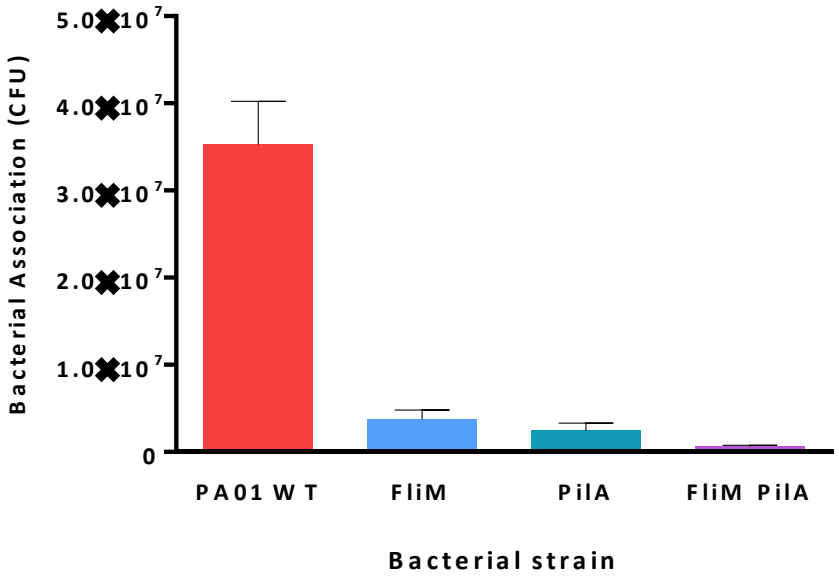

Figure 3.4 Association of wild type and mutant PAO1 bacteria to corneal fibroblasts

Corneal fibroblasts were challenged separately with 10^7 CFU/mL GFP-expressing wild type PAO1 and with mutant strains FliM, PilA and FliM PilA for 3h. Mutant PAO1 strains deficient in TFP and/or flagella demonstrated lower rates of association to corneal fibroblasts than wild type bacteria, suggesting that TFP and flagella play an important role in bacterial association to those cells. The bars represent the mean number of associated bacteria and the error bars the standard error of the mean of 3 independent experiments.

Table 3.1 Difference in bacterial association between wild type and mutant PAO1 strain

Bacterial strains		**Mean difference**	**P-value**
PAO1WT	PAO1Δ*fliM*	31539999.67*	0.000
	PAO1Δ*pilA*	32871333*	0.000
	PAO1Δ*fliM pilA*	34624444.33*	0.000
PAO1Δ*fliM pilA*	PAO1Δ*fliM*	-3084444.67	0.419
	PAO1Δ*pilA*	-1753111.33	0.641

* The mean difference in bacterial count between the mutant strains and the wild type is significant at the 0.05 level.

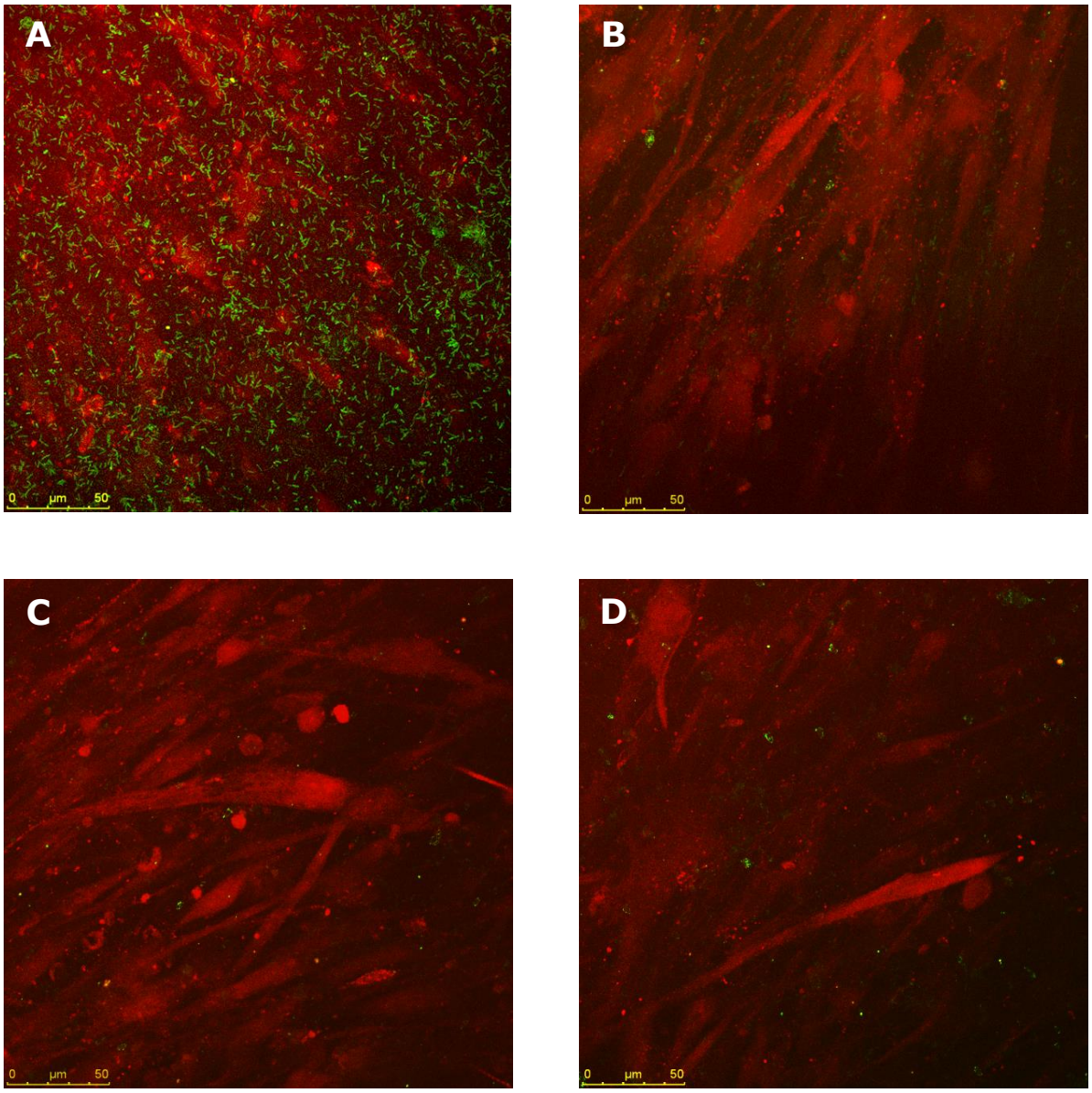

Figure 3.5 Laser scanning confocal microscopy of PAO1 bacteria adhering to corneal fibroblasts

Corneal fibroblasts were challenged separately with 10^7 CFU/mL GFP-expressing wild type PAO1 and with mutant strains FliM, PilA and FliM PilA for 3h. The number of mutant GFP expressing PAO1 bacteria (green dots) deficient in TFP (B), Flagella (C) and both TFP and flagella (C) associated to corneal fibroblasts (red) was evidently less than the number of associated wild type bacteria (A). [Field of view=246 μm^3; Objective lens=63x]

3.2 Bacterial invasion of corneal fibroblasts

3.2.1 Gentamicin protection assays

The SEM experiments above (Section 3.1.2) suggest that PAO1 may be capable of invading corneal fibroblasts. In order to investigate this further, a group of corneal fibroblast monolayers was infected with 10^2 and 10^4 CFU/mL bacteria (MOI 0.001 and 0.1, respectively) and another group was infected with 10^7 CFU/mL (MOI 100). Cellular invasion over time was quantified using the gentamicin assay, with the high infective dose assessed at 3h and the lower doses at 9h. Gentamicin was the antibiotic of choice since it effectively killed concentrations of PAO1 bacteria at growth levels expected in the culture medium after 3 and 9h (>99% bacterial killing, data not shown) and also because it is unable to penetrate the cells and kill intracellular bacteria.[423] Cytochalasin D (CD) was added to the monolayers to investigate whether the internalization of PAO1 bacteria by corneal fibroblasts occurred by an actin microfilament-dependent process.

Cellular invasion was detectable by 9h post challenge with the lower infective doses. The number of internalized bacteria recovered from cell monolayers treated with cytochalasin (CD+G) was significantly lower than untreated cells ($p<0.01$, Table 3.2), suggesting that these bacteria were internalized by fibroblasts using an actin micro filament dependent process (Figure 3.6 A and B). With the higher infective dose (10^7 CFU/mL; MOI 100), PAO1 bacteria invaded corneal fibroblasts by 3h post challenge, and the number of internalized bacteria recovered from cell monolayers treated with cytochalasin D was also significantly lower than untreated cells ($p<0.01$), similar to lower infective doses and longer duration (Figure 3.6 C and Table 3.2).

On the other hand, cytochalasin D had no significant effect on the number of bacteria adhering to fibroblasts in any of the infective doses or time points ($p>0.1$, Table 3.2), suggesting that the reduced number of recovered bacteria seen with cytochalasin D is not related to a reduction number in association.

In order to further analyze these data, an invasion index was calculated and expressed as a percentage of the total number of associated bacteria. The rate of invasion was higher with higher infecting dose and shorter duration, with a geometric mean level of invasion (±95% confidence limits) of 1.4% (0.68,2.87%); than with lower infecting dose and longer duration, with 0.3% (0.04,2.61%). However, this difference was not statistically significant ($P>0.05$).

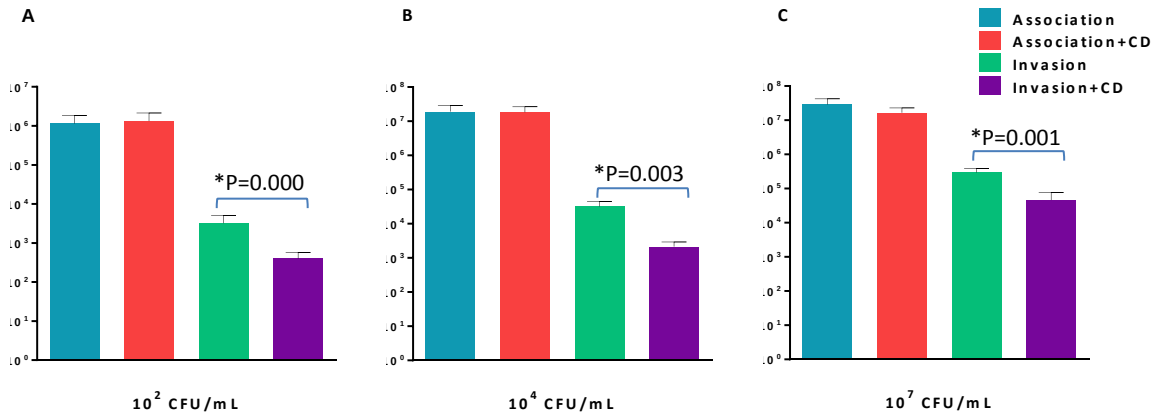

Figure 3.6 Gentamicin protection assay of bacterial invasion of human corneal fibroblasts.

A group of corneal fibroblasts was challenged with low infective doses (10^2 and 10^4 CFU/mL) and assessed at 9h post challenge (A and B), and another group was challenged with a higher infective dose (10^7 CFU/mL) and assessed at 3h post challenge (C). Cytochalasin D decreases bacterial internalization by inhibiting actin microfilaments. The bars represent the number of recovered bacteria with and without gentamicin treatment and with and without pre-treatment with cytochalasin D, and the error bars represent the standard error of the mean from 8 independent experiments. The asterisks indicate statistically significant differences ($p<0.05$)

Table 3.2 Comparison between invasion rates in fibroblasts pre-treated with cytochalasin D and untreated cells.

	Bacterial Inoculum	Without Cytochalasin D		With Cytochalasin D		P-value
		Mean	SEM	Mean	SEM	
Invasion	10^2 CFU/mL	1913	268	395	92	0.000
	10^4 CFU/mL	39446	10300	2189	429	0.003
	10^7 CFU/mL	294778	51378	46200	16017	0.001
Association	10^2 CFU/mL	1218000	300340	1463077	410052	0.634
	10^4 CFU/mL	14820000	3820312	17082667	3720244	0.675
	10^7 CFU/mL	29011111	6720335	16511111	3477205	0.124

*The mean difference is significant at the 0.05 level.

3.2.2 Electron microscopy

Results from the gentamicin assay suggested that PAO1 bacteria may possibly be internalized by corneal fibroblasts during bacterial challenge and transmission electron microscopy (TEM) was used to visually confirm the presence of bacteria inside the fibroblasts. After examining several sections of fibroblasts monolayers infected with PAO1, bacterial internalization was observed occurring at different stages (Figures 3.7A-E). PAO1 bacteria were detected in close proximity to the surface of corneal fibroblasts (Figures 3.7Aand B), with a cup-like invagination from the surface of the cell, where PAO1 bacteria were observed to be inside (Figures 3.7C). More advanced stages of invasion were also observed with PAO1 bacteria within cell-bound vacuoles completely inside host cells (Figures 3.7D). As a result, the ability of PAO1 to invade corneal fibroblasts was confirmed by TEM, although invasion was likely to be a rare event.

3.2.3 Effect of ciprofloxacin on internalized bacteria

Ciprofloxacin has been shown to penetrate the intact cornea and into the anterior chamber,[424] and is considered the gold standard for treatment of clinical *P. aeruginosa* microbial keratitis.[425] We sought to investigate the effect of ciprofloxacin on intracellular bacteria for two reasons; firstly, to confirm that the recovered bacteria from the gentamicin assays are truly intracellular and not from extracellular compartments/folds inaccessible to gentamicin; secondly, to test the ability of ciprofloxacin to accumulate inside corneal fibroblasts. The doses were chosen either to reflect MIC ranges used clinically or to match the dose of gentamicin we used.

The number of recovered bacteria from ciprofloxacin-treated infected fibroblasts was significantly less than that of gentamicin-treated cells (Table 3.3), and was inversely proportional to the dose of ciprofloxacin, indicating that ciprofloxacin accumulates inside corneal fibroblasts in a dose dependant manner, killing intracellular susceptible bacteria. The number of bacteria recovered from gentamicin-treated cells was approximately 10^5 CFU, whereas that from ciprofloxacin-treated cells was between 10^3 and 10^4 CFU (Figure 3.8).

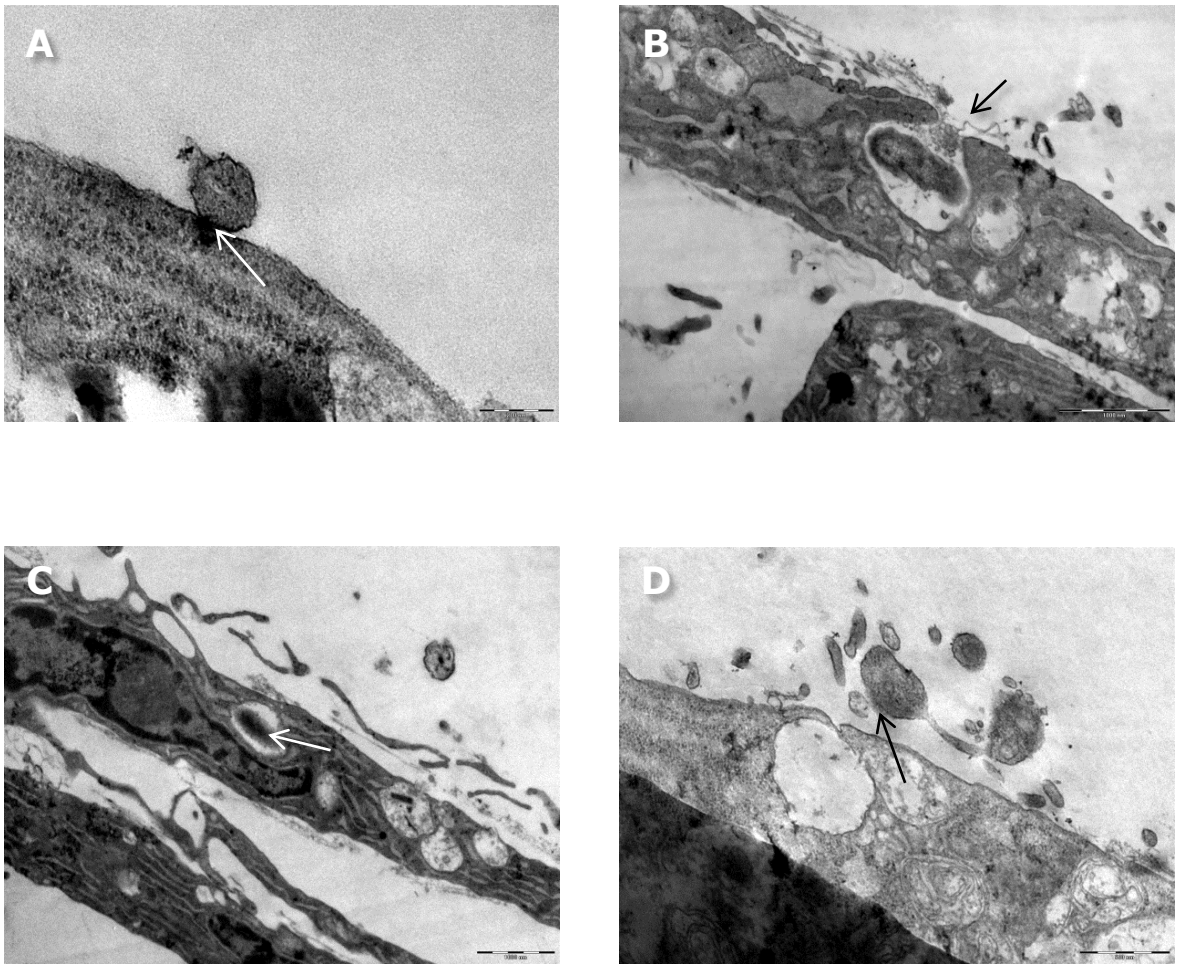

Figure 3.7 Transmission electron micrograph of PAO1 bacteria invading corneal fibroblasts.

The arrows point to bacteria adhering to the cell (A), internalized by endocytosis through a cup like invagination of the fibroblast cell membrane (B), residing inside a cytoplasmic endocytotic vesicle (C), and possibly externalizing out of the fibroblast (D). [Magnification= x45000 (A), x18500 (B) and

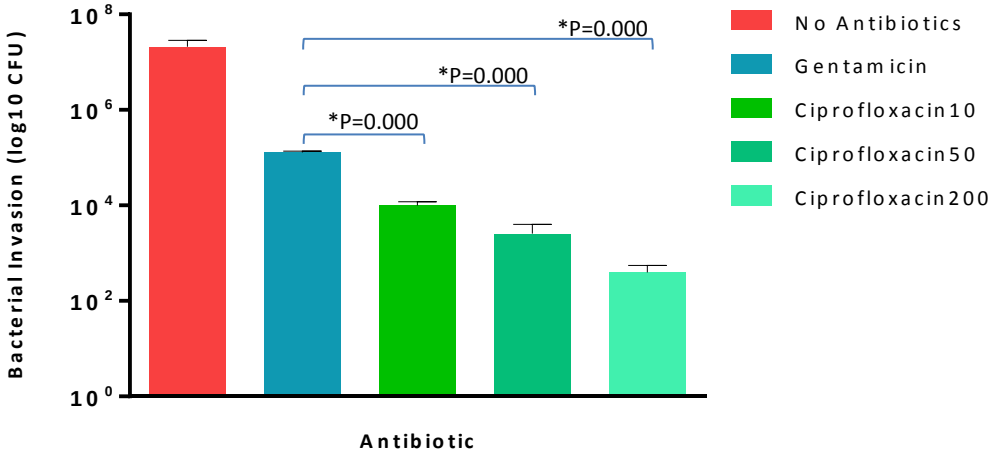

Figure 3.8 Gentamicin-ciprofloxacin invasion assay

Infected fibroblasts were treated with gentamicin (200 µg/mL) and ciprofloxacin (10, 50 and 200 µg/mL) The bars represent the number of recovered bacteria without antibiotics and with gentamicin and ciprofloxacin treatment, and the error bars represent the standard error of the mean from 8 independent experiments. The asterisks indicate statistically significant differences ($p<0.05$)

Table 3.3 Difference between the number of recovered bacteria in gentamicin-treated and ciprofloxacin-treated fibroblasts

Antibiotic		Mean difference	P-value
Gentamicin	Cipofloxacin10	119281*	0.000
	Cipofloxacin50	126582*	0.000
	Cipofloxacin200	128749*	0.000

*The mean difference is significant at the 0.05 level.

The number of recovered bacteria from ciprofloxacin treated fibroblasts was significantly lower than that from gentamicin treated cells.

3.2.4 Bacterial survival and replication inside invaded fibroblasts

Because higher bacterial doses caused almost complete destruction of cell monolayers, which hindered accurate assessment of bacterial association and invasion of fibroblasts at the 24h time point, a subset of fibroblast monolayers was treated with gentamicin to destroy all extracellular bacteria and hence protect the fibroblasts from the bacteria replicating freely in the culture medium, changing its pH and expressing exotoxins and other virulence factors that eventually destroy the cells. This allowed us to assess the survival and replication of bacteria that had already invaded the fibroblasts prior to the addition of gentamicin, and at 24h, cell monolayers were still visually mostly intact. The number of recovered bacteria increased significantly in a time dependent manner (Table 3.4), suggesting that PAO1 bacteria survived and replicated inside corneal fibroblasts (Figure 3.9). In uninfected wells, monolayers treated with gentamicin were also intact, suggesting that gentamicin alone doesn't have a detrimental effect on cultured corneal fibroblasts, which is consistent with evidence in other cell lines.[426] Table 3.4 shows the statistical analysis of the difference between the numbers of intracellular bacteria recovered at 3, 6, 9 and 24h. There was no statistically significant difference between the number of intracellular bacteria recovered at 3h and at 6h, or between the number at 6h and at 9h. There was, however, a statistically significant difference between the numbers of intracellular bacteria at 3 and 9h ($P < 0.05$), and at 3 and 24h ($P < 0.005$). The difference between the numbers of intracellular bacteria was significantly higher at 24h than at all other time points.

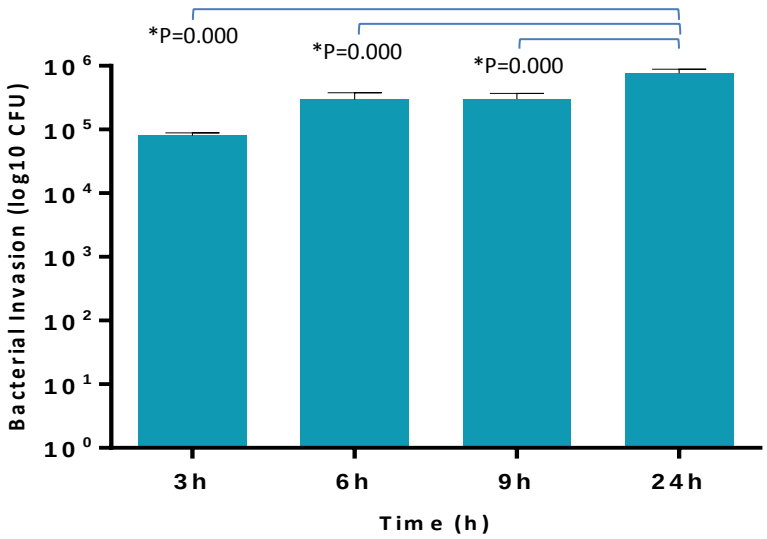

Figure 3.9 Bacterial survival and replication inside corneal fibroblasts.

Gentamicin was added 3h post challenge to preserve the cells for the 24h duration. The bars represent the number of retrieved bacteria, and the error bars represent the standard error of the mean from 3 independent experiments. The asterisks indicate statistically significant differences ($p<0.05$)

Table 3.4 Difference between intracellular bacterial counts at different time points.

Time		Mean Difference	P-value
3h	6h	214056	0.078
	9h	221900	0.068
	24h	681878*	0.000
6h	3h	214056	0.078
	9h	7844	0.947
	24h	467822*	0.000
9h	3h	221900*	0.068
	6h	7844	0.947
	24h	4599778*	0.000
24h	3h	6818778*	0.000
	6h	467822*	0.000
	9h	459978*	0.000

* The mean difference is significant at the 0.05 level.

The number of recovered intracellular bacteria at 24h was significantly higher than the numbers at 3, 6 and 9h.

3.2.5 The role of the SRC kinase system in bacterial internalization

The SRC tyrosine kinase family of enzymes[427] and the actin microfilament system[314] play an important role in the internalization of *P.aeruginosa* into eukaryotic cells. We sought to investigate the role of these systems in bacterial internalization into corneal fibroblasts by inhibiting SRC tyrosine kinase and the actin microfilament system in corneal fibroblasts and then assessing the rate of bacterial invasion using a standard gentamicin protection assay.

Initially, to rule out the possibility that the observed inhibition was due to inefficient association of *P.aeruginosa* to pretreated corneal fibroblasts, bacterial association was assessed. We found that none of the tested inhibitors had a significant effect on bacterial association to corneal fibroblasts (Table 3.5 and Figure 3.10).

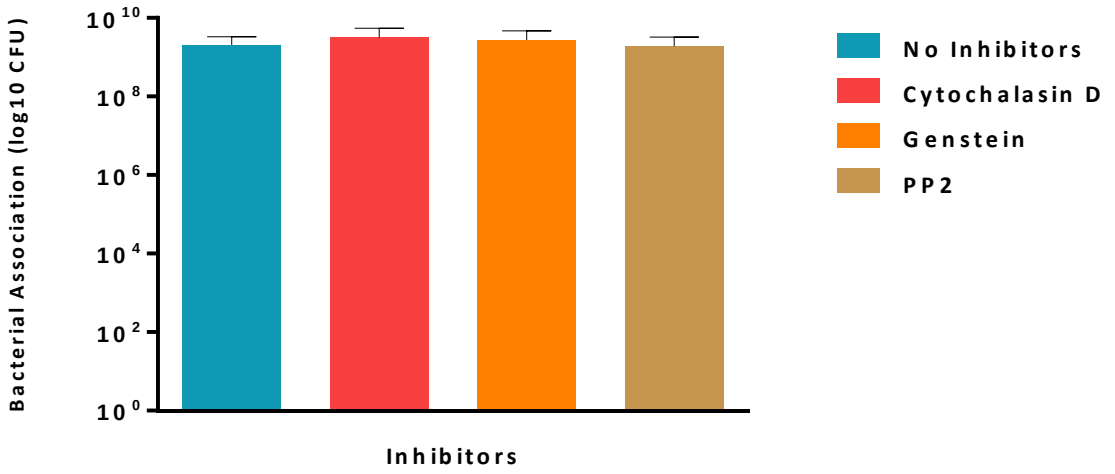

Figure 3.10 Bacterial association to corneal fibroblasts pre-treated with inhibitors

Corneal fibroblasts were pre-treated separately with genistein, PP2, and cytochalasin D for 30 min, and then challenged with 10^7 CFU/mL PAO1 bacteria for 3h, and gentamicin was added for a further 90 min. Bacterial association was not affected by pre-treatment of corneal fibroblasts with genistein, PP2 or cytochalasin D. The bars represent the mean number of bacteria and the error bars the standard error of the mean of 3 independent experiments.

Table 3.5 Difference in bacterial association in the presence and absence of inhibitors

Inhibitors		Mean difference	P-value
No inhibitors	Cytochalasin D	-1078888888.9	0.419
	Genistein	-720333333.3	0.589
	PP2	126555555.6	0.924

* The mean difference is significant at the 0.05 level.

There was no significant difference in bacterial association between pre-treated and untreated fibroblasts

In the gentamicin protection assay, the number of bacteria recovered from corneal fibroblasts pre-treated with the SRC tyrosine kinase general inhibitors genistein and PP2 was significantly less than that from untreated cells (Figure 3.11), and the number of bacteria recovered from corneal fibroblasts pre-treated with cytochalasin D was significantly less than that from untreated cells (Table 3.6), suggesting that the SRC tyrosine kinase system and the actin-microfilament system also plays an important role in bacterial internalization in our model of microbial keratitis (Figure 3.11A).

Upon investigating the presence and upregulation of SRC tyrosine kinase by SDS-PAGE and Western blotting, we found that corneal fibroblasts expressed a higher level of the enzyme compared to uninfected cells, suggesting that the expression of SRC tyrosine kinase is upregulated in response to infection to facilitate bacterial internalization into the cells (Figure 3.11B). Beta actin expression was tested and was equal across all samples, confirming equal expression of proteins in all cells.

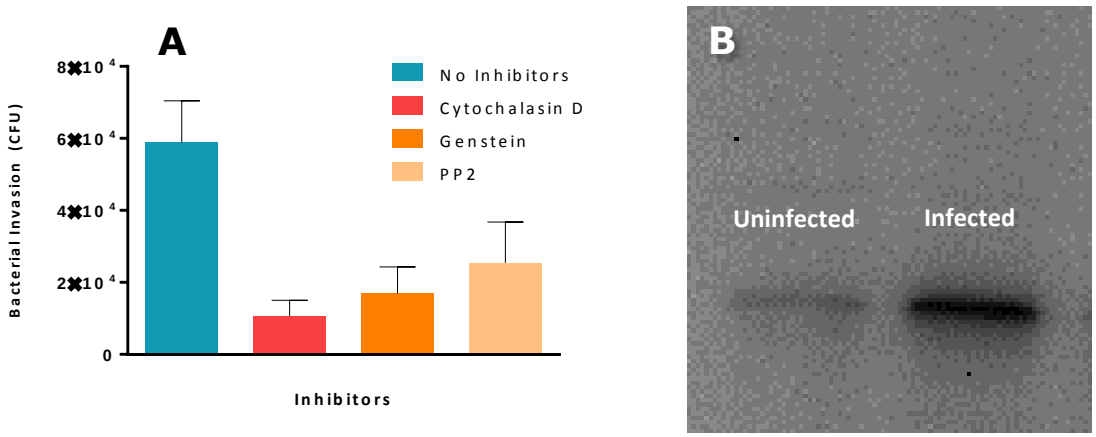

Figure 3.11 Role of SRC tyrosine kinase and the actin microfilament system in bacterial internalisation

Corneal fibroblasts were pre-treated separately with genistein, PP2, and cytochalasin D for 30 min, and then challenged with 10^7 CFU/mL PAO1 bacteria for 3h, and gentamicin was added for a further 90 min. For the Western blot, fibroblasts were challenged with 10^7 CFU/mL PAO1 bacteria for 3h, and then lysed, and the supernatants were run. Genistein, PP2, and cytochalasin D significantly reduced bacterial internalisation into corneal fibroblasts (A), and infected cells demonstrated heightened expression of SRC tyrosine kinase (B). The bars represent the mean number of recovered internalized bacteria and the error bars the standard error of the mean of 3 independent experiments. .

Table 3.6 Comparison between bacterial internalisation in corneal fibroblasts pre-treated with SRC tyrosine kinase and actin microfilament system inhibitors and untreated cells

Inhibitors		Mean difference	P-value
No inhibitors	Cytochalasin D	48244.4*	0.000
	Genistein	41911.1*	0.000
	PP2	33455.6*	0.000

* The mean difference in recovered bacterial counts is significant at the 0.05 level.

The number of recovered bacteria from untreated fibroblasts was significantly higher than that from cells pre-treated with cytochalasin D, Genistein and PP2.

3.3 Bacterial cytotoxic effect on corneal fibroblasts

3.3.1 Lactate dehydrogenase (LDH) Assays

In order to further investigate the apparent death and destruction of cell monolayers induced by PAO1 bacteria, the release of LDH from corneal fibroblasts was quantified. In our experiments, corneal fibroblasts monolayers were infected with bacteria at a MOI ranging from 0.0001 to 1000 to assess the capacity of PAO1 bacteria to induce cell injury. Measurement of LDH release obtained for each bacterial inoculum was converted to a percentage of the maximum LDH release value that was measured from lysed uninfected cells. Measurements were taken at 9h post infection as it was demonstrated from infection experiments (Section 3.1.1) that cell death was most likely to occur at or after this time, and visual inspection of fibroblast monolayers showed them to be mostly intact at 9h. In addition, we found in our pilot experiments that there was no induction of LDH release at 3h and 6h post challenge, and cytotoxicity was not assessed at these time points thereafter. LDH release was detectable at 9h post challenge, and the maximum LDH release occurred at an MOI of 1, after which LDH release declined (Figure 3.12).

3.3.2 Effect of intracellular bacteria on fibroblast viability

Results from invasion experiments suggest that PAO1 bacteria survive and replicate inside gentamicin protected cells (section 3.1.3). We sought to investigate whether this presence had a significant effect on corneal fibroblast viability to gain a better understanding of whether bacterial internalization is a part of the pathogenesis, or if the bacteria invade fibroblasts for a different purpose, for example, as a reservoir for re-infection or to avoid contact with immune cells.

We found that, contrary to infected unprotected fibroblasts, which released significantly higher levels of LDH than uninfected cells, fibroblasts protected with gentamicin, and containing intracellular bacteria, only released LDH in amounts similar to spontaneous release by uninfected cells (Figure 3.13A). There was no significant difference between cytotoxicity in fibroblasts containing intracellular bacteria and uninfected cells at 9 or 24h (Table 3.7), suggesting that cell viability was not affected by the presence of replicating bacteria inside them. This agrees with other evidence, and in one study of intestinal epithelial cells, *L. monocytogenes* was found to multiply readily intracellularly without affecting intestinal epithelial cell viability.[428]

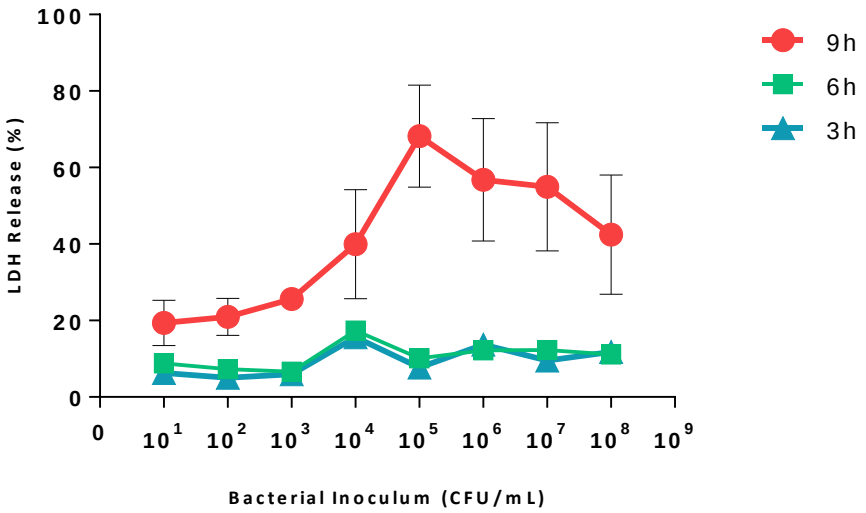

Figure 3.12 LDH release from infected fibroblasts as a percentage of maximum release by complete lysis of cells.

Corneal fibroblasts were challenged with various doses (10^1-10^8 CFU/mL) of PAO1 bacteria for 9h. The cytopathic effect was elucidated at 3, 6 and 9h post challenge. LDH released by infected corneal fibroblasts at 3 and 6h were similar to constitutive levels released by uninfected cells, so cytotoxicity was not assessed at these time points after the pilot experiments. The data symbols represent the mean value of LDH release percentage and the error bars in the 9h curve represent the standard error of the mean of 3 independent experiments. Where no error bars are visible, they fall within the symbol.

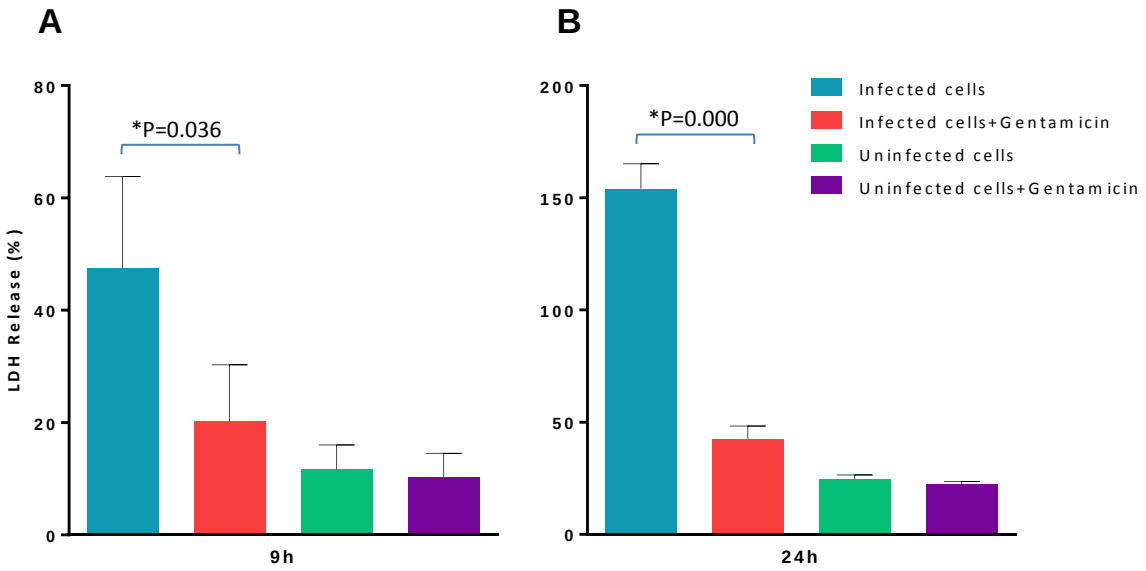

Figure 3.13 Effect of intracellular bacteria on LDH release

Corneal fibroblasts were challenged with 10^7 CFU/mL of PAO1 bacteria for 9 and 24h and gentamicin was added at 3h post challenge to preserve the fibroblasts for the duration of the experiment. LDH release in protected fibroblasts was similar to spontaneous release by unchallenged cells at 9h (A) and at 24h (B). The bars represent the percentage of LDH release, and the error bars represent the standard error of the mean from 3 independent experiments. The asterisks indicate statistically significant differences.

Table 3.7 Comparison between LDH release percentage in infected and unifected fibroblasts with and without gentamicin protection

Cytotoxicity at 9h		**Mean Difference**	**P-value**
Infected	Uninfected	35.86667*	0.036
Infected+Gentamicin	Uninfected	8.66667	0.560
Cytotoxicity at 24h		**Mean Difference**	**P-value**
Infected	Uninfected	129.30000*	0.000
Infected+Gentamicin	Uninfected	17.90000	0.081

* The mean difference is significant at the 0.05 level.

Infected fibroblasts produced significantly higher rise in percentage of LDH release compared to uninfected cells. With gentamicin protection, there was no significant difference in the percentage of LDH release between infected and uninfected cells.

3.3.3 Effect of bacterial virulence on cytotoxicity

Pseudomonas aeruginosa PA14 is a highly virulent strain and is known to be more virulent than the moderately virulent PAO1 strain.[429] We sought to investigate whether higher bacterial virulence impacts the cytotoxic effect of these bacterial strains by comparing LDH release by corneal fibroblasts when infected by those 2 strains.

We found that infection by PA14 caused significantly more LDH release by corneal fibroblasts than PAO1 (Table 3.8) suggesting that higher bacterial virulence induces more cytotoxicity in infected corneal fibroblasts (Figure 3.14).

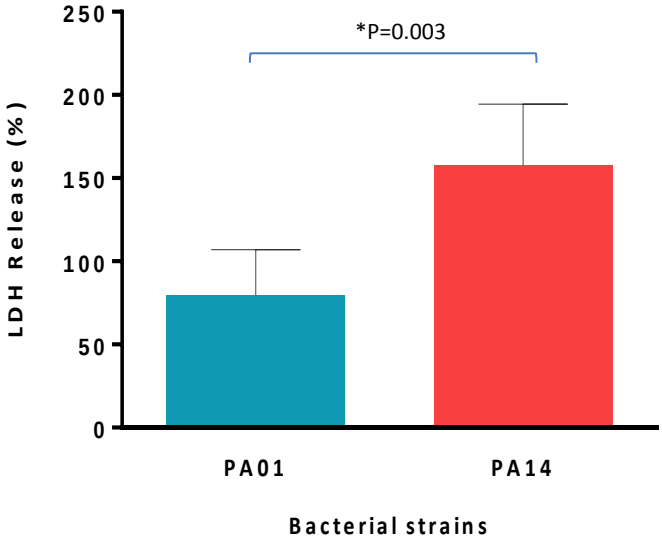

Figure 3.14 Effect of bacterial virulence on LDH release
Corneal fibroblasts were separately challenged with 10^7 CFU/mL PAO1 and PA14 for 9h. Corneal fibroblasts infected with PA14 released significantly more LDH than those infected with PAO1, suggesting that cytotoxity may be correlated with bacterial virulence. The bars represent the percentage of LDH release, and the error bars represent the standard error of the mean from 3 independent experiments. The asterisks indicate statistically significant differences ($p<0.05$).

Table 3.8 Difference between cytotoxicity induced by PA14 and PAO1 strains

Bacterial strains		Mean Difference	P-value
PAO1	PA14	80.56*	0.003

* The mean difference is significant at the 0.05 level.

Fibroblasts infected with PA14 produced a significantly higher rise in percentage of LDH release compared to those infected with PAO1.

To rule out the possibility that the difference in cytotoxicity noticed was due to a variation in bacterial association to fibroblasts, bacterial association was assessed. We found that there was no statistically significant difference in bacterial association between the two strains (Table 3.9), indicating that the difference in cytotoxic effect noted was not because of a difference in the efficiency of association between the two bacterial strains (Figure 3.15).

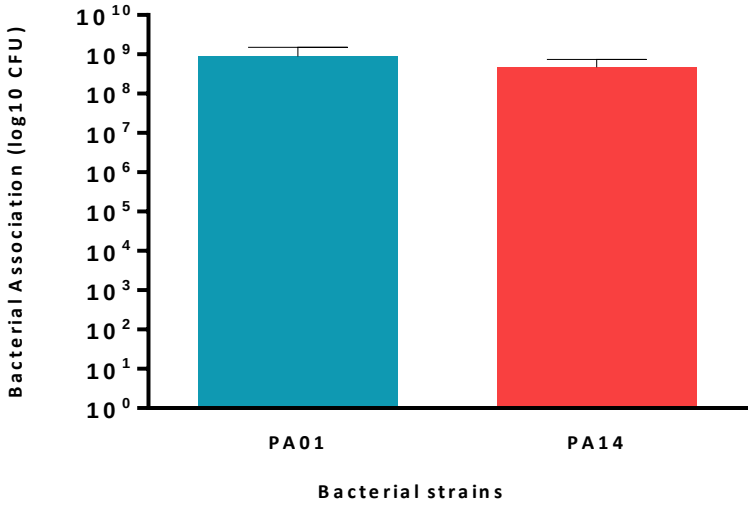

Figure 3.15 Bacterial association to corneal fibroblasts infected with PAO1 and PA14

Corneal fibroblasts were infected with 10^7 CFU/mL of PAO1 and PA14, and bacterial association was assessed at 3h. There was no difference in bacterial association between the 2 strains. The bars represent the number of bacteria, and the error bars represent the standard error of the mean from 3 independent experiments.

Table 3.9 Difference in association between PA14 and PAO1 strains

Bacterial strains		Mean Difference	P-value
PAO1	PA14	415611111.7	0.578

* The mean difference in bacterial counts is significant at the 0.05 level.

There was no significant difference in bacterial association between PAO1 and PA14

3.3.4 The role of flagella and type III secretion system in cytotoxicity

Pseudomonas aeruginosa utilize flagella for motility and association to target cells,[156] and then uses the type III secretion system (TTSS) to inject its toxins into host cells.[213] We sought to investigate the role of these virulence factors in inducing cytotoxicity is corneal fibroblasts during acute microbial keratitis. Our experiments on the effect of bacterial virulence on cytotoxicity showed that the more virulent PA14 causes more cytotoxicity to fibroblasts, so we used a wild type PA14 strain and compared it to mutant strains PA14*Δpopb* deficient in the PopB translocator protein essential for normal TTSS function, and PA14*ΔflgK* deficient in flagella.

We found that corneal fibroblasts challenged with mutant strains PA14*Δpopb* and PA14*ΔflgK* released significantly less LDH than fibroblasts challenged with wild type PA14, suggesting that the cytotoxic effect of *P. aeruginosa* is highly dependent on their flagella and type III secretion systems (Figure 3.16). The difference between cytotoxicity induced by PA14*Δpopb* and by PA14*ΔflgK* was not statistically significant (Table 3.10).

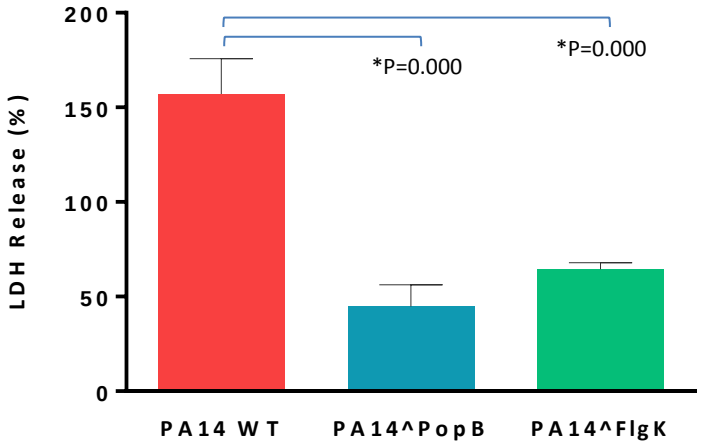

Figure 3.16 The role of bacterial flagella and type III secretion system in bacterial cytotoxic effects
Corneal fibroblasts were separately challenged with 10^7 CFU/mL wild type PA14 and mutant strains PA14*Δpopb* and PA14*ΔflgK* for 9h. Corneal fibroblasts infected with mutant PA14 deficient in flagella and TTSS released less LDH than those infected with wild type PA14, suggesting that these virulence factors play an important role in inducing cytotoxity. The bars represent the percentage of LDH release, and the error bars represent the standard error of the mean from 3 independent experiments. The asterisks indicate statistically significant differences ($p<0.05$).

Table 3.10 Difference between cytotoxicity induced by wild type and mutant PA14 strains

Bacterial strains		Mean difference	P-value
PA14 WT	PA14*Δpopb*	112.33*	0.000
	PA14*ΔflgK*	92.67*	0.000
PA14*ΔflgK*	PA14*Δpopb*	19.67	0.287

* The mean difference in percentage of LDH release is significant at the 0.05 level.

To rule out the possibility that the difference in cytotoxicity noticed was due to a variation in bacterial association to fibroblasts, bacterial association was assessed. We found that, although associated bacteria were numerically less in PA14FlgK than the other strains (Figure 3.17), there was no statistically significant difference in bacterial association between the three mutant strains (Table 3.11). This might be explained by the presence of other intact bacterial association mechanisms, such as the pilus, which is normal in all strains, so the bacteria can associate to some extent to the fibroblasts, but cannot cause cytotoxicity to the same extent as the wild type strain, suggesting that cytotoxicity might be flagellum dependent as well.

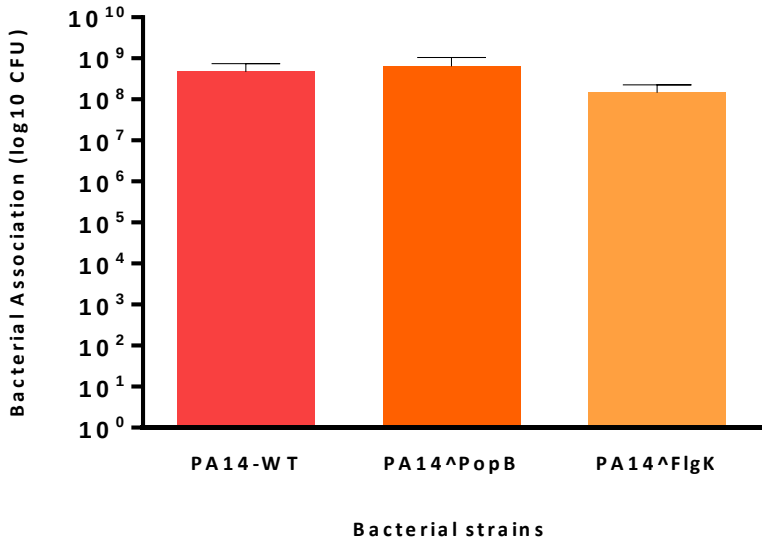

Figure 3.17 Bacterial Association to fibroblasts infected with wild type and mutant PA14

Corneal fibroblasts were infected with 10^7 CFU/mL of wild type PA14 and mutant strains PA14*Δpopb* and PA14*ΔflgK*, and bacterial association was assessed at 3h. There was no difference in bacterial association between the 3 strains. The bars represent the number of bacteria, and the error bars represent the standard error of the mean from 3 independent experiments.

Table 3.11 Difference in association between wild type and mutant PA14 strains

Bacterial strains		Mean difference	P-value
PA14 WT	PA14*Δpopb*	-170122222.6	0.693
	PA14*ΔflgK*	318255555.3	0.467

* The mean difference in bacterial counts is significant at the 0.05 level.

There was no significant difference in bacterial association between wild type and mutant PA14 strains.

Chapter 4 : **RESULTS**

CORNEAL FIBROBLAST RESPONSE TO PSEUDOMONAS AERUGINOSA INFECTION

4.1 Cytokine production by corneal fibroblasts

4.1.1 Cytokine production in response to live PAO1 infection

Culture supernatants from all infection experiments were collected and analysed for pro-inflammatory cytokine release by corneal fibroblasts. Cytokines tested included Interleukin-1 beta (IL-1ß), Granulocyte macrophage-colony stimulating factor (GM-CSF), Interferon gamma(IFN-γ), Interleukin-2 (IL-2), Interleukin-6 (IL-6), Interleukin-8 (IL-8), Interleukin-10 (IL-10), Interleukin-12 (IL-12) and Tumour necrosis factor alpha (TNF-α). In the initial experiments, supernatants were collected at 24h, by which point complete destruction of cell monolayers was observed for all infecting doses. Results showed that with the exception of IL-1ß, which showed significantly higher levels of release (P =0.004), all tested cytokines showed lower levels than constitutive levels released by uninfected cells (Figure 4.1).

4.1.2 Cytokine production by infected corneal fibroblasts protected with gentamicin

We hypothesized that the above results were due to destruction of corneal fibroblasts before they had a chance to release the cytokines, and that IL-1ß was possibly produced early before fibroblast destruction was significant. To test this hypothesis, we challenged the fibroblasts with bacteria for 3h, then added gentamicin to kill all extracellular bacteria and protect the fibroblasts for the remainder of the 24h period. We found that cytokine levels were higher, to varying degrees, in infected cells than controls for most tested cytokines (Figure 4.2); however, the differences were not statistically significant, with the exception of IL-1ß and GM-CSF, which showed significantly higher levels (Table 4.1). This may indicate that, when given enough time, corneal fibroblasts upregulate their release of pro-inflammatory cytokines in response to live infection by PAO1 bacteria.

4.1.3 Early cytokine production by infected corneal fibroblasts

To test whether IL-1ß was released early shortly after challenge, culture supernatants were collected at 9h post challenge, with and without the addition of gentamicin at 3h. We found that IL-1ß release by infected fibroblasts was higher than that by uninfected controls (Figure 4.3), although the difference was not statistically significant (Table 4.2). All other tested cytokines showed lower levels than uninfected controls with and without gentamicin protection (data not shown), which may merely reflect the amount of cell loss caused by 9h of bacterial challenge.

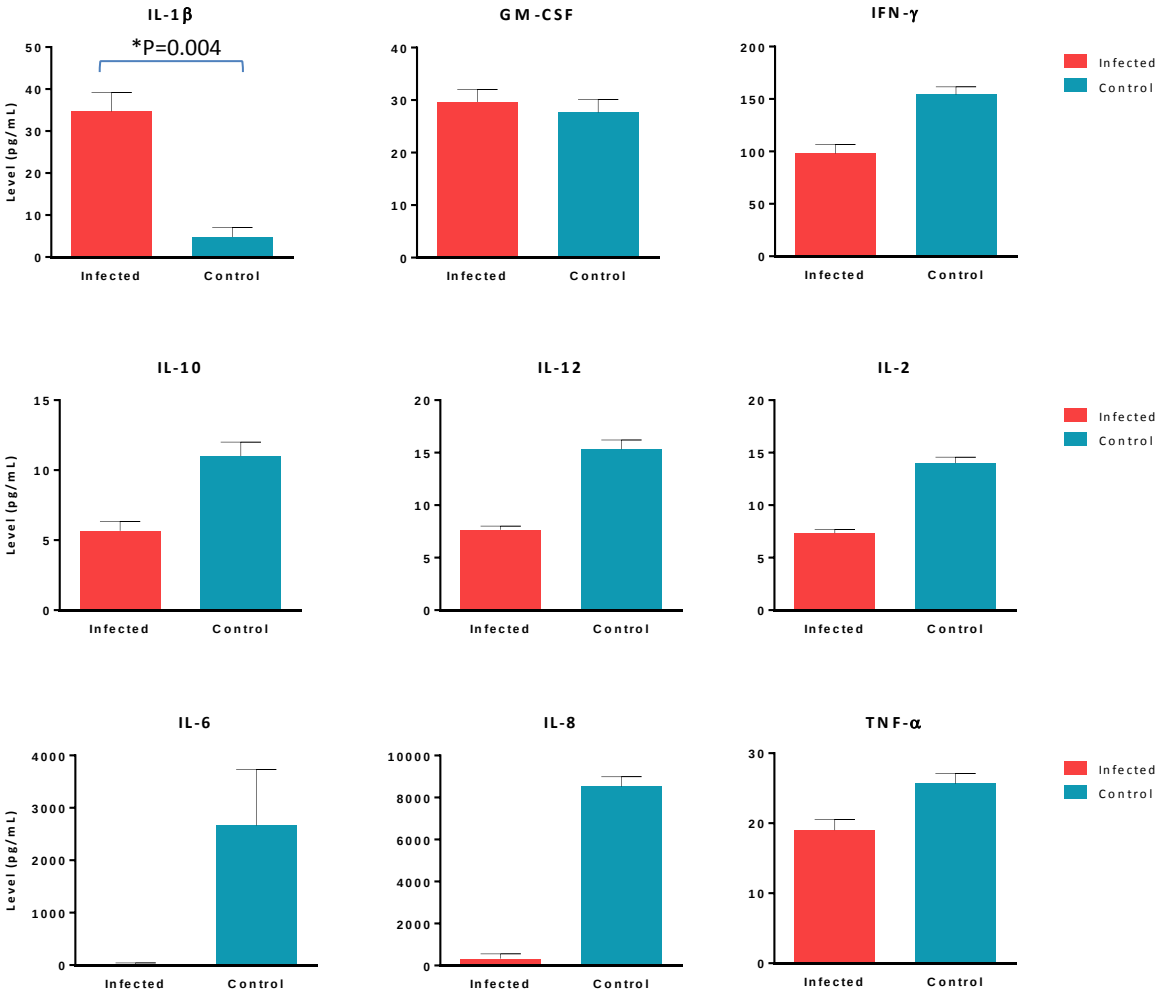

Figure 4.1 Cytokine production with live uninterrupted infection of corneal fibroblasts.

Corneal fibroblasts were infected with 10^7 CFU/mL of live bacteria for 24h, and supernatants were tested for cytokine levels by a sandwich immune technique. All tested cytokines demonstrated lower levels than constitutive release by uninfected cells, with the exception of IL-1ß, which was higher. The bars represent the mean level of cytokine release, and the error bars represent the standard error of the mean from 3 independent experiments. The asterisk represents statistically significant difference ($p<0.05$).

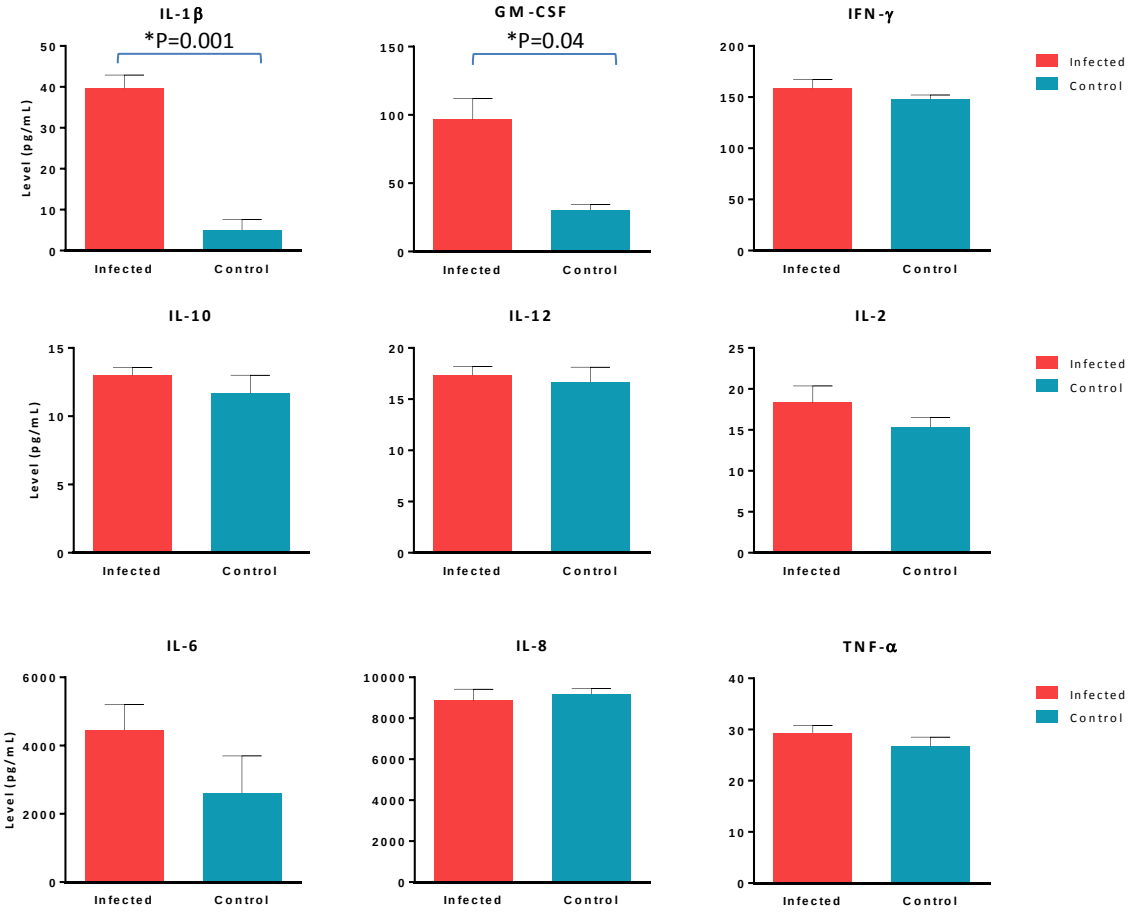

Figure 4.2. Cytokine production with gentamicin protection of corneal fibroblasts.

Corneal fibroblasts were infected with 10^7 CFU/mL of live bacteria for 24h, and gentamicin was added at 3h post challenge to preserve the fibroblasts for the duration of the experiment. Infected protected fibroblasts produced significantly higher levels of IL-1β and GM-CSF than uninfected cells, although the difference was not statistically significant with the other tested cytokines. The bars represent the level of cytokine release, and the error bars represent the standard error of the mean from 3 independent experiments. The asterisks represent statistically significant differences ($p<0.05$).

Table 4.1 Comparison between cytokine levels released by uninfected cells and corneal fibroblasts protected with gentamicin after 24h of bacterial challenge.

Cytokine	Infection		Mean difference	P-Value
IL-1ß	Infected	Uninfected	34.68*	0.001
GM-CSF	Infected	Uninfected	66.33*	0.041
IFN-γ	Infected	Uninfected	10.67	0.337
IL-10	Infected	Uninfected	1.33	0.433
IL-12	Infected	Uninfected	0.67	0.719
IL-2	Infected	Uninfected	3.00	0.286
IL-6	Infected	Uninfected	1845.00	0.243
IL-8	Infected	Uninfected	322.00	0.644
TNF-α	Infected	Uninfected	2.67	0.324

* The mean difference (pg/mL) is significant at the 0.05 level.

The level of cytokines released by infected fibroblasts was significantly higher than that by uninfected cells.

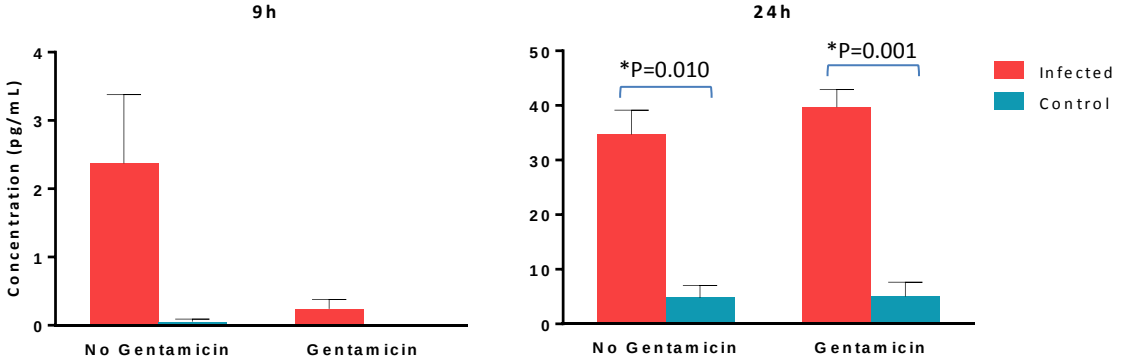

Figure 4.3. IL-1ß production by infected corneal fibroblasts at 9 and 24h post challenge as compared to uninfected controls.

Corneal fibroblasts were infected with 10^7 CFU/mL of live bacteria for 9 and 24h, and gentamicin was added at 3h post challenge to preserve the fibroblasts for the duration of the experiment. Infected fibroblasts produced a higher level of IL-1ß than uninfected cells. The bars represent the level of cytokine production, and the error bars represent the standard error of the mean from 3 independent experiments. The asterisks represent statistically significant differences ($p<0.05$).

Table 4.2 Comparison between IL-1ß release by corneal fibroblasts protected with gentamicin and uninfected cells after 9 and 24h of bacterial challenge.

Time	**No gentamicin protection**		**Mean difference**	**P-Value**
9h	Infected	Uninfected	2.32	0.148
24h	Infected	Uninfected	29.90*	0.010
Time	**Gentamicin protection**		**Mean difference**	**P-Value**
9h	Infected	Uninfected	0.23	0.230
24h	Infected	Uninfected	34.68*	0.001

* The mean difference is significant at the 0.05 level.

The level of IL-1ß released by infected fibroblasts was significantly higher than that by uninfected cells at 24h, regardless of gentamicin protection.

4.1.4 The role of individual bacterial cellular components on cytokine production

To investigate whether corneal fibroblasts produced cytokines in response to individual bacterial components to an extent similar to their response to infection by live bacteria, we tested the levels of IL-1ß production. Similar to section 4.1.4, we used 3 different cell lines from 3 different donors and although there was some inter-donor variability, we found that, while fibroblasts challenged with live bacteria produced significantly higher levels of IL-1ß (Table 4.3), fibroblasts challenged with heat killed bacteria, freeze-thaw killed bacteria and lipopolysaccharide produced IL-1ß in levels similar to constitutive levels produced by unchallenged cells, suggesting that IL-1ß production is related to active interaction between the fibroblasts and the live bacteria rather than in response to certain exotoxins or bacterial cellular components (Figure 4.4). Lysed uninfected fibroblasts Released slightly higher IL-1ß level than uninfected cells (Figure 4.4), and the difference was statistically significant in one out of the three donors, but not significant in the other two (Table 4.3).

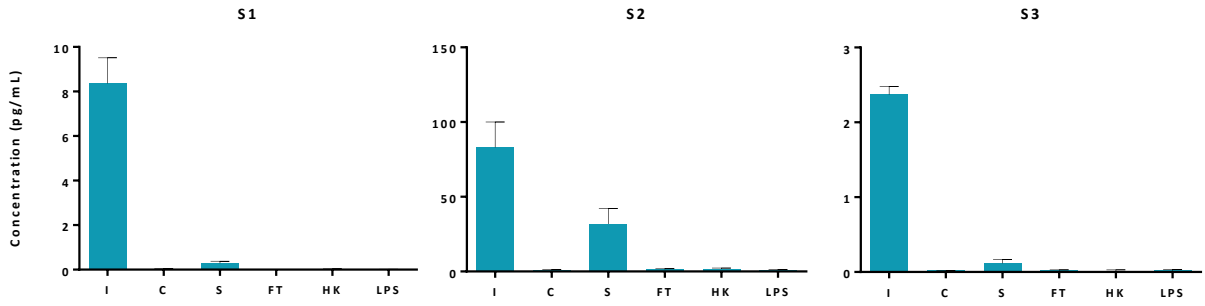

Figure 4.4 Interleukin-1ß production by corneal fibroblasts in response to challenge with live bacteria and various exotoxins and bacterial cellular components

Corneal fibroblasts were challenged with with 10^7 CFU/mL of live bacteria (I), heat killed bacteria (HK), freeze-thaw killed bacteria (FT) and lipopolysaccharide (LPS). Controls included uninfected cells (C) and lysed uninfected cells (S). At 24h, infected fibroblasts produced higher levels of IL-1ß levels than uninfected or bacterial component-challenged cells. The bars represent the level of cytokine release, and the error bars represent the standard error of the mean from 3 independent experiments. S1,S2 and S3 are cell lines from different donor

Table 4.3 Difference between IL-1ß production by lysed uninfected corneal fibroblasts, and cells challenged with live bacteria and various exotoxins and bacterial cellular components

Cell Line	IL-1ß concentration (pg/mL)		Mean difference	P-Value
S1	Infected	Heat killed	8.33333*	0.000
		Freeze-thaw killed	8.35333*	0.000
		Lipopolysaccharide	8.35000*	0.000
		Lysed uninfected	8.07000*	0.000
		Uninfected	8.32667*	0.000
	Uninfected	Heat killed	0.00667	0.992
		Freeze-thaw killed	0.02667	0.966
		Lipopolysaccharide	0.02333	0.971
		Lysed uninfected	-0.25667	0.685
S2	Infected	Heat killed	81.14000*	0.000
		Freeze-thaw killed	81.57000*	0.000
		Lipopolysaccharide	81.99000*	0.000
		Lysed uninfected	51.22667*	0.000
		Uninfected	82.14667*	0.000
	Uninfected	Heat killed	-1.00667	0.928
		Freeze-thaw killed	-0.57667	0.958
		Lipopolysaccharide	-0.15667	0.989
		Lysed uninfected	-30.92000*	0.013
S3	Infected	Heat killed	2.35795*	0.000
		Freeze-thaw killed	2.35376*	0.000
		Lipopolysaccharide	2.35599*	0.000
		Lysed uninfected	2.25525*	0.000
		Uninfected	2.35163*	0.000
	Uninfected	Heat killed	0.00632	0.923
		Freeze-thaw killed	0.00213	0.974
		Lipopolysaccharide	0.00436	0.947
		Lysed uninfected	-.09638	0.154

* The mean difference is significant at the 0.05 level.

4.1.5 Effect of bacterial virulence on cytokine production

As discussed above, *P. aeruginosa* PA14 is more virulent than PAO1, and our results show that this higher virulence is associated with a more potent cytotoxic effect on corneal fibroblasts. We sought to investigate whether higher bacterial virulence also impacts IL-1ß production by corneal fibroblasts, as we hypothesized that a more virulent strain may be associated with more damage to the cornea, and hence, the amount of cytokine produced might be released earlier and in higher amounts to stop the offending pathogen.

We used 3 different cell lines from 3 different donors, and analyzed IL-1ß production at 9 and 24h. Although we noticed some variability in cytokine production between the different donors, we found that at 9h, infection by PA14 caused significantly more IL-1ß production by corneal fibroblasts than PAO1 for each cell line (Table 4.4). At 24h, however, IL-1ß production was higher with infection by PAO1 than with infection by PA14, possibly due to earlier destruction of fibroblasts by the more virulent PA14 (Figure 4.5), which also reflects the higher pattern of cytotoxicity seen with PA14 (section 3.3.3). This suggests that higher bacterial virulence induces an earlier and more potent IL-1ß production, which is in agreement with our hypothesis.

4.1.6 The role of flagellin and type III secretion system in cytokine production

Our experiments on the effect of bacterial virulence factors on its cytotoxic effects on corneal fibroblasts demonstrate that mutant bacteria deficient in the type III secretion system and flagella induce significantly less cytotoxic effects on corneal fibroblasts than wild type bacteria (Section3.3.4). We sought to investigate if these same virulence factors had a similar effect on IL-1ß production by corneal fibroblasts; especially that higher bacterial virulence was associated with an earlier and more potent IL-1ß production (as described above).

Similar to section 4.1.4, we used three different cell lines from three different donors, and analyzed IL-1ß production at 9 and 24h. Although we noticed the same variability in cytokine production between the different donors, we found that at 9h, infection by wild type PA14 caused significantly more IL-1ß production by corneal fibroblasts than mutant PA14 strains PA14*Δpopb* and PA14*ΔflgK* for each cell line (Table 4.5). At 24h, however, similar to the pattern observed in section 4.1.4, IL-1ß production was higher with infection by mutant PA14 strains PA14*Δpopb* and PA14*ΔflgK* than with infection by wild typePA14, although the difference was occasionally not statistically significant (Figure 4.6 and Table 4.5).

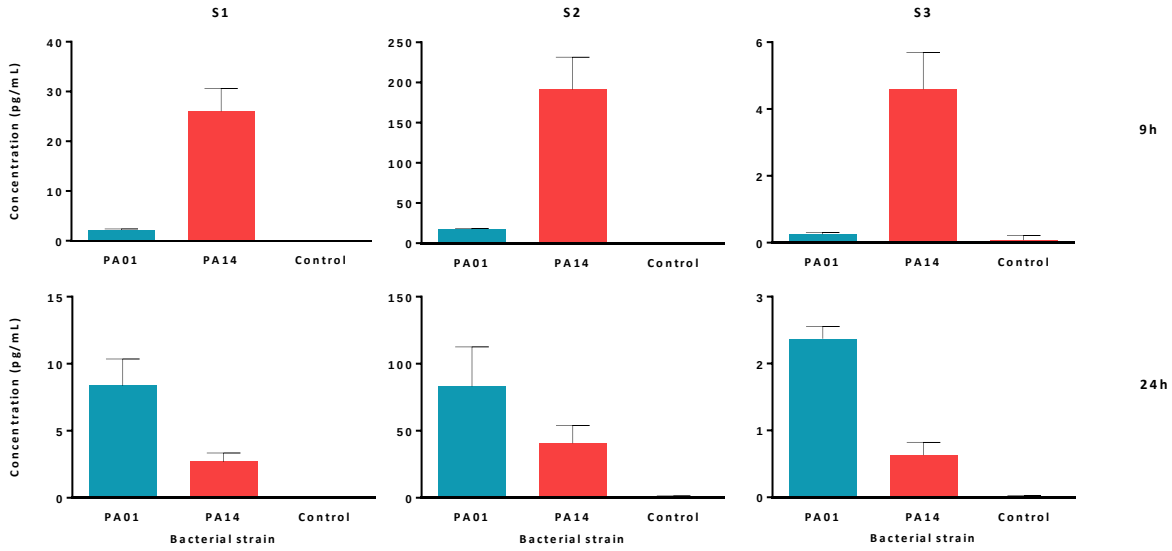

Figure 4.5 Effect of bacterial virulence on cytokine production
Corneal fibroblasts were infected with 10^7 CFU/mL of PAO1 and PA14 for 24h and supernatants were collected at 9 and 24h. Cytokine production was compared between fibroblasts infected with PAO1 bacteria (PAO1), PA14 bacteria (PA14) and uninfected cells (control). At 9h, corneal fibroblasts infected with PA14 produced more IL-1ß than those infected with PAO1, whereas at 24h, this pattern was reversed. The bars represent the level of cytokine release, and the error bars represent the standard deviation from 3 independent experiments (n=3).

Table 4.4 Difference in IL-1β production between fibroblasts challenged with PA14 and with PAO1 across 3 different cell lines

Time	Cell Line	IL-1ß concentration (pg/mL)		Mean difference	P-Value
9h	**S1**	PAO1	PA14	-23.8*	0.012
	S2	PAO1	PA14	-173.9*	0.002
	S3	PAO1	PA14	-4.3*	0.021
24h	**S1**	PAO1	PA14	5.7*	0.029
	S2	PAO1	PA14	42.3	0.086
	S3	PAO1	PA14	1.7*	0.000

* The mean difference in IL-1ß levels (pg/mL) is significant at the 0.05 level.

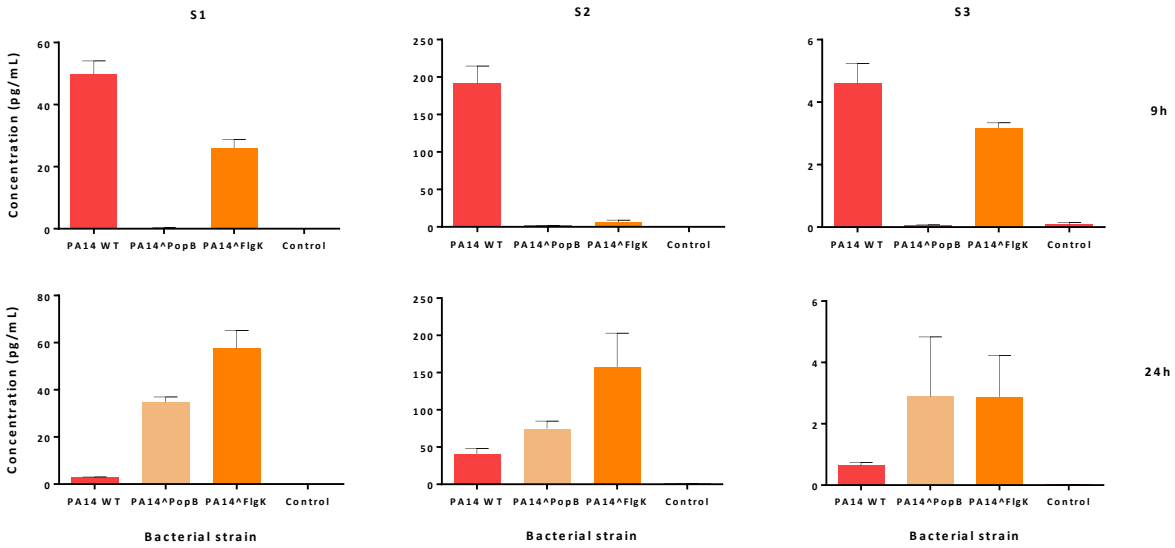

Figure 4.6 The role of bacterial flagella and type III secretion system in cytokine production

Corneal fibroblasts were infected with 10^7 CFU/mL of wild type PA14 and mutant strains PA14*Δpopb* and PA14*ΔflgK* for 24h and supernatants were collected at 9 and 24h. Cytokine production was compared between fibroblasts infected with different PA14 strains (PA14WT, PA14*Δpopb* and PA14*ΔflgK)* and uninfected cells (control). At 9h, corneal fibroblasts infected with wild type PA14 produced more IL-1ß than those infected with mutant PA14 strains PA14*Δpopb* and PA14*ΔflgK*, whereas at 24h, this pattern was reversed, although the difference was mostly not statistically significant. The bars represent the level of cytokine release, and the error bars represent the standard deviation from 3 independent experiments.

Table 4.5 Difference in cytokine production between corneal fibroblasts infected with wild type PA14 and with mutant PA14 strains PA14*Δpopb* and PA14*ΔflgK*

Time	Cell Line	IL-1ß concentration (pg/mL)		Mean difference	P-Value
9h	**S1**	PA14 WT	PA14*Δpopb*	49.4*	0.000
			PA14*ΔflgK*	23.7*	0.001
		PA14*ΔflgK*	PA14*Δpopb*	25.7*	0.001
	S2	PA14 WT	PA14*Δpopb*	189.4*	0.000
			PA14*ΔflgK*	185.2*	0.000
		PA14*ΔflgK*	PA14*Δpopb*	4.2	0.832
	S3	PA14 WT	PA14*Δpopb*	4.5*	0.000
			PA14*ΔflgK*	1.4*	0.039
		PA14*ΔflgK*	PA14*Δpopb*	3.1*	0.001
24hh	**S1**	PA14 WT	PA14*Δpopb*	-32.0*	0.003
			PA14*ΔflgK*	-54.8*	0.000
		PA14*ΔflgK*	PA14*Δpopb*	22.8*	0.013
	S2	PA14 WT	PA14*Δpopb*	-33.9	0.412
			PA14*ΔflgK*	-116.9*	0.023
		PA14*ΔflgK*	PA14*Δpopb*	83.0	0.075
	S3	PA14 WT	PA14*Δpopb*	-2.24854	0.290
			PA14*ΔflgK*	-2.24595	0.291
		PA14*ΔflgK*	PA14*Δpopb*	-.00259	0.999

* The mean difference in IL-1ß levels (pg/mL) is significant at the 0.05 level.

4.2 Matrix Metalloprotease (MMP) Production by Corneal Fibroblasts

4.2.1 Gelatine Zymography

In order to assess whether MMPs were produced by corneal fibroblasts in response to bacterial components or endotoxins, or whether it was related to exotoxins released by live bacteria, our live infection model was tested against different controls with isolated bacterial virulence factors and cellular components. These controls included heat killed (HK) bacteria, which preserved the cellular integrity of the bacteria with all the cell wall and membrane associated virulence factors; freeze-thaw (FT) killed bacteria, which destroyed the cell wall and membrane exposing all intracellular components and virulence factors without denaturing them, and pure *Pseudomonas aeruginosa* lipopolysaccharide (LPS). Our positive controls included bacteria alone with no cells and lysed uninfected fibroblasts. A subset of fibroblasts was treated with gentamicin 3h post challenge to test whether intracellular bacteria had a different effect on MMP production. Culture supernatants were collected at 9 and 24h to test whether there was a difference in MMP production between early and late stages of infection.

We found that fibroblasts challenged with HK bacteria, FT bacteria and LPS produced a constitutive 65 kDa gelatinase, possibly inactive MMP-2, similar to unchallenged cells. The same was true for cells treated with gentamicin after 3h of infection. Bacteria alone produced a 54 kDa gelatinase, possibly alkaline protease, whereas fibroblasts challenged by live bacteria released several gelatinases that were specific to the interaction between them and live bacteria. These could be other bacterial gelatinases only released upon contact with host cells, other host gelatinases, degradation products of MMP-2 and MMP-9 or a combination of the above. Our pilot experiments showed that there was no change in MMP production from constitutive levels at 9h for all challenging factors, and MMP production was not tested at this time point thereafter.

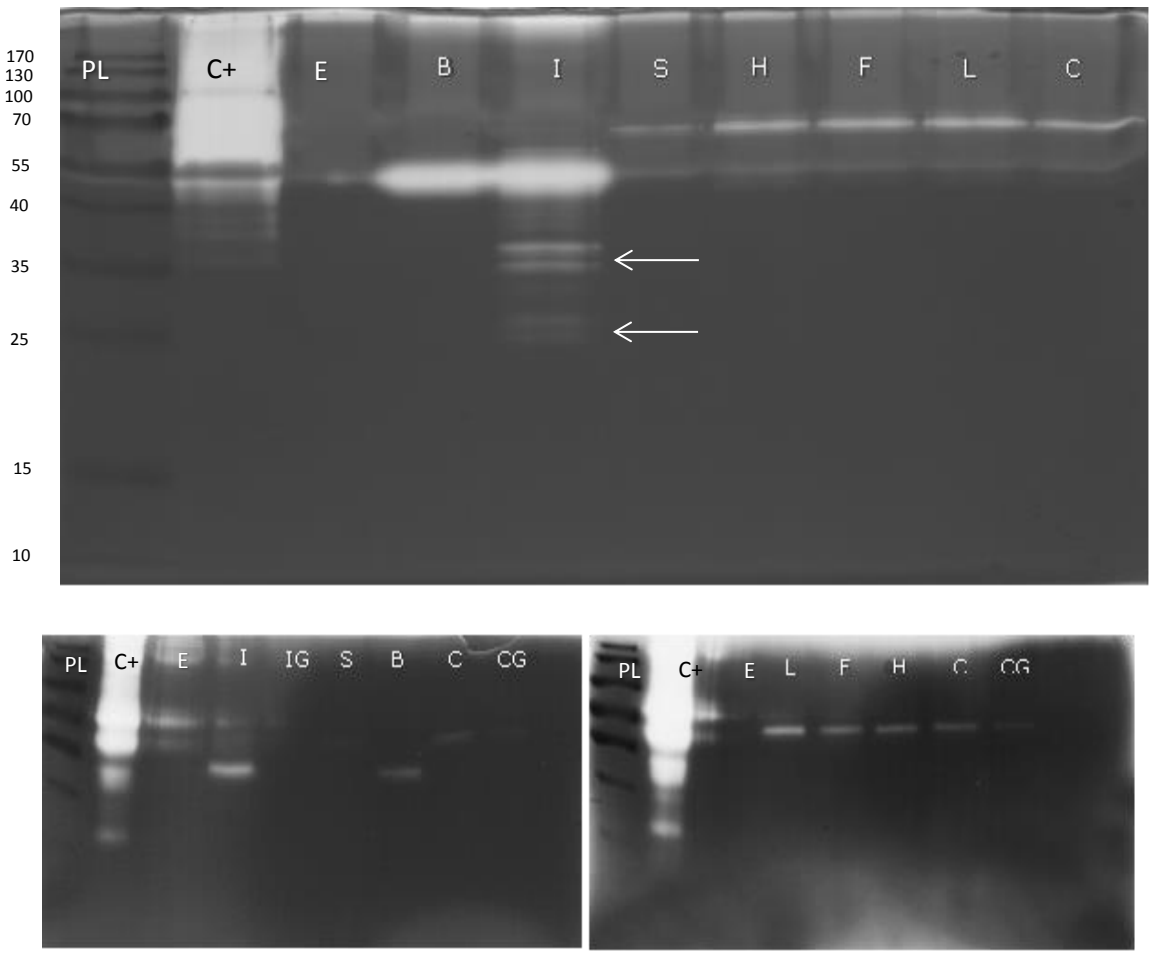

Figure 4.7 Gelatine zymogram showing MMP release by corneal fibroblasts.

Corneal fibroblasts were challenged with live bacteria and controls for 24h. In the upper gel, the two well on the left contain the protein ladder (PL) and the MMP positive control (C+). The third well had no samples (E). B represents bacteria alone, I is cells challenged with live bacteria, S is lysed uninfected cells, H is cells challenged with heat killed bacteria, F is cells challenged with freeze/thaw killed bacteria, L is cells challenged with LPS, and C is unchallenged cells. In the lower 2 gels, IG is infected cells treated with gentamicin 3h post challenge, and CG is uninfected treated with gentamicin 3h post challenge. The light coloured bands represent areas in the gelatin gel digested by the MMPs as they deposit according to their weight during the gel electrophoresis. The arrows point to MMPs released in response to live infection.

4.2.2 Sandwich immunoassay

4.2.2.1 Effect of individual cellular components on MMP production

The results of our gelatine zymography show that infected corneal fibroblasts released specific gelatinases only in response to challenge by live bacteria. We sought to further identify those gelatinases by specifically investigating the presence of MMP-1, MMP-2, MMP-3 and MMP-9 in culture supernatants. MMP-1, also known as interstitial collagenase, MMP-2 and MMP-9, also known as gelatinase A and B, respectively, and MMP-3, also known as stromelysin-1, are all zinc dependant endopeptidases that play important roles in extracellular matrix degradation, leukocyte migration and immune modulation associated with acute infections.[430] By using a sandwich immunoassay technique, we were able to detect the levels of expression of these MMPs in our model of microbial keratitis.

We found that infected corneal fibroblasts produced a higher level of MMP-1 and MMP-9 than constitutive secretion by uninfected cells, although the difference was not statistically significant, and individual cellular components produced MMP levels similar to uninfected cells, which supports our zymography results.

With regard to MMP-2 and MMP-3, infected fibroblasts produced a lower level of MMPs than uninfected cells, whereas individual bacterial cellular components produced MMP-2 levels similar to uninfected cells and MMP-3 levels lower than uninfected cells. This may indicate that challenge of corneal fibroblasts by live bacteria or individual cellular components can inhibit the production of, or destroy the already produced, MMP-2 and MMP-3.

4.2.2.2 Effect of gentamicin protection on MMP production

Because we noticed a difference in cytokine production between corneal fibroblasts protected with gentamicin and unprotected fibroblasts (section 4.1.2), we sought to investigate whether gentamicin protection would have a similar effect on MMP production. We found that with gentamicin protection, the level of MMP-1, MMP-3 and MMP-9 produced by corneal fibroblasts was significantly higher than with no protection (Table 4.6), although the difference in production between infected and uninfected gentamicin protected fibroblasts was not statistically significant (Figure 4.9). For MMP-2, however, gentamicin protection did not have any effect on MMP production by fibroblasts, and MMP-2 production by infected fibroblasts was consistently lower than constituent levels. We hypothesized that this may be related to the destruction or inhibition of production of the MMP by the bacteria. Lysed uninfected cells released MMP levels slightly higher than constitutive levels, with the exception of MMP-3 where the level was lower than constitutive.

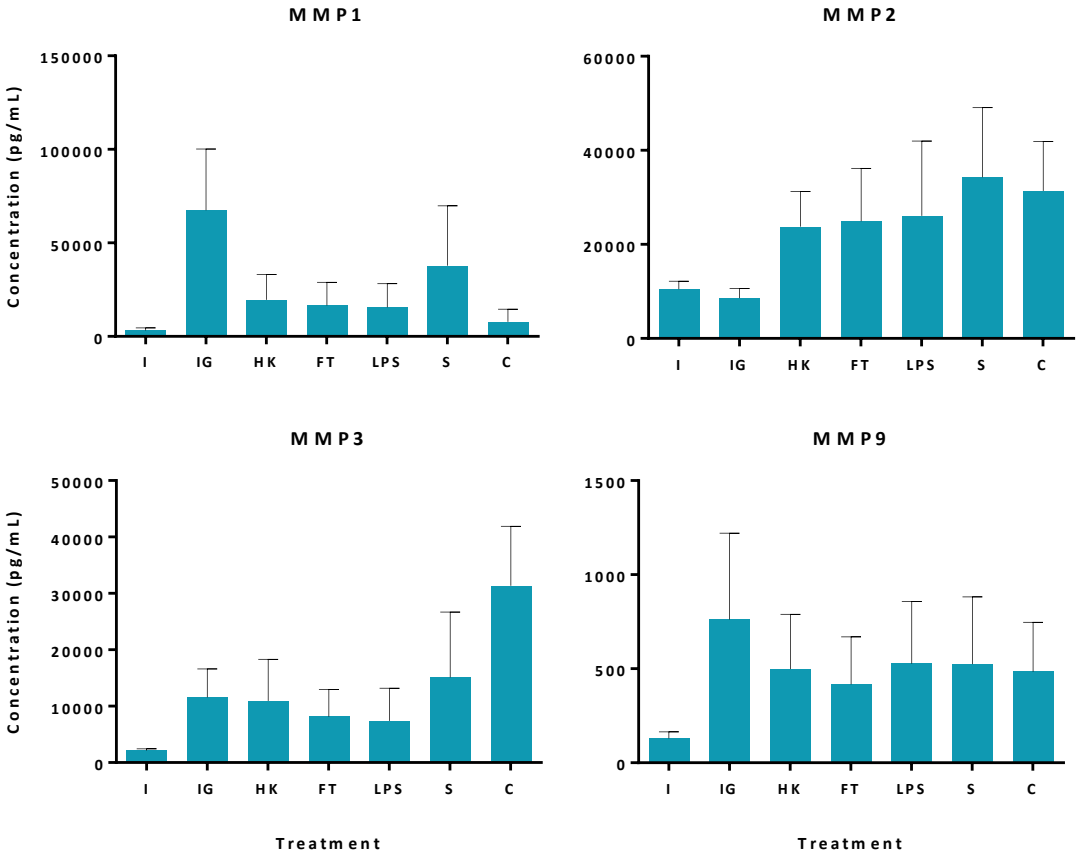

Figure 4.8 MMP production by corneal fibroblasts in response to challenge with live bacteria and individual bacterial components

Corneal fibroblasts were infected with 10^7 CFU/mL of live bacteria (I), 10^7 CFU/mL of live bacteria with gentamicin protection (IG), heat killed bacteria (HK), freeze-thaw killed bacteria (FT) and lipopolysaccharide (LPS). Controls included uninfected cells (C) and lysed uninfected cells (S), and MMP production was assessed by a sandwich immunoassay technique at 24h. The levels of MMP-1 and MMP-9 produced by infected fibroblasts were higher than those produced by uninfected cells, whereas the levels of MMP-2 and MMP-3 were lower than constitutive levels. Individual cellular components induced a similar level of production of MMPs by corneal fibroblasts, except for MMP-3, where the levels were higher. The bars represent the level of MMP production, and the error bars represent the standard error of the mean from 3 independent experiments.

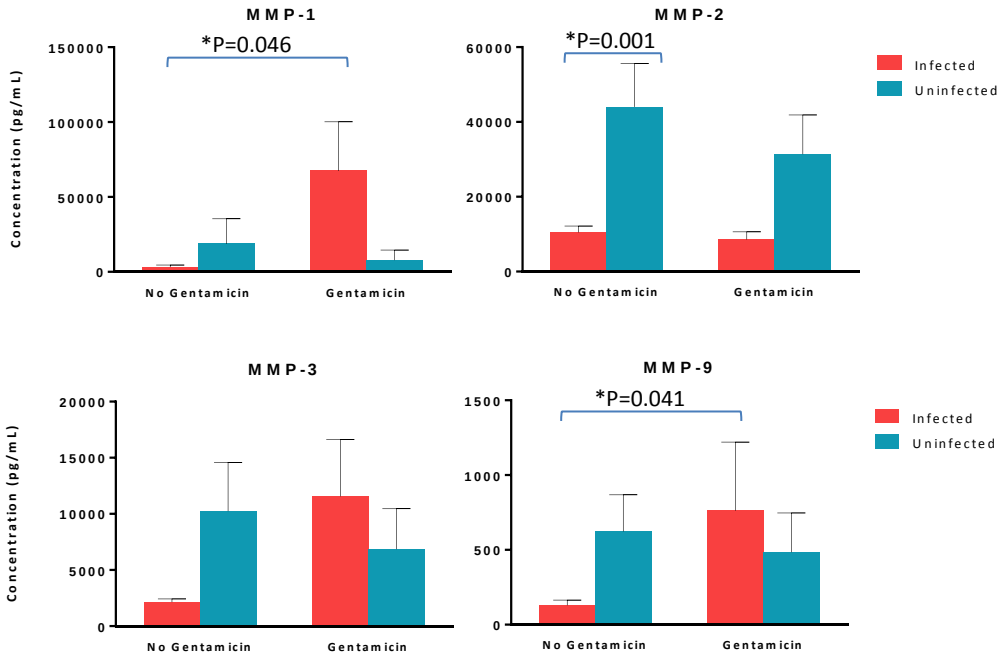

Figure 4.9 MMP production by fibroblasts protected by gentamicin and unprotected cells

Corneal fibroblasts were infected with 10^7 CFU/mL of PAO1 and gentamicin was added at 3h post challenge to preserve the fibroblasts for the duration of the experiment. Corneal fibroblasts protected with gentamicin produced more MMPs than uninfected cells, with the exception of MMP-2, where the level of production by infected cells was consistently lower than constitutive levels. The bars represent the level of MMP production, and the error bars represent the standard error of the mean from 3 independent experiments.

Table 4.6 MMP production by infected gentamicin protected and unprotected corneal fibroblasts

MMP	Gentamicin protection		Mean difference	P-Value
MMP-1	Protected	Unprotected	64265*	0.046
MMP-2	Protected	Unprotected	1915.1	0.363
MMP-3	Protected	Unprotected	9419.4*	0.026
MMP-9	Protected	Unprotected	631.6*	0.041

* The mean difference is significant at the 0.05 level.

Table 4.7 MMP production by infected and uninfected gentamicin protected fibroblasts

MMP	Infection		Mean difference	P-Value
MMP-1	Infected	Uninfected	40351.5	0.182
MMP-2	Infected	Uninfected	-22795.9*	0.001
MMP-3	Infected	Uninfected	3667.3	0.371
MMP-9	Infected	Uninfected	215.5	0.471

* The mean difference is significant at the 0.05 level.

4.2.2.3 Effect of bacterial virulence on MMP production

As discussed above, *P. aeruginosa* PA14 is more virulent than PAO1, and our results show that this higher virulence is associated with a higher level of cytokine production and a more potent cytotoxic effect on corneal fibroblasts. We sought to investigate whether higher bacterial virulence also impacts MMP production by corneal fibroblasts, and whether there was a difference in production between the different MMPs. Because we observed a higher cytokine production at 9h (Section 4.1.4), we decided to also assess MMP production at 9h as well as 24h.

We found that, contrary to cytotoxicity and cytokine production, infection of corneal fibroblasts with the more virulent PA14 did not result in production of higher levels of MMPs at 9h (Figure 4.10). This is consistent with the results of our earlier experiments that showed that there was no significant MMP production at 9h (Section 4.1.4) and the even lower detected level of MMPs may be secondary to a faster destruction of corneal fibroblasts by PA14 compared to PAO1 before they were able to produce the MMPs.

Similarly, at 24h, the level of MMP production by corneal fibroblasts infected with PA14 was lower than the level by fibroblasts infected with PAO1. This is also probably due to the faster destruction of corneal fibroblasts by PA14 before they were able to produce the MMPs.

4.2.2.4 The role of flagellin and type III secretion system in MMP production

Our experiments on the effect of bacterial virulence factors on corneal fibroblast cytotoxicity and cytokine production demonstrate that mutant bacteria deficient in the type III secretion system and flagella induce significantly less cytotoxic effects on corneal fibroblasts and less cytokine production than wild type bacteria (Sections 4.1.5 and 4.1.6). We sought to investigate if these virulence factors had an impact on MMP production by corneal fibroblasts, and whether there was a difference between different time points, so we investigated MMP production at 9 and 24h.

We found that at both 9 and 24h, corneal fibroblasts infected with wild type PA14 produced less MMPs than mutant PA14 strains PA14*Δpopb* and PA14*ΔflgK* (Figure 4.12 and Figure 4.13), although the difference was mostly statistically significant at 9h and non-significant at 24h (Table 4.10 and Table 4.11). We hypothesized that this reflects the pattern of cytotoxicity, where the cells are destroyed earlier by the more virulent wild type strain before they were able to produce the MMPs.

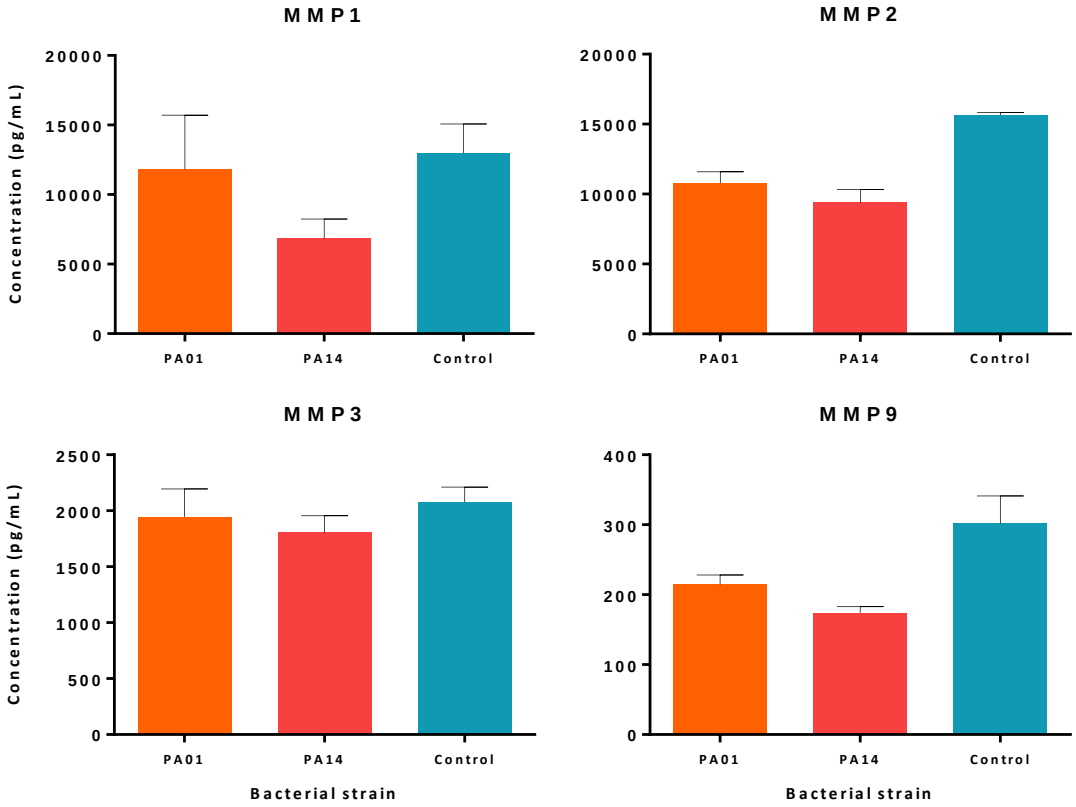

Figure 4.10 MMP production by corneal fibroblasts infected with PAO1 and PA14 at 9h

Corneal fibroblasts were infected with 10^7 CFU/mL of PA14 and PAO1 for 9h. Infection with PA14 did not induce a higher level of MMP production by corneal fibroblasts than infection with PAO1. The bars represent the level of MMP production, and the error bars represent the standard error of the mean from 3 different experiments.

Table 4.8 Difference in MMP production between fibroblasts infected with PAO1 and PA14 at 9h

MMP	MMP concentration (pg/mL)		Mean difference	P-Value
MMP-1	PAO1	PA14	4981.6	0.107
MMP-2	PAO1	PA14	1413.3	0.117
MMP-3	PAO1	PA14	138.9	0.455
MMP-9	PAO1	PA14	40.4*	0.012

* The mean difference is significant at the 0.05 level.

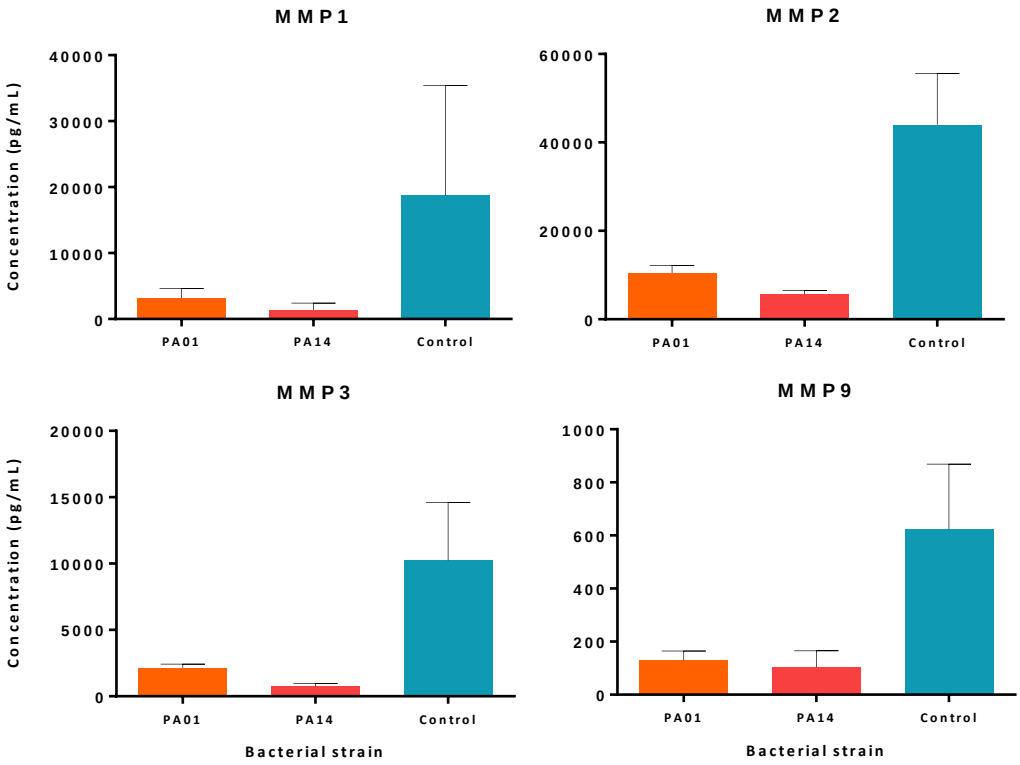

Figure 4.11 MMP production by corneal fibroblasts infected with PAO1 and PA14 at 24h

Corneal fibroblasts were infected with 10^7 CFU/mL of PA14 and PAO1 for 24h. Infection with PA14 did not induce a higher level of MMP production by corneal fibroblasts than infection with PAO1. The bars represent the level of MMP production, and the error bars represent the standard error of the mean from 3 different experiments.

Table 4.9 Difference in MMP production between fibroblasts infected with PAO1 and PA14 at 24h

MMP	MMP concentration (pg/mL)		Mean difference	P-Value
MMP-1	PAO1	PA14	1807.4	0.364
MMP-2	PAO1	PA14	4812.6	0.060
MMP-3	PAO1	PA14	1397.6*	0.020
MMP-9	PAO1	PA14	25.5	0.735

* The mean difference is significant at the 0.05 level.

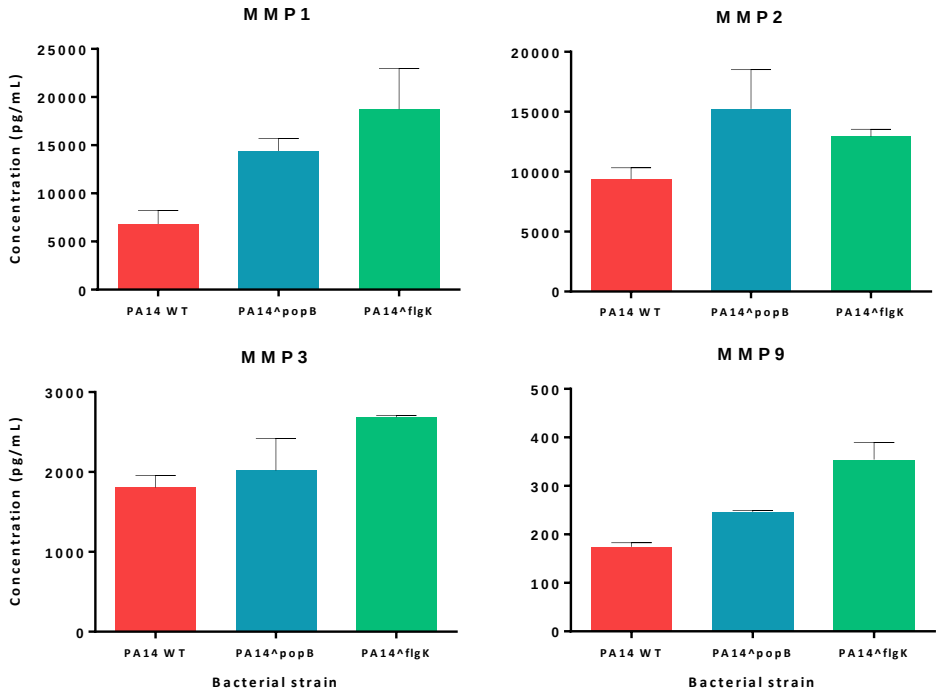

Figure 4.12 MMP production by corneal fibroblasts infected with wild type and mutant PA14 strains at 9h

Corneal fibroblasts were infected with wild type PA14 and mutant PA14 strains PA14*Δpopb* and PA14*ΔflgK* for 9h, and MMP production was assessed. Fibroblasts infected with wild type PA14 produced less MMPs than those infected with mutant strains PA14*Δpopb* and *PA14ΔflgK.* The bars represent the level of MMP production, and the error bars represent the standard deviation of the mean from 3 different experiments.

Table 4.10 Difference in MMP production between corneal fibroblasts infected for 9h with wild type and mutant PA14 strains

MMP	MMP concentration (pg/mL)		Mean difference	P-Value
MMP-1	PA14 WT	PA14*Δpopb*	-7587.90300*	0.013
		PA14*ΔflgK*	-11920.19300*	0.002
	PA14*ΔflgK*	PA14*Δpopb*	4332.29000	0.094
MMP-2	PA14 WT	PA14*Δpopb*	-5862.85200*	0.011
		PA14*ΔflgK*	-3546.75867	0.072
	PA14*ΔflgK*	PA14*Δpopb*	-2316.09333	0.204
MMP-3	PA14 WT	PA14*Δpopb*	-211.60900	.338
		PA14*ΔflgK*	-879.86833*	.005
	PA14*ΔflgK*	PA14*Δpopb*	668.25933*	0.017
MMP-9	PA14 WT	PA14*Δpopb*	-72.08080*	0.006
		PA14*ΔflgK*	-179.98297*	0.000
	PA14*ΔflgK*	PA14*Δpopb*	107.90217*	0.001

* The mean difference is significant at the 0.05 level.

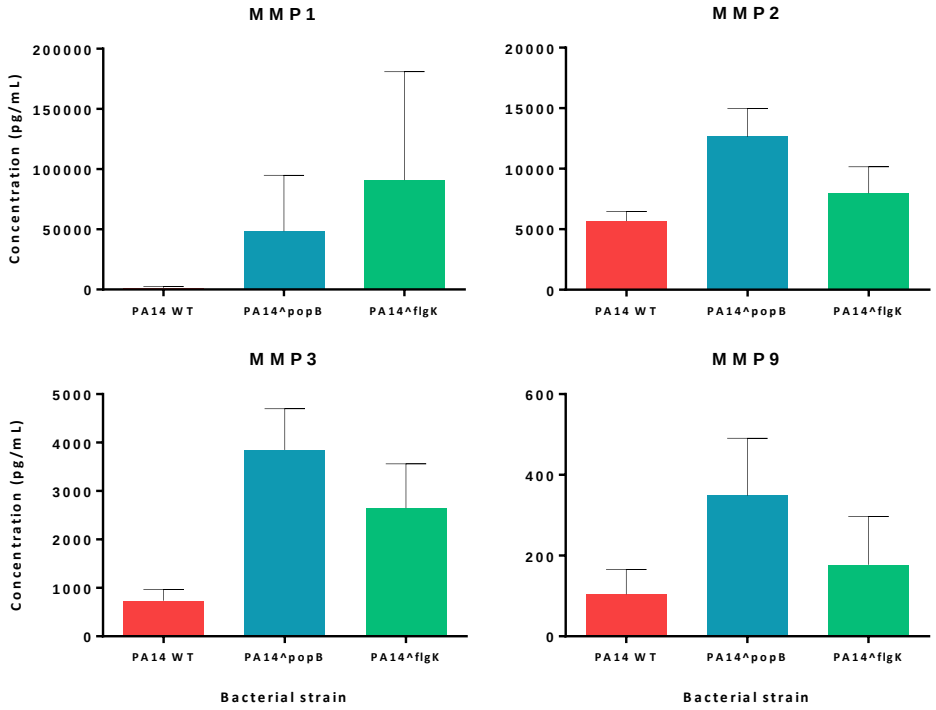

Figure 4.13 MMP production by corneal fibroblasts infected with wild type and mutant PA14 strains at 24h

Fibroblasts infected with wild type PA14 produced less MMPs than those infected with mutant strains PA14*Δpopb* and *PA14ΔflgK.* The bars represent the level of MMP production, and the error bars represent the standard deviation of the mean from 3 different experiments.

Table 4.11 Difference in MMP production between corneal fibroblasts infected for 24h with wild type and mutant PA14 strains

MMP	MMP concentration (pg/mL)		Mean difference	P-Value
MMP-1	PA14 WT	PA14*Δpopb*	-47100.37433	0.589
		PA14*ΔflgK*	-89594.60487	0.320
	PA14*ΔflgK*	PA14*Δpopb*	42494.23053	0.626
MMP-2	PA14 WT	PA14*Δpopb*	-6961.82500*	0.041
		PA14*ΔflgK*	-2288.59700	0.427
	PA14*ΔflgK*	PA14*Δpopb*	-4673.22800	0.133
MMP-3	PA14 WT	PA14*Δpopb*	-3110.90840*	0.024
		PA14*ΔflgK*	-1909.44473	0.115
	PA14*ΔflgK*	PA14*Δpopb*	-1201.46367	0.291
MMP-9	PA14 WT	PA14*Δpopb*	-244.77193	.176
		PA14*ΔflgK*	-73.07958	.663
	PA14*ΔflgK*	PA14*Δpopb*	-171.69235	0.323

* The mean difference is significant at the 0.05 level.

Chapter 5 : **RESULTS**

INTERACTIONS OF PSEUDOMONAS AERUGINOSA WITH THE CORNEA AS AN ORGAN

5.1 Model Design

In Descemet's stripping endothelial keratoplasty (DSEK) partial corneal transplants procedures, only the donor corneal endothelium and a small part of the posterior stroma are used in the procedure [Figure 5.1 (A)], leaving behind the majority of the stroma, Bowman's layer and the epithelium [Figure 5.1 (B)] to be discarded.

After obtaining the necessary ethical approvals, the left over donor DSEK buttons were collected and used for the experiments. These buttons were live and contained all the anatomical components of the cornea involved in early microbial keratitis, and so, when infected with bacteria in a controlled environment, they provided a good model for human corneal infection, albeit without the tears, nerves, blood vessels and immune cells. Such arrangement is probably more representative of infectious crystalline keratopathy (ICK), where the infection is associated with little or no corneal or the anterior segment inflammation, usually due to a local or systemic immunocompromised state.[431, 432] In these cases, the absence of the host immune response allows for the visualization of the formation and spread of the infection through the transparent cornea.[432]

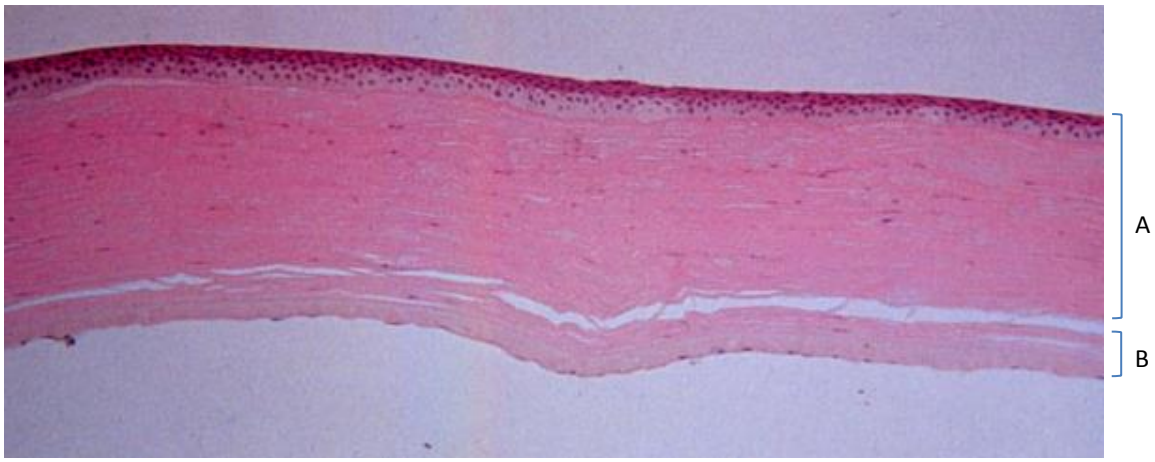

Figure 5.1 Human corneal DSEK button model

The anterior part of the cornea (A), comprising the epithelium and the majority of the stroma, is used in our model. The posterior part (B) is used in corneal endothelial transplant procedures (DSEK)

5.2 Bacterial association to the corneal epithelium

5.2.1 Scanning electron microscopy

Pseudomonas aeruginosa bacteria were shown to associate to and penetrate the superficial layers of the murine corneal epithelium up to the anterior basement membrane.[173] We sought to investigate the association and penetration of PAO1 bacteria with whole-layer human corneal epithelium by SEM. Figure 5.2 A and B show the appearance of the normal corneal epithelium with the characteristic smooth surface and the normal minimal exfoliation of superficial epithelial cells.

When infected with PAO1 bacteria for 3h, the epithelial surface appeared much rougher, and the number of exfoliating cells increased dramatically (Figure 5.2 C and D). With higher magnifications, the bacteria appeared to associate to the surface of the superficial epithelial cells, and some appeared to be invading those cells (Figure 5.2 E and F). This mechanism of exfoliating superficial epithelial cells is an important defence mechanism whereby the bacterial load is reduced and thus minimizing the number of bacteria progressing further through the tissue.

In order to investigate the penetration of bacteria in the event of an epithelial breech, the epithelial barrier was overcome by scoring the surface of the buttons before infecting them. PAO1 bacteria appeared to associate to superficial and deeper cells within the score, possibly penetrating to deeper tissue (See Figure 5.4).

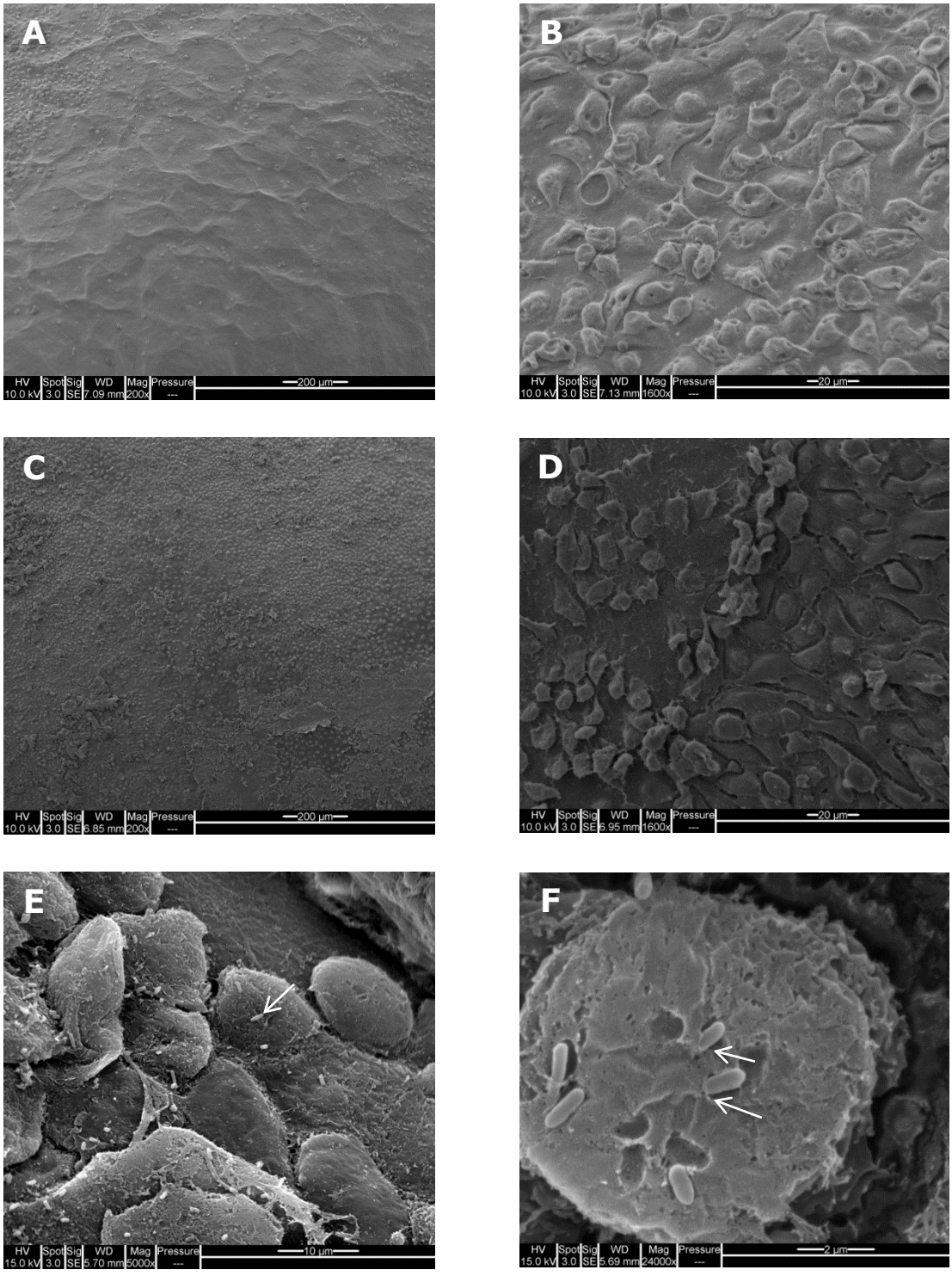

Figure 5.2 Scanning electron micrograph of bacterial association to the intact corneal epithelium.

Whole corneal buttons were infected with 10^7 CFU/mL of bacteria for 3h before being fixed and processed for SEM. A and B are scans of uninfected buttons; C, D, E and F are infected buttons with increasing magnification. The arrows point to bacteria adhering to (E) and penetrating the surface of (F) superficial cells [Original magnification; A and C= x200, B and D= x1600, E= x5000 and F= x24000].

5.3 Bacterial penetration into corneal stroma

5.3.1 Light Microscopy

In studies of murine models of microbial keratitis, bacteria could not penetrate the intact epithelial basement membrane, mainly because the size of its pores is too small for bacteria to pass through.[173] In our model, vertical scores were made so that they bypass the epithelial basement membrane and extend deep into the stroma, and we used both scarified and non-scarified corneal buttons to test the ability of bacteria to penetrate deeper into the stroma in the presence or absence of an intact basement membrane.

Figure 5.3 shows a light microscopic section of a scored button, showing the depth of the scores. The scores were made so that they bypass the epithelial basement membrane and into the stroma. Epithelial cells were seen to migrate to fill the gap as part of the normal wound healing response, which demonstrates that these corneal buttons are viable, with normally active cells. This is important, as it means that this model closely resembles a clinical situation, and the interactions seen here between bacteria and live corneal epithelial and stromal cells may be very similar to what occurs in a real-life human microbial keratitis.

5.3.2 Transmission electron microscopy (TEM)

In our SEM examination of scored corneal buttons, bacteria were seen to possibly associate to deeper cells within the scores, but the extent of the penetration could not be assessed due to the limitation of SEM (Figure 5.4). To further assess the penetration of bacteria into the stroma, TEM was used to examine sections of the infected corneal buttons taken at the level of the epithelial scores. In the button with an intact basement membrane, although the bacteria could penetrate through the layers of epithelium to reach the basement membrane, they were seen to line up on its epithelial side, but no bacteria were seen penetrating into the adjacent stroma (Figure 5.5 A). In the scarified button, however, the area of the epithelial score showed epithelial cells migrating to fill it, and PAO1 bacteria could be seen within the score and gaining access into the adjacent stroma (Figure 5.5 B, C and D). At later time points, bacteria were seen to start aggregating into a colony, seemingly establishing the infection within the stroma (Figure 5.5 E and F).

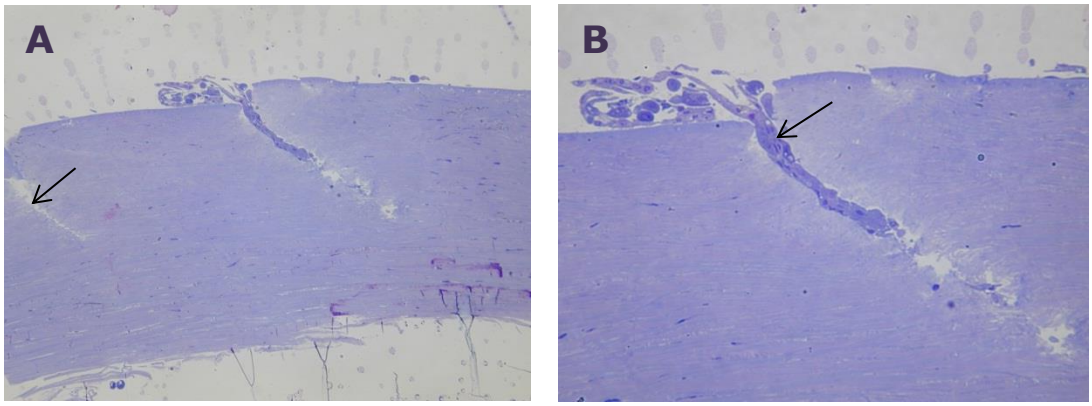

Figure 5.3 Light micrograph of human corneal button.

Whole corneal buttons were infected with 10^7 CFU/mL of bacteria for 3h. The corneal epithelium was scarified by a needle to bypass the basement membrane and allow the bacteria to penetrate into the stroma (A, arrow). Epithelial cell can be seen migrating to fill the gap in a classical wound healing response (B, arrow).

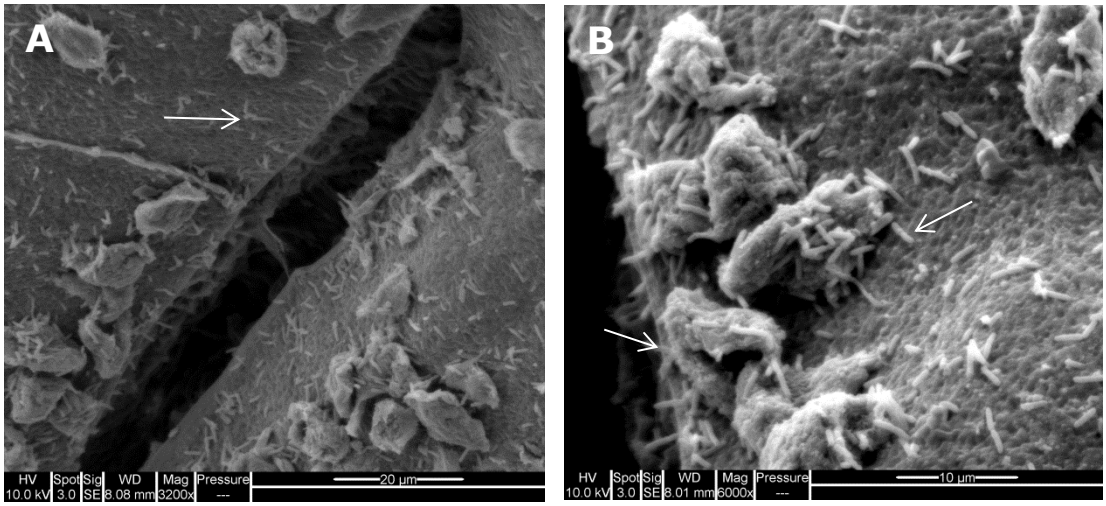

Figure 5.4 Scanning electron micrograph of bacterial association to scarified corneal epithelium

Whole corneal buttons were infected with 10^7 CFU/mL of bacteria for 3h. Bacteria (arrows) associated to the surface of superficial cells (A, original magnification= x3200), and possibly deeper cells within the score (B, original magnification= x6000).

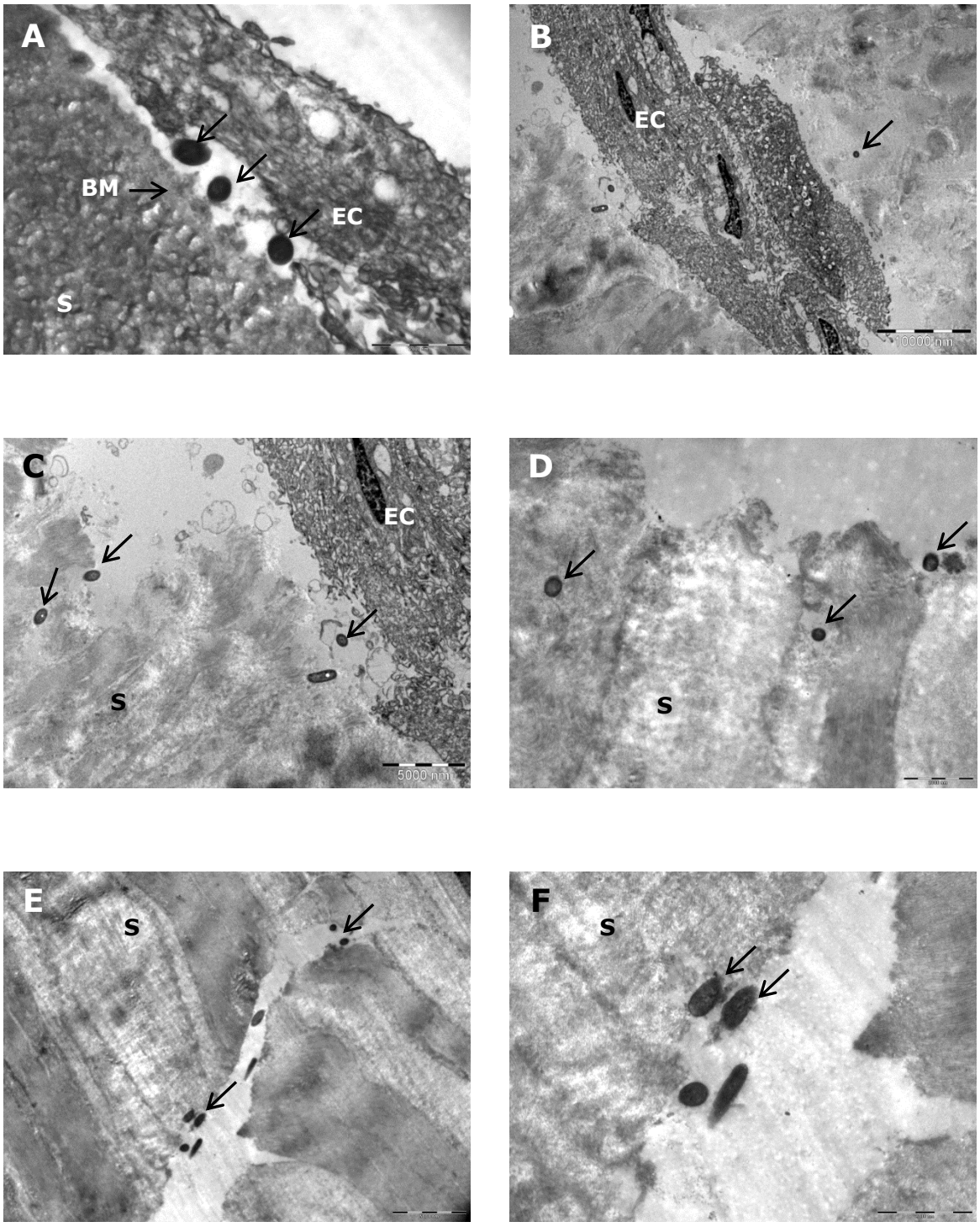

Figure 5.5 Transmission electron micrograph of bacterial penetration into the corneal stroma.

Corneal buttons were challenged 10^7 CFU/mL of bacteria for 3 and 9h before fixation and processing. The arrows point to bacteria penetrating into the stroma (S), and epithelial cells (EC) are seen to be migrating into the score. [Original magnification; A and C= x200, B and D= x1600, E= x5000 and F= x24000]

Chapter 6 : **DISCUSSION**

6.1 Host-pathogen interactions in microbial keratitis

On the cellular level, we hypothesized that if corneal fibroblasts do have a role in immune activation, they probably interact with bacteria on different levels, and that this interaction possibly leads to the release of cytokines and/or other mediators that modulate the immune system and possibly recruit immune cells. There are several main interactions between pathogens and host cells. The first essential step for further pathogen/host interactions is association of the bacteria to the host cells;[433] then there is invasion and dissemination, which enables bacteria to propagate within the tissue and reach new sites; and cytotoxicity, which is related to the virulence and pathogenicity of the offending pathogen. Host cell response is a subsequent important interaction that normally follows some or all of the other pathogen/host interactions.

6.1.1 *P. aeruginosa* bacteria associate to corneal fibroblasts

Association of bacteria to cell surfaces is a primary essential step in bacterial colonization of the tissue at the onset of infection.[434, 435] In our model, when the initial multiplicity of infection (MOI) was lower than or equal to 0.1 CFU/mL, PAO1 bacteria associated to primary corneal fibroblasts in a linear dose- and time-dependant manner up to 9h post challenge, which is consistent with other systems with well-established host-pathogen interactions.[436] When the MOI was higher, however, the association was almost at its highest at 3h post challenge and did not increase much on subsequent time points. This is probably due to saturation of fibroblast monolayers with bacteria, and also due to cell destruction, which we have noted to start at 9h with MOI of 1 CFU/mL or higher. At 24h post challenge, severe cytotoxicity and complete monolayer destruction was noted with all infecting doses, indicating that cytotoxicity is indeed another important interaction in this model.

We also demonstrated that mutant PAO1 bacteria deficient in PilA, responsible for normal TFP functions, could not associate efficiently to corneal fibroblasts, neither could bacteria deficient in FliM, essential for normal flagellar functions, which confirms the role of these two important adhesins in the pathogenesis of microbial keratitis, and paves the way for investigating possible therapeutic strategies targeting them. This is consistent with infection models in other systems. In a murine pulmonary infection model, mutant *P.aeruginosa* PAK strains deficient in PilA and FliC led to significantly lower rates of pneumonia and mortality in infected mice.[155] Mutant PAO1 strains deficient in PilA and FliM demonstrated deficient cap formations in their biofilms.[437]

The association of bacteria to host cells involves specialized interactions between bacterial adhesins and their specific receptors on the surface of target cells.[161] *P.aeruginosa* adhesins include alginate,[438] surface-associated exoenzyme S,[439] the flagellum,[156] the pilus,[160] and outer

membrane proteins.[440] The pilus is believed to be involved in the initial contact between the bacteria and the target cell, mainly due to of its extension from the cell surface, and type IV pilus (TFP) accounts for about 90% of the association capability of *P. aeruginosa* to human lung cells.[161]

Integrins and cadherins are among the known cellular receptors for bacterial association.[441] Integrins are a family of cell surface receptors that recognize specific ECM submolecular structures, and bacteria were found to utilize integrins to associate to many extracellular matrix molecules, including fibronectin, collagens, laminin, elastin, heparin, heparan sulphate, and chondroitin sulphate[442]. Saccharide epitopes of globo series cell membrane glycolipids,[443] and mannosylated integral membrane glycoproteins (uroplakins) have been shown to be involved in bacterial association in *E.coli* cystitis.[444] Piliated bacteria can also bind to immunoglobulins, such as CD147, which was shown to be a vascular endothelial cell receptor for *N. meningitides* infection.[445] Glycoconjugates, such as glycolipids, glycosylated proteins, and proteoglycans, act as receptors for *P. aeruginosa* binding in respiratory infections, and they demonstrate distinct apical and basolateral localization for the polarized airway epithelial cells.[446]

6.1.2 *P. aeruginosa* bacteria invade corneal fibroblasts

Another important host-pathogen interaction is bacterial internalization into host cells. In our model, *P. aeruginosa* invasion of corneal fibroblasts could be detected by 3h post challenge, although it was a relatively rare event, occurring in about 2% of the time. This is probably because in a clinical microbial keratitis, *P. aeruginosa* bacteria do not particularly need to invade corneal fibroblasts in order to traverse the stroma. The stroma is mostly formed of collagen and extracellular matrix proteoglycans with a relatively small number of fibroblasts, and bacteria produce proteases that digest these proteins to help them propagate through the tissue. On the other hand, bacteria may use this internalization to evade host defences and antibiotics, and this is noticed clinically when reactivation of the pathology occurs despite antibiotic treatment. Our results show that PAO1 survived and even multiplied inside invaded corneal fibroblasts. This is not surprising if the main purpose of invading the corneal fibroblasts was to avoid the host immune cells, and is consistent with observationsin other systems. Many bacteria replicate within the host cytosol, like *Salmonella* that reside in a cytosolic vacuole to avoid phagolysosomal fusion, or *Shigella* and some pathogenic *Burkholderia* spp. that live freely in the host cytosol.[447]

In our TEM studies, PAO1 bacteria were noticed to enter the cells by endocytosis, where they reside within membrane-bound vacuoles. In a previous study, Fleiszig and co-authors predicted that bacterial entry to cells was an endocytic process when they observed the presence of bacteria in

intracellular vacuoles.[448] Our TEM photographs show the invagination of the cell membrane and the actual formation of the endocytic vesicle around a bacterium during internalization.

When bacteria encounter host cells, different strains behave in a different manner, according to the type of the host cell. Some bacteria evolved specialised strategies to invade initial cellular barriers and disseminate through tissues, like for example *N.meningitidis* which invade meningeal cells cross the blood-cerebrospinal fluid barrier to enter the subarachnoid space.[449] On the other hand, several bacterial species classically known to be extracellular pathogens have evolved molecular strategies to actively induce their entry into target cells for replication and/or dissemination to other host tissues, and many have been shown to internalise into host cells, probably using intracellular compartments for persistence in target tissues.[441]

Some bacteria inhibit internalization into professional immune cells, which phagocytise bacteria and kill them by lytic enzymes secreted into the bacteria-containing phagosomes, by utilising the ExsA-regulated effector molecules exoenzyme T (ExoT), which causes epithelial cell rounding and inhibition of bacterial internalization.[231, 258] These strains are generally branded as cytotoxic because of their ability to kill host cells through their type III secreted toxins. Invasive strains, on the other hand, invade and multiply within host cells.[314] Bacterial invasion may contribute to the pathogenesis or to the progression of the infection by allowing the bacteria to evade host immune effectors and induce changes in host cell function[450], or evading antibiotics used clinically whenever these agents are unable to penetrate the host cell membrane.[451]

Bacteria use several mechanisms for internalization utilizing the existing signalling pathways of the host cells, particularly tyrosine kinases and the induction of tyrosine phosphorylation in target cells. Among the different tyrosine kinase systems, the family of Src tyrosine kinases seems to be significantly involved in the induction of bacterial internalization by cellular tyrosine phosphorylation in several bacterial species.[452] In our model, pre-treating corneal fibroblasts with the Src tyrosine kinase inhibitors significantly reduced bacterial internalization into these cells. Additionally, corneal fibroblasts upregulated their expression of Src tyrosine kinase when infected with bacteria. Inhibition of the actin microfilament system also reduced bacterial internalization into corneal fibroblasts. This suggests that corneal fibroblasts utilize the Src kinase and the actin microfilament systems for bacterial internalization, much like corneal epithelial cells and other cellular environments around the body. On the other hand, bacterial association was not affected by the inhibition of Src tyrosine kinase, indicating that this system is not required for bacterial association, which is consistent with other evidence.[453]

The Src family of protein tyrosine kinases plays important roles in the regulation of signal transduction by a large number of cell surface receptors in multiple cellular environments. They play an important role in regulating fundamental cellular processes, including cell growth, differentiation, cell shape, migration and survival, and specialized cell signals.[454] All Src tyrosine kinases consist of an N-terminal SH3 and SH2 domain, the kinase domain, and a regulatory C-terminal tyrosine residue; and are generally kept in an inactive state by tyrosine phosphorylation of the C-terminal regulatory tyrosine. Dephosphorylation of the tyrosine residue results in conformational changes in the protein that opens the kinase domain, and this results in auto-phosphorylation of a stimulatory tyrosine in the kinase domain (Tyr-416) and full activation of the kinase.[452] It has been previously shown that inhibition of tyrosine kinases prevents the invasion of rabbit corneal epithelial cells by *P. aeruginosa*, indicating that tyrosine kinases play a role in the internalization of by *P. aeruginosa* into those cells.[455] There is other evidence of the important role of Src tyrosine kinases for *P. aeruginosa* internalization by mammalian cells. For instance, infection of different types of cells with various *P. aeruginosa* strains results in rapid activation of Src tyrosine kinase, detectable as early as 5-10 minutes after initiation of infection, preceding the internalization of the bacteria which happens at 15 minutes. In addition, activation of Src-like tyrosine kinases results in tyrosine phosphorylation of several cellular proteins.[453] The activation of Src tyrosine kinases has been elucidated in the internalization of several other bacterial species, including *Yersinia enterocolitica*, *S. flexneri*, *L. monocytogenes*, and *Neisseria gonorrhoeae.* [456-459]This may indicate that the processes of bacterial internalization into cells are conserved, and different bacteria may utilize similar signalling pathways for it.[453]

6.1.3 *P. aeruginosa* bacteria destroy corneal fibroblasts

Although PAO1 is an invasive strain, it does retain some cytotoxic properties on human cells.[460] In our bacterial association experiments, all fibroblast monolayers were completely destroyed at 24h for all infective doses, even those as low as 10 bacteria per monolayer. We investigated that by quantifying lactate dehydrogenase (LDH) released by corneal fibroblasts and comparing it to the maximum LDH release that was measured from lysed uninfected cells. Our results showed that cell death was noted at 9h post challenge, with 50% of LDH release detected with a MOI of 0.1 CFU/cell, and a maximum release with an MOI of 1 CFU/cell. With higher MOIs, the level of LDH declines, and this is probably due to the rapid cell death and hence the reduced amount of overall LDH released by dying “leaky” fibroblasts into the medium. It could also be due to degradation of LDH already released by the lytic enzymes released with cellular apoptosis or pyroptosis.

In our prolonged gentamicin protection studies, we demonstrated that PAO1 bacteria were able to survive and replicate inside corneal fibroblasts, and in spite of that, cell monolayers were visually fairly intact for up to 24h post challenge. This led us to hypothesize that the presence of replicating bacteria inside fibroblasts did not kill them, and to test that hypothesis, we measured the LDH released by infected cells as compared to that released by gentamicin protected cells containing bacteria. We found that fibroblasts with intracellular bacteria only released LDH in an amount similar to spontaneous release by uninfected cells, suggesting that cell viability was not affected by the presence of replicating bacteria inside the cells. This supports the assumption that *P. aeruginosa* use corneal fibroblasts as reservoirs for infection, and hence they need to preserve the cells within which they hide.

P. aeruginosa has a number of different strains that employ different strategies to effect their pathogenicity. Some strains are predominantly invasive, like PAO1, but do retain some cytotoxic effects in mammalian cells,[460] while cytotoxic strains are inherently capable of invasion, and low levels of invasion are detectable in corneal epithelial cells before cytotoxicity starts, and their invasive properties are still detectable even if cytotoxicity is disabled by gene mutation.[455] Invasive and cytotoxic strains differ in certain genes that are regulated by the transcriptional activator ExsA, encoded by *exsA*. Only invasive strains have the 49-kDa form of exoenzyme S (*exoS*) whereas ExoU (*exoU*) is present only in cytotoxic strains.[250] Although invasion and cytotoxicity were originally thought to be sequential events, where cytotoxicity was thought to be dependent on invasion, it has been shown that that invasion and cytotoxicity are not sequential, and that they are independent events, although they both require protein tyrosine kinase.[455]

P. aeruginosa isolates demonstrate a high degree of variability in virulence, ranging from moderately virulent strains, like PAO1, which belongs to a relatively uncommon clonal group, to highly virulent strains like PA14 which belongs to one of the most common clonal groups isolated.[461] The PA14 genome contains two pathogenicity islands that are absent in PAO1 which carry several genes implicated in virulence, like exoU and the Rcs/Pvr systems, and the deletion of these pathogenicity islands impacts the virulence of PA14 in several murine infection models.[462-464] In our model, PA14 demonstrated significantly higher cytotoxic effects on corneal fibroblasts than PAO1, which is consistent with the other evidence.

P. aeruginosa utilize the highly regulated type III secretion system to inject its effector proteins into target cells. These proteins cause host cells death either directly, through pore-mediated increases in membrane permeability;[212-215] or indirectly, through the activation of broad cellular defence responses.[216] *P. aeruginosa* type III secretion system triggers the inflammasome-mediated

activation of caspase 1, resulting in the production of the interleukins IL-1β and IL-18 and in pyroptosis.[212, 218, 219] The type III secretion system is composed of a needle complex, translocator proteins, regulator proteins, chaperone proteins and effector proteins. It is an extremely efficient system, but it requires the full function of all its components to function properly.

In our experiments, we chose to use wild type and mutant PA14 strains to investigate the role of individual virulence factors, because PA14 is predominantly cytotoxic and would have the full machinery required for cytotoxicity. We used a mutant PA14 strain deficient in the popB translocator hydrophobic protein, which is essential for target cell pore formation critical for a normal type III secretion system function. This allowed us to assess the role of this system in bacterial cytotoxicity in our model. We also used PA14 deficient in flgK, one of the flagellar hook associated proteins essential for its function,[465] and this allowed us to assess the significance of bacterial association as a prerequisite for further interactions, including cytotoxicity. Our results showed that wild type PA14 bacteria induced significantly more cytotoxicity on corneal fibroblasts than both mutant strains, confirming the important role of type III secretion system in bacterial cytotoxic effects on corneal fibroblasts. Our results also suggest that cytotoxicity is flagellum dependent, demonstrated by the significant reduction of the cytotoxic effect of flagella-deficient mutant to a similar level to TTSS deficient mutants, despite the latter being intact in that strain.

6.1.4 Corneal fibroblasts produce cytokines in response to *P. aeruginosa* infection

All the above studies and results suggested to us that there are indeed active interactions between PAO1 bacteria and primary human corneal fibroblasts. We hence sought to investigate whether corneal fibroblasts respond to these interactions by releasing cytokines and other mediators that modulate the pathogenesis of microbial keratitis. We were particularly interested in two classes of mediators: pro-inflammatory cytokines and matrix metalloproteases (MMP).

In our model, we measured the level of 9 pro-inflammatory cytokines in culture supernatants from our early infection experiments, but found that IL-1β was the only cytokine that showed a significantly higher level than constitutive levels released by uninfected cells at 24h post challenge. We hypothesized that this may be due to destruction of corneal fibroblasts before the transcription and release of those cytokines, and that IL-1ß was possibly released early before fibroblast destruction was significant. IL-1β is produced as an inactive cytoplasmic precursor that is cleaved to generate the mature active form by caspase-1 on activation of the inflammasome pathway,[370] so it is plausible that its activation and release occurs much earlier than all the other cytokines. This was indeed confirmed when we tested cytokine release after 9h of infection, when IL-1ß level was also higher than constitutive levels. Moreover, when gentamicin was used to protect the fibroblasts for

the duration of the challenge, most tested cytokines showed a higher level than constitutive release, suggesting that corneal fibroblasts do have a role in immune activation.

Classically, when pathogen recognition receptors, such as TLRs, are stimulated by offending pathogens, inflammatory pathways are initiated, and this typically involves recruitment of MyD88, leading to NF-κB translocation to the nucleus and expression of pro-inflammatory and chemotactic cytokines. These include CXCL1/KC, IL-1α and IL-1β which recruit neutrophils from limbal capillaries to the corneal stroma, and activate macrophages and resident corneal epithelial cells and keratocytes.[350] IL-1β in particular is involved in the generation of systemic and local responses to infection, injury, and immunological challenges and is the primary cause of chronic and acute inflammation.[366] It is also likely that neutrophil mediated IL-1β processing has a broad role in early stage infection, with macrophage and possibly neutrophil inflammasome activity contributing at a later stage.[365] The fact that IL-1β was released early by corneal fibroblasts in our model in response to infection by *P.aeruginosa* supports the assumption that these cells are not simple bystanders but are in fact sentinel cells that actively modulate immune pathways.

Our group has shown previously that activated corneal fibroblasts isolated from microbial keratitis patients upregulate their TLR4 receptors and release several pro-inflammatory cytokines when treated with pure LPS. Naïve corneal fibroblasts isolated from normal corneas, however, did not behave in the same manner.[466] We tried to identify whether cytokine production was related to the active infection process by live bacteria itself, or whether it could also be induced by bacterial cellular components and endotoxins. We challenged fibroblasts with heat killed bacteria that have preserved cell wall and external components, freeze-thaw killed bacteria that have ruptured cell walls exposing intracellular components and pure *P. aeruginosa* LPS which activate pathogen recognition receptors like TLR4. Our results show that only fibroblasts challenged with live cells produced significantly higher levels of cytokines than unchallenged cells, and cells challenged with bacterial components alone produced similar levels of cytokines as constitutive levels. This suggests that it is the interaction between live bacteria and the fibroblasts that induces this response, and since intracellular bacteria in fibroblasts protected with gentamicin produced IL-1β in a level similar to unprotected cells, we concluded that cytokine production is probably impacted by a combination of the association and the type III secretion system interactions.

This led us to investigate the effect of bacterial virulence on cytokine production. We hypothesized that since PA14 is more virulent than PAO1, it may induce a stronger response from corneal fibroblasts. Our results show that PA14 infection induced a significantly higher level of IL-1β by corneal fibroblasts than PAO1 at least at 9h post challenge, but this was reversed at 24h. This

suggests that corneal fibroblasts respond earlier and more potently to infection by highly virulent strains than they do to less virulent strains, possibly to start the immune cascade earlier and recruit more immune cells to the site of infection. The finding that the pattern of IL-1β production was reversed at 24h, where the level of the cytokine was higher with infection by PAO1 than by PA14 suggests that corneal fibroblast were possibly destroyed earlier in the process and hence IL-1β level stopped increasing at that time compared to the other fibroblasts that continued their production for a longer period so that the level climbed to a higher level. Another explanation is that bacteria are capable of destroying the already secreted cytokine, and that the more virulent PA14 have a higher capacity of destroying the cytokine than PAO1. This could be verified in future studies by measuring the levels of IL-1β by the 2 strains at more time points.

Interleukin-1β production through the inflammasome pathway has been previously demonstrated.[220] NLRC4 activates caspase-1-dependent-IL-1β release, and is believed to be a general innate immune sensor that mediates caspase-1 activation during bacterial infection.[218] It was concluded that the most likely triggers for NLRC4 activation are cytosolic flagellin and the inner rod protein of TTSS.[447] Interestingly, both flagellin and the rod protein share a similar structural organization characterized by two long parallel α helices, and mutation in the conserved hydrophobic residues of these α helices disrupts the triggering of NLRC4 inflammasome activation activity of both flagellin and rod proteins.[467, 468] Similar to flagellin, the TTSS rod protein and the needle protein form a hollow structure as part of their secretion apparatus. Notably the needle protein and the rod are very similar in size and in three-dimensional structure[469]. The rod protein, however, is erroneously secreted out of the bacteria by the TTSS, whereas the needle protein is essential for the function of the TTSS needle complex.[447] The biochemical activity of the TTSS rod protein and the TTSS needle protein were demonstrated in activating the NLRC4 inflammasome, both in murine and human macrophages.[470, 471] The NLRC4 inflammasome, therefore, serves as an effective cytosolic surveillance system to detect bacterial flagella and/or TTSS.

The TTSS is believed to have evolved from the flagellum. They both have many structural resemblances, like the resemblance of the base of the TTSS to the basal body of the flagellum, and the needle to the flagellar hook. In addition, many of the structural proteins in the TTSS and flagellum systems bear significant sequence homology; the two systems display a highly similar three-dimensional architecture.[447] When we investigated the role of TTSS and flagellum in cytokine production, we found that wild type PA14 bacteria induced significantly higher production of IL-1β than mutant strains. We have also showed that these mutant strains are less virulent and induced less cytotoxicity than the wild type strain. It is not merely the presence of the bacteria or their

cellular components that stimulate the cells and initiate the pathology. The loss of either the flagellum or the TTSS in the PA14 mutant strains caused significant reduction in both the cytotoxicity and the IL-1β production by corneal fibroblasts in our model.

6.1.5 Corneal fibroblasts produce MMPs in response to *P. aeruginosa* infection

The other class of mediators we were interested in is the MMPs. Matrix metalloproteinases (MMPs) are a family of proteolytic enzymes that have multiple roles in extracellular matrix (ECM) remodelling and immune pathways. In health, they have roles in normal development, menstruation and bone remodelling, and in disease, they are implicated in processes involving abnormal ECM turnover, like arthritis, atherosclerosis and neoplasia[472]. They also have important roles in immune modulation, facilitating white blood cell recruitment, cytokine and chemokine cleavage and defensin activation.[430] MMPs are important for successful resolution of acute infection; they facilitate the migration of immune cells, elimination of the offending pathogen, resolution of inflammation and eventually remodelling of the ECM. MMPs also activate pro-IL-1β,[473] cleave activated IL-1β,[474] and modulate chemokine activity. Tissue destruction by MMPs during excessive inflammation, however, may favour pathogen dissemination or persistence, by breaking down barriers or creating areas that are poorly accessed by host immune cells.

Corneal fibroblasts maintain the structural homeostasis of the corneal stroma by regulating synthesis and degradation of ECM components using MMPs.[137] In clinical microbial keratitis, host tissue destruction is caused by lytic enzymes released from the pathogen, corneal cells and immune cells. Bacterial proteases can be implemented in the early events of microbial keratitis, but further tissue destruction is mainly caused by proteases released by resident corneal cells[390] and infiltrating leukocytes.[372]

In our model, we demonstrated by gelatine zymography that corneal fibroblasts released several MMPs in response to challenge by live bacteria that were not released when fibroblasts were challenged with heat or freeze/thaw killed bacteria or with LPS, nor were they secreted when bacteria were protected inside the cells or when the cells were completely lysed. This suggests that these MMPs are specific to the interaction between the bacteria and the cells and are only released with live infection. Thus, as these MMPs secreted by corneal fibroblasts contribute to the tissue necrosis seen in microbial keratitis, this further supports the notion that fibroblasts have an active local role in combating the infection.

The cornea mainly produces four MMPs; MMP-1 (collagenase-1), MMP-2 (gelatinase A), MMP-3 (stromelysin-1) and MMP-9 (gelatinase B).[406] In normal corneas, however, only MMP-2 is secreted

constitutively.[407] MMP-1 mainly degrades type I collagen, the most abundant protein in the body, so it is widely expressed during several physiological and pathological tissue remodelling.[475] The cornea is composed mainly of type I collagen, so MMP-1 is commonly isolated from the cornea. MMP-2 mainly degrades type IV collagen, and may be important in ECM remodelling in the late stages of microbial keratitis.[476] MMP-3 degrades collagen types II, III, IV, IX, and X, proteoglycans, fibronectin, laminin, and elastin, in addition to activating MMP-1, MMP-7, and MMP-9.[477] It is also implicated in of immune cell migration and MMP-3-deficient mice have deficient neutrophil migration to infected tissue.[430] MMP-9 degrades type IV collagen, and can upregulate chemotactic cytokines/chemokines IL-1β and MIP-2.[478] Activated MMP-2 and MMP-9 were detected in the tear fluid of microbial keratitis patients, and it was concluded that their expression may be related to the severity of ulceration.[479]

In our model, infected unprotected corneal fibroblasts produced a consistently lower level of all tested MMPs which probably indicates the destruction of the fibroblasts before the transcription and activation of the MMPs took place. This was supported by the finding that the levels of MMP-1, MMP-3 and MMP-9 produced by corneal fibroblasts were significantly higher with gentamicin protection than with no protection. Infected gentamicin-protected cells produced slightly higher levels of MMP-1 and MMP-9 than constitutive secretion by uninfected cells, although the difference was not statistically significant, suggesting that corneal fibroblasts may upregulate the production of these MMPs if given enough time. Lower levels of MMP-2 and MMP-3, however, were detected in infected protected fibroblasts than uninfected cells, which may indicate that challenge of corneal fibroblasts by live bacteria can inhibit the production of, or destroy the already produced, MMP-2 and MMP-3.

When investigating MMP levels in corneal fibroblasts challenged with individual bacterial cellular components, the MMP levels produced by infected protected fibroblasts were similar those in uninfected cells, suggesting that this process may be related to certain virulence factors only expressed by live bacteria. This led us to investigate the role of bacterial virulence and virulence factors, specifically flagella and type III secretion system, in this process, as they had a significant role in IL-1β production. We found that fibroblasts challenged with more virulent bacteria always produced less MMPs, which merely reflects the pattern of increased cytotoxicity associated with these strains. It seems that infection with less virulent strains, like PAO1 or mutant PA14 strains, allowed the fibroblasts more time to produce higher levels of MMPS than cells infected with more virulent strains, like wild type PA14. Although IL-1β has been shown to induce the expression of

MMPs in corneal epithelial cells and fibroblasts,[476] we could not identify a correlation in our model. This is probably because the fibroblasts were killed before the effect of IL-1β was elucidated.

Our strategy for protecting the fibroblasts long enough to investigate the production of different mediators has worked well when the relatively short initial challenge with bacteria was enough to activate the immune pathways in the cells. On the other hand, removing all extracellular bacteria may have stopped the activation of other pathways by externally associated bacteria and their type III secretion system, thereby limiting the scope of studying these pathways in our model. Lower infective doses or different infection strategies may be used in future studies to avoid these aforementioned limitations.

6.2 A model of microbial keratitis

We have developed a model of human microbial keratitis that has 2 components: a whole tissue model of microbial keratitis, where we used whole human corneal tissue to examine the interactions in an environment that closely resembles a clinical situation, and this allowed us to study the pathology from a global tissue stand point; and a tissue culture model of human corneal fibroblasts that allowed us to examine the cellular and molecular components of the pathology.

Although the human corneal fibroblast monolayer model of microbial keratitis provides critical information about the pathogenesis of the disease, we felt it was also crucial to design another model, where the interactions of bacteria with the cornea as an organ can also be studied in detail to mimic a real life clinical situation more closely. Many investigators designed similar models in mice and other animals to study the disease, and there is, indeed, a wealth of information on the topic. But animal models, although usefully representative of the pathology, are still limited by the anatomical differences between human corneas and other mammalian corneas. The mouse cornea, for example, is much smaller than a human cornea, and mouse cells express different mediators to human cells, and yet murine microbial keratitis remains the most heavily utilized model.

We sought to investigate the sequence of events that occurs in the early stages of microbial keratitis, so we developed a human microbial keratitis model utilizing live human corneal tissue remaining after corneal transplant procedures. In a real life situation, clinical *P. aeruginosa* microbial keratitis rarely occurs with an intact epithelium; rather, it occurs when there is some form of epithelial injury. This can be surprising if one considers the fact that the corneal epithelium is a part of the external body surface that is continuously exposed to pathogens and offending agents. But the epithelium, like other body surfaces, has an entire arsenal of defence mechanisms that protects against a full blown pathology. In our whole tissue model, we studied the corneal tissue after infection with a high

dose of bacteria (MOI 100) for 3h by SEM and TEM. We showed that *P. aeruginosa* bacteria successfully associated to corneal epithelial cells, and even managed to penetrate the entire epithelium but could not penetrate further into the stroma unless there was a breach in the epithelial basement membrane. When there was a breach, bacteria were able to penetrate and colonize the stroma quite efficiently. This is consistent with studies utilizing mouse models, in which *P. aeruginosa* bacteria were unable to penetrate beyond the intact epithelial membrane into the stroma, but could reach the stroma through the discontinuous basement membrane.[100]

The corneal epithelium has several defence mechanisms to combat infection. An important mechanical mechanism is the desquamation of superficial epithelial cells containing offending bacteria into tears. In a rat model, when *P. aeruginosa* was inoculated onto a healthy cornea, most internalized bacteria were found in cells that were readily desquamated from the cornea with rinsing,[314] which led the investigators to conclude that internalization coupled with desquamation is a mechanism for clearing bacteria that manage to associate to the surface. In our model, infected corneal buttons showed a rougher surface and more apparently desquamating cells than uninfected cells by scanning electron microscopy. This probably indicates that the internalization/desquamation sequence is a defence mechanism that the human cornea employs as well, suggesting that this mechanism may be conserved across the different species.

6.2.1 Sequence of events in early microbial keratitis

We propose that in the healthy cornea, bacterial inocula are readily eliminated from the surface of the eye by the formidable epithelial defenses. Only in the presence of a breach are bacteria able to penetrate through the layers of the epithelial and the discontinuous basement membrane into the corneal stroma, where they can colonize and multiply. Because of the immune privilege of the eye, and the lack of mature immune cells to maintain visual function in the cornea, corneal fibroblasts are equipped to detect the presence of, and interact with, offending bacteria. Corneal fibroblasts are then able to produce IL-1β, which activates the resident CD14+ undifferentiated monocyte precursor cells to mature dendritic cells and macrophages, which in turn secrete cytokines and chemokines that attract neutrophils and other leukocytes, starting the immune cascade. Corneal fibroblasts also secrete MMPs to aid in leukocyte migration, basement membrane degradation and ECM remodelling.

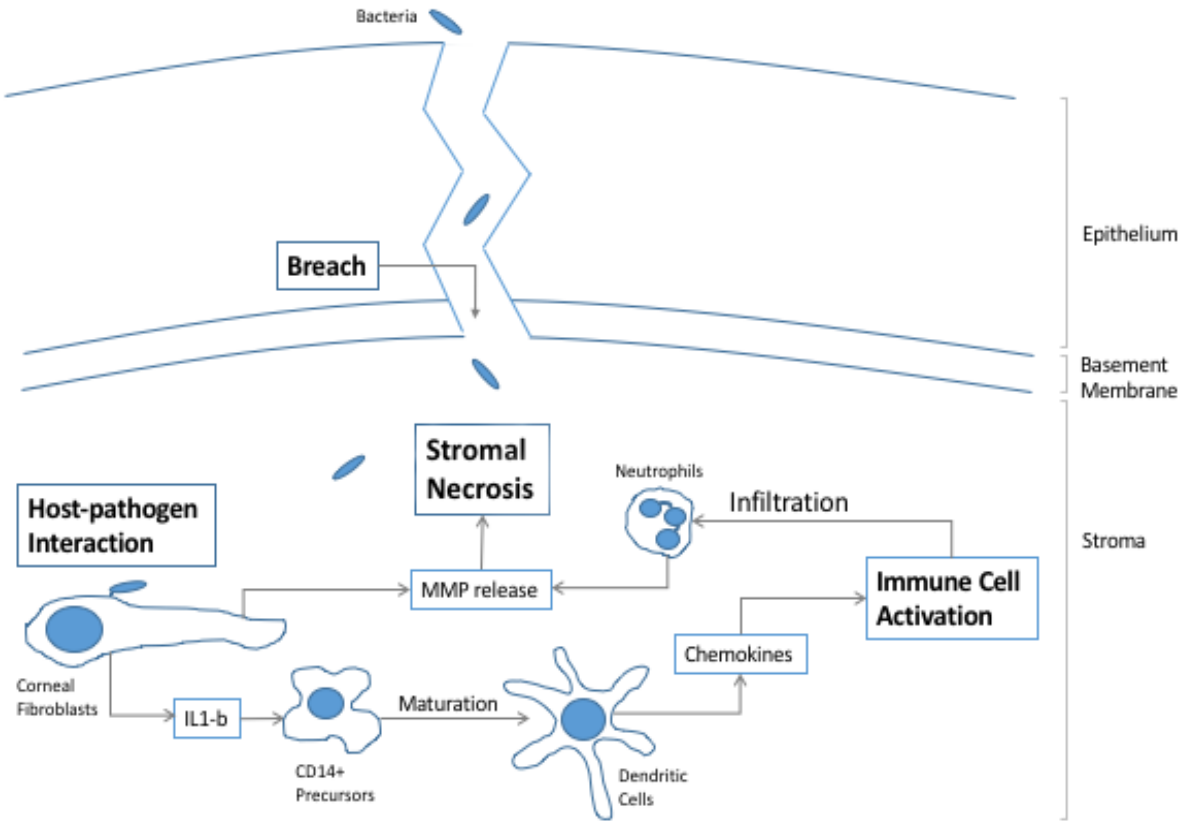

Figure 6.1 Flow diagram of the sequence of events in early microbial keratitis

In the event of an epithelial breach, bacteria are able to penetrate to the stroma, where they interact with stromal fibroblasts. These cells are equipped to be able to produce IL-1β in response to this interaction, which in turn activates the resident CD14+ undifferentiated monocyte precursor cells to mature dendritic cells and macrophages. These cells then start the immune cascade by secreting cytokines and chemokines that attract neutrophils and other leukocytes to the cornea, and these secrete proteolytic enzymes that ultimately lead to the stromal necrosis seen in progressive corneal ulceration.

6.3 Limitations and future work

6.3.1 Comparing different tissue fibroblasts to keratocyte-derived fibroblasts

Keratocytes embryologically develop from the neural crest, unlike other fibroblasts, like skin fibroblasts that develop from the mesenchyme. When keratocyte are activated, like in the event of trauma or infection, they attain a classical fibroblast phenotype, but they may behave differently from other tissue fibroblasts. In future studies, host-pathogen interactions can be studied in skin or gut fibroblasts and compared to the interactions we observed in this work.

6.3.2 Assessment of bacterial association and invasion in different strains

In our experiments, we tested for variations in bacterial association between wild type and mutant strains, and examined the effect of the absence of TFP and flagella on bacterial association early in the process, up to 3h. The total association in those strains, however, was not characterized in detail as it was in our early experiments with wild type PAO1 bacteria, and that was because our main focus was the early events of the process. In future studies, a more detailed characterisation can be pursued, and total bacterial association can be measured over more time points and with more infective doses to determine whether or not it was dose and time dependant in those mutant strains as it was in wild type strains. Different wild type strains, including isolates from clinical cases of microbial keratitis, can be used as well for that purpose, studying, for example, the difference between clinical isolates and laboratory strains in that regard. Bacterial typing of clinical isolates and correlating their virulence characteristics with the clinical picture of the corresponding patient may provide some very useful information about the prognosis of the disease and may help devise new strategies for treatment.

Similarly, bacterial invasion can be assessed and compared over more wild type and mutant strains and clinical isolates to better characterise the difference between those strains, in terms of bacterial internalisation. In addition, the role of the different virulence factors in bacterial internalisation, like TFP, flagella and TTSS, can also be assessed in future studies.

6.3.3 Removing infective medium to maintain steady infective dose

Our strategy for protecting the fibroblasts long enough to investigate the production of different mediators has worked well when the relatively short initial challenge with bacteria was enough to activate the immune pathways in the cells. On the other hand, removing all extracellular bacteria may have stopped the activation of other pathways by externally associated cells and their type III secretion system, thereby limiting the scope of studying these pathways in our model. Lower

infective doses or different infection strategies may be used in future studies to avoid these aforementioned limitations. For example, regularly replacing the infective medium with fresh medium containing known bacterial inocula may avoid the limitation of the uncontrolled exponential growth of bacteria in the culture medium over the course of the experiment.

6.3.4 Testing the gene expression of cytokines and MMPs in our experiments

In our experiments to test cytokine release by corneal fibroblasts in response to infection by different bacterial strains, and by mutant and wild type strains, we observed that the amount of cytokines seemed to decrease with time, and we proposed that this could either be because the fibroblasts are dying before producing the cytokines, or because the bacteria are destroying the cytokines after their release. One strategy to differentiate would be to test the gene expression of cytokines in our experiments; if the gene expression was similar, then this would suggest that the bacteria are destroying the already released cytokines. If, on the other hand, the gene expression detection was reduced, this may mean that the fibroblasts are destroyed before producing the cytokines or MMPs.

6.3.5 Assessment of cytokines and MMP release at more time points

In our experiments, cytokine production was assessed at 9 and 24h, mainly to allow enough time for gene transcription, translation and protein production. IL-1β release was assessed at 9h when its levels were elevated despite the destruction of the fibroblasts at 24h, but the levels at earlier time points were not measured. This can be explored in future studies to try to determine a more accurate timeline for the activation and release of IL-1β from corneal fibroblasts.

6.3.6 Testing the global cytokines and MMP release in the whole tissue model

Our main focus in our whole tissue model was to use this model to visually confirm our findings using electron microscopy, so the corneal buttons were fixed and processed immediately after the infective challenge. In future studies, and to assess the global tissue response to bacterial challenge, infective culture medium can be collected before fixing the buttons, and cytokine and MMP levels can be measured. This would ideally involve longer and more numerous time points to accurately assess the timelines of cytokine and MMP production.

6.3.7 Assessment of naïve corneal fibroblast response to a conditioned medium

In a study by Wong et al, activated corneal fibroblasts isolated from microbial keratitis patients upregulate their TLR4 receptors and release several pro-inflammatory cytokines when treated with pure LPS. In contrast, naïve corneal fibroblasts isolated from normal corneas, did not behave in the

same manner.[466] Initially we thought that these cells were only challenged with LPS, so live infection may show a similar effect, but this was not the case. It might be possible that these fibroblasts were exposed to a different array of cytokines and other mediators within the milieu of a clinical microbial keratitis that led to the their "activation" and their increased propensity to upregulate their inflammatory signalling. One way to examine that is to expose naïve corneal fibroblasts to a conditioned medium. In this medium, known doses of bacteria would be added to known numbers of neutrophils for specified times, and then the supernatant is added to naïve corneal fibroblasts for different intervals of time. The original and the resulting supernatants can be tested for cytokine production, and the results compared to estimate the induced cytokine production. These fibroblasts can also be tested for further activation and TLR4 upregulation when challenged with LPS or live bacteria.

6.3.8 Assessment of leukocyte response to cytokines released by infected fibroblasts

Supernatants resulting from live infection of corneal fibroblasts with *P. aeruginosa* can be added to polymorphonuclear leukocytes (PNL) and other immune cells to assess the effect of the liberated cytokines on immune cell activation, comparing resting cytokine levels to levels after exposure to the supernatant. This can also be assessed and compared among different wild type and mutant strains.

6.3.9 Introduction of leukocytes to the whole tissue model

In the whole tissue model, PNLs and other leukocytes can be added to the medium before and after bacterial challenge, and the resulting supernatant can be tested for cytokine levels. The buttons can also be fixed and examined by scanning and transmission electron microscopy at different time points to try to gain a better understanding of the sequence of events of microbial keratitis in this model. Scanning laser fluorescence microscopy can also be used for the same purpose using GFP expressing bacteria.

6.3.10 Introduction of epithelial cells into the tissue culture model

One of the main limitations of our tissue culture model is that it is devoid of epithelial cells. The interactions between epithelial cells and the underlying fibroblasts are very important in the pathogenesis and progression of microbial keratitis in a real life clinical situation, so the introduction of epithelial cells into the model can be pursued in future studies, and the host cell response can be studied in more detail and compared to our current data. The host-pathogen interactions between epithelial cells and *P.aeruginosa* has been extensively studied previously, so we elected not to study them again. However, these interactions can be studied as part of the introduction of epithelial cells

into our model, in order to further dissect and understand the early sequence of events in microbial keratitis.

Chapter 7 : **APPENDICES**

7.1 Reagents for Bacterial Culture

7.1.1 Luria-Bertani agar with 60µg/mL gentamicin

- Used to grow PAO1 tn7-GFP strains.
- To prepare 500 mL, add ingredients shown in Table 7.1 to 500 mL distilled water.

Table 7.1 Luria-Bertani agar with gentamicin

Product	Source	Amount
Tryptone	Oxoid, Basingstoke, UK	5 g
Yeast extract	Bectod-Dickinson, Sparks, MD, USA	2.5 g
Sodium chloride	Fischer, Loughborough, UK	5 g
Bacterial agar	Oxoid, Basingstoke, UK	7.5 g
Gentamicin	Sigma-Aldrich, Dorset, UK	4 mL

- Sterilize by autoclaving at 120^{o}C, 2.7Kg cm^{2}
- Add gentamicin when temperature drops to 55-60^{o}C

7.2 Reagents for Cell Culture and Infection

7.2.1 Corneal fibroblast culture medium (CFCM)

- Used for isolating and growing corneal fibroblasts in preparation for infection experiments.
- To prepare 500 mL, ingredients were added as shown in Table 7.2.

Table 7.2 Corneal fibroblast culture medium (CFCM)

Product	Source	Concentration	Amount
Dulbecco's Modified Eagle's Medium/Nutrient Mixture F-12 Ham	Sigma-Aldrich, Dorset, UK	-	500 mL
Decomplemented foetal bovine serum (dFBS)	Sigma-Aldrich, Dorset, UK	10%	50 mL
Penicillin/Streptomycin A	Sigma-Aldrich, Dorset, UK	2%	10 mL
Gentamicin	Sigma-Aldrich, Dorset, UK	5 µg/ml	250 µL
Amphotericin B	Sigma-Aldrich, Dorset, UK	0.2%	1 mL
Cholera toxin	Sigma-Aldrich, Dorset, UK	0.1 µg/ml	50 µL
Insulin	Invitrogen, Paisley, UK	5 µg/ml	625 µL
Epidermal Growth Factor	Invitrogen, Paisley, UK	10 ng/ml	500 µL

- Sterilize ingredients using polysulfone membrane filter (pore size 0.2 m, Pall Life Sciences, Portsmouth, UK) before addition to medium base.

7.2.2 Corneal fibroblast infection medium (CFIM)

- Used to prepare bacterial suspensions in corneal fibroblasts infection experiments.
- To prepare 500 mL, add ingredients as shown in Table 7.3. Sterilize as above

Table 7.3 Corneal fibroblast infection medium

Product	Source	Concentration	Amount
Dulbecco's Modified Eagle's Medium/Nutrient Mixture F-12 Ham	Sigma-Aldrich, Dorset, UK	-	500 mL
Decomplemented foetal bovine serum (dFBS)*	Sigma-Aldrich, Dorset, UK	1%	5 mL
Cholera toxin	Sigma-Aldrich, Dorset, UK	0.1 µg/ml	50 µL
Insulin	Invitrogen, Paisley, UK	5 µg/ml	625 µL
Epidermal Growth Factor	Invitrogen, Paisley, UK	10 ng/ml	500 µL

*When testing for proteins, such as in gelatin zymography or in SDS-PAGE, the FCS was omitted from CFIM to improve the accuracy of the results.

7.3 Reagents for cell culture

7.3.1 Decomplemented foetal bovine serum (dFBS)

- Used in cell culture media.
- Prepared by placing the sealed 500 mL FBS bottle (Sigma-Aldrich, Dorset, UK) into water bath at 56^{o}C for 1h.
- Store in aliquots in a -20^{o}C freezer.

7.3.2 Cytochalasin D (CD) solution

- Used to block bacterial internalization in invasion assays.
- A working stock (10µg/mL) is prepared by adding 100 µL of CD neat stock solution (1mg/mL; Sigma-Aldrich, Dorset, UK) to 9.9 mL CFIM.
- For an experiment, this is further diluted 1/5 to a final concentration of 2µg/mL.
- Store in aliquots in a -20^{o}C freezer.

7.3.3 Saponin lysis solution

- Used to lyse corneal fibroblasts infection experiments.
- To prepare 10 mL, add ingredients as shown in Table 7.4

Table 7.4 Saponin lysis solution

Product	Source	Concentration	Amount
Phosphate buffered saline (PBS)	Sigma-Aldrich, Dorset, UK	-	10 mL
Saponin powder	Sigma-Aldrich, Dorset, UK	1% (w/v)	0.1 g
Decomplemented foetal bovine serum	Sigma-Aldrich, Dorset, UK	1% (v/v)	100 µL

- Mix well until completely dissolved and sterilize using polysulfone membrane filter (pore size 0.2 µm, Pall Life Sciences, Portsmouth, UK).

7.4 Reagents used in polymerase chain reaction (PCR)

7.4.1 Agarose gel

- Used for running gel in PCR experiments.
- Prepared by adding 1g of Hi-res agarose (Geneflow, Elmhurst, UK) to 50 mL of Tris-acetate-EDTA buffer (40 mM Tris-acetate, 1 mM EDTA, pH 8.0)
- Mixture is dissolved by placing in microwave for 4 min on medium power.
- While hot, the dissolved gel is poured into a gel tray with a 5 mm comb in place.
- Gel is left to set for 30 min.

7.5 Reagents used in sandwich immunoassays

7.5.1 Reagents used in the Pro-Inflammatory 9-Plex assay

7.5.1.1 Calibrator solutions

- Used to prepare calibration curves.
- Add 1 mL to calibrator stock powder and leave for 5 min.
- From this 1µg/mL, prepare an 8-point calibration curve with solutions of 10000, 2500, 625, 156, 39, 9.8 and 0 pg/mL.
- Discard after use.

7.5.1.2 Detection antibody solution

- Used for the detection step of the assay.
- Add 3 mL Diluent 100 to Detection Antibody stock.
- Discard after use.

7.5.1.3 Reading Buffer

- Used for reading the plates.
- Add 10 mL of Read Buffer T stock to 10 mL deionized water.
- Discard after use.

7.5.2 Reagents used in the V-PLEX Human IL-1β assay

7.5.2.1 Calibrator solutions

- Used to prepare calibration curves.
- Add 1000 µL of proprietary Diluent 2 to lyophilized calibrator vial, vortex mix well and leave for 5 min. This becomes the highest calibrator.
- Prepare 7 Eppendorf tubes with 300 µL Diluent 2 in each tube
- Transfer 100 µL from the highest calibrator to the next tube.
- Repeat 4-fold serial dilution 5 more times.
- Use the last tube with only 300 µL Diluent 2 as the blank calibrator (Figure 7.1).

Figure 7.1 Serial dilution for calibrator solutions

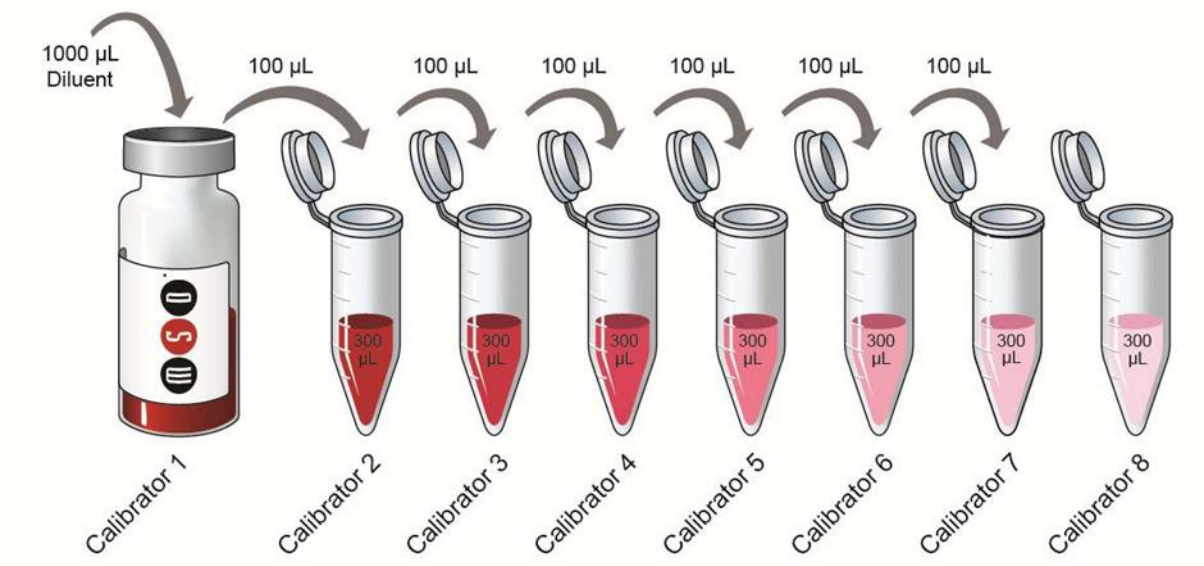

7.5.2.2 Detection antibody solution

- Used for the detection step of the assay.
- Add 60 µL of SULFO-TAG stock antibody to 2.94 mL proprietary Diluent 3.
- Discard after use.

7.5.3 Reagents used in the Human MMP Ultra-Sensitive assays

7.5.3.1 Calibrator solutions

- Used to prepare calibration curves.
- Prepare 8 Eppendorf tubes marked SD-01 to SD-08.
- Prepare the highest calibrator (SD-01) by adding 15 µL of the Human MMP Calibrator Blend to 135 µL Diluent 2.
- Prepare SD-02 by adding 40 µL of SD-01 to 120 µL Diluent 2.
- Repeat 4-fold serial dilution 5 more times.
- Use the last tube with only 120 µL Diluent 2 as the blank calibrator.

7.5.3.2 Detection antibody solution

- Used for the detection step of the assay.
- Add 60 µL of the stock antibody blend to 2.94 mL proprietary Diluent 3.
- Discard after use.

7.6 Reagents used in Zymography

7.6.1 Zymogram sample buffer (2X):

- Added to samples prior to adding to the wells on the gel.
- To prepare 10 mL, add ingredients as shown in Table 7.5 Zymogram sample buffer.

Table 7.5 Zymogram sample buffer

Reagent	Amount
0.5 M Tris-HCl pH6.8	2.5 mL
100% Glycerol	2.0 mL
10% SDS	4.0 mL
0.1% Bromophenol blue	0.5 mL
Deionized water	1.0 mL

- Store in aliquots of 500 µL in a -20^{o}C freezer.

7.6.2 Zymogram running buffer (5X):

- Used to fill the electrophoresis tank alongside the gels.
- To prepare 1L, add ingredients as shown in Table 7.6.

Table 7.6 Zymogram running buffer

Reagent	Amount
Tris base	15g
Glycine	72g
SDS	5g
Deionized water	1L

- For an experiment, this is further diluted 1/5.
- Store at room temperature.

7.6.3 Zymogram staining buffer:

- Used to stain the gels.
- To prepare 1L, add ingredients as shown in Table 7.7 Zymogram staining buffer

Table 7.7 Zymogram staining buffer

Reagent	Amount
Coomassie Blue R-250	5 mL
Methanol	300 mL
Acetic acid	100 mL

- Store protected from light at room temperature
- Can be recycled after use.

7.6.4 Zymogram de-staining buffer:

- Used to de-stain the gels.
- To prepare 1L, add ingredients as shown in Table 7.8.

Table 7.8 Zymogram de-staining buffer

Reagent	Amount
Methanol	300 mL
Acetic acid	100 mL
Deionized water	600 mL

- Store at room temperature

7.7 Reagents used in SDS-PAGE and Western blots

7.7.1 Separating (resolving) gel

- Used to run the proteins in the gel electrophoresis.
- To prepare 4 gels, add ingredients as shown in Table 7.9

Table 7.9 Separating gel for SDS-PAGE

Reagent	Amount
30% Acrylamide/0.8% bisacrylamide	6.0 mL
Separating buffer (1.5 M Tris-HCl, pH 8.8)	3.75 mL
Deionized water	5.25 mL
Ammonium persulfate 10% (w/v)	50 µL
TEMED	10 µL

7.7.2 Stacking gel

- Used to concentrate and pack proteins in the gel electrophoresis.
- To prepare 4 gels, add ingredients as shown in Table 7.10

Table 7.10 Stacking gel for SDS-PAGE

Reagent	Amount
30% Acrylamide/0.8% bisacrylamide	0.65 mL
Stacking buffer (0.5 M Tris-HCl, pH 6.8)	1.25 mL
Deionized water	3.05 mL
Ammonium persulfate 10% (w/v)	25 µL
TEMED	5 µL

7.7.3 Sample buffer

- Used to prepare and load samples in the gel electrophoresis.
- To prepare a 4x solution, add ingredients as shown in Table 7.11

Table 7.11 Sample buffer for SDS-PAGE

Reagent	Amount
0.5 M Tris-HCl pH6.8	4.8 mL
100% Glycerol	4.0 mL
SDS	0.8 g
Bromophenol blue	5.0 mg
Deionized water	0.7 mL

7.7.4 Running buffer

- Used to fill the electrophoresis tank alongside the gels.
- To prepare a 10x solution, add ingredients as shown in Table 7.12

Table 7.12 Running buffer for SDS-PAGE

Reagent	Amount
Tris-HCl pH 8.3	30.3 g
Glycine	144 g
SDS	10 g
Deionized water	1L

7.7.5 Transfer (blotting) buffer

- Used to blot the proteins from the gels onto the membranes.
- To prepare 250 mL, add 50 mL methanol to 200 mL running buffer (Table 7.12).

7.7.6 Blocking buffer

- Used to block all unbound protein.
- To prepare 20 mL, add 2 g powdered skimmed milk to 20 mL PBS-Tween (Appendix 7.8.1).
- Use 20 mL per gel.

7.7.7 Pierce™ BCA Protein Assay

- Used to quantify proteins in samples.
- Pierce™ BCA Protein Assay Kit components are shown in Table 7.13

Table 7.13 Pierce™ BCA Protein Assay Kit

Reagent	Constituents	Solvent
BCA reagent A	Sodium carbonate Sodium bicarbonate Bicinchoninic acid Sodium tartrate	0.1 M sodium hydroxide
BCA reagent B	4% (w/v) cupric sulfate	
Albumin standard	0.2 mg/mL bovine serum albumin	0.9% (w/v) saline 0.05% (w/v) sodium azide

7.7.8 Serial dilutions of albumin standard

- Albumin standards were used in the BCA protein assay
- The concentrations were prepared as shown in Table 7.14

Table 7.14 Serial dilutions of albumin standard in BCA assay

Label	Volume of diluent	Volume and source of BSA	Final concentration of BSA (µg/mL)
A	0	300 µL from stock	2000
B	125 µL	375 µL from stock	1500
C	325 µL	325 µL from stock	1000
D	175 µL	175 µL from B	750
E	325 µL	325 µL from C	500
F	325 µL	325 µL from E	250
G	325 µL	325 µL from F	125
H	400 µL	100 µL from G	25
I	400 µL	0	0 (Blank)

7.8 Miscellaneous reagents

7.8.1 PBS-Tween

- Used to wash plates during SDS-PAGE and cytokine and MMP analysis.
- To prepare, add 250 µl tween to 500 mL PBS.

LIST OF REFERENCES

1. Pascolini, D. and S.P. Mariotti, *Global estimates of visual impairment: 2010.* Br J Ophthalmol, 2012. **96**(5): p. 614-8.
2. Robaei, D. and S. Watson, *Corneal blindness: a global problem.* Clin Experiment Ophthalmol, 2014. **42**(3): p. 213-4.
3. Foster, A., *Vision 2020--the Right to Sight.* Trop Doct, 2003. **33**(4): p. 193-4.
4. Thulasiraj, R.D., et al., *Blindness and vision impairment in a rural south Indian population: the Aravind Comprehensive Eye Survey.* Ophthalmology, 2003. **110**(8): p. 1491-8.
5. Dandona, L., et al., *Blindness in the Indian state of Andhra Pradesh.* Invest Ophthalmol Vis Sci, 2001. **42**(5): p. 908-16.
6. National Programme for control of blindness, D.G.o.H.S., Ministry of Health and Family Welfare Government of India, *National survey on blindness and visual outcome after cataract surgery*. 2002: New Delhi
7. Tabbara, K.F., *Blindness in the eastern Mediterranean countries.* Br J Ophthalmol, 2001. **85**(7): p. 771-5.
8. Chirambo, M.C., et al., *Blindness and visual impairment in southern Malawi.* Bull World Health Organ, 1986. **64**(4): p. 567-72.
9. Khan, M.U., E. Haque, and M.R. Khan, *Prevalence & causes of blindness in rural Bangladesh.* Indian J Med Res, 1985. **82**: p. 257-62.
10. Solomon, A., *State of the World's Sight. Vision 2020: the Right to Sight 1999–2005*. 2005, World Health Organization: Geneva.
11. Foster, A. and A. Sommer, *Childhood blindness from corneal ulceration in Africa: causes, prevention, and treatment.* Bull World Health Organ, 1986. **64**(5): p. 619-23.
12. Keay, L., et al., *Microbial keratitis predisposing factors and morbidity.* Ophthalmology, 2006. **113**(1): p. 109-16.
13. Whitcher, J.P., M. Srinivasan, and M.P. Upadhyay, *Corneal blindness: a global perspective.* Bull World Health Organ, 2001. **79**(3): p. 214-21.
14. *Global initiative for the elimination of avoidable blindness*. 1997, World Health Organization: Geneva.
15. Boatin, B.A., *The current state of the Onchocerciasis Control Programme in West Africa.* Trop Doct, 2003. **33**(4): p. 209-14.
16. John, D. and E. Daniel, *Infectious keratitis in leprosy.* Br J Ophthalmol, 1999. **83**(2): p. 173-6.
17. Garg, P., et al., *The value of corneal transplantation in reducing blindness.* Eye (Lond), 2005. **19**(10): p. 1106-14.
18. Wang, H., et al., *Prevalence and causes of corneal blindness.* Clin Experiment Ophthalmol, 2014. **42**(3): p. 249-53.
19. Rapoza, P.A., et al., *Etiology of corneal opacification in central Tanzania.* Int Ophthalmol, 1993. **17**(1): p. 47-51.
20. Bowman, R.J., et al., *Non-trachomatous corneal opacities in the Gambia--aetiology and visual burden.* Eye (Lond), 2002. **16**(1): p. 27-32.
21. Brilliant, L.B., et al., *Epidemiology of blindness in Nepal.* Bull World Health Organ, 1985. **63**(2): p. 375-86.
22. Whitcher, J.P. and M. Srinivasan, *Corneal ulceration in the developing world--a silent epidemic.* Br J Ophthalmol, 1997. **81**(8): p. 622-3.
23. Shah, A., et al., *Geographic variations in microbial keratitis: an analysis of the peer-reviewed literature.* Br J Ophthalmol, 2011. **95**(6): p. 762-7.
24. Ray, K.J., et al., *Fluoroquinolone treatment and susceptibility of isolates from bacterial keratitis.* JAMA Ophthalmol, 2013. **131**(3): p. 310-3.

25. Oldenburg, C.E., et al., *Moxifloxacin susceptibility mediates the relationship between causative organism and clinical outcome in bacterial keratitis.* Invest Ophthalmol Vis Sci, 2013. **54**(2): p. 1522-6.
26. Sengupta, S., et al., *Changing referral patterns of infectious corneal ulcers to a tertiary care facility in south India - 7-year analysis.* Ophthalmic Epidemiol, 2012. **19**(5): p. 297-301.
27. Wong, T., et al., *Severe infective keratitis leading to hospital admission in New Zealand.* Br J Ophthalmol, 2003. **87**(9): p. 1103-8.
28. Laspina, F., et al., *Epidemiological characteristics of microbiological results on patients with infectious corneal ulcers: a 13-year survey in Paraguay.* Graefes Arch Clin Exp Ophthalmol, 2004. **242**(3): p. 204-9.
29. Otri, A.M., et al., *Profile of sight-threatening infectious keratitis: a prospective study.* Acta Ophthalmol, 2013. **91**(7): p. 643-51.
30. Mascarenhas, J., et al., *Differentiation of etiologic agents of bacterial keratitis from presentation characteristics.* Int Ophthalmol, 2012. **32**(6): p. 531-8.
31. Leck, A.K., et al., *Aetiology of suppurative corneal ulcers in Ghana and south India, and epidemiology of fungal keratitis.* Br J Ophthalmol, 2002. **86**(11): p. 1211-5.
32. Kimura, H., et al., *Keratoconjunctivitis caused by echovirus type 13 in Japanese children.* Pediatr Infect Dis J, 2003. **22**(8): p. 758-9.
33. Kasova, V., et al., *Poliovirus type 3 keratoconjunctivitis.* J Infect Dis, 1980. **142**(2): p. 292.
34. Thanathanee, O., et al., *Outbreak of Pythium keratitis during rainy season: a case series.* Cornea, 2013. **32**(2): p. 199-204.
35. Reddy, A.K., et al., *Dictyostelium polycephalum infection of human cornea.* Emerg Infect Dis, 2010. **16**(10): p. 1644-5.
36. Sreejith, R.S., et al., *Oestrus ovis ophthalmomyiasis with keratitis.* Indian J Med Microbiol, 2010. **28**(4): p. 399-402.
37. Alexandrakis, G., D. Miller, and A.J. Huang, *Amebic keratitis due to Vahlkampfia infection following corneal trauma.* Arch Ophthalmol, 1998. **116**(7): p. 950-1.
38. Stapleton, F., et al., *Risk factors for moderate and severe microbial keratitis in daily wear contact lens users.* Ophthalmology, 2012. **119**(8): p. 1516-21.
39. Ahn, M., et al., *Clinical aspects and prognosis of mixed microbial (bacterial and fungal) keratitis.* Cornea, 2011. **30**(4): p. 409-13.
40. Amescua, G., D. Miller, and E.C. Alfonso, *What is causing the corneal ulcer? Management strategies for unresponsive corneal ulceration.* Eye (Lond), 2012. **26**(2): p. 228-36.
41. Bharathi, M.J., et al., *Analysis of the risk factors predisposing to fungal, bacterial & Acanthamoeba keratitis in south India.* Indian J Med Res, 2009. **130**(6): p. 749-57.
42. Upadhyay, M.P., et al., *The Bhaktapur eye study: ocular trauma and antibiotic prophylaxis for the prevention of corneal ulceration in Nepal.* Br J Ophthalmol, 2001. **85**(4): p. 388-92.
43. Srinivasan, M., et al., *Epidemiology and aetiological diagnosis of corneal ulceration in Madurai, south India.* Br J Ophthalmol, 1997. **81**(11): p. 965-71.
44. Ormerod, L.D., et al., *Epidemiology of microbial keratitis in southern California. A multivariate analysis.* Ophthalmology, 1987. **94**(10): p. 1322-33.
45. Bourcier, T., et al., *Bacterial keratitis: predisposing factors, clinical and microbiological review of 300 cases.* Br J Ophthalmol, 2003. **87**(7): p. 834-8.
46. Stapleton, F., et al., *The incidence of contact lens-related microbial keratitis in Australia.* Ophthalmology, 2008. **115**(10): p. 1655-62.
47. Hoddenbach, J.G., et al., *Clinical presentation and morbidity of contact lens-associated microbial keratitis: a retrospective study.* Graefes Arch Clin Exp Ophthalmol, 2014. **252**(2): p. 299-306.
48. Tabbara, K.F., H.F. El-Sheikh, and B. Aabed, *Extended wear contact lens related bacterial keratitis.* Br J Ophthalmol, 2000. **84**(3): p. 327-8.

49. Patrinely, J.R., et al., *Bacterial keratitis associated with extended wear soft contact lenses.* CLAO J, 1985. **11**(3): p. 234-6.
50. Galentine, P.G., et al., *Corneal ulcers associated with contact lens wear.* Arch Ophthalmol, 1984. **102**(6): p. 891-4.
51. Krachmer, J.H., M.J. Mannis, and E.J. Holland, *Cornea: Fundamentals , Diagnosis and Management*. 2nd ed. Vol. 1. 2005, St Louis: Elsevier Mosby.
52. Mishima, S., *Corneal thickness.* Surv Ophthalmol, 1968. **13**(2): p. 57-96.
53. Rozsa, A.J. and R.W. Beuerman, *Density and organization of free nerve endings in the corneal epithelium of the rabbit.* Pain, 1982. **14**(2): p. 105-20.
54. Al-Aqaba, M.A., et al., *Architecture and distribution of human corneal nerves.* Br J Ophthalmol, 2010. **94**(6): p. 784-9.
55. Jones, M.A. and C.F. Marfurt, *Peptidergic innervation of the rat cornea.* Exp Eye Res, 1998. **66**(4): p. 421-35.
56. Lehtosalo, J.I., *Substance P-like immunoreactive trigeminal ganglion cells supplying the cornea.* Histochemistry, 1984. **80**(3): p. 273-6.
57. Marfurt, C.F., C.J. Murphy, and J.L. Florczak, *Morphology and neurochemistry of canine corneal innervation.* Invest Ophthalmol Vis Sci, 2001. **42**(10): p. 2242-51.
58. Uusitalo, H., K. Krootila, and A. Palkama, *Calcitonin gene-related peptide (CGRP) immunoreactive sensory nerves in the human and guinea pig uvea and cornea.* Exp Eye Res, 1989. **48**(4): p. 467-75.
59. Stone, R.A., *Neuropeptide Y and the innervation of the human eye.* Exp Eye Res, 1986. **42**(4): p. 349-55.
60. Ueda, S., et al., *Peptidergic and catecholaminergic fibers in the human corneal epithelium. An immunohistochemical and electron microscopic study.* Acta Ophthalmol Suppl, 1989. **192**: p. 80-90.
61. Stone, R.A., et al., *Vasoactive intestinal polypeptide-like immunoreactive nerves to the human eye.* Acta Ophthalmol (Copenh), 1986. **64**(1): p. 12-8.
62. Terenghi, G., et al., *Morphological changes of sensory CGRP-immunoreactive and sympathetic nerves in peripheral tissues following chronic denervation.* Histochemistry, 1986. **86**(1): p. 89-95.
63. Aguayo, J.B., et al., *Dynamic monitoring of corneal carbohydrate metabolism using high-resolution deuterium NMR spectroscopy.* Exp Eye Res, 1988. **47**(2): p. 337-43.
64. Brandell, B.W., et al., *Tissue oxygen uptake from the atmosphere by a new, noninvasive polarographic technique with application to corneal metabolism.* Adv Exp Med Biol, 1988. **222**: p. 275-84.
65. Gottsch, J.D., et al., *Glycolytic activity in the human cornea monitored with nuclear magnetic resonance spectroscopy.* Arch Ophthalmol, 1986. **104**(6): p. 886-9.
66. Weissman, B.A., I. Fatt, and J. Rasson, *Diffusion of oxygen in human corneas in vivo.* Invest Ophthalmol Vis Sci, 1981. **20**(1): p. 123-5.
67. Thoft, R.A. and J. Friend, *Biochmical aspects of contact lens wear.* Am J Ophthalmol, 1975. **80**(1): p. 139-45.
68. Sack, R.A., K.O. Tan, and A. Tan, *Diurnal tear cycle: evidence for a nocturnal inflammatory constitutive tear fluid.* Invest Ophthalmol Vis Sci, 1992. **33**(3): p. 626-40.
69. Sack, R.A., et al., *Towards a closed eye model of the pre-ocular tear layer.* Prog Retin Eye Res, 2000. **19**(6): p. 649-68.
70. Holly, F.J. and M.A. Lemp, *Tear physiology and dry eyes.* Surv Ophthalmol, 1977. **22**(2): p. 69-87.
71. van Setten, G.B., et al., *Epidermal growth factor is a constant component of normal human tear fluid.* Graefes Arch Clin Exp Ophthalmol, 1989. **227**(2): p. 184-7.
72. Gupta, A., et al., *Transforming growth factor beta-1 and beta-2 in human tear fluid.* Curr Eye Res, 1996. **15**(6): p. 605-14.

73. van Setten, G.B., *Basic fibroblast growth factor in human tear fluid: detection of another growth factor.* Graefes Arch Clin Exp Ophthalmol, 1996. **234**(4): p. 275-7.
74. Barton, K., et al., *Inflammatory cytokines in the tears of patients with ocular rosacea.* Ophthalmology, 1997. **104**(11): p. 1868-74.
75. Vesaluoma, M., et al., *Platelet-derived growth factor-BB (PDGF-BB) in tear fluid: a potential modulator of corneal wound healing following photorefractive keratectomy.* Curr Eye Res, 1997. **16**(8): p. 825-31.
76. Watanabe, K., S. Nakagawa, and T. Nishida, *Stimulatory effects of fibronectin and EGF on migration of corneal epithelial cells.* Invest Ophthalmol Vis Sci, 1987. **28**(2): p. 205-11.
77. Nishida, T. and T. Tanaka, *Extracellular matrix and growth factors in corneal wound healing.* Curr Opin Ophthalmol, 1996. **7**(4): p. 2-11.
78. Fini, M.E., et al., *Unique regulation of the matrix metalloproteinase, gelatinase B.* Invest Ophthalmol Vis Sci, 1995. **36**(3): p. 622-33.
79. Kumagai, N., et al., *Active matrix metalloproteinases in the tear fluid of individuals with vernal keratoconjunctivitis.* J Allergy Clin Immunol, 2002. **110**(3): p. 489-91.
80. Malecaze, F., et al., *Interleukin-6 in tear fluid after photorefractive keratectomy and its effects on keratocytes in culture.* Cornea, 1997. **16**(5): p. 580-7.
81. Afonso, A.A., et al., *Tear fluid gelatinase B activity correlates with IL-1alpha concentration and fluorescein clearance in ocular rosacea.* Invest Ophthalmol Vis Sci, 1999. **40**(11): p. 2506-12.
82. Maurice, D.M., *The cornea and sclera*, in *The Eye*, H. Davson, Editor. 1984, Academic Press: Orlando. p. 1-158.
83. Beitch, I., *The induction of keratinization in the corneal epithelium. A comparison of the "dry" and vitamin A-deficient eyes.* Invest Ophthalmol, 1970. **9**(11): p. 827-43.
84. Pfister, R.R., *The normal surface of corneal epithelium: a scanning electron microscopic study.* Invest Ophthalmol, 1973. **12**(9): p. 654-68.
85. Argueso, P. and I.K. Gipson, *Epithelial mucins of the ocular surface: structure, biosynthesis and function.* Exp Eye Res, 2001. **73**(3): p. 281-9.
86. Esco, M.A., et al., *Potential role for laminin 5 in hypoxia-mediated apoptosis of human corneal epithelial cells.* J Cell Sci, 2001. **114**(Pt 22): p. 4033-40.
87. Ma, X. and H.E. Bazan, *Platelet-activating factor (PAF) enhances apoptosis induced by ultraviolet radiation in corneal epithelial cells through cytochrome c-caspase activation.* Curr Eye Res, 2001. **23**(5): p. 326-35.
88. Li, L., et al., *Annexin V binding to rabbit corneal epithelial cells following overnight contact lens wear or eyelid closure.* CLAO J, 2002. **28**(1): p. 48-54.
89. Estil, S., E.J. Primo, and G. Wilson, *Apoptosis in shed human corneal cells.* Invest Ophthalmol Vis Sci, 2000. **41**(11): p. 3360-4.
90. Doran, T.I., A. Vidrich, and T.T. Sun, *Intrinsic and extrinsic regulation of the differentiation of skin, corneal and esophageal epithelial cells.* Cell, 1980. **22**(1 Pt 1): p. 17-25.
91. Sun, T.T. and H. Green, *Cultured epithelial cells of cornea, conjunctiva and skin: absence of marked intrinsic divergence of their differentiated states.* Nature, 1977. **269**(5628): p. 489-93.
92. Hanna, C., D.S. Bicknell, and J.E. O'Brien, *Cell turnover in the adult human eye.* Arch Ophthalmol, 1961. **65**: p. 695-8.
93. Gipson, I.K., S.J. Spurr-Michaud, and A.S. Tisdale, *Anchoring fibrils form a complex network in human and rabbit cornea.* Invest Ophthalmol Vis Sci, 1987. **28**(2): p. 212-20.
94. Berman, M., et al., *Ulceration is correlated with degradation of fibrin and fibronectin at the corneal surface.* Invest Ophthalmol Vis Sci, 1983. **24**(10): p. 1358-66.
95. Tran, C.S., et al., *Host cell polarity proteins participate in innate immunity to Pseudomonas aeruginosa infection.* Cell Host Microbe, 2014. **15**(5): p. 636-43.

96. Bucior, I., J.F. Pielage, and J.N. Engel, *Pseudomonas aeruginosa pili and flagella mediate distinct binding and signaling events at the apical and basolateral surface of airway epithelium.* PLoS Pathog, 2012. **8**(4): p. e1002616.
97. Engel, J. and Y. Eran, *Subversion of mucosal barrier polarity by pseudomonas aeruginosa.* Front Microbiol, 2011. **2**: p. 114.
98. Watanabe, K., S. Nakagawa, and T. Nishida, *Chemotactic and haptotactic activities of fibronectin for cultured rabbit corneal epithelial cells.* Invest Ophthalmol Vis Sci, 1988. **29**(4): p. 572-7.
99. Suzuki, K., et al., *Coordinated reassembly of the basement membrane and junctional proteins during corneal epithelial wound healing.* Invest Ophthalmol Vis Sci, 2000. **41**(9): p. 2495-500.
100. Alarcon, I., et al., *Role of the corneal epithelial basement membrane in ocular defense against Pseudomonas aeruginosa.* Infect Immun, 2009. **77**(8): p. 3264-71.
101. Rodrigues, M.M., et al., *Langerhans cells in the normal conjunctiva and peripheral cornea of selected species.* Invest Ophthalmol Vis Sci, 1981. **21**(5): p. 759-65.
102. Lang, R.M., M.H. Friedlaender, and B.J. Schoenrock, *A new morphologic manifestation of Langerhans cells in guinea pig corneal transplants.* Curr Eye Res, 1981. **1**(3): p. 161-7.
103. Gillette, T.E., J.W. Chandler, and J.V. Greiner, *Langerhans cells of the ocular surface.* Ophthalmology, 1982. **89**(6): p. 700-11.
104. Rubsamen, P.E., et al., *On the Ia immunogenicity of mouse corneal allografts infiltrated with Langerhans cells.* Invest Ophthalmol Vis Sci, 1984. **25**(5): p. 513-8.
105. Whitsett, C.F. and R.D. Stulting, *The distribution of HLA antigens on human corneal tissue.* Invest Ophthalmol Vis Sci, 1984. **25**(5): p. 519-24.
106. Ward, B.R., et al., *Local thermal injury elicits immediate dynamic behavioural responses by corneal Langerhans cells.* Immunology, 2007. **120**(4): p. 556-72.
107. Komai, Y. and T. Ushiki, *The three-dimensional organization of collagen fibrils in the human cornea and sclera.* Invest Ophthalmol Vis Sci, 1991. **32**(8): p. 2244-58.
108. Gordon, M.K., et al., *Type V collagen and Bowman's membrane. Quantitation of mRNA in corneal epithelium and stroma.* J Biol Chem, 1994. **269**(40): p. 24959-66.
109. Jacobsen, I.E., O.A. Jensen, and J.U. Prause, *Structure and composition of Bowman's membrane. Study by frozen resin cracking.* Acta Ophthalmol (Copenh), 1984. **62**(1): p. 39-53.
110. Wilson, S.E. and J.W. Hong, *Bowman's layer structure and function: critical or dispensable to corneal function? A hypothesis.* Cornea, 2000. **19**(4): p. 417-20.
111. Hassell, J.R. and D.E. Birk, *The molecular basis of corneal transparency.* Exp Eye Res, 2010. **91**(3): p. 326-35.
112. Linsenmayer, T.F., J.M. Fitch, and R. Mayne, *Extracellular matrices in the developing avian eye: type V collagen in corneal and noncorneal tissues.* Invest Ophthalmol Vis Sci, 1984. **25**(1): p. 41-7.
113. Konomi, H., et al., *Localization of type V collagen and type IV collagen in human cornea, lung, and skin. Immunohistochemical evidence by anti-collagen antibodies characterized by immunoelectroblotting.* Am J Pathol, 1984. **116**(3): p. 417-26.
114. Yue, B.Y., J. Sugar, and K. Schrode, *Collagen staining in corneal tissues.* Curr Eye Res, 1986. **5**(8): p. 559-64.
115. Kern, P., M. Menasche, and L. Robert, *Relative rates of biosynthesis of collagen type I, type V and type VI in calf cornea.* Biochem J, 1991. **274 (Pt 2)**: p. 615-7.
116. Doane, K.J., G. Yang, and D.E. Birk, *Corneal cell-matrix interactions: type VI collagen promotes adhesion and spreading of corneal fibroblasts.* Exp Cell Res, 1992. **200**(2): p. 490-9.
117. Ueda, A., et al., *Electron-microscopic studies on the presence of gap junctions between corneal fibroblasts in rabbits.* Cell Tissue Res, 1987. **249**(2): p. 473-5.
118. Poole, C.A., N.H. Brookes, and G.M. Clover, *Confocal imaging of the human keratocyte network using the vital dye 5-chloromethylfluorescein diacetate.* Clin Experiment Ophthalmol, 2003. **31**(2): p. 147-54.

119. West-Mays, J.A. and D.J. Dwivedi, *The keratocyte: corneal stromal cell with variable repair phenotypes.* Int J Biochem Cell Biol, 2006. **38**(10): p. 1625-31.
120. Nishida, T., et al., *Interactions of extracellular collagen and corneal fibroblasts: morphologic and biochemical changes of rabbit corneal cells cultured in a collagen matrix.* In Vitro Cell Dev Biol, 1988. **24**(10): p. 1009-14.
121. Tomasek, J.J., E.D. Hay, and K. Fujiwara, *Collagen modulates cell shape and cytoskeleton of embryonic corneal and fibroma fibroblasts: distribution of actin, alpha-actinin, and myosin.* Dev Biol, 1982. **92**(1): p. 107-22.
122. Giraud, J.P., et al., *Statistical morphometric studies in normal human and rabbit corneal stroma.* Exp Eye Res, 1975. **21**(3): p. 221-9.
123. Freegard, T.J., *The physical basis of transparency of the normal cornea.* Eye (Lond), 1997. **11 (Pt 4)**: p. 465-71.
124. Morishige, N., et al., *Three-dimensional analysis of collagen lamellae in the anterior stroma of the human cornea visualized by second harmonic generation imaging microscopy.* Invest Ophthalmol Vis Sci, 2011. **52**(2): p. 911-5.
125. Liles, M., et al., *Differential relative sulfation of Keratan sulfate glycosaminoglycan in the chick cornea during embryonic development.* Invest Ophthalmol Vis Sci, 2010. **51**(3): p. 1365-72.
126. Saika, S., et al., *TGFbeta2 in corneal morphogenesis during mouse embryonic development.* Dev Biol, 2001. **240**(2): p. 419-32.
127. Fitch, J.M., et al., *The spatial organization of Descemet's membrane-associated type IV collagen in the avian cornea.* J Cell Biol, 1990. **110**(4): p. 1457-68.
128. Fujikawa, L.S., et al., *Fibronectin in healing rabbit corneal wounds.* Lab Invest, 1981. **45**(2): p. 120-9.
129. Suda, T., et al., *Fibronectin appears at the site of corneal stromal wound in rabbits.* Curr Eye Res, 1981. **1**(9): p. 553-6.
130. Tuft, S.J. and D.J. Coster, *The corneal endothelium.* Eye (Lond), 1990. **4 (Pt 3)**: p. 389-424.
131. Joyce, N.C., et al., *Cell cycle protein expression and proliferative status in human corneal cells.* Invest Ophthalmol Vis Sci, 1996. **37**(4): p. 645-55.
132. Joyce, N.C., *Proliferative capacity of the corneal endothelium.* Prog Retin Eye Res, 2003. **22**(3): p. 359-89.
133. Laule, A., et al., *Endothelial cell population changes of human cornea during life.* Arch Ophthalmol, 1978. **96**(11): p. 2031-5.
134. Hogan, M.J., J.A. Alvarado, and J.E. Weddell, *Histology of the human cornea*. 1971, Philadelphia.
135. Ringvold, A., M. Davanger, and E.G. Olsen, *On the spatial organization of the cornea endothelium.* Acta Ophthalmol (Copenh), 1984. **62**(6): p. 911-8.
136. Hirsch, M., et al., *Study of the ultrastructure of the rabbit corneal endothelium by the freeze-fracture technique: apical and lateral junctions.* Exp Eye Res, 1977. **25**(3): p. 277-88.
137. Fini, M.E. and B.M. Stramer, *How the cornea heals: cornea-specific repair mechanisms affecting surgical outcomes.* Cornea, 2005. **24**(8 Suppl): p. S2-S11.
138. Lederberg, J., *Pseudomonas*, in *Encyclopedia of Microbiology*. 2000, Academic Press: San Diego. p. 876-891.
139. *Classics in infectious diseases. On the blue and green coloration that appears on bandages. By Carle Gessard (1850-1925).* Rev Infect Dis, 1984. **6 Suppl 3**: p. S775-6.
140. Costerton, W. and H. Anwar, *Pseudomonas aeruginosa: The Microbe and Pathogen*, in *Pseudomonas aeruginosa Infections and Treatment*. 1994. p. 1-17.
141. Romanov, V.L., et al., *[Oxidative dehalogenation of 2-chloro- and 2,4-dichlorobenzoates by Pseudomonas aeruginosa].* Mikrobiologiia, 1993. **62**(5): p. 887-96.
142. Favero, M.S., et al., *Pseudomonas aeruginosa: growth in distilled water from hospitals.* Science, 1971. **173**(3999): p. 836-8.

143. Oberhofer, T.R., *Growth of nonfermentative bacteria at 42 degrees C.* J Clin Microbiol, 1979. **10**(6): p. 800-4.
144. Goldberg, J.B., *Pseudomonas: global bacteria.* Trends Microbiol, 2000. **8**(2): p. 55-7.
145. Yoon, S.S., et al., *Pseudomonas aeruginosa anaerobic respiration in biofilms: relationships to cystic fibrosis pathogenesis.* Dev Cell, 2002. **3**(4): p. 593-603.
146. Eschbach, M., et al., *Long-term anaerobic survival of the opportunistic pathogen Pseudomonas aeruginosa via pyruvate fermentation.* J Bacteriol, 2004. **186**(14): p. 4596-604.
147. Song, R., et al., *Biodegradation of petroleum hydrocarbons by two Pseudomonas aeruginosa strains with different uptake modes.* J Environ Sci Health A Tox Hazard Subst Environ Eng, 2006. **41**(4): p. 733-48.
148. Itah, A.Y., et al., *Biodegradation of international jet A-1 aviation fuel by microorganisms isolated from aircraft tank and joint hydrant storage systems.* Bull Environ Contam Toxicol, 2009. **83**(3): p. 318-27.
149. Zhang, Z., et al., *Degradation of n-alkanes and polycyclic aromatic hydrocarbons in petroleum by a newly isolated Pseudomonas aeruginosa DQ8.* Bioresour Technol, 2011. **102**(5): p. 4111-6.
150. Gilardi, G., *Cultural and Biochemical Aspects for Identification of Glucose-Nonfermenting Gram-Negative Rods*, in *Nonfermenting Gram-Negative Rods*. 1985. p. 17-24.
151. Maybury, B.A., et al., *Antimicrobial susceptibilities of rough, smooth, and mucoid colony types of Pseudomonas isolated from cystic fibrosis patients.* Antimicrob Agents Chemother, 1979. **15**(3): p. 494-6.
152. Fito-Boncompte, L., et al., *Full virulence of Pseudomonas aeruginosa requires OprF.* Infect Immun, 2011. **79**(3): p. 1176-86.
153. Knirel, Y.A., *Polysaccharide antigens of Pseudomonas aeruginosa.* Crit Rev Microbiol, 1990. **17**(4): p. 273-304.
154. Stanislavsky, E.S. and J.S. Lam, *Pseudomonas aeruginosa antigens as potential vaccines.* FEMS Microbiol Rev, 1997. **21**(3): p. 243-77.
155. Ansorg, R.A., et al., *Differentiation of the major flagellar antigens of Pseudomonas aeruginosa by the slide coagglutination technique.* J Clin Microbiol, 1984. **20**(1): p. 84-8.
156. Feldman, M., et al., *Role of flagella in pathogenesis of Pseudomonas aeruginosa pulmonary infection.* Infect Immun, 1998. **66**(1): p. 43-51.
157. Belas, R., *Biofilms, flagella, and mechanosensing of surfaces by bacteria.* Trends Microbiol, 2014. **22**(9): p. 517-27.
158. Sircar, R., et al., *Assembly states of FliM and FliG within the flagellar switch complex.* J Mol Biol, 2015. **427**(4): p. 867-86.
159. Gode-Potratz, C.J., et al., *Surface sensing in Vibrio parahaemolyticus triggers a programme of gene expression that promotes colonization and virulence.* Mol Microbiol, 2011. **79**(1): p. 240-63.
160. Doig, P., et al., *Role of pili in adhesion of Pseudomonas aeruginosa to human respiratory epithelial cells.* Infect Immun, 1988. **56**(6): p. 1641-6.
161. Hahn, H.P., *The type-4 pilus is the major virulence-associated adhesin of Pseudomonas aeruginosa--a review.* Gene, 1997. **192**(1): p. 99-108.
162. Mattick, J.S., *Type IV pili and twitching motility.* Annu Rev Microbiol, 2002. **56**: p. 289-314.
163. Watts, T.H., C.M. Kay, and W. Paranchych, *Spectral properties of three quaternary arrangements of Pseudomonas pilin.* Biochemistry, 1983. **22**(15): p. 3640-6.
164. Folkhard, W., et al., *Structure of polar pili from Pseudomonas aeruginosa strains K and O.* J Mol Biol, 1981. **149**(1): p. 79-93.
165. Persat, A., et al., *Type IV pili mechanochemically regulate virulence factors in Pseudomonas aeruginosa.* Proc Natl Acad Sci U S A, 2015. **112**(24): p. 7563-8.
166. Gold, V.A., et al., *Structure of a type IV pilus machinery in the open and closed state.* Elife, 2015. **4**.

167. Ishimoto, K.S. and S. Lory, *Formation of pilin in Pseudomonas aeruginosa requires the alternative sigma factor (RpoN) of RNA polymerase.* Proc Natl Acad Sci U S A, 1989. **86**(6): p. 1954-7.
168. Totten, P.A., J.C. Lara, and S. Lory, *The rpoN gene product of Pseudomonas aeruginosa is required for expression of diverse genes, including the flagellin gene.* J Bacteriol, 1990. **172**(1): p. 389-96.
169. Stover, C.K., et al., *Complete genome sequence of Pseudomonas aeruginosa PAO1, an opportunistic pathogen.* Nature, 2000. **406**(6799): p. 959-64.
170. Lee, D.G., et al., *Genomic analysis reveals that Pseudomonas aeruginosa virulence is combinatorial.* Genome Biol, 2006. **7**(10): p. R90.
171. McCallum, S.J., et al., *Spread of an epidemic Pseudomonas aeruginosa strain from a patient with cystic fibrosis (CF) to non-CF relatives.* Thorax, 2002. **57**(6): p. 559-60.
172. Roy, P.H., et al., *Complete genome sequence of the multiresistant taxonomic outlier Pseudomonas aeruginosa PA7.* PLoS One, 2010. **5**(1): p. e8842.
173. Evans, D.J. and S.M. Fleiszig, *Why does the healthy cornea resist Pseudomonas aeruginosa infection?* Am J Ophthalmol, 2013. **155**(6): p. 961-970 e2.
174. Sensakovic, J.W. and P.F. Bartell, *Biological activity of fragments derived from the extracellular slime glycolipoprotein of Pseudomonas aeruginosa.* Infect Immun, 1975. **12**(4): p. 808-12.
175. Wretlind, B. and O.R. Pavlovskis, *Pseudomonas aeruginosa elastase and its role in pseudomonas infections.* Rev Infect Dis, 1983. **5 Suppl 5**: p. S998-1004.
176. Galloway, D.R., *Pseudomonas aeruginosa elastase and elastolysis revisited: recent developments.* Mol Microbiol, 1991. **5**(10): p. 2315-21.
177. Caballero, A.R., et al., *Pseudomonas aeruginosa protease IV enzyme assays and comparison to other Pseudomonas proteases.* Anal Biochem, 2001. **290**(2): p. 330-7.
178. Engel, L.S., et al., *Protease IV, a unique extracellular protease and virulence factor from Pseudomonas aeruginosa.* J Biol Chem, 1998. **273**(27): p. 16792-7.
179. Inoue, H., T. Nakagawa, and K. Morihara, *Pseudomonas aeruginosa proteinase. II. Molecular weight and molecular dimension.* Biochim Biophys Acta, 1963. **73**: p. 125-31.
180. Morihara, K., *Production of Elastase and Proteinase by Pseudomonas Aeruginosa.* J Bacteriol, 1964. **88**: p. 745-57.
181. Peters, J.E. and D.R. Galloway, *Purification and characterization of an active fragment of the LasA protein from Pseudomonas aeruginosa: enhancement of elastase activity.* J Bacteriol, 1990. **172**(5): p. 2236-40.
182. Schad, P.A. and B.H. Iglewski, *Nucleotide sequence and expression in Escherichia coli of the Pseudomonas aeruginosa lasA gene.* J Bacteriol, 1988. **170**(6): p. 2784-9.
183. Marquart, M.E., et al., *Identification of a novel secreted protease from Pseudomonas aeruginosa that causes corneal erosions.* Invest Ophthalmol Vis Sci, 2005. **46**(10): p. 3761-8.
184. Baumann, U., et al., *Three-dimensional structure of the alkaline protease of Pseudomonas aeruginosa: a two-domain protein with a calcium binding parallel beta roll motif.* EMBO J, 1993. **12**(9): p. 3357-64.
185. Folders, J., et al., *Identification of a chitin-binding protein secreted by Pseudomonas aeruginosa.* J Bacteriol, 2000. **182**(5): p. 1257-63.
186. Morihara, K., *Pseudolysin and other pathogen endopeptidases of thermolysin family.* Methods Enzymol, 1995. **248**: p. 242-53.
187. Kessler, E. and D.E. Ohman, *Handbook of Proteolytic Enzymes*. 1998, London: Academic Press.
188. Kessler, E., et al., *Elastase and the LasA protease of Pseudomonas aeruginosa are secreted with their propeptides.* J Biol Chem, 1998. **273**(46): p. 30225-31.
189. Braun, P. and J. Tommassen, *Function of bacterial propeptides.* Trends Microbiol, 1998. **6**(1): p. 6-8.

190. Kessler, E. and M. Safrin, *The propeptide of Pseudomonas aeruginosa elastase acts an elastase inhibitor.* J Biol Chem, 1994. **269**(36): p. 22726-31.
191. Braun, P., W. Bitter, and J. Tommassen, *Activation of Pseudomonas aeruginosa elastase in Pseudomonas putida by triggering dissociation of the propeptide-enzyme complex.* Microbiology, 2000. **146 (Pt 10)**: p. 2565-72.
192. McIver, K.S., J.C. Olson, and D.E. Ohman, *Pseudomonas aeruginosa lasB1 mutants produce an elastase, substituted at active-site His-223, that is defective in activity, processing, and secretion.* J Bacteriol, 1993. **175**(13): p. 4008-15.
193. Kuang, Z., et al., *Pseudomonas aeruginosa elastase provides an escape from phagocytosis by degrading the pulmonary surfactant protein-A.* PLoS One, 2011. **6**(11): p. e27091.
194. Parmely, M., et al., *Proteolytic inactivation of cytokines by Pseudomonas aeruginosa.* Infect Immun, 1990. **58**(9): p. 3009-14.
195. Scharmann, W., F. Jacob, and J. Porstendorfer, *The cytotoxic action of leucocidan from Pseudomonas aeruginosa on human polymorphonuclear leucocytes.* J Gen Microbiol, 1976. **93**(2): p. 303-8.
196. Berka, R.M. and M.L. Vasil, *Phospholipase C (heat-labile hemolysin) of Pseudomonas aeruginosa: purification and preliminary characterization.* J Bacteriol, 1982. **152**(1): p. 239-45.
197. Boukhalfa, H. and A.L. Crumbliss, *Chemical aspects of siderophore mediated iron transport.* Biometals, 2002. **15**(4): p. 325-39.
198. Braun, V., *Iron uptake by Escherichia coli.* Front Biosci, 2003. **8**: p. s1409-21.
199. Braun, V. and H. Killmann, *Bacterial solutions to the iron-supply problem.* Trends Biochem Sci, 1999. **24**(3): p. 104-9.
200. Schalk, I.J., et al., *Copurification of the FpvA ferric pyoverdin receptor of Pseudomonas aeruginosa with its iron-free ligand: implications for siderophore-mediated iron transport.* Biochemistry, 1999. **38**(29): p. 9357-65.
201. Lau, G.W., et al., *The role of pyocyanin in Pseudomonas aeruginosa infection.* Trends Mol Med, 2004. **10**(12): p. 599-606.
202. Braud, A., et al., *The Pseudomonas aeruginosa pyochelin-iron uptake pathway and its metal specificity.* J Bacteriol, 2009. **191**(11): p. 3517-25.
203. Hauser, A.R., *The type III secretion system of Pseudomonas aeruginosa: infection by injection.* Nat Rev Microbiol, 2009. **7**(9): p. 654-65.
204. Hoiczyk, E. and G. Blobel, *Polymerization of a single protein of the pathogen Yersinia enterocolitica into needles punctures eukaryotic cells.* Proc Natl Acad Sci U S A, 2001. **98**(8): p. 4669-74.
205. Cordes, F.S., et al., *Helical structure of the needle of the type III secretion system of Shigella flexneri.* J Biol Chem, 2003. **278**(19): p. 17103-7.
206. Kubori, T., et al., *Supramolecular structure of the Salmonella typhimurium type III protein secretion system.* Science, 1998. **280**(5363): p. 602-5.
207. Pastor, A., et al., *PscF is a major component of the Pseudomonas aeruginosa type III secretion needle.* FEMS Microbiol Lett, 2005. **253**(1): p. 95-101.
208. Soscia, C., et al., *Cross talk between type III secretion and flagellar assembly systems in Pseudomonas aeruginosa.* J Bacteriol, 2007. **189**(8): p. 3124-32.
209. Banerjee, A., et al., *Binding mode analysis of a major T3SS translocator protein PopB with its chaperone PcrH from Pseudomonas aeruginosa.* Proteins, 2014. **82**(12): p. 3273-85.
210. Schoehn, G., et al., *Oligomerization of type III secretion proteins PopB and PopD precedes pore formation in Pseudomonas.* Embo j, 2003. **22**(19): p. 4957-67.
211. Sundin, C., et al., *Polarisation of type III translocation by Pseudomonas aeruginosa requires PcrG, PcrV and PopN.* Microb Pathog, 2004. **37**(6): p. 313-22.
212. Dacheux, D., et al., *Pore-forming activity of type III system-secreted proteins leads to oncosis of Pseudomonas aeruginosa-infected macrophages.* Mol Microbiol, 2001. **40**(1): p. 76-85.

213. Goure, J., et al., *The V antigen of Pseudomonas aeruginosa is required for assembly of the functional PopB/PopD translocation pore in host cell membranes.* Infect Immun, 2004. **72**(8): p. 4741-50.
214. Lee, V.T., et al., *Activities of Pseudomonas aeruginosa effectors secreted by the Type III secretion system in vitro and during infection.* Infect Immun, 2005. **73**(3): p. 1695-705.
215. Shafikhani, S.H., C. Morales, and J. Engel, *The Pseudomonas aeruginosa type III secreted toxin ExoT is necessary and sufficient to induce apoptosis in epithelial cells.* Cell Microbiol, 2008. **10**(4): p. 994-1007.
216. Roy, D., et al., *A process for controlling intracellular bacterial infections induced by membrane injury.* Science, 2004. **304**(5676): p. 1515-8.
217. Franchi, L., et al., *Critical role for Ipaf in Pseudomonas aeruginosa-induced caspase-1 activation.* Eur J Immunol, 2007. **37**(11): p. 3030-9.
218. Sutterwala, F.S., et al., *Immune recognition of Pseudomonas aeruginosa mediated by the IPAF/NLRC4 inflammasome.* J Exp Med, 2007. **204**(13): p. 3235-45.
219. Galle, M., et al., *The Pseudomonas aeruginosa Type III secretion system plays a dual role in the regulation of caspase-1 mediated IL-1beta maturation.* J Cell Mol Med, 2008. **12**(5A): p. 1767-76.
220. Miao, E.A., et al., *Pseudomonas aeruginosa activates caspase 1 through Ipaf.* Proc Natl Acad Sci U S A, 2008. **105**(7): p. 2562-7.
221. Parsot, C., C. Hamiaux, and A.L. Page, *The various and varying roles of specific chaperones in type III secretion systems.* Curr Opin Microbiol, 2003. **6**(1): p. 7-14.
222. Yahr, T.L., et al., *Transcriptional analysis of the Pseudomonas aeruginosa exoenzyme S structural gene.* J Bacteriol, 1995. **177**(5): p. 1169-78.
223. Shen, D.K., et al., *Orf1/SpcS chaperones ExoS for type three secretion by Pseudomonas aeruginosa.* Biomed Environ Sci, 2008. **21**(2): p. 103-9.
224. Finck-Barbancon, V., T.L. Yahr, and D.W. Frank, *Identification and characterization of SpcU, a chaperone required for efficient secretion of the ExoU cytotoxin.* J Bacteriol, 1998. **180**(23): p. 6224-31.
225. Fleiszig, S.M., et al., *Pseudomonas aeruginosa-mediated cytotoxicity and invasion correlate with distinct genotypes at the loci encoding exoenzyme S.* Infect Immun, 1997. **65**(2): p. 579-86.
226. Schulert, G.S., et al., *Secretion of the toxin ExoU is a marker for highly virulent Pseudomonas aeruginosa isolates obtained from patients with hospital-acquired pneumonia.* J Infect Dis, 2003. **188**(11): p. 1695-706.
227. Pederson, K.J., et al., *The amino-terminal domain of Pseudomonas aeruginosa ExoS disrupts actin filaments via small-molecular-weight GTP-binding proteins.* Mol Microbiol, 1999. **32**(2): p. 393-401.
228. Goehring, U.M., et al., *The N-terminal domain of Pseudomonas aeruginosa exoenzyme S is a GTPase-activating protein for Rho GTPases.* J Biol Chem, 1999. **274**(51): p. 36369-72.
229. Frithz-Lindsten, E., et al., *Intracellular targeting of exoenzyme S of Pseudomonas aeruginosa via type III-dependent translocation induces phagocytosis resistance, cytotoxicity and disruption of actin microfilaments.* Mol Microbiol, 1997. **25**(6): p. 1125-39.
230. Garrity-Ryan, L., et al., *The arginine finger domain of ExoT contributes to actin cytoskeleton disruption and inhibition of internalization of Pseudomonas aeruginosa by epithelial cells and macrophages.* Infect Immun, 2000. **68**(12): p. 7100-13.
231. Cowell, B.A., et al., *ExoT of cytotoxic Pseudomonas aeruginosa prevents uptake by corneal epithelial cells.* Infect Immun, 2000. **68**(1): p. 403-6.
232. Riese, M.J., et al., *Auto-ADP-ribosylation of Pseudomonas aeruginosa ExoS.* J Biol Chem, 2002. **277**(14): p. 12082-8.
233. Henriksson, M.L., et al., *A nonphosphorylated 14-3-3 binding motif on exoenzyme S that is functional in vivo.* Eur J Biochem, 2002. **269**(20): p. 4921-9.

234. Rocha, C.L., et al., *Characterization of Pseudomonas aeruginosa exoenzyme S as a bifunctional enzyme in J774A.1 macrophages.* Infect Immun, 2003. **71**(9): p. 5296-305.
235. Pederson, K.J. and J.T. Barbieri, *Intracellular expression of the ADP-ribosyltransferase domain of Pseudomonas exoenzyme S is cytotoxic to eukaryotic cells.* Mol Microbiol, 1998. **30**(4): p. 751-9.
236. Barbieri, A.M., et al., *ADP-ribosylation of Rab5 by ExoS of Pseudomonas aeruginosa affects endocytosis.* Infect Immun, 2001. **69**(9): p. 5329-34.
237. Fraylick, J.E., et al., *Independent and coordinate effects of ADP-ribosyltransferase and GTPase-activating activities of exoenzyme S on HT-29 epithelial cell function.* Infect Immun, 2001. **69**(9): p. 5318-28.
238. Kaufman, M.R., et al., *Pseudomonas aeruginosa mediated apoptosis requires the ADP-ribosylating activity of exoS.* Microbiology, 2000. **146 (Pt 10)**: p. 2531-41.
239. Krall, R., et al., *Pseudomonas aeruginosa ExoT is a Rho GTPase-activating protein.* Infect Immun, 2000. **68**(10): p. 6066-8.
240. Kazmierczak, B.I. and J.N. Engel, *Pseudomonas aeruginosa ExoT acts in vivo as a GTPase-activating protein for RhoA, Rac1, and Cdc42.* Infect Immun, 2002. **70**(4): p. 2198-205.
241. Shafikhani, S.H. and J. Engel, *Pseudomonas aeruginosa type III-secreted toxin ExoT inhibits host-cell division by targeting cytokinesis at multiple steps.* Proc Natl Acad Sci U S A, 2006. **103**(42): p. 15605-10.
242. Deng, Q., J. Sun, and J.T. Barbieri, *Uncoupling Crk signal transduction by Pseudomonas exoenzyme T.* J Biol Chem, 2005. **280**(43): p. 35953-60.
243. Shaver, C.M. and A.R. Hauser, *Relative contributions of Pseudomonas aeruginosa ExoU, ExoS, and ExoT to virulence in the lung.* Infect Immun, 2004. **72**(12): p. 6969-77.
244. Garrity-Ryan, L., et al., *The ADP ribosyltransferase domain of Pseudomonas aeruginosa ExoT contributes to its biological activities.* Infect Immun, 2004. **72**(1): p. 546-58.
245. Geiser, T.K., et al., *Pseudomonas aeruginosa ExoT inhibits in vitro lung epithelial wound repair.* Cell Microbiol, 2001. **3**(4): p. 223-36.
246. Cho, S.Y. and R.L. Klemke, *Extracellular-regulated kinase activation and CAS/Crk coupling regulate cell migration and suppress apoptosis during invasion of the extracellular matrix.* J Cell Biol, 2000. **149**(1): p. 223-36.
247. Sato, H., et al., *The mechanism of action of the Pseudomonas aeruginosa-encoded type III cytotoxin, ExoU.* EMBO J, 2003. **22**(12): p. 2959-69.
248. Phillips, R.M., et al., *In vivo phospholipase activity of the Pseudomonas aeruginosa cytotoxin ExoU and protection of mammalian cells with phospholipase A2 inhibitors.* J Biol Chem, 2003. **278**(42): p. 41326-32.
249. Hauser, A.R., P.J. Kang, and J.N. Engel, *PepA, a secreted protein of Pseudomonas aeruginosa, is necessary for cytotoxicity and virulence.* Mol Microbiol, 1998. **27**(4): p. 807-18.
250. Finck-Barbancon, V., et al., *ExoU expression by Pseudomonas aeruginosa correlates with acute cytotoxicity and epithelial injury.* Mol Microbiol, 1997. **25**(3): p. 547-57.
251. Kurahashi, K., et al., *Pathogenesis of septic shock in Pseudomonas aeruginosa pneumonia.* J Clin Invest, 1999. **104**(6): p. 743-50.
252. Yahr, T.L., et al., *ExoY, an adenylate cyclase secreted by the Pseudomonas aeruginosa type III system.* Proc Natl Acad Sci U S A, 1998. **95**(23): p. 13899-904.
253. Pearson, J.P., et al., *Structure of the autoinducer required for expression of Pseudomonas aeruginosa virulence genes.* Proc Natl Acad Sci U S A, 1994. **91**(1): p. 197-201.
254. Preston, M.J., et al., *Contribution of proteases and LasR to the virulence of Pseudomonas aeruginosa during corneal infections.* Infect Immun, 1997. **65**(8): p. 3086-90.
255. Willcox, M.D., et al., *Role of quorum sensing by Pseudomonas aeruginosa in microbial keratitis and cystic fibrosis.* Microbiology, 2008. **154**(Pt 8): p. 2184-94.
256. Hentzer, M., et al., *Attenuation of Pseudomonas aeruginosa virulence by quorum sensing inhibitors.* EMBO J, 2003. **22**(15): p. 3803-15.

257. Ichikawa, J.K., et al., *Genome-wide analysis of host responses to the Pseudomonas aeruginosa type III secretion system yields synergistic effects.* Cell Microbiol, 2005. **7**(11): p. 1635-46.
258. Vallis, A.J., et al., *Biological effects of Pseudomonas aeruginosa type III-secreted proteins on CHO cells.* Infect Immun, 1999. **67**(4): p. 2040-4.
259. Cowell, B.A., D.J. Evans, and S.M. Fleiszig, *Actin cytoskeleton disruption by ExoY and its effects on Pseudomonas aeruginosa invasion.* FEMS Microbiol Lett, 2005. **250**(1): p. 71-6.
260. Sayner, S.L., et al., *Paradoxical cAMP-induced lung endothelial hyperpermeability revealed by Pseudomonas aeruginosa ExoY.* Circ Res, 2004. **95**(2): p. 196-203.
261. Vance, R.E., A. Rietsch, and J.J. Mekalanos, *Role of the type III secreted exoenzymes S, T, and Y in systemic spread of Pseudomonas aeruginosa PAO1 in vivo.* Infect Immun, 2005. **73**(3): p. 1706-13.
262. Kleerebezem, M., et al., *Quorum sensing by peptide pheromones and two-component signal-transduction systems in Gram-positive bacteria.* Mol Microbiol, 1997. **24**(5): p. 895-904.
263. Schuster, M., et al., *Identification, timing, and signal specificity of Pseudomonas aeruginosa quorum-controlled genes: a transcriptome analysis.* J Bacteriol, 2003. **185**(7): p. 2066-79.
264. Wagner, V.E., et al., *Microarray analysis of Pseudomonas aeruginosa quorum-sensing regulons: effects of growth phase and environment.* J Bacteriol, 2003. **185**(7): p. 2080-95.
265. Gambello, M.J., S. Kaye, and B.H. Iglewski, *LasR of Pseudomonas aeruginosa is a transcriptional activator of the alkaline protease gene (apr) and an enhancer of exotoxin A expression.* Infect Immun, 1993. **61**(4): p. 1180-4.
266. Passador, L., et al., *Expression of Pseudomonas aeruginosa virulence genes requires cell-to-cell communication.* Science, 1993. **260**(5111): p. 1127-30.
267. Storey, D.G., et al., *Pseudomonas aeruginosa lasR transcription correlates with the transcription of lasA, lasB, and toxA in chronic lung infections associated with cystic fibrosis.* Infect Immun, 1998. **66**(6): p. 2521-8.
268. Toder, D.S., et al., *lasA and lasB genes of Pseudomonas aeruginosa: analysis of transcription and gene product activity.* Infect Immun, 1994. **62**(4): p. 1320-7.
269. Deziel, E., et al., *Analysis of Pseudomonas aeruginosa 4-hydroxy-2-alkylquinolines (HAQs) reveals a role for 4-hydroxy-2-heptylquinoline in cell-to-cell communication.* Proc Natl Acad Sci U S A, 2004. **101**(5): p. 1339-44.
270. Smith, R.S., et al., *The Pseudomonas autoinducer N-(3-oxododecanoyl) homoserine lactone induces cyclooxygenase-2 and prostaglandin E2 production in human lung fibroblasts: implications for inflammation.* J Immunol, 2002. **169**(5): p. 2636-42.
271. Vikstrom, E., F. Tafazoli, and K.E. Magnusson, *Pseudomonas aeruginosa quorum sensing molecule N-(3 oxododecanoyl)-l-homoserine lactone disrupts epithelial barrier integrity of Caco-2 cells.* FEBS Lett, 2006. **580**(30): p. 6921-8.
272. Hazlett, L.D., M. Zucker, and R.S. Berk, *Distribution and kinetics of the inflammatory cell response to ocular challenge with Pseudomonas aeruginosa in susceptible versus resistant mice.* Ophthalmic Res, 1992. **24**(1): p. 32-9.
273. Hazlett, L.D., *Role of innate and adaptive immunity in the pathogenesis of keratitis.* Ocul Immunol Inflamm, 2005. **13**(2-3): p. 133-8.
274. Hazlett, L.D., D.D. Rosen, and R.S. Berk, *Age-related susceptibility to Pseudomonas aeruginosa ocular infections in mice.* Infect Immun, 1978. **20**(1): p. 25-9.
275. Hazlett, L.D., et al., *Penetration of the unwounded immature mouse cornea and conjunctiva by Pseudomonas: SEM-TEM analysis.* Invest Ophthalmol Vis Sci, 1980. **19**(6): p. 694-7.
276. Hoiby, N., et al., *Pseudomonas aeruginosa and the in vitro and in vivo biofilm mode of growth.* Microbes Infect, 2001. **3**(1): p. 23-35.
277. Costerton, J.W., et al., *Biofilms, the customized microniche.* J Bacteriol, 1994. **176**(8): p. 2137-42.

278. Brown, M.R., P.J. Collier, and P. Gilbert, *Influence of growth rate on susceptibility to antimicrobial agents: modification of the cell envelope and batch and continuous culture studies.* Antimicrob Agents Chemother, 1990. **34**(9): p. 1623-8.
279. Davies, D.G., et al., *The involvement of cell-to-cell signals in the development of a bacterial biofilm.* Science, 1998. **280**(5361): p. 295-8.
280. Hancock, R.E., *Resistance mechanisms in Pseudomonas aeruginosa and other nonfermentative gram-negative bacteria.* Clin Infect Dis, 1998. **27 Suppl 1**: p. S93-9.
281. Henwood, C.J., et al., *Antimicrobial susceptibility of Pseudomonas aeruginosa: results of a UK survey and evaluation of the British Society for Antimicrobial Chemotherapy disc susceptibility test.* J Antimicrob Chemother, 2001. **47**(6): p. 789-99.
282. Mah, T.F. and G.A. O'Toole, *Mechanisms of biofilm resistance to antimicrobial agents.* Trends Microbiol, 2001. **9**(1): p. 34-9.
283. Lambert, P.A., *Mechanisms of antibiotic resistance in Pseudomonas aeruginosa.* J R Soc Med, 2002. **95 Suppl 41**: p. 22-6.
284. Gilad, J., *Burkholderia mallei and Burkholderia pseudomallei: the causative micro-organisms of glanders and melioidosis.* Recent Pat Antiinfect Drug Discov, 2007. **2**(3): p. 233-41.
285. Mesaros, N., et al., *Pseudomonas aeruginosa: resistance and therapeutic options at the turn of the new millennium.* Clin Microbiol Infect, 2007. **13**(6): p. 560-78.
286. Maschmeyer, G. and I. Braveny, *Review of the incidence and prognosis of Pseudomonas aeruginosa infections in cancer patients in the 1990s.* Eur J Clin Microbiol Infect Dis, 2000. **19**(12): p. 915-25.
287. *Pseudomonas septicaemia.* Br Med J, 1980. **280**(6226): p. 1240-1.
288. Finkelstein, R., et al., *Bone and joint infections due to Pseudomonas aeruginosa: clinical aspects and treatment.* Isr J Med Sci, 1989. **25**(3): p. 123-6.
289. Miskew, D.B., et al., *Pseudomonas aeruginosa bone and joint infection in drug abusers.* J Bone Joint Surg Am, 1983. **65**(6): p. 829-32.
290. Wise, B.L., J.L. Mathis, and E. Jawetz, *Infections of the central nervous system due to pseudomonas aeruginosa.* J Neurosurg, 1969. **31**(4): p. 432-4.
291. Wang, M.C., et al., *Ear problems in swimmers.* J Chin Med Assoc, 2005. **68**(8): p. 347-52.
292. Vrochides, D., W.C. Feng, and A.K. Singh, *Mycotic ascending aortic pseudoaneurysm secondary to pseudomonas mediastinitis at the aortic cannulation site.* Tex Heart Inst J, 2003. **30**(4): p. 322-4.
293. Schmitt, T.M., et al., *Pseudomonas aeruginosa pseudoaneurysm of the ascending aorta after coronary artery bypass graft surgery.* Tex Heart Inst J, 2003. **30**(2): p. 137-9.
294. Marshall, J.C., N.V. Christou, and J.L. Meakins, *The gastrointestinal tract. The "undrained abscess" of multiple organ failure.* Ann Surg, 1993. **218**(2): p. 111-9.
295. Chastre, J. and J.Y. Fagon, *Ventilator-associated pneumonia.* Am J Respir Crit Care Med, 2002. **165**(7): p. 867-903.
296. Ratjen, F., *Diagnosing and managing infection in CF.* Paediatr Respir Rev, 2006. **7 Suppl 1**: p. S151-3.
297. Nicotra, M.B., et al., *Clinical, pathophysiologic, and microbiologic characterization of bronchiectasis in an aging cohort.* Chest, 1995. **108**(4): p. 955-61.
298. Shaw, M.J., *Ventilator-associated pneumonia.* Curr Opin Pulm Med, 2005. **11**(3): p. 236-41.
299. Gaynes, R.P., et al., *Surgical site infection (SSI) rates in the United States, 1992-1998: the National Nosocomial Infections Surveillance System basic SSI risk index.* Clin Infect Dis, 2001. **33 Suppl 2**: p. S69-77.
300. Wilson, M.A., *Skin and soft-tissue infections: impact of resistant gram-positive bacteria.* Am J Surg, 2003. **186**(5A): p. 35S-41S; discussion 42S-43S, 61S-64S.
301. Greene, S.L., W.P. Su, and S.A. Muller, *Pseudomonas aeruginosa infections of the skin.* Am Fam Physician, 1984. **29**(1): p. 193-200.

302. Leyden, J.J., K.J. McGinley, and O.H. Mills, *Pseudomonas aeruginosa gram-negative folliculitis.* Arch Dermatol, 1979. **115**(10): p. 1203-4.
303. Obritsch, M.D., et al., *Nosocomial infections due to multidrug-resistant Pseudomonas aeruginosa: epidemiology and treatment options.* Pharmacotherapy, 2005. **25**(10): p. 1353-64.
304. Hamasuna, R., et al., *Bacteria of preoperative urinary tract infections contaminate the surgical fields and develop surgical site infections in urological operations.* Int J Urol, 2004. **11**(11): p. 941-7.
305. Barker, C.F. and R.E. Billingham, *Immunologically privileged sites.* Adv Immunol, 1977. **25**: p. 1-54.
306. Niederkorn, J.Y., *Immune privilege and immune regulation in the eye.* Adv Immunol, 1990. **48**: p. 191-226.
307. Zhou, R. and R.R. Caspi, *Ocular immune privilege.* F1000 Biol Rep, 2010. **2**.
308. Knop, N. and E. Knop, *Conjunctiva-associated lymphoid tissue in the human eye.* Invest Ophthalmol Vis Sci, 2000. **41**(6): p. 1270-9.
309. Chen, L., *Ocular lymphatics: state-of-the-art review.* Lymphology, 2009. **42**(2): p. 66-76.
310. Streilein, J.W. and J.Y. Niederkorn, *Characterization of the suppressor cell(s) responsible for anterior chamber-associated immune deviation (ACAID) induced in BALB/c mice by P815 cells.* J Immunol, 1985. **134**(3): p. 1381-7.
311. Knisely, T.L., et al., *The presence of biologically significant concentrations of glucocorticoids but little or no cortisol binding globulin within aqueous humor: relevance to immune privilege in the anterior chamber of the eye.* Invest Ophthalmol Vis Sci, 1994. **35**(10): p. 3711-23.
312. Sohn, J.H., et al., *Complement, innate immunity and ocular disease.* Chem Immunol Allergy, 2007. **92**: p. 105-14.
313. Mun, J.J., et al., *Clearance of Pseudomonas aeruginosa from a healthy ocular surface involves surfactant protein D and is compromised by bacterial elastase in a murine null-infection model.* Infect Immun, 2009. **77**(6): p. 2392-8.
314. Fleiszig, S.M., T.S. Zaidi, and G.B. Pier, *Pseudomonas aeruginosa invasion of and multiplication within corneal epithelial cells in vitro.* Infect Immun, 1995. **63**(10): p. 4072-7.
315. Fleiszig, S.M., et al., *Epithelial cell polarity affects susceptibility to Pseudomonas aeruginosa invasion and cytotoxicity.* Infect Immun, 1997. **65**(7): p. 2861-7.
316. Selinger, D.S., R.C. Selinger, and W.P. Reed, *Resistance to infection of the external eye: the role of tears.* Surv Ophthalmol, 1979. **24**(1): p. 33-8.
317. Flanagan, J.L. and M.D. Willcox, *Role of lactoferrin in the tear film.* Biochimie, 2009. **91**(1): p. 35-43.
318. Fleiszig, S.M., M.S. Kwong, and D.J. Evans, *Modification of Pseudomonas aeruginosa interactions with corneal epithelial cells by human tear fluid.* Infect Immun, 2003. **71**(7): p. 3866-74.
319. Kwong, M.S., et al., *Human tear fluid protects against Pseudomonas aeruginosa keratitis in a murine experimental model.* Infect Immun, 2007. **75**(5): p. 2325-32.
320. Mun, J.J., et al., *Modulation of epithelial immunity by mucosal fluid.* Sci Rep, 2011. **1**: p. 8.
321. Fleiszig, S.M., et al., *Modulation of Pseudomonas aeruginosa adherence to the corneal surface by mucus.* Infect Immun, 1994. **62**(5): p. 1799-804.
322. Ni, M., et al., *Surfactant protein D is present in human tear fluid and the cornea and inhibits epithelial cell invasion by Pseudomonas aeruginosa.* Infect Immun, 2005. **73**(4): p. 2147-56.
323. Masinick, S.A., et al., *Secretory IgA inhibits Pseudomonas aeruginosa binding to cornea and protects against keratitis.* Invest Ophthalmol Vis Sci, 1997. **38**(5): p. 910-8.
324. Johansson, M.E., et al., *The inner of the two Muc2 mucin-dependent mucus layers in colon is devoid of bacteria.* Proc Natl Acad Sci U S A, 2008. **105**(39): p. 15064-9.
325. Meyer-Hoffert, U., et al., *Secreted enteric antimicrobial activity localises to the mucus surface layer.* Gut, 2008. **57**(6): p. 764-71.

326. McDermott, A.M., et al., *Defensin expression by the cornea: multiple signalling pathways mediate IL-1beta stimulation of hBD-2 expression by human corneal epithelial cells.* Invest Ophthalmol Vis Sci, 2003. **44**(5): p. 1859-65.
327. Redfern, R.L., R.Y. Reins, and A.M. McDermott, *Toll-like receptor activation modulates antimicrobial peptide expression by ocular surface cells.* Exp Eye Res, 2011. **92**(3): p. 209-20.
328. Willcox, M.D., *Pseudomonas aeruginosa infection and inflammation during contact lens wear: a review.* Optom Vis Sci, 2007. **84**(4): p. 273-8.
329. Viriyakosol, S., et al., *MD-2 binds to bacterial lipopolysaccharide.* J Biol Chem, 2001. **276**(41): p. 38044-51.
330. Hazlett, L.D., *Bacterial infections of the cornea (Pseudomonas aeruginosa).* Chem Immunol Allergy, 2007. **92**: p. 185-94.
331. Hazlett, L.D. and R.L. Hendricks, *Reviews for immune privilege in the year 2010: immune privilege and infection.* Ocul Immunol Inflamm, 2010. **18**(4): p. 237-43.
332. Alarcon, I., et al., *Factors impacting corneal epithelial barrier function against Pseudomonas aeruginosa traversal.* Invest Ophthalmol Vis Sci, 2011. **52**(3): p. 1368-77.
333. Gupta, G. and A. Surolia, *Collectins: sentinels of innate immunity.* Bioessays, 2007. **29**(5): p. 452-64.
334. Tam, C., et al., *3D quantitative imaging of unprocessed live tissue reveals epithelial defense against bacterial adhesion and subsequent traversal requires MyD88.* PLoS One, 2011. **6**(8): p. e24008.
335. Pearlman, E., et al., *Toll-like receptors at the ocular surface.* Ocul Surf, 2008. **6**(3): p. 108-16.
336. McDermott, A.M., *The role of antimicrobial peptides at the ocular surface.* Ophthalmic Res, 2009. **41**(2): p. 60-75.
337. Kumar, A. and F.S. Yu, *Toll-like receptors and corneal innate immunity.* Curr Mol Med, 2006. **6**(3): p. 327-37.
338. Kumar, A., et al., *Modulation of corneal epithelial innate immune response to pseudomonas infection by flagellin pretreatment.* Invest Ophthalmol Vis Sci, 2007. **48**(10): p. 4664-70.
339. Mc, N.N., et al., *Ocular surface epithelia express mRNA for human beta defensin-2.* Exp Eye Res, 1999. **69**(5): p. 483-90.
340. Augustin, D.K., et al., *Role of defensins in corneal epithelial barrier function against Pseudomonas aeruginosa traversal.* Infect Immun, 2011. **79**(2): p. 595-605.
341. Abrams, G.A., et al., *Nanoscale topography of the basement membrane underlying the corneal epithelium of the rhesus macaque.* Cell Tissue Res, 2000. **299**(1): p. 39-46.
342. Ko, J.A., R. Yanai, and T. Nishida, *IGF-1 released by corneal epithelial cells induces up-regulation of N-cadherin in corneal fibroblasts.* J Cell Physiol, 2009. **221**(1): p. 254-61.
343. Kenyon, K.R., et al., *Prevention of stromal ulceration in the alkali-burned rabbit cornea by glued-on contact lens. Evidence for the role of polymorphonuclear leukocytes in collagen degradation.* Invest Ophthalmol Vis Sci, 1979. **18**(6): p. 570-87.
344. Foster, C.S., et al., *Immunosuppression and selective inflammatory cell depletion. Studies on a guinea pig model of corneal ulceration after ocular alkali burning.* Arch Ophthalmol, 1982. **100**(11): p. 1820-4.
345. Shimazu, R., et al., *MD-2, a molecule that confers lipopolysaccharide responsiveness on Toll-like receptor 4.* J Exp Med, 1999. **189**(11): p. 1777-82.
346. Visintin, A., et al., *Secreted MD-2 is a large polymeric protein that efficiently confers lipopolysaccharide sensitivity to Toll-like receptor 4.* Proc Natl Acad Sci U S A, 2001. **98**(21): p. 12156-61.
347. Schultz, C.L., et al., *Lipopolysaccharide induced acute red eye and corneal ulcers.* Exp Eye Res, 1997. **64**(1): p. 3-9.
348. Gioannini, T.L., et al., *Isolation of an endotoxin-MD-2 complex that produces Toll-like receptor 4-dependent cell activation at picomolar concentrations.* Proc Natl Acad Sci U S A, 2004. **101**(12): p. 4186-91.

349. Gioannini, T.L., et al., *Monomeric endotoxin:protein complexes are essential for TLR4-dependent cell activation.* J Endotoxin Res, 2005. **11**(2): p. 117-23.
350. Sun, Y., et al., *TLR4 and TLR5 on corneal macrophages regulate Pseudomonas aeruginosa keratitis by signaling through MyD88-dependent and -independent pathways.* J Immunol, 2010. **185**(7): p. 4272-83.
351. Kawai, T. and S. Akira, *TLR signaling.* Semin Immunol, 2007. **19**(1): p. 24-32.
352. Raman, M., W. Chen, and M.H. Cobb, *Differential regulation and properties of MAPKs.* Oncogene, 2007. **26**(22): p. 3100-12.
353. Pearson, G., et al., *Mitogen-activated protein (MAP) kinase pathways: regulation and physiological functions.* Endocr Rev, 2001. **22**(2): p. 153-83.
354. Lee, M.S. and Y.J. Kim, *Signaling pathways downstream of pattern-recognition receptors and their cross talk.* Annu Rev Biochem, 2007. **76**: p. 447-80.
355. Yamamoto, M., et al., *Role of adaptor TRIF in the MyD88-independent toll-like receptor signaling pathway.* Science, 2003. **301**(5633): p. 640-3.
356. Oganesyan, G., et al., *Critical role of TRAF3 in the Toll-like receptor-dependent and -independent antiviral response.* Nature, 2006. **439**(7073): p. 208-11.
357. Huang, X., et al., *TLR4 is required for host resistance in Pseudomonas aeruginosa keratitis.* Invest Ophthalmol Vis Sci, 2006. **47**(11): p. 4910-6.
358. Kumar, A., J. Zhang, and F.S. Yu, *Toll-like receptor 2-mediated expression of beta-defensin-2 in human corneal epithelial cells.* Microbes Infect, 2006. **8**(2): p. 380-9.
359. Ueta, M., et al., *Intracellularly expressed TLR2s and TLR4s contribution to an immunosilent environment at the ocular mucosal epithelium.* J Immunol, 2004. **173**(5): p. 3337-47.
360. Sun, Y. and E. Pearlman, *Inhibition of corneal inflammation by the TLR4 antagonist Eritoran tetrasodium (E5564).* Invest Ophthalmol Vis Sci, 2009. **50**(3): p. 1247-54.
361. Visintin, A., et al., *MD-2 expression is not required for cell surface targeting of Toll-like receptor 4 (TLR4).* J Leukoc Biol, 2006. **80**(6): p. 1584-92.
362. Zhang, J., et al., *Lack of MD-2 expression in human corneal epithelial cells is an underlying mechanism of lipopolysaccharide (LPS) unresponsiveness.* Immunol Cell Biol, 2009. **87**(2): p. 141-8.
363. Roy, S., Y. Sun, and E. Pearlman, *Interferon-gamma-induced MD-2 protein expression and lipopolysaccharide (LPS) responsiveness in corneal epithelial cells is mediated by Janus tyrosine kinase-2 activation and direct binding of STAT1 protein to the MD-2 promoter.* J Biol Chem, 2011. **286**(27): p. 23753-62.
364. Hazlett, L.D., et al., *NKT cells are critical to initiate an inflammatory response after Pseudomonas aeruginosa ocular infection in susceptible mice.* J Immunol, 2007. **179**(2): p. 1138-46.
365. Pearlman, E., et al., *Host defense at the ocular surface.* Int Rev Immunol, 2013. **32**(1): p. 4-18.
366. Dinarello, C.A., *Interleukin-1 beta, interleukin-18, and the interleukin-1 beta converting enzyme.* Ann N Y Acad Sci, 1998. **856**: p. 1-11.
367. Alnemri, E.S., et al., *Human ICE/CED-3 protease nomenclature.* Cell, 1996. **87**(2): p. 171.
368. Cerretti, D.P., et al., *Molecular cloning of the interleukin-1 beta converting enzyme.* Science, 1992. **256**(5053): p. 97-100.
369. Thornberry, N.A., et al., *A novel heterodimeric cysteine protease is required for interleukin-1 beta processing in monocytes.* Nature, 1992. **356**(6372): p. 768-74.
370. Martinon, F., K. Burns, and J. Tschopp, *The inflammasome: a molecular platform triggering activation of inflammatory caspases and processing of proIL-beta.* Mol Cell, 2002. **10**(2): p. 417-26.
371. Gross, O., et al., *The inflammasome: an integrated view.* Immunol Rev, 2011. **243**(1): p. 136-51.
372. Schroder, K. and J. Tschopp, *The inflammasomes.* Cell, 2010. **140**(6): p. 821-32.

373. Black, R.A., et al., *Generation of biologically active interleukin-1 beta by proteolytic cleavage of the inactive precursor.* J Biol Chem, 1988. **263**(19): p. 9437-42.
374. Hazuda, D.J., et al., *Processing of precursor interleukin 1 beta and inflammatory disease.* J Biol Chem, 1990. **265**(11): p. 6318-22.
375. Leal, S.M., Jr., et al., *Fungal antioxidant pathways promote survival against neutrophils during infection.* J Clin Invest, 2012. **122**(7): p. 2482-98.
376. Nathan, C., *Neutrophils and immunity: challenges and opportunities.* Nat Rev Immunol, 2006. **6**(3): p. 173-82.
377. Sano, Y., B.R. Ksander, and J.W. Streilein, *Fate of orthotopic corneal allografts in eyes that cannot support anterior chamber-associated immune deviation induction.* Invest Ophthalmol Vis Sci, 1995. **36**(11): p. 2176-85.
378. Williamson, J.S., S. DiMarco, and J.W. Streilein, *Immunobiology of Langerhans cells on the ocular surface. I. Langerhans cells within the central cornea interfere with induction of anterior chamber associated immune deviation.* Invest Ophthalmol Vis Sci, 1987. **28**(9): p. 1527-32.
379. Hamrah, P., et al., *Corneal immunity is mediated by heterogeneous population of antigen-presenting cells.* J Leukoc Biol, 2003. **74**(2): p. 172-8.
380. Smith, R.S., et al., *Fibroblasts as sentinel cells. Synthesis of chemokines and regulation of inflammation.* Am J Pathol, 1997. **151**(2): p. 317-22.
381. Sempowski, G.D., P.R. Chess, and R.P. Phipps, *CD40 is a functional activation antigen and B7-independent T cell costimulatory molecule on normal human lung fibroblasts.* J Immunol, 1997. **158**(10): p. 4670-7.
382. Sempowski, G.D., et al., *CD40 mediated activation of gingival and periodontal ligament fibroblasts.* J Periodontol, 1997. **68**(3): p. 284-92.
383. Hobden, J.A., *Pseudomonas aeruginosa proteases and corneal virulence.* DNA Cell Biol, 2002. **21**(5-6): p. 391-6.
384. Steuhl, K.P., et al., *Relevance of host-derived and bacterial factors in Pseudomonas aeruginosa corneal infections.* Invest Ophthalmol Vis Sci, 1987. **28**(9): p. 1559-68.
385. Moon, M.M., et al., *Monoclonal antibodies provide protection against ocular Pseudomonas aeruginosa infection.* Invest Ophthalmol Vis Sci, 1988. **29**(8): p. 1277-84.
386. Ohman, D.E., R.P. Burns, and B.H. Iglewski, *Corneal infections in mice with toxin A and elastase mutants of Pseudomonas aeruginosa.* J Infect Dis, 1980. **142**(4): p. 547-55.
387. Kernacki, K.A. and R.S. Berk, *Characterization of arachidonic acid metabolism and the polymorphonuclear leukocyte response in mice infected intracorneally with Pseudomonas aeruginosa.* Invest Ophthalmol Vis Sci, 1995. **36**(1): p. 16-23.
388. Kernacki, K.A., et al., *In vivo bacterial protease production during Pseudomonas aeruginosa corneal infection.* Invest Ophthalmol Vis Sci, 1995. **36**(7): p. 1371-8.
389. Hazlett, L.D., D.D. Rosen, and R.S. Berk, *Pseudomonas eye infections in cyclophosphamide-treated mice.* Invest Ophthalmol Vis Sci, 1977. **16**(7): p. 649-52.
390. Lausch, R.N., et al., *Early cytokine synthesis in the excised mouse cornea.* J Interferon Cytokine Res, 1996. **16**(1): p. 35-40.
391. Strieter, R.M., et al., *"The good, the bad, and the ugly." The role of chemokines in models of human disease.* J Immunol, 1996. **156**(10): p. 3583-6.
392. Hazlett, L.D., et al., *Aging alters the phagocytic capability of inflammatory cells induced into cornea.* Curr Eye Res, 1990. **9**(2): p. 129-38.
393. Salonen, E.M., et al., *Plasmin in tear fluid of patients with corneal ulcers: basis for new therapy.* Acta Ophthalmol (Copenh), 1987. **65**(1): p. 3-12.
394. Wang, H.M., M. Berman, and M. Law, *Latent and active plasminogen activator in corneal ulceration.* Invest Ophthalmol Vis Sci, 1985. **26**(4): p. 511-24.
395. Saksela, O. and D.B. Rifkin, *Cell-associated plasminogen activation: regulation and physiological functions.* Annu Rev Cell Biol, 1988. **4**: p. 93-126.

396. Dano, K., et al., *Plasminogen activators, tissue degradation, and cancer.* Adv Cancer Res, 1985. **44**: p. 139-266.
397. Berman, M., R. Leary, and J. Gage, *Evidence for a role of the plasminogen activator--plasmin system in corneal ulceration.* Invest Ophthalmol Vis Sci, 1980. **19**(10): p. 1204-21.
398. Cejkova, J., et al., *The histochemical pattern of mechanically or chemically injured rabbit cornea after aprotinin treatment: relationships with the plasmin concentration of the tear fluid.* Histochem J, 1993. **25**(6): p. 438-45.
399. Ye, S., S. Humphries, and A. Henney, *Matrix metalloproteinases: implication in vascular matrix remodelling during atherogenesis.* Clin Sci (Lond), 1998. **94**(2): p. 103-10.
400. Kieseier, B.C., et al., *Matrix metalloproteinases in inflammatory demyelination: targets for treatment.* Neurology, 1999. **53**(1): p. 20-5.
401. Park, A.J., et al., *Mutational analysis of the transin (rat stromelysin) autoinhibitor region demonstrates a role for residues surrounding the "cysteine switch".* J Biol Chem, 1991. **266**(3): p. 1584-90.
402. Windsor, L.J., et al., *An internal cysteine plays a role in the maintenance of the latency of human fibroblast collagenase.* Biochemistry, 1991. **30**(3): p. 641-7.
403. Werb, z. and c. Alexander, *Cell biology of extracellular matrix*. 1993, New York: Plenum.
404. Brinckerhoff, C.E., *Regulation of metalloproteinase gene expression: implications for osteoarthritis.* Crit Rev Eukaryot Gene Expr, 1992. **2**(2): p. 145-64.
405. Ottino, P., F. Taheri, and H.E. Bazan, *Platelet-activating factor induces the gene expression of TIMP-1, -2, and PAI-1: imbalance between the gene expression of MMP-9 and TIMP-1 and -2.* Exp Eye Res, 2002. **74**(3): p. 393-402.
406. Fini, M.E. and M.T. Girard, *Expression of collagenolytic/gelatinolytic metalloproteinases by normal cornea.* Invest Ophthalmol Vis Sci, 1990. **31**(9): p. 1779-88.
407. Matsubara, M., et al., *Differential roles for two gelatinolytic enzymes of the matrix metalloproteinase family in the remodelling cornea.* Dev Biol, 1991. **147**(2): p. 425-39.
408. Matsubara, M., J.D. Zieske, and M.E. Fini, *Mechanism of basement membrane dissolution preceding corneal ulceration.* Invest Ophthalmol Vis Sci, 1991. **32**(13): p. 3221-37.
409. Ando, H., et al., *MMPs and proteinase inhibitors in the human aqueous humor.* Invest Ophthalmol Vis Sci, 1993. **34**(13): p. 3541-8.
410. Brown, D., et al., *Characterization of the major matrix degrading metalloproteinase of human corneal stroma. Evidence for an enzyme/inhibitor complex.* Exp Eye Res, 1991. **52**(1): p. 5-16.
411. Fini, M.E., et al., *The rabbit gene for 92-kDa matrix metalloproteinase. Role of AP1 and AP2 in cell type-specific transcription.* J Biol Chem, 1994. **269**(46): p. 28620-8.
412. Girard, M.T., et al., *Stromal fibroblasts synthesize collagenase and stromelysin during long-term tissue remodeling.* J Cell Sci, 1993. **104 (Pt 4)**: p. 1001-11.
413. Fini, M.E., J.R. Cook, and R. Mohan, *Proteolytic mechanisms in corneal ulceration and repair.* Arch Dermatol Res, 1998. **290 Suppl**: p. S12-23.
414. Barletta, J.P., et al., *Inhibition of pseudomonal ulceration in rabbit corneas by a synthetic matrix metalloproteinase inhibitor.* Invest Ophthalmol Vis Sci, 1996. **37**(1): p. 20-8.
415. Kernacki, K.A., R. Barrett, and L.D. Hazlett, *Evidence for TIMP-1 protection against P. aeruginosa-induced corneal ulceration and perforation.* Invest Ophthalmol Vis Sci, 1999. **40**(13): p. 3168-76.
416. Adachi, W., et al., *Isolation and characterization of human cathepsin V: a major proteinase in corneal epithelium.* Invest Ophthalmol Vis Sci, 1998. **39**(10): p. 1789-96.
417. Yamada, T., S. Hara, and M. Tamai, *Immunohistochemical localization of cathepsin D in ocular tissues.* Invest Ophthalmol Vis Sci, 1990. **31**(7): p. 1217-23.
418. Persson, H., S. Kawashima, and J.O. Karlsson, *Immunohistochemical localization of calpains and calpastatin in the rabbit eye.* Brain Res, 1993. **611**(2): p. 272-8.

419. Shiono, T., S. Hayasaka, and K. Mizuno, *Acid hydrolases in the bovine corneal epithelium.* Graefes Arch Clin Exp Ophthalmol, 1986. **224**(5): p. 467-8.
420. el-Hifnawi, E., *Localization of cathepsin D in rat ocular tissues. An immunohistochemical study.* Ann Anat, 1995. **177**(1): p. 11-7.
421. Birkedal-Hansen, H., *Role of cytokines and inflammatory mediators in tissue destruction.* J Periodontal Res, 1993. **28**(6 Pt 2): p. 500-10.
422. Dong, Z., et al., *Expression of cathepsins B, D and L in mouse corneas infected with Pseudomonas aeruginosa.* Eur J Biochem, 2001. **268**(24): p. 6408-16.
423. Fleiszig, S.M., et al., *Relationship between cytotoxicity and corneal epithelial cell invasion by clinical isolates of Pseudomonas aeruginosa.* Infect Immun, 1996. **64**(6): p. 2288-94.
424. Price, F.W., Jr., et al., *Corneal tissue levels of topically applied ciprofloxacin.* Cornea, 1995. **14**(2): p. 152-6.
425. Leibowitz, H.M., *Clinical evaluation of ciprofloxacin 0.3% ophthalmic solution for treatment of bacterial keratitis.* Am J Ophthalmol, 1991. **112**(4 Suppl): p. 34s-47s.
426. Fischer, A.B., *Gentamicin as a bactericidal antibiotic in tissue culture.* Med Microbiol Immunol, 1975. **161**(1): p. 23-39.
427. Kannan, S., et al., *Src kinase Lyn is crucial for Pseudomonas aeruginosa internalization into lung cells.* Eur J Immunol, 2006. **36**(7): p. 1739-52.
428. Gaillard, J.L., et al., *In vitro model of penetration and intracellular growth of Listeria monocytogenes in the human enterocyte-like cell line Caco-2.* Infect Immun, 1987. **55**(11): p. 2822-9.
429. Mikkelsen, H., R. McMullan, and A. Filloux, *The Pseudomonas aeruginosa reference strain PA14 displays increased virulence due to a mutation in ladS.* PLoS One, 2011. **6**(12): p. e29113.
430. Elkington, P.T., C.M. O'Kane, and J.S. Friedland, *The paradox of matrix metalloproteinases in infectious disease.* Clin Exp Immunol, 2005. **142**(1): p. 12-20.
431. Sridhar, M.S., et al., *Infectious crystalline keratopathy in an immunosuppressed patient.* Clao j, 2001. **27**(2): p. 108-10.
432. Butler, T.K., et al., *In vitro model of infectious crystalline keratopathy: tissue architecture determines pattern of microbial spread.* Invest Ophthalmol Vis Sci, 2001. **42**(6): p. 1243-6.
433. Finlay, B.B. and S. Falkow, *Common themes in microbial pathogenicity revisited.* Microbiol Mol Biol Rev, 1997. **61**(2): p. 136-69.
434. Beachey, E.H., *Bacterial adherence: adhesin-receptor interactions mediating the attachment of bacteria to mucosal surface.* J Infect Dis, 1981. **143**(3): p. 325-45.
435. Finlay, B.B. and S. Falkow, *Common themes in microbial pathogenicity.* Microbiol Rev, 1989. **53**(2): p. 210-30.
436. Azghani, A.O., A.Y. Kondepudi, and A.R. Johnson, *Interaction of Pseudomonas aeruginosa with human lung fibroblasts: role of bacterial elastase.* Am J Respir Cell Mol Biol, 1992. **6**(6): p. 652-7.
437. Barken, K.B., et al., *Roles of type IV pili, flagellum-mediated motility and extracellular DNA in the formation of mature multicellular structures in Pseudomonas aeruginosa biofilms.* Environ Microbiol, 2008. **10**(9): p. 2331-43.
438. Doig, P., et al., *Characterization of the binding of Pseudomonas aeruginosa alginate to human epithelial cells.* Infect Immun, 1987. **55**(6): p. 1517-22.
439. Baker, N.R., et al., *Pseudomonas aeruginosa exoenzyme S is an adhesion.* Infect Immun, 1991. **59**(9): p. 2859-63.
440. Ramphal, R., et al., *Adhesion of Pseudomonas aeruginosa pilin-deficient mutants to mucin.* Infect Immun, 1991. **59**(4): p. 1307-11.
441. Pizarro-Cerda, J. and P. Cossart, *Bacterial adhesion and entry into host cells.* Cell, 2006. **124**(4): p. 715-27.

442. Ljungh, A., A.P. Moran, and T. Wadstrom, *Interactions of bacterial adhesins with extracellular matrix and plasma proteins: pathogenic implications and therapeutic possibilities.* FEMS Immunol Med Microbiol, 1996. **16**(2): p. 117-26.
443. Striker, R., et al., *Structural requirements for the glycolipid receptor of human uropathogenic Escherichia coli.* Mol Microbiol, 1995. **16**(5): p. 1021-9.
444. Mulvey, M.A., et al., *Induction and evasion of host defenses by type 1-piliated uropathogenic Escherichia coli.* Science, 1998. **282**(5393): p. 1494-7.
445. Bernard, S.C., et al., *Pathogenic Neisseria meningitidis utilizes CD147 for vascular colonization.* Nat Med, 2014. **20**(7): p. 725-31.
446. Bucior, I., K. Mostov, and J.N. Engel, *Pseudomonas aeruginosa-mediated damage requires distinct receptors at the apical and basolateral surfaces of the polarized epithelium.* Infect Immun, 2010. **78**(3): p. 939-53.
447. Zhao, Y. and F. Shao, *The NAIP-NLRC4 inflammasome in innate immune detection of bacterial flagellin and type III secretion apparatus.* Immunol Rev, 2015. **265**(1): p. 85-102.
448. Fleiszig, S.M., et al., *Pseudomonas aeruginosa invades corneal epithelial cells during experimental infection.* Infect Immun, 1994. **62**(8): p. 3485-93.
449. Slanina, H., et al., *Entry of Neisseria meningitidis into mammalian cells requires the Src family protein tyrosine kinases.* Infect Immun, 2010. **78**(5): p. 1905-14.
450. Eckmann, L., M.F. Kagnoff, and J. Fierer, *Epithelial cells secrete the chemokine interleukin-8 in response to bacterial entry.* Infect Immun, 1993. **61**(11): p. 4569-74.
451. Finlay, B.B. and S. Falkow, *Comparison of the invasion strategies used by Salmonella cholerae-suis, Shigella flexneri and Yersinia enterocolitica to enter cultured animal cells: endosome acidification is not required for bacterial invasion or intracellular replication.* Biochimie, 1988. **70**(8): p. 1089-99.
452. Schwartzberg, P.L., *The many faces of Src: multiple functions of a prototypical tyrosine kinase.* Oncogene, 1998. **17**(11 Reviews): p. 1463-8.
453. Esen, M., et al., *Invasion of human epithelial cells by Pseudomonas aeruginosa involves src-like tyrosine kinases p60Src and p59Fyn.* Infect Immun, 2001. **69**(1): p. 281-7.
454. Parsons, S.J. and J.T. Parsons, *Src family kinases, key regulators of signal transduction.* Oncogene, 2004. **23**(48): p. 7906-9.
455. Evans, D.J., et al., *Pseudomonas aeruginosa invasion and cytotoxicity are independent events, both of which involve protein tyrosine kinase activity.* Infect Immun, 1998. **66**(4): p. 1453-9.
456. Dehio, C., M.C. Prevost, and P.J. Sansonetti, *Invasion of epithelial cells by Shigella flexneri induces tyrosine phosphorylation of cortactin by a pp60c-src-mediated signalling pathway.* Embo j, 1995. **14**(11): p. 2471-82.
457. Hauck, C.R., et al., *CD66-mediated phagocytosis of Opa52 Neisseria gonorrhoeae requires a Src-like tyrosine kinase- and Rac1-dependent signalling pathway.* Embo j, 1998. **17**(2): p. 443-54.
458. Isberg, R.R. and J.M. Leong, *Multiple beta 1 chain integrins are receptors for invasin, a protein that promotes bacterial penetration into mammalian cells.* Cell, 1990. **60**(5): p. 861-71.
459. Van Langendonck, N., P. Velge, and E. Bottreau, *Host cell protein tyrosine kinases are activated during the entry of Listeria monocytogenes. Possible role of pp60c-src family protein kinases.* FEMS Microbiol Lett, 1998. **162**(1): p. 169-76.
460. Nouwens, A.S., et al., *Proteomic comparison of membrane and extracellular proteins from invasive (PAO1) and cytotoxic (6206) strains of Pseudomonas aeruginosa.* Proteomics, 2002. **2**(9): p. 1325-46.
461. Wiehlmann, L., et al., *Population structure of Pseudomonas aeruginosa.* Proc Natl Acad Sci U S A, 2007. **104**(19): p. 8101-6.

462. He, J., et al., *The broad host range pathogen Pseudomonas aeruginosa strain PA14 carries two pathogenicity islands harboring plant and animal virulence genes.* Proc Natl Acad Sci U S A, 2004. **101**(8): p. 2530-5.
463. Mikkelsen, H., et al., *Expression of Pseudomonas aeruginosa CupD fimbrial genes is antagonistically controlled by RcsB and the EAL-containing PvrR response regulators.* PLoS One, 2009. **4**(6): p. e6018.
464. Harrison, E.M., et al., *Pathogenicity islands PAPI-1 and PAPI-2 contribute individually and synergistically to the virulence of Pseudomonas aeruginosa strain PA14.* Infect Immun, 2010. **78**(4): p. 1437-46.
465. Homma, M., D.J. DeRosier, and R.M. Macnab, *Flagellar hook and hook-associated proteins of Salmonella typhimurium and their relationship to other axial components of the flagellum.* J Mol Biol, 1990. **213**(4): p. 819-32.
466. Wong, Y., et al., *Lipopolysaccharide regulation of toll-like receptor-4 and matrix metalloprotease-9 in human primary corneal fibroblasts.* Invest Ophthalmol Vis Sci, 2011. **52**(5): p. 2796-803.
467. Miao, E.A., et al., *Innate immune detection of the type III secretion apparatus through the NLRC4 inflammasome.* Proc Natl Acad Sci U S A, 2010. **107**(7): p. 3076-80.
468. Lightfield, K.L., et al., *Critical function for Naip5 in inflammasome activation by a conserved carboxy-terminal domain of flagellin.* Nat Immunol, 2008. **9**(10): p. 1171-8.
469. Lefebre, M.D. and J.E. Galan, *The inner rod protein controls substrate switching and needle length in a Salmonella type III secretion system.* Proc Natl Acad Sci U S A, 2014. **111**(2): p. 817-22.
470. Zhao, Y., et al., *The NLRC4 inflammasome receptors for bacterial flagellin and type III secretion apparatus.* Nature, 2011. **477**(7366): p. 596-600.
471. Yang, J., et al., *Human NAIP and mouse NAIP1 recognize bacterial type III secretion needle protein for inflammasome activation.* Proc Natl Acad Sci U S A, 2013. **110**(35): p. 14408-13.
472. Brinckerhoff, C.E. and L.M. Matrisian, *Matrix metalloproteinases: a tail of a frog that became a prince.* Nat Rev Mol Cell Biol, 2002. **3**(3): p. 207-14.
473. Schonbeck, U., F. Mach, and P. Libby, *Generation of biologically active IL-1 beta by matrix metalloproteinases: a novel caspase-1-independent pathway of IL-1 beta processing.* J Immunol, 1998. **161**(7): p. 3340-6.
474. Ito, A., et al., *Degradation of interleukin 1beta by matrix metalloproteinases.* J Biol Chem, 1996. **271**(25): p. 14657-60.
475. Pardo, A. and M. Selman, *MMP-1: the elder of the family.* Int J Biochem Cell Biol, 2005. **37**(2): p. 283-8.
476. Xue, M.L., et al., *Regulation of MMPs and TIMPs by IL-1beta during corneal ulceration and infection.* Invest Ophthalmol Vis Sci, 2003. **44**(5): p. 2020-5.
477. Ye, S., et al., *Progression of coronary atherosclerosis is associated with a common genetic variant of the human stromelysin-1 promoter which results in reduced gene expression.* J Biol Chem, 1996. **271**(22): p. 13055-60.
478. McClellan, S.A., et al., *Matrix metalloproteinase-9 amplifies the immune response to Pseudomonas aeruginosa corneal infection.* Invest Ophthalmol Vis Sci, 2006. **47**(1): p. 256-64.
479. Sakimoto, T., J. Shoji, and M. Sawa, *Active form of gelatinases in tear fluidin patients with corneal ulcer or ocular burn.* Jpn J Ophthalmol, 2003. **47**(5): p. 423-6.